Individualising anti-cancer treatment:

Optimising tracking accuracy and dose delivery in Stereotactic Body Radiotherapy (SBRT)

Dr Christy Saron Goldsmith,
MBBS, B.Sc., MRCP, FRCR

Submitted for MD (Res)

Abstract

Introduction:

Stereotactic Body Radiotherapy (SBRT) is a form of highly focal radiation therapy. Treatment delivery is largely guided ("tracked") by gold-marker fiducials for non-spinal body sites. CyberKnife (CK) is purpose-built todeliver SBRT.

Methods:

An experimental system, using a radiotherapy "phantom", was designed to assess the accuracy of the CK system in imaging static and migrating fiducials (Chapter 2). An assumption in fiducial-tracked treatments is that the exact arrangement of fiducials at planning CT is maintained at treatment. It is also crucial that relative Organ At Risk (OAR) and tumour position, is consistent between planning CT scan and treatment. The validity of this assumption was assessed by comparing fiducial locations on Planning and Treatment CTs (Chapter 3). The feasibility of achieving consistent bladder filling, and the impact of consistent filling on the ability to track translations/rotations in prostate cancer therapy was explored (Chapter 4). Uncertainties in treatment planning/delivery for CK prostate patients was explored, and ideal planning margins were calculated (Chapter 5). Optimum SBRT dose for localised pancreatic cancer, lymph node oligometastasis and oligometastatic breast cancer was explored (Chapter 6).

Results:

Imaging of fiducial position was accurate and reproducible across a clinically appropriate tracking range. However, findings highlighted the need for vigilance at treatment delivery. The reliability and "trackability" of implanted fiducials, as well as consistency of OAR position, varied according to tumour and implantation site. Guidelines were generated accordingly. Bladder filling/Margins guidelines have been generated. Radiobiological analysis has indicated that there is scope for cautious dose escalation in the SBRT treatment of pancreatic cancer. Analysis of SBRT-treated lymph node oligometastases has demonstrated that Local Control is 100% when SBRT is prescribed to a threshold $72Gy_{10.}$

Conclusion:

Refinements in patient preparation, fiducial placement, and dose/fractionation selection can optimise tracking accuracy and dose delivery in SBRT.

Table of Contents

CHAPTER 1

Background and Introduction

1.1 Conventionally fractionated Conformal Radiotherapy

1.1.1: Treatment planning

- Simulation
- ICRU Target Concepts
- Tumour localisation
- Planning
- Limitations of Conformal radiotherapy

1.1.2: Dose Fractionation issues

1.2 Intensity Modulated RadioTherapy

1.2.1 Treatment planning

1.2.2 Clinical evidence for gain over Conformal radiotherapy

1.3 Stereotactic Body Radiotherapy

1.3.1 Definition

1.3.2 Key Components

- Immobilisation
- Tumour motion

1.3.3 SBRT Treatment delivery systems

1.3.4 Conformality

1.3.5 Dose-fractionation issues

1.4 Summary

1.5 Aims of this Research

CHAPTER 1

Background and Introduction

1.1 Conventionally fractionated Conformal Radiotherapy

Radiotherapy is the medical use of ionising radiation to kill malignant cells in order to control cancer. Ionising radiation is able to kill cancer cells (but also normal body cells), by damaging cellular DNA, via a number of different mechanisms. Radiotherapy is a local form of treatment, and as normal tissue is radiosensitive, it is important that the deposition of radiation dose is accurately deposited on the tumour and spares collateral damage to adjacent normal healthy tissues.

Once a patient is seen in clinic and consented for Radiotherapy, there a number of important steps in the Radiotherapy Planning Process which must occur before a patient can receive their treatment.

1.1.1 Treatment Planning Process:

Simulation

The Radiotherapy planning process starts with the process of "simulation". The process of "simulation", for many years, involved a patient being immobilised in their treatment position on a couch. A "conventional" radiotherapy simulator would then capture two-dimensional (2D) information. A conventional simulator comprised a diagnostic X-ray tube mounted to reproduce the geometric movements of a radiotherapy treatment machine, which was capable of imaging with fluoroscopy and diagnostic film. Three-Dimensional (3D) information was inferred by taking orthogonal X-Ray films. As conventional planning can only infer 3D information, this is a limitation of the technique, as accurate dosimetry requires full 3D information in order to fully evaluate attenuation of the photon beam within tissue.

In order to overcome this limitation, conventional simulators have now largely been replaced by Computed Tomography (CT), or "virtual" CT simulators. These simulators comprise a CT scanner, laser marking system, and 3D work-station to allow the visualisation and manipulation of the CT data for treatment localisation. The information derived through CT is inherently 3D, and contains both contour and tissue density information which is required for the planning process (1). A 3D based

environment for imaging, planning and radiotherapy delivery is the current baseline standard according to the most recent National Radiotherapy Advisory Group (NRAG) report (2).

Scanned images taken at virtual simulation are linked into treatment planning software that allows Clinical Oncologists to visualise and localise the tumour target in 3D.

The International Commission on Radiation Units and Measurements Guidelines (ICRU): Target Concepts

The ICRU 50 report (1993) defines standards for describing Radiotherapy prescription volumes.
Gross Tumour Volume (GTV) represents the gross palpable or visible extent of disease.
Clinical Target Volume (CTV) incorporates a margin of normal tissue for unknown subclinical or microscopic disease.
Planning Target Volume (PTV) includes all other errors and uncertainties e.g. tumour motion and set-up errors (3).

The ICRU 62 report (1999) acknowledges the effect of organ/tumour movement, the resulting uncertainties are accommodated by expanding the CTV to an Internal Target Volume (ITV) by an Internal Margin (IM). The report also accounts for uncertainties in treatment delivery due to errors in beam-patient positioning, called the Set Up margin (SM), to develop a Planning Target Volume (PTV) (4). See Figure 1.

Figure 1: Diagram to illustrate the concepts of GTV, CTV, ITV, and PTV

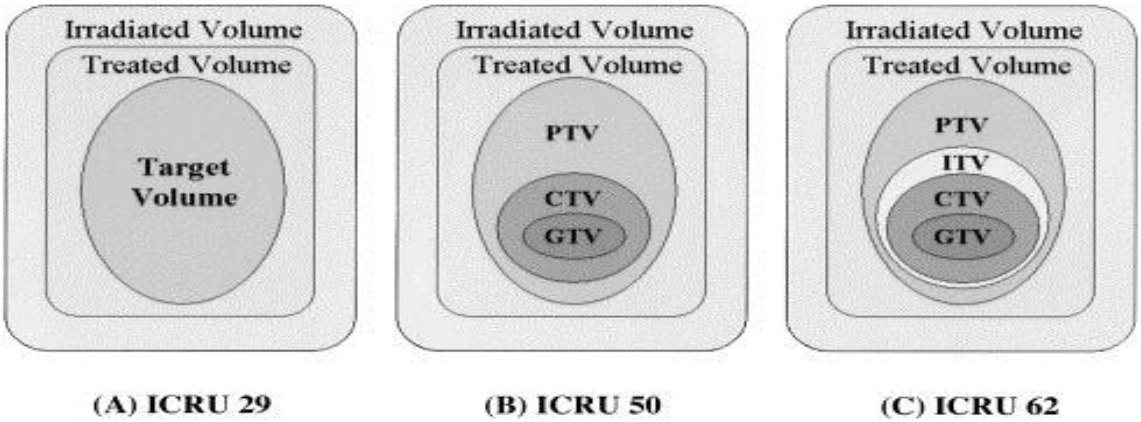

(A) ICRU 29 (B) ICRU 50 (C) ICRU 62

Tumour localisation

There have been a number of advances in recent years that have made it possible to more accurately delineate a target.

It is now possible to fuse the 3D CT data set with Magnetic Resonance Imaging (MRI) scans. This aids the outlining process, as some tumours, e.g. brain and prostate are more easily seen on MRI than CT (5). In a study by Sannazzari et al, the CTV for localised prostate cancer (prostate plus seminal vesicles) was delineated on both CT and MRI studies. Image fusion was achieved by fusing to anatomical fiducial markers. There was a mean over-estimation of CTV of 34% with CT compared with MRI (6).

The outlining of other tumours that are glucose-avid, e.g. Non-Small Cell Lung Cancer (NSCLC), Squamous cell cancers of the Head and Neck is helped by the ability to fuse Positron Emission Tomography (PET) scans to the Primary CT scan (7, 8).

PET scans are performed following the administration of ^{18}F-Fluoro-DeoxyGlucose (FDG), a glucose analogue. As the FDG is labeled with ^{18}F at the 2-prime hydroxyl position, the normal degradation that occurs during glycolysis is prevented, and the radio-labelled FDG accumulates within the tissue (9). In this way, PET scans provide functional information (metabolic rate), and are good for identifying nodal disease Head &Neck cancers (see Figure 2, page 8), as well as areas of atelectasis in Thoracic cancer.

Studies have demonstrated a change in the PTV in approximately 30% of cases of NSCLC, which may have important consequences for both toxicity and tumour control. PET-fusion may allow smaller volumes to be outlined (especially likely in cases of atelectasis), this would allow smaller volumes of normal lung to be irradiated, which should improve the toxicity profile of the treatment (10). Alternatively, PET may increase the outlined tumour volumes (due to positive lymph nodes), which is likely to have a positive impact on tumour control (11).

A disadvantage to PET (compared to CT), however, is that PET has poorer spatial resolution (12).

Figure 2: Image A shows a CT image taken at the level of the thoracic inlet. The arrow shows a pathological lymph node which is relatively difficult to identify. Image B shows a co-registered PET-CT image. The arrowed node avidly takes up radio-labelled FDG and is now easy to identify.

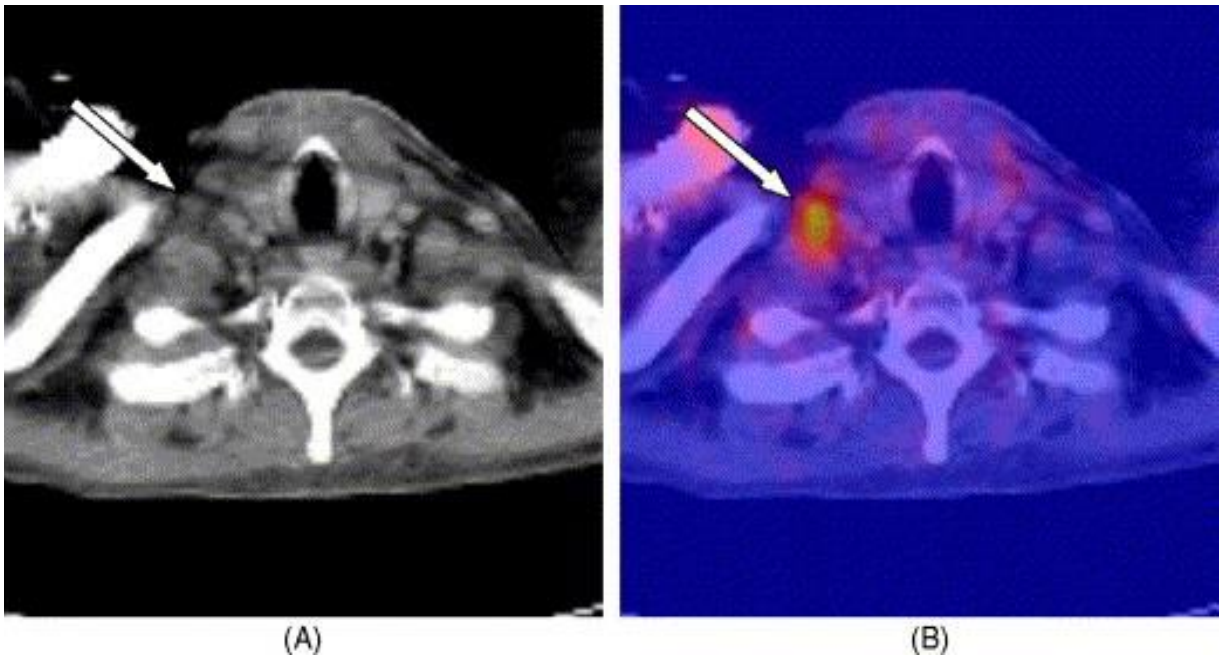

The localisation of tumours can also be improved by the use of intravenous (or oral) contrast agents. If CT is being used as the imaging modality, contrast agents are iodinated. These agents improve the delineation of anatomic structures, especially vascular structures, and improve the accuracy of lesion characterisation (13).

Planning

Once a tumour has been outlined on the primary CT (possibly with reference to other imaging e.g. MRI, PET), the planning process can begin. As well as localising the target, it is important to also localise "Organs at Risk" (OAR), these are the adjacent critical normal body structures that limit the dose that can be safely delivered to target. If safe doses to OARs are not respected the consequence will be increased toxicity of treatment (14). Conformal planning techniques modify the shape of the beam, to match the shape of the tumour, hence decreasing the volume of normal tissue that is irradiated. The beam shape is modified by the use of computer-controlled Multi-Leaf Collimators (MLCs) which are 0.5cm thick and are mounted in the treatment head of the Linear Accelerators (the machines used to deliver MegaVoltage (MV) Radiotherapy). The movement of the MLCs at the time of treatment is pre-specified in the generated radiotherapy plan. The use of MLCs for Conformal radiotherapy delivery represents an advance over previous shaping techniques both in terms of

conformality of treatment, and resources. Previous techniques either employed the straight edges of the jaws in the treatment head (e.g. for a "4-field brick" prostate plan following 2D conventional simulation). Alternatively, custom-made lead alloy blocks were used for beam shaping. This technique had many resource implications as the blocks were time-consuming to make, and there were manual-handling issues as the blocks were heavy (15). In Conformal radiotherapy, the fluence is uniform across the radiation field.

Limitations of conformal radiotherapy

Despite the improvements described above with respect to conformality of treatment with conformal over conventional radiotherapy technique, there are limitations. It is not possible for conformal radiotherapy to cover concave clinical targets such as prostate and seminal vesicles, or thyroid, without irradiating normal tissue contained within the concavity as shown in Figure 3 (page 10).

Conformal radiotherapy has limitations also, in that it does not include any inherent motion management strategies. This means that for tumours such as lung cancer, which are subject to a considerable degree of movement during a treatment fraction, generous CTV to PTV margins are required in order to ensure no geographic miss of target at any stage of the respiratory cycle. The unfortunate consequence of this, however, is that a large volume of normal lung is irradiated.

These limitations have been addressed in more recent advances in radiotherapy, which are discussed subsequently in this chapter.

Figure 3:

Three-dimensional conformal radiotherapy (3D-CRT) plan-showing the isodose distribution for the prostate gland (royal blue outline) and surrounding structures (bladder=pink outline, rectum=yellow outline, femoral heads = red and sky blue outline). The 3D analysis shows the extent of the high-dose area (red shaded area) with regards to covering the prostate and allows an appreciation for the volume of the rectum and bowel within the high-dose area.

Image taken from "Technological advances in radiotherapy for the treatment of localised prostate cancer", Mangar SA et al, European Journal of Cancer 41 (2005) 908–921.

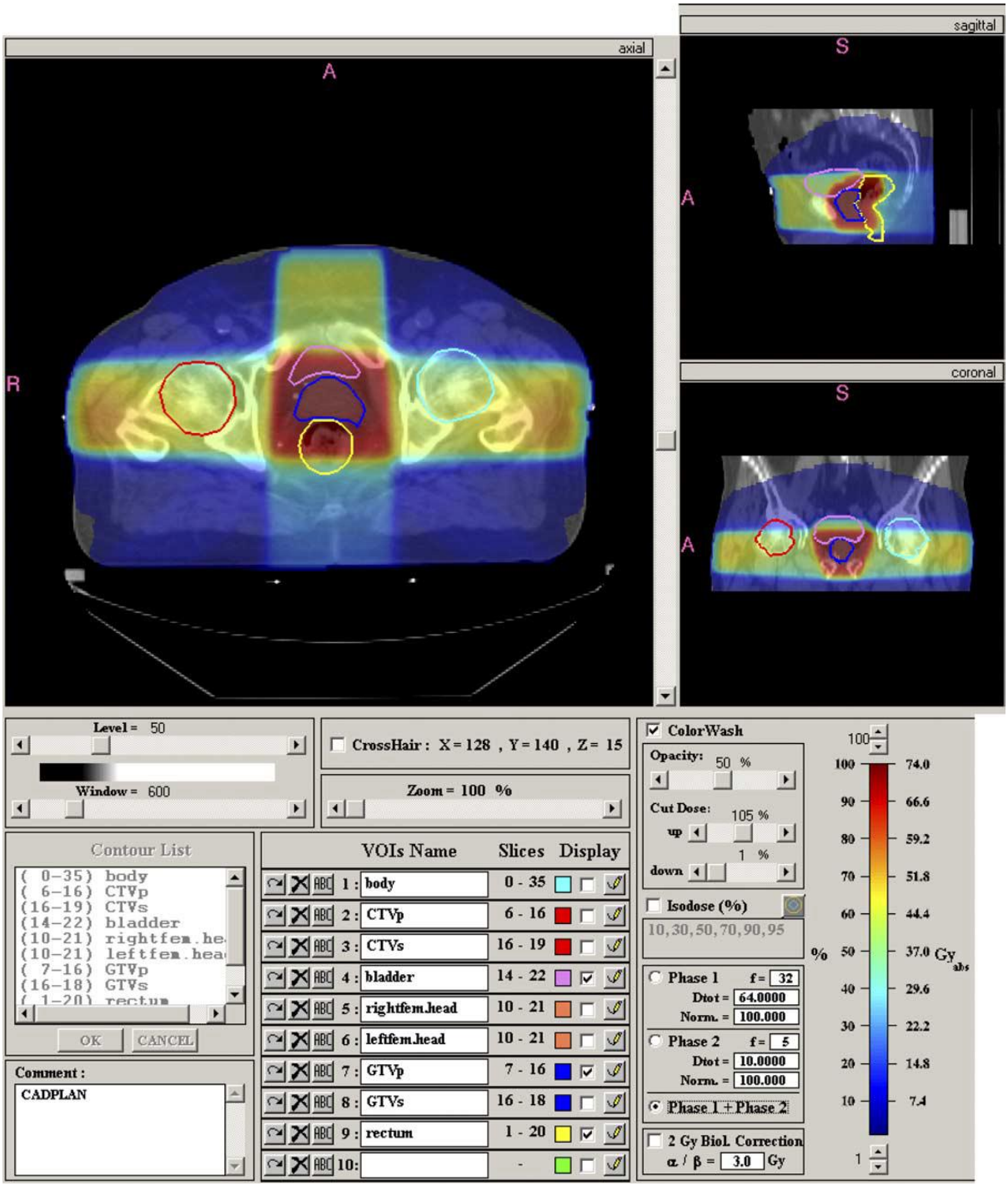

1.1.2 Dose-fractionation issues

Conventionally fractionated radiotherapy involves the delivery of 2Gy in a single fraction each day to tumour. By convention, radiotherapy tends to be delivered on working days, therefore delivery of 5 x 2Gy fractions of radiotherapy per week is standard. The total dose to be delivered to tumour will depend partly on the aim of treatment (radical vs palliative). Other considerations include the radiation sensitivity of the tumour: lymphoma is radio-sensitive and doses of 30-40Gy delivered at 2Gy per fraction can be curative. In contrast, NSCLC would require around 64Gy delivered at 2Gy per fraction to give a possibility of cure. Total dose to the tumour also needs to take account of the nearby Organs At Risk (OARs). Organs At Risk are the normal organs located near the tumour target which may be damaged during exposure to radiotherapy. In practice, it is primarily dose to surrounding OARs that limits the dose that can be safely delivered to tumour targets. Most radical treatments (where the aim of treatment is cure) deliver total doses of radiotherapy on the steep part of the Dose-Response curve as shown in Figure 4 (page 12). This means that if it were possible to refine our radiotherapy technique in order that we could safely minimise irradiation of OARs (without compromising tumour coverage), dose escalation to tumour would be possible, and this would improve tumour control (for an equivalent level of toxicity).

Figure 4:

Typical paired sigmoid dose-response curves for Tumour Control (A) and Normal Tissue Complications (B)

Image taken from "Impact of PET on Radiation Therapy planning in lung cancer", MacManus M et al, Radiologic Clinics of North America, 45 (4) 627-638, 2007.

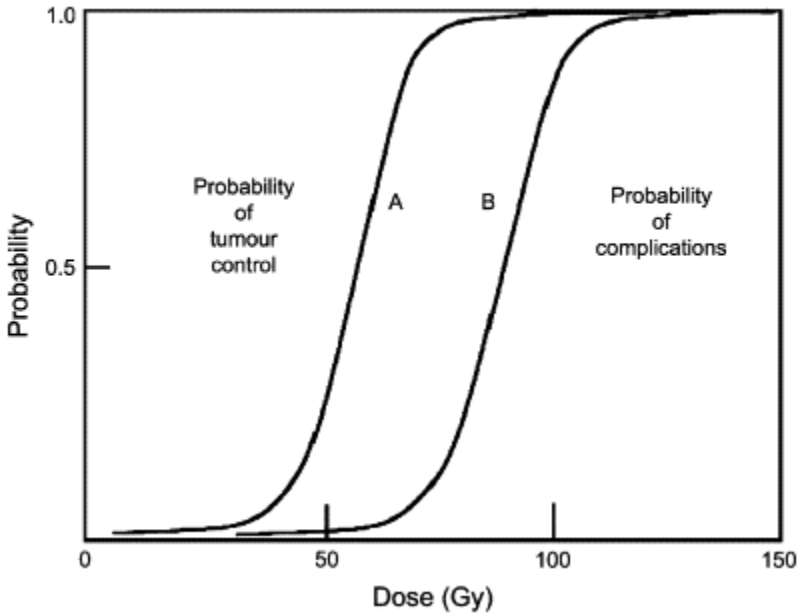

The aim of fractionation (splitting the total radiotherapy dose into multiple 2Gy daily fractions) is to spare late effects of radiotherapy on irradiated normal tissues, more than the tumour. Normal body cells have an ability to repair the DNA damage inflicted by radiotherapy, which is superior to that of tumour cells. Protracting the dose (i.e. giving multiple 2Gy daily doses, rather than a large single fraction of radiotherapy), allows DNA repair to occur, more so in normal body cells than tumour cells.

Fractionation also aims to beat the phenomenon of hypoxia. Hypoxic cells are resistant to radiation. When oxygenated cells are killed by irradiation, the perfusion of previously hypoxic cells is improved, making them more susceptible to radiation-induced cell death on the delivery of the next fraction. See Figure 5 (page 13).

Figure 5:

The mechanism by which Fractionation overcomes Hypoxic Radioresistance.

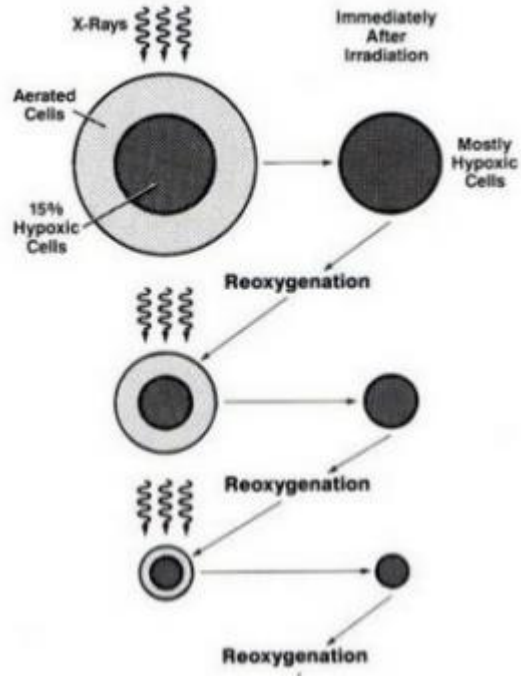

The delivery of radiotherapy at a rate of 2Gy daily fractions, tends to prolong overall treatment time, which is advantageous to limit early (acute) side effects of radiotherapy. The disadvantage of a prolonged overall treatment time, however, is the phenomenon of accelerated repopulation. This is especially relevant for courses of radiotherapy of over 3 weeks. Accelerated repopulation describes the phenomenon whereby as a tumour shrinks with radiotherapy, surviving clonogens proliferate at an accelerated rate (this may have a negative impact on tumour control). A further disadvantage to a prolonged course of radiotherapy, is patient convenience. In fact, some cancer patients do not have the physical stamina required to undergo a course of radical radiotherapy lasting 6 weeks.

Alternative dose/fractionation regimes are discussed later in this Chapter.

1.2 Intensity Modulated RadioTherapy (IMRT)

1.2.1 Treatment planning for IMRT

As described in the previous section, certain tumour targets e.g. thyroid, and prostate and seminal vesicles, cannot be covered with a high degree of conformality due to their complex shape. If a number of beams are brought together around an isocentre, and each beam is of uniform fluence, the volume of intersection of such beams will be convex, and will contain no concavities.

IMRT is an advance compared to 3D conformal radiotherapy. The radiation fluence within any given radiation field can be varied, this enables the 3D high-dose volume to have concavities within it to conform nearly perfectly with the 3D shape of the tumour. The fluence may be varied by using multiple static fields where each segment, shaped by MLCs, contributes to the total treatment (Step and Shoot IMRT). See Figure 6.

Figure 6:

Multiple Static Fields shaped by MLCs (green) to create the desired fluence profile (grey).

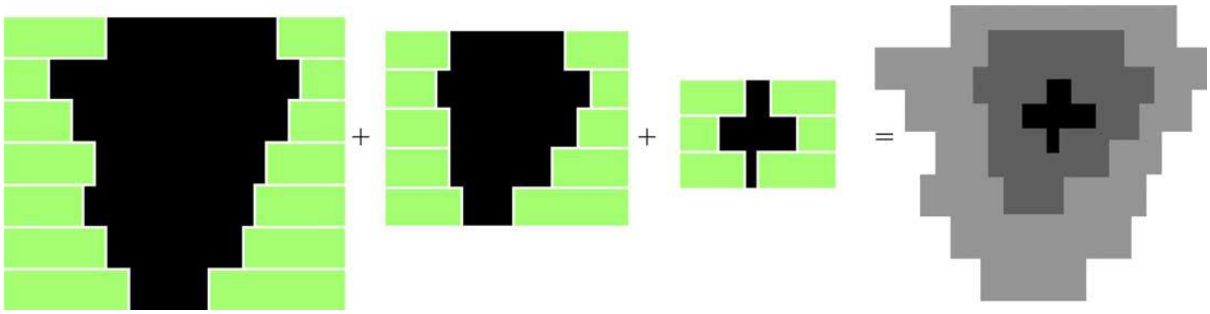

Alternatively, the MLCs can be moved during beam delivery to create the desired fluence profile (Dynamic MLC delivery).

Using either technique IMRT can achieve dose plans where the Target Volume has concavities within it, see Figure 7 (page 15).

Figure 8:

IMRT Dose distribution for pelvic lymph nodes. The high-dose volume (shaded red) has a concavity within it which allows dose to the Bladder to be minimised.

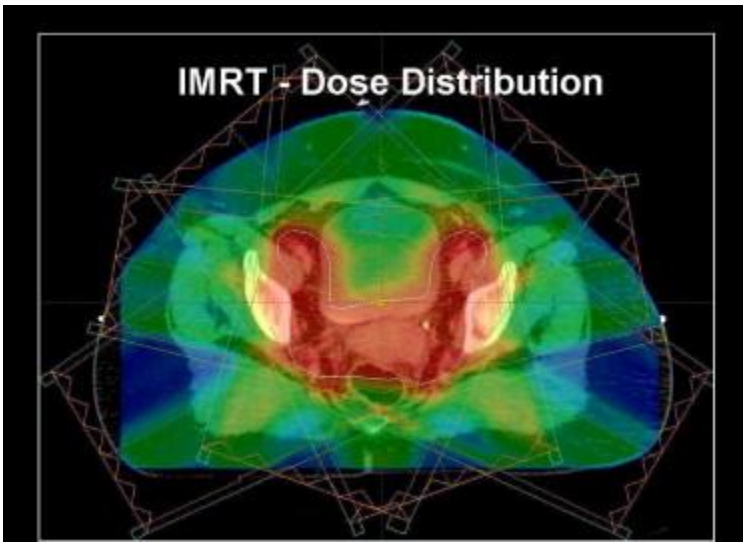

In addition, the ability to vary the fluence within each radiation field enables the production of plans that have optimum dose homogeneity.

Equally, planned dose inhomogeneities can be introduced into a radiotherapy plan in order to match the dose delivered with risk for tumour recurrence (16). This approach is being trialled in the IMPORT-High trial for breast cancer (17).

The desired 3D dose distribution can be reached via either “forward planned” or “inverse planned” techniques. “Forward planning” involves the planner trying a variety of configurations of beams, wedges and beam weightings until a suitable match is found to the dose prescription. Forward planning is possible for some forms of IMRT in which only a few beams will be employed, each with just a few “segments” (which will vary the fluence of each beam) e.g. Breast.

“Inverse planning” requires the planner/oncologist to specify dose-volume constraints and/or dose limits to target and OARs. These specifications drive the planning computer to satisfy the constraints as much as possible. Inverse planning tends to be the preferred planning technique with more complex targets, and where more beams are likely to be needed to create an optimal 3D dose distribution e.g. head and neck target, and prostate/seminal vesicles (18).

IMRT delivery techniques vary. They include (but are not limited to) multiple-static-field MLC technique, dynamic MLC technique (where MLCs will be moving while the beam is turned on) and robotic IMRT.

As the complexity of radiotherapy planning and delivery techniques increases, there is increased potential for a plan to not be delivered as intended. Quality assurance (QA) is therefore especially important for IMRT techniques. An ESTRO report from 2008 gives practical guidance on recommended QA procedures (including phantom measurements and in vivo dosimetry) for departments which deliver IMRT (19).

In summary, the perceived advantage of IMRT is sparing collateral damage to adjacent normal tissues by shaping the high-dose target volume more accurately to the borders of the irregular shaped tumour. Alternatively, for any given dose to the adjacent normal structures, the dose to the tumour may be higher.

1.2.2 Clinical evidence for gain over Conformal radiotherapy.

A number of "planning studies" have shown potential advantages for IMRT planning and delivery, over 3D Conformal radiotherapy. Arbea et al compared these techniques for the treatment of locally advanced rectal cancer (20). Target coverage and normal tissue avoidance were compared using standard planning parameters. Target dose distribution showed greater dose inhomogeneity after IMRT planning. 3D Conformal radiotherapy plans had significantly poorer conformality, as measured by the Conformity Index (CI). The CI is the ratio between the target volume (PTV) and the irradiated volume at specified prescription dose (Vol PTV/Vol IR95%) (21). The V40 (i.e. the volume receiving 40Gy or more) and the D5 (the doses to 5% of the volume) for OARs were significantly lower in the IMRT plans.

However, for a new radiotherapy technique to represent a true clinical gain over its predecessor, the potential dosimetric advantages outlined above should translate into improved toxicity profiles. A new technique should either show equivalent tumour control, with reduced normal tissue toxicity; or improved tumour control with equivalent normal tissue toxicity.

An observational cohort study using data from the SEER-Medicare database compared men over 65 years of age who had received radiotherapy for non-metastatic prostate cancer. A cohort of over 5000 men had received IMRT, whilst a further cohort of over 6000 men had received conformal radiotherapy. The primary outcome measure was bowel complications. IMRT was associated with reductions in composite bowel complications (24-month cumulative incidence, 18.8% vs 22.5% , HR=0.86, 95%CI=0.79-0.83)(22).

Similar clinical gains for IMRT have been demonstrated for Breast (16) and Head and Neck (23) tumour sites.

Overall, having given consideration to the improved dosimetry and clinical gains of IMRT over 3DCRT, the importance of IMRT nationally has been reviewed by the National Radiotherapy Advisory Group (NRAG). NRAG produced a report in 2007 recommending that IMRT should become the standard of care between 2012 and 2017 (2).

1.3 Stereotactic Body Radiotherapy (SBRT)

1.3.1 Definition

This is a form of high-precision radiotherapy delivered to extra-cranial sites characterised by: reproducible immobilisation to avoid patient movement during radiation delivery; measures to account for tumour motion during treatment planning and delivery; dose distributions tightly covering the tumour, with rapid dose fall-off in surrounding normal tissues in order to minimise toxicity; and most importantly, the use of extremely high doses of radiation, usually delivered in 3-5 treatment fractions over a week (24).

CyberKnife (Accuray, Sunnyvale, USA) is an image-guided robotic radiosurgery system purpose-built for delivery of SBRT. A compact 6MV X-band linac is mounted onto a six-joint robotic arm. This provides flexibility in beam pattern generation, allowing the system to produce very conformal non-isocentric treatment plans. A typical CyberKnife plan will utilise 100-250 beams to give optimum conformality. Whilst conformality is clearly important, a CyberKnife planner and their Clinical Oncologist must always weigh up the clinical gains of conformality against the inconvenience to the patient of longer treatment times (which can be over an hour for CyberKnife vs <10mins for 3DCRT). The CyberKnife system also features a robotic couch with six degrees of freedom and near real-time kV image guidance (25) .

The technique represents a step forward as “body” (extra-cranial) tumour sites can now be treated with hypofractionated radiotherapy to a radical dose, over a short overall treatment time, with an acceptable toxicity profile, and excellent rates of tumour control.

1.3.2 Key Components

Immobilisation

The immobilisation which is most appropriate depends on the target site and the SBRT delivery system which is being used.

Certain target sites (e.g. lungs) are more difficult to immobilise than others (e.g. spine).

A further consideration as to the degree of immobilisation that is required, is the image guidance system that is available (i.e. Real-time tracking vs. Cone-beam CT pre-treatment fraction).

Immobilisation for SBRT treatments is often achieved with the use of a vacuum-formed personalised immobilisation device (Vacbag). A treatment position must be chosen that the patient can comfortably maintain for the duration of treatment. Consideration should also be given to arm position, as well as supine vs. prone, to allow the optimum range of beam angles to treat tumour, without passing through unnecessary non-target tissue e.g. arms, and without being constrained by the treatment couch. (The CyberKnife system does not allow beams to enter through the treatment couch).

Tumour motion

Irrespective of the SBRT system being used, it is imperative that tumour motion can be accurately evaluated and accounted for, in order to avoid geographical miss. This is especially critical for tumours which are subject to respiratory motion e.g. thoracic, pancreatic, and hepatic tumours. Some SBRT systems can track such targets (e.g. Cyberknife, using the Synchrony system, see Section 1.3.6). Others are capable of gated delivery, i.e. the delivery of radiation only at certain pre-defined phases of the respiratory cycle (e.g. Gated RapidArc). All systems require appropriate CTV to PTV expansions.

The functions of the different commercially available SBRT system are discussed in Section 1.3.3.

1.3.3 SBRT Treatment Delivery Systems

A number of modern Linear Accelerators (linacs) with on-board imaging capabilities meet the basic image guidance requirements for delivering SBRT, e.g. Varian Trilogy: RapidArc (Varian Medical Systems, Palo Alto, CA, USA) and Elekta Synergy (Elekta, Stockholm, Sweden). A micro MLC can be added to produce the required degree of conformality for stereotactic plans.

Newer developments include fully-integrated SBRT delivery systems. Novalis TX has a Varian Trilogy linac base with micro (2.5mm) MLC. This system incorporates the BrainLAB "ExacTrac X-ray 6D" system, which provides near real-time image guidance with six degrees of freedom, and a corresponding robotic treatment couch with associated software (BrainLAB, Munich, Germany). The TrueBeam (Varian) and Elekta Axesse are similar integrated systems.

The TomoTherapy Hi-Art System (TomoTherapy, Madison, WI, USA) has a ring gantry as used in diagnostic CT scanners and delivers helical IMRT via thousands of small beamlets. The system has on-board image guidance with megavoltage CT.

CyberKnife (Accuray, Sunnyvale, CA, USA) is an image-guided robotic radiosurgery system. The system was outlined in Section 1.3.1 (page 17). Treatment delivery is guided by 2 orthogonal X-ray sources mounted in the ceiling of the CyberKnife room, these cameras are orientated to point at the imaging centre of the room and X-Rays are received by plates in the floor of the room. See Figure 9 (page 20). Extra-cranial, non-spine treatments are largely guided by fiducial tracking, because soft tissue tumours tend to be poorly visualised on the X-ray based image guidance system. Fiducials are gold markers implanted in or around tumour, which act as a surrogate for tumour position.

A key advantage of the CyberKnife system is the Respiratory Tracking System: Synchrony™. This is a hybrid tracking system for lung tumour targets, and tumours that will move with respiratory motion. The system tracks tumour movements with 2 methods: a) Light Emitting Diodes (LEDs) that are placed on the patient's upper abdomen. 3 cameras (see Figure 9, page 20) continually track the LEDs, b) Live X-rays taken of the tumour with implanted fiducial surrogates. This information is fed into the Synchrony system and a breathing "model" of the patient's breathing is created, which is used to allow the CyberKnife to accurately target treatment beams to a moving tumour (26).

Figure 9: An image to demonstrate the CyberKnife Treatment Delivery System.

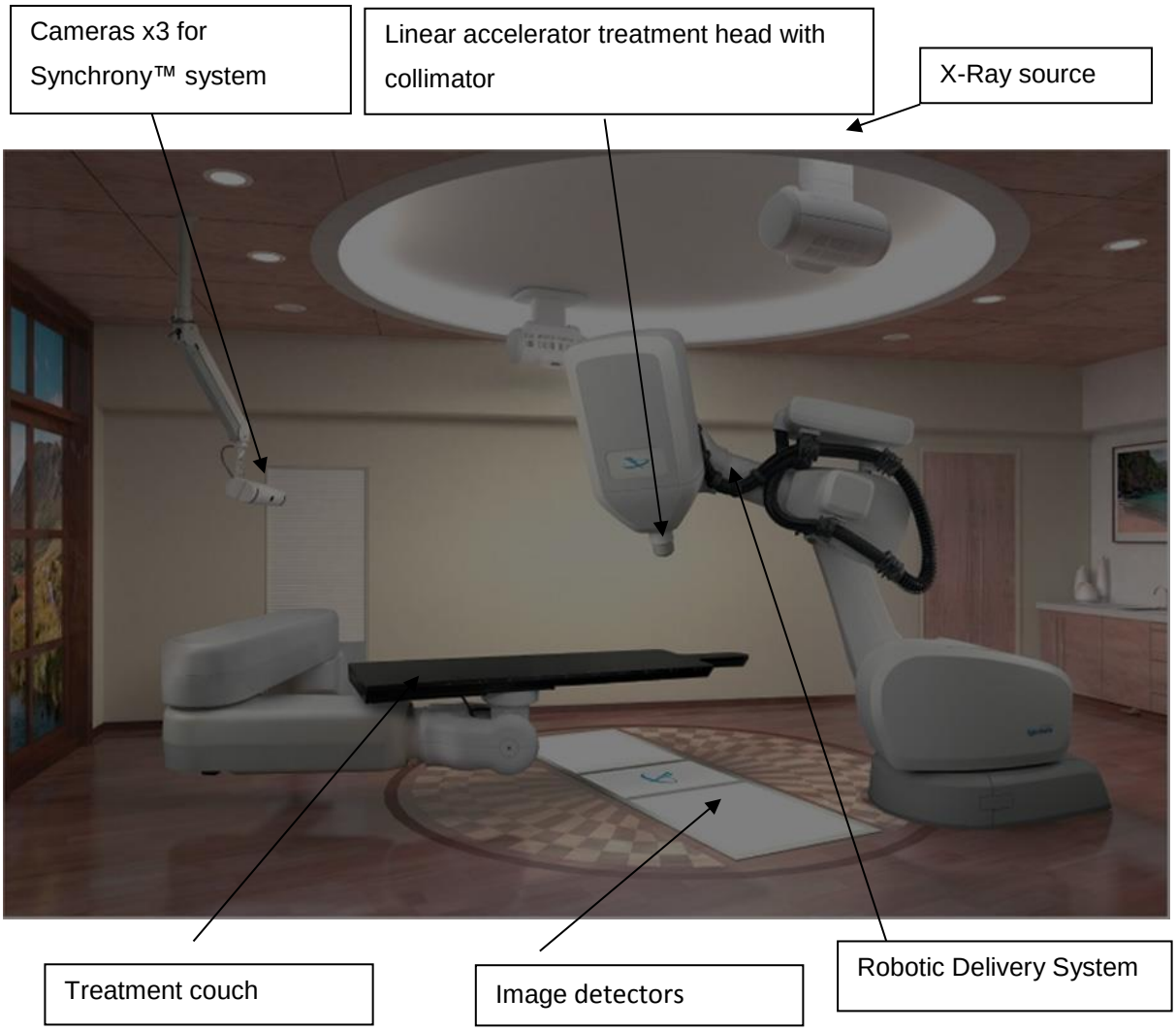

1.3.4 Conformality

As SBRT delivers an ablative dose to the target, it is essential that the target is covered with a high degree of conformality, with a sharp dose fall-off in the surrounding normal tissues. This can be achieved due to complex inverse-planning computer systems, as always, guided by physicists and planning radiographers to achieve the desired dose-distribution. Depending on the SBRT system being used, the IMRT delivery techniques described in section 1.2 can help to achieve the required

degree of conformality. In addition, the ability to deliver non-coplanar, non-isocentric beams can also help to achieve optimum conformality. See Figure 10 (page 21).

Whilst optimum conformality is critical in SBRT, there are a number of caveats to this approach. Given the tight GTV to PTV margins that are applied with this technique, it is absolutely critical that target delineation is accurate. This technique is potentially vulnerable to geographical target miss (with possible consequences of reduced tumour control and/or increased normal tissue toxicity) if there are errors in target localisation, or in treatment delivery.

Figure 10:

A CyberKnife treatment plan, (CT scan: axial slice), for treatment of a primary lung tumour. A fiducial can be seen (arrowed) in the tumour. The thick green line is the isodose prescription line. The key in the top right hand corner of the image gives a scale for the isodoses (in cGy). The plan shows a sharp fall-off in dose with distance from the tumour.

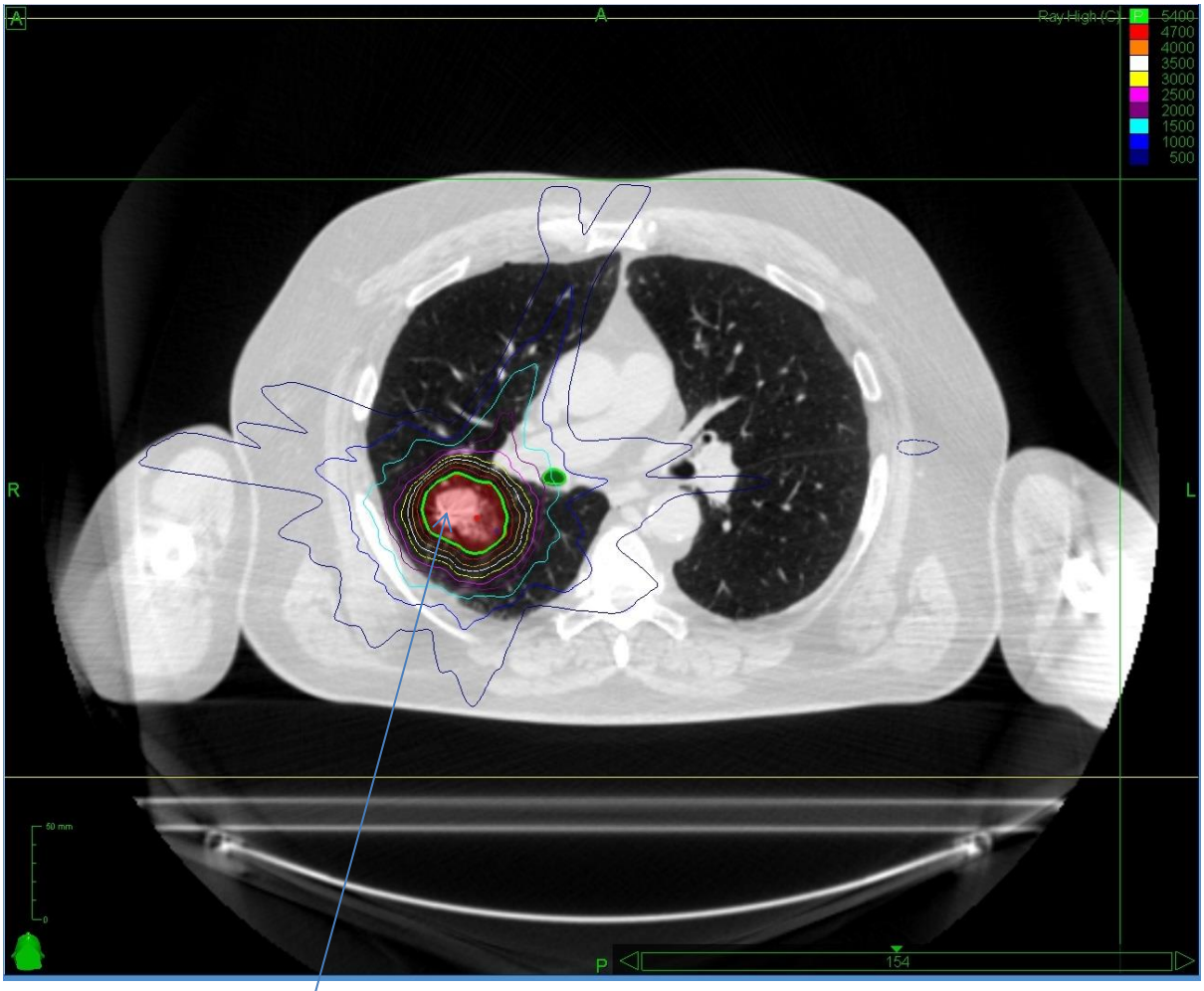

1.3.5 Dose-fractionation issues

As described in section 1.1.2, conventionally fractionated conformal radiotherapy delivers 2Gy per fraction to the tumour volume, together with a margin to account for inaccuracies of planning, set-up and delivery. Total dose will vary according to the intrinsic radiation sensitivity of the tumour, as well as the radiation tolerance of the adjacent organs at risk. The therapeutic benefit achieved with this dose fractionation has been appreciated for over 100 years, and clinical experience of the effects of this fractionation on both tumour, and normal tissues, has been accumulating over this time period. The development of radiobiological concepts such as the linear quadratic model (27) and the "4 R's" of radiotherapy (Repair, Reassortment, Repopulation, and Reoxygenation)(28), as well as key clinical observations, have led to further understanding of the tissue effects of fractionation. The radiotherapy community has accumulated a considerable body of evidence of "safe" dose limits to organs at risk when conventional fractionation is employed (14, 29).

Conformality was known to be an important goal even in 1938 (30), although the necessary technical advances to achieve the desired conformality followed many years later. Dose homogeneity delivered to the target was also considered an important principle. The ICRU 50 report recommended that the target is covered with a homogenous dose, i.e. -5% to +7% of the prescription dose (3). The aim of radiotherapy has always been to damage every single potentially malignant cell to such an extent that it cannot continue to proliferate, and it is known that increasing total dose makes this more likely (31). However, this has to be weighed up against expected normal tissue toxicity.

In practice, conventionally fractionated radiotherapy delivers a total dose to tumour which aims to prevent proliferation, whilst staying within "safe" dose constraints to nearby organs at risk.

In contrast, the dose fractionation regimes employed in SBRT represent a departure from conventional dose fractionation. Large doses per fraction (e.g. >8 Gy/#) are delivered with the aim of ablating all tissue within the PTV. A moderate internal dose gradient is achieved, as SBRT is typically prescribed to a prescription isodose of 60-80%. This creates considerable dose inhomogeneity within the target volume, certainly beyond that which is recommended in the ICRU 50 report. However, there is some evidence to suggest that carefully planned target dose inhomogeneity may enhance the tumoricidal effect (32).

Whilst the potential benefits of ablative radiotherapy can be appreciated in terms of improved tumour control, there are also potential risks.

Extra-cranial sites can be prone to significant inter- and intra-fraction movement of both tumour, and organs at risk. As previously explained, this increases the risk of tumour miss, and increases the risk of irradiating normal tissue to ablative doses.

Another note of caution is that the overwhelming experience with treating extra-cranial sites is with conventional dose fractionation. There is concern, also, that the linear quadratic (LQ) model (which is used by Clinical Oncologists to predict tissue response to altered fractionation regimes), may not accurately predict cell response at the higher doses per fraction used in SBRT regimes (33).

As a consequence of these uncertainties, there is wide variation in the SBRT dose fractionation regimes employed. Current SBRT regimens have largely been based on cautious dose escalation in Phase I clinical trials (34), (35),(36).

The radiation schedules used in SBRT cannot be directly compared with those used in conventional radiotherapy, as explained, because the dose per fraction is different. To compare the regimes, therefore, Biologically Effective Dose (BED) must be calculated (37). To take primary lung cancer as an example, conventionally fractionated schedules delivered with curative intent e.g. 64Gy/32#, or 70Gy/35#, typically have a BED of 70-80Gy. These schedules are associated with a disappointing Overall Survival rate of 34% at 3 years (38). In contrast, modern SBRT schedules use doses equivalent to a BED>100Gy, and a frequently used schedule for peripheral lung tumours is 20Gy x 3 which delivers a BED as high as 180Gy (34). These high-BED regimes result in superior tumour cell kill, and superior tumour control to conventional fractionation. The RTOG 0236 was a Phase II multi-centre trial of SBRT for early stage NSCLC treating to 18Gy x 3 over 1.5 - 2 weeks. Estimated 3-year primary tumour control rate was impressive at 97.6%. Treatment was reasonably well tolerated (39).

1.4 Summary

There has been a paradigm shift in recent years in the radical radiotherapy treatment of cancer (i.e. treatment with curative intent).

For over 60 years, the radiotherapy community has been delivering 2Gy/#, treating 5 days a week, to a "radical" total dose. In practice, the total dose prescribed would be a dose considered to have a reasonable prospect of cure (or long-term local control), whilst also having an acceptable toxicity profile.

There were concerns that increasing the dose per fraction over 2Gy/# could increase especially the late effects of radiotherapy.

A number of recent advances in radiotherapy, however, have enabled the safe delivery of SBRT regimes, which deliver a high dose per fraction, and a high BED. These high-BED regimes achieve excellent rates of tumour control.

SBRT marks a step change in radiotherapy delivery. Whilst the benefits of this new approach can be appreciated, further developments are required to optimise effective dose delivery to tumour, and protect normal tissue.

1.5 **Aims of this Research:**

1. To assess if the imaging and interpretation of fiducial position by the CyberKnife in-room imaging system is accurate and appropriate.

   I will create an experimental system that will utilise a solid water phantom with 3 fixed, and 1 migrating, fiducials. I will rigorously assess the ability of the CyberKnife imaging system to accurately identify and analyse fiducial position and migration.

   (Chapter 2)

2. To evaluate whether the "Rigid Body Geometry" of fiducial arrangement, which is established at the time of planning CT, is maintained at the time of treatment?

   The accuracy of fixed fiducial tracked treatments is critically dependent on the assumption that there is "Rigid Body Geometry" i.e. that fiducial position will be identical at time of planning CT and at the time of Treatment CT.

   I will assess the magnitude of any fiducial movement between Planning and Treatment CT scans, in a range of body sites, evaluating the clinical scenarios and fiducial positions associated with the highest probability of fiducial migration. My analysis will inform advice to be given on optimal fiducial placement to minimise risks of migration.

   (Chapter 3)

3. To develop bladder filling guidelines for Radiotherapy and CyberKnife patients, based on optimal dosimetry and reproducibility.
   To determine the relationship between the consistency of bladder filling (between planning and treatment), and the ability to track rotations of the tumour target for the CK treatment of prostate cancer.
   (Chapter 4)

4. To explore uncertainties in treatment planning/delivery for CK prostate patients, and to calculate ideal planning margins for the CK treatment of localised prostate cancer.

   (Chapter 5)

5. To perform a radiobiological comparison between a conventional radiotherapy schedule and SBRT schedule for the treatment of localised pancreatic cancer.
   To analyse the outcome of SBRT to lymph node oligometastases according to delivered Biologically Effective Dose (BED).
   To evaluate the outcome of SBRT to oligometastatic breast cancer according to delivered BED.
   (Chapter 6)

References:

1. Driver D, Dobbs HJ. Improvements in radiotherapy practice: the impact of new imaging technologies. Cancer Imaging. 2004;4(2):142-50.
2. NRAG. Radiotherapy - developing a world class service for England. Report to Ministers. 2007.
3. ICRU. International Commission on Radiation Units and Measurements Report 50: Prescribing, Recording and Reporting Photon Beam Therapy. ICRU Reports. 1993;50.
4. ICRU. Prescribing, Recording and Reporting Photon Beam Therapy. Report 62. 1999.
5. Tanaka H, Hayashi S, Ohtakara K, Hoshi H, Iida T. Usefulness of CT-MRI fusion in radiotherapy planning for localized prostate cancer. J Radiat Res. 2011;52(6):782-8.
6. Sannazzari GL, Ragona R, Ruo Redda MG, Giglioli FR, Isolato G, Guarneri A. CT-MRI image fusion for delineation of volumes in three-dimensional conformal radiation therapy in the treatment of localized prostate cancer. Br J Radiol. 2002;75(895):603-7.
7. Ashamalla H, Rafla S, Parikh K, Mokhtar B, Goswami G, Kambam S, et al. The contribution of integrated PET/CT to the evolving definition of treatment volumes in radiation treatment planning in lung cancer. Int J Radiat Oncol Biol Phys. 2005;63(4):1016-23.
8. Deniaud-Alexandre E, Touboul E, Lerouge D, Grahek D, Foulquier JN, Petegnief Y, et al. Impact of computed tomography and 18F-deoxyglucose coincidence detection emission tomography image fusion for optimization of conformal radiotherapy in non-small-cell lung cancer. Int J Radiat Oncol Biol Phys. 2005;63(5):1432-41.
9. Visioni A, Kim J. Positron emission tomography for benign and malignant disease. Surg Clin North Am. 2011;91(1):249-66.
10. De Ruysscher D, Kirsch CM. PET scans in radiotherapy planning of lung cancer. Radiother Oncol. 2010;96(3):335-8.
11. Padma S, Sundaram PS, George S. Role of positron emission tomography computed tomography in carcinoma lung evaluation. J Cancer Res Ther. 2011;7(2):128-34.
12. Pysz MA, Gambhir SS, Willmann JK. Molecular imaging: current status and emerging strategies. Clin Radiol. 2010;65(7):500-16.
13. Antoch G, Freudenberg LS, Beyer T, Bockisch A, Debatin JF. To enhance or not to enhance? 18F-FDG and CT contrast agents in dual-modality 18F-FDG PET/CT. J Nucl Med. 2004;45 Suppl 1:56S-65S.
14. Marks LB, Ten Haken RK, Martel MK. Guest Editor's Introduction to QUANTEC: A Users Guide. International Journal of Radiation Oncology • Biology • Physics.76(3):S1-S2.
15. LoSasso T, Kutcher GJ. Multileaf collimation versus alloy blocks: analysis of geometric accuracy. Int J Radiat Oncol Biol Phys. 1995;32(2):499-506.
16. Donovan E, Bleakley N, Denholm E, Evans P, Gothard L, Hanson J, et al. Randomised trial of standard 2D radiotherapy (RT) versus intensity modulated radiotherapy (IMRT) in patients prescribed breast radiotherapy. Radiother Oncol. 2007;82(3):254-64.
17. Coles C, Yarnold J. The IMPORT trials are launched (September 2006). Clin Oncol (R Coll Radiol). 2006;18(8):587-90.
18. Webb S. The physical basis of IMRT and inverse planning. Br J Radiol. 2003;76(910):678-89.
19. al Ae. Guidelines for the Verification of IMRT. ESTRO report. 2007.
20. Arbea L, Ramos LI, Martinez-Monge R, Moreno M, Aristu J. Intensity-modulated radiation therapy (IMRT) vs. 3D conformal radiotherapy (3DCRT) in locally advanced rectal cancer (LARC): dosimetric comparison and clinical implications. Radiat Oncol. 2010;5:17.
21. Knoos T, Kristensen I, Nilsson P. Volumetric and dosimetric evaluation of radiation treatment plans: radiation conformity index. Int J Radiat Oncol Biol Phys. 1998;42(5):1169-76.
22. Bekelman JE, Mitra N, Efstathiou J, Liao K, Sunderland R, Yeboa DN, et al. Outcomes after intensity-modulated versus conformal radiotherapy in older men with nonmetastatic prostate cancer. Int J Radiat Oncol Biol Phys. 2011;81(4):e325-34.
23. Chen AM, Farwell DG, Luu Q, Vazquez EG, Lau DH, Purdy JA. Intensity-modulated radiotherapy is associated with improved global quality of life among long-term survivors of head-and-neck cancer. Int J Radiat Oncol Biol Phys. 2012;84(1):170-5.
24. Kavanagh BD, McGarry RC, Timmerman RD. Extracranial radiosurgery (stereotactic body radiation therapy) for oligometastases. Semin Radiat Oncol. 2006;16(2):77-84.

25. Martin A, Gaya A. Stereotactic body radiotherapy: a review. Clin Oncol (R Coll Radiol). 2010;22(3):157-72.
26. Pepin EW, Wu H, Zhang Y, Lord B. Correlation and prediction uncertainties in the CyberKnife Synchrony respiratory tracking system. Medical Physics. 2011;38(7):4036-44.
27. Fowler JF. The linear-quadratic formula and progress in fractionated radiotherapy. Br J Radiol. 1989;62(740):679-94.
28. F P, E V, WH M. Radiation resistance of cancer stem cells: The 4 R's of Radiobiology revisited. Stem Cells. 2010;28(4):639-48.
29. Emami B, Lyman J, Brown A, Coia L, Goitein M, Munzenrider JE, et al. Tolerance of normal tissue to therapeutic irradiation. Int J Radiat Oncol Biol Phys. 1991;21(1):109-22.
30. Praestholm J. [Producing the third dimension of flat radiographic images: analogue tomography - computer tomography]. Dan Medicinhist Arbog. 1995:122-44.
31. Munro TR, Gilbert CW. The relation between tumour lethal doses and the radiosensitivity of tumour cells. Br J Radiol. 1961;34:246-51.
32. Tome WA, Fowler JF. Selective boosting of tumor subvolumes. Int J Radiat Oncol Biol Phys. 2000;48(2):593-9.
33. Guerrero M, Li XA. Extending the linear-quadratic model for large fraction doses pertinent to stereotactic radiotherapy. Phys Med Biol. 2004;49(20):4825-35.
34. McGarry RC, Papiez L, Williams M, Whitford T, Timmerman RD. Stereotactic body radiation therapy of early-stage non–small-cell lung carcinoma: Phase I study. International Journal of Radiation Oncology • Biology • Physics.63(4):1010-5.
35. Schefter TE, Kavanagh BD, Timmerman RD, Cardenes HR, Baron A, Gaspar LE. A phase I trial of stereotactic body radiation therapy (SBRT) for liver metastases. Int J Radiat Oncol Biol Phys. 2005;62(5):1371-8.
36. Koong AC, Le QT, Ho A, Fong B, Fisher G, Cho C, et al. Phase I study of stereotactic radiosurgery in patients with locally advanced pancreatic cancer. Int J Radiat Oncol Biol Phys. 2004;58(4):1017-21.
37. Fowler J, Tome W, Fenwick J, Mehta M. A challenge to traditional radiation oncology. Int J Radiat Oncol Biol Phys. 2004;60:1241 - 56.
38. Qiao X, Tullgren O, Lax I, Sirzén F, Lewensohn R. The role of radiotherapy in treatment of stage I non-small cell lung cancer. Lung Cancer.41(1):1-11.
39. Timmerman R, Paulus R, Galvin J, Michalski J, Straube W, Bradley J, et al. Stereotactic Body Radiation Therapy for Inoperable Early Stage Lung Cancer. JAMA : the journal of the American Medical Association. 2010;303(11):1070-6.

Chapter 2

Fixed fiducial tracking in a phantom: an experimental model

2.1. INTRODUCTION

Stereotactic Body Radiotherapy (SBRT) requires a robust system for tracking accuracy.

Non-spine/Brain SBRT treatments delivered by the CyberKnife system are tracked by the use of fiducials.

Fiducials are radio-opaque markers e.g. gold seeds, which are inserted in, or close to, tumour. They act as surrogates for tumour position and can be imaged by the integral in-room KV imaging system. There are a number of fiducial placement criteria which must be fulfilled in order to achieve optimum fiducial tracking accuracy. Ideally 3 - 6 fiducials are placed in or around the tumour, with a minimum of 2 cm spacing between fiducials to minimise uncertainty in measuring rotation. A minimum of 3 fiducials, ideally located in more than one axial plane, is required to track rotations. The fiducials should be placed no more than 5 -6 cm from the target lesion. This is firstly in order that the fiducials can all be captured on the Field of View (FOV) for live images of the CyberKnife treatment consoles, which measure 20cm x 20cm. In addition, the greater the distance between a fiducial and tumour, the greater the risk of disparity between fiducial position and true tumour position. There must also be at least a 15° angle between any grouping of 3 fiducials i.e. they must not be collinear (1).

Fiducial tracking is the primary tracking option for treating any soft tissue tumours where it is not possible to use bony structures for reference. The technique was explored in detail by Kitamura et al (2). The aim of fiducial tracking is to find the relative translation and rotation (6D transformation including roll, pitch and yaw) between the patient position on the treatment couch, and that of the Computed Tomography (CT)-planning scan. The fiducial tracking procedure implicitly assumes that the geometry in the planning CT scan (which establishes the relative position of the fiducials to the tumour), is reproduced on the day of treatment i.e. there is an assumption that there is Rigid Body Geometry (3).

The fiducial tracking method is often considered the "gold standard" in performance evaluation of other registration algorithms (4). The CyberKnife system uses the Concurrent Viterbi with Association (CVA) algorithm to track fiducials. The algorithm relies partially on analysis from DRRs (from the Planning CT). The algorithm then locates the fiducials at the time of treatment in additional steps.

The fiducial tracking flowchart is shown below (Figure 1):

Figure 1*:* Fiducial tracking flowchart

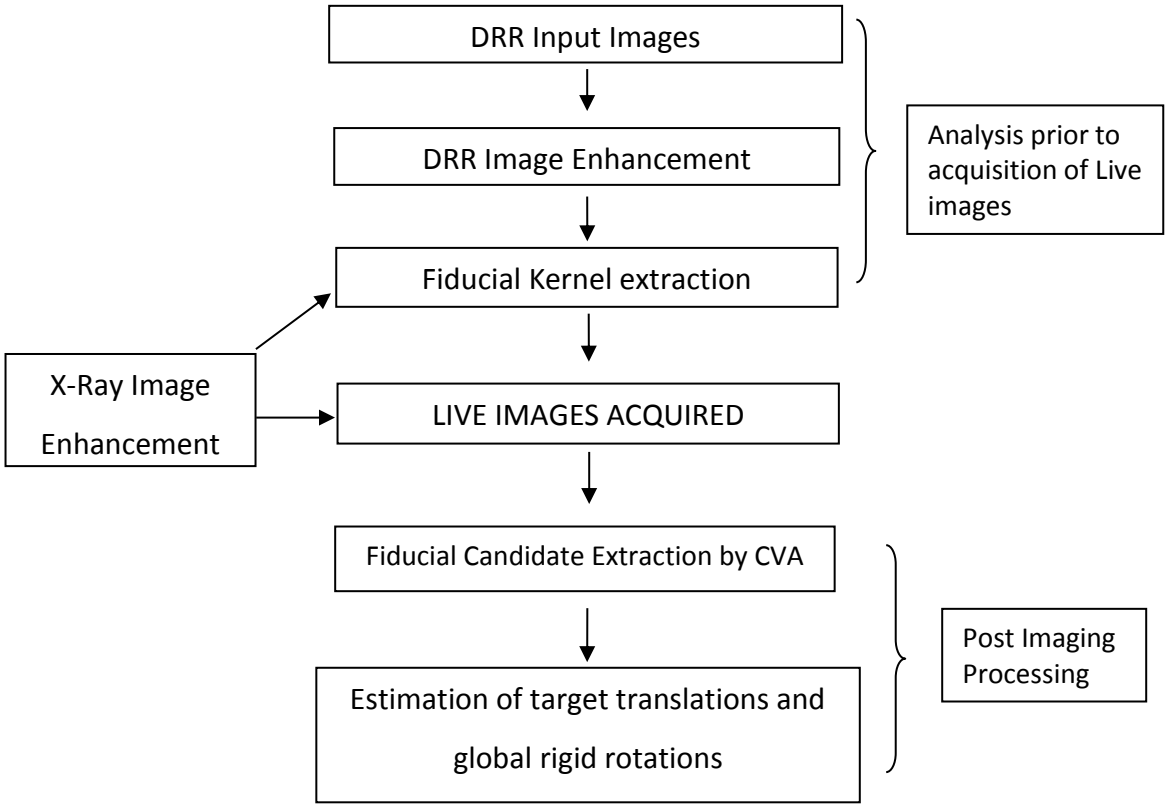

The fiducial tracking algorithm works on prior knowledge (DRRs from the Planning CT) of 4 key criteria:

1. Number of fiducials.
2. Size of the fiducials.
3. Location of the fiducials.
4. "X" axis point will be the same in both cameras.

The DRR's are reviewed first in a process called "Bandpass filtering" (BPF). The images are filtered once to remove "features" smaller than a threshold size (which is just below the size of one fiducial). The images are then filtered to remove "features" smaller than another threshold (which is just above the size of one fiducial). By subtracting these two the system gets an image containing "features" with a size comparable to one fiducial (5). See Figure 2A and 2B. Figures 2A-4 are taken from Hatipoglu et al (5).

Figure 2A: DRR image showing 5 implanted fiducials before BPF (Images from Hatipoglu et al)

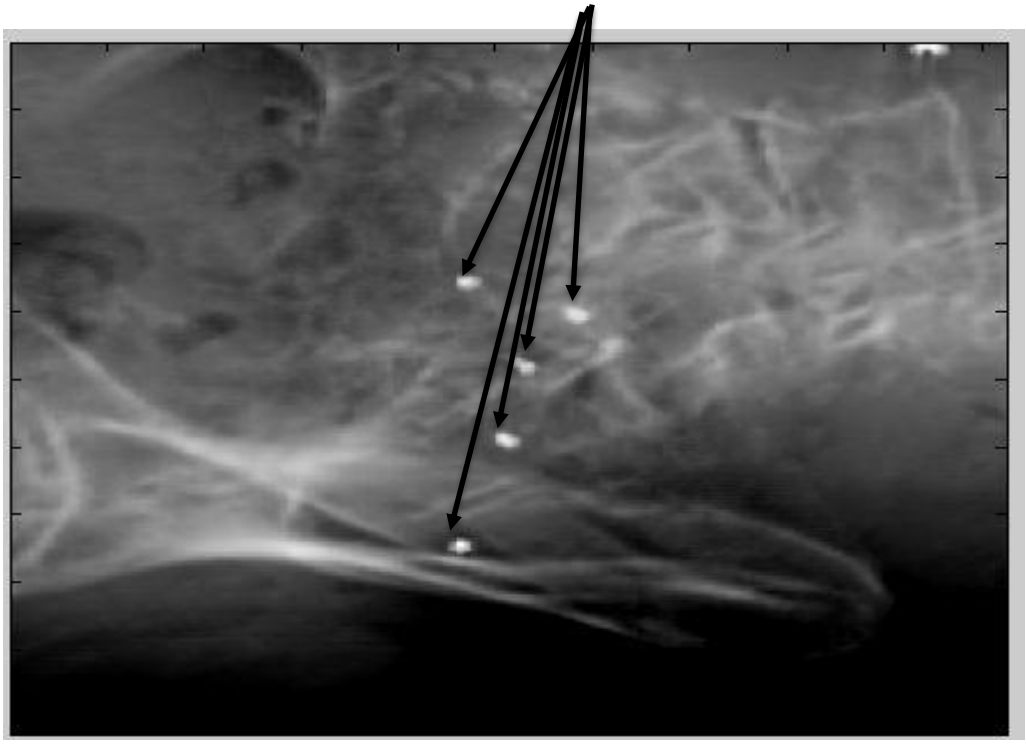

Figure 2B: DRR image after BPF: Implanted fiducials can now be seen more clearly.

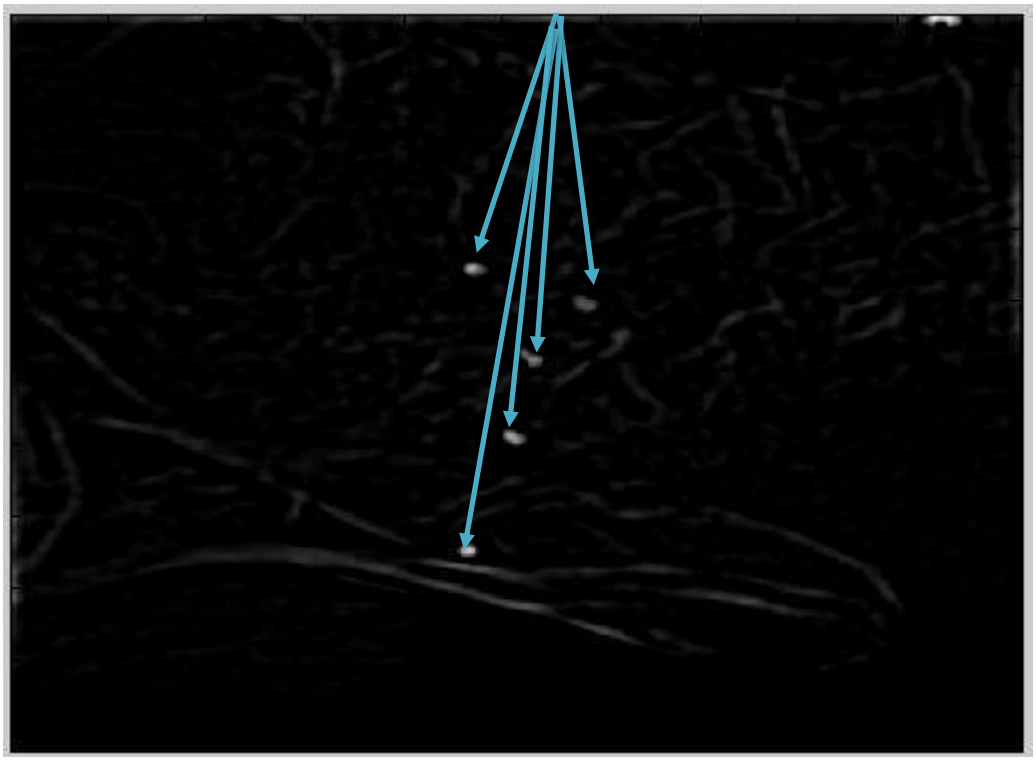

The next step is Fiducial kernel extraction. Fiducial "kernels" are extracted from the DRR's. The location of each fiducial in the Planning CT is known so the system knows which part of the image to use as a kernel. The DRR's are then enhanced to capture the kernel as a miniature image with the kernel displayed as white, with a small surrounding area of black. The purpose of this step is to isolate the fiducial(s) and to eliminate "noise". See Figure 3 below.

Figure 3*:*

Fiducial kernel extraction has identified fiducial kernels for finding candidates in the Live images

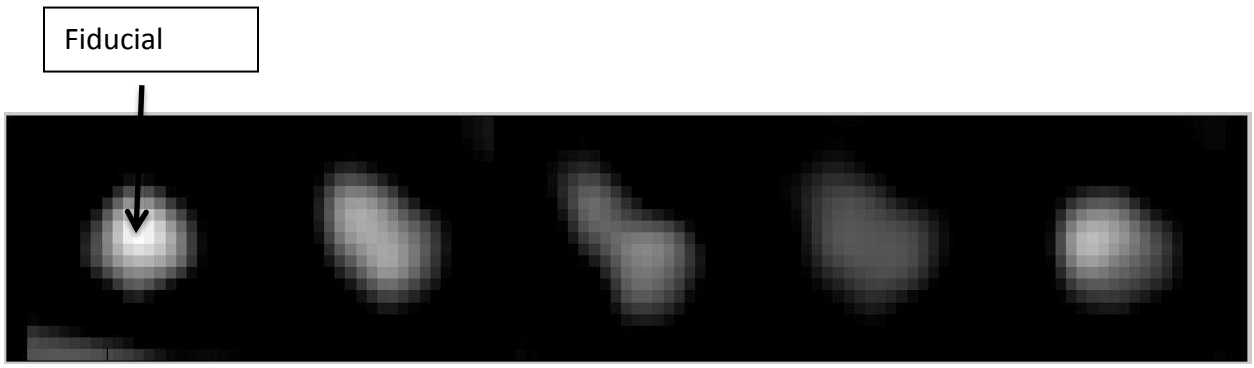

"Live" images are then acquired at the time of treatment. The two in-room X-Ray imagers capture orthogonal patient projections in the region of interest. This step needs to be sensitive and avoid missing any potential fiducials, many hundreds of "candidate" fiducials are detected in this step. Candidate maps are generated (one map for each fiducial) by comparing each kernel from the enhanced DRR with the enhanced live images. See Figure 4 below.

Figure 4*:*

Candidate maps for each fiducial

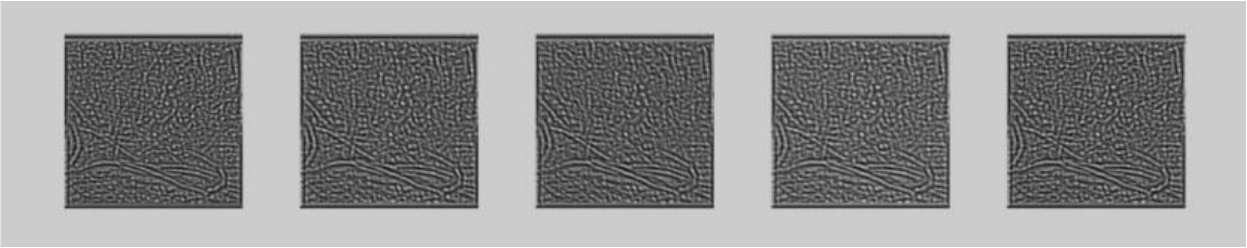

The next step is image correlation. The imaging system looks for focal areas of radio-intensity. The likelihoods of "candidates" for each fiducial on the orthogonal patient projections are then updated. The next step involves calculating the association likelihoods of candidates for the same fiducial in the two images (as a fiducial's x-axis position is identical, or almost identical, in the paired images this helps the system to accurately identify a fiducial). The probability of a fiducial candidate being an actual fiducial also depends partly on it being an "expected" (expected from DRR) distance away from other fiducials.

Finally, the likelihoods of candidates in each image are updated again with the association likelihoods. In this way, the algorithm converges on the "candidate of maximum likelihood" for each fiducial in the paired images. The "candidates of maximum likelihood" generated, should represent the true fiducials. The "success rate" of this algorithm is reported by Accuray Inc to be >99%. The accuracy was tested by reviewing a collection of images from more than 35 patient treatments with 3 fiducials in situ, and more than 10,000 image pairs (5).

As described, SBRT delivers hypofractionated, high BED, ablative doses of radiotherapy to the tumour target, with acceptable levels of toxicity. The fiducial tracking process is complex as described above. At the time of treatment delivery issues related to fiducial tracking can cause treatment delivery to be interrupted until specific interventions are made. It is important that radiographers are given adequate guidance so that the interventions applied are appropriate to the specific clinical situation.

It is critical that fiducial tracking is accurate, if not there are significant potential consequences: decreased tumour control and/or increased toxicity.

I will investigate the accuracy of the fiducial tracking process in phantom and clinical models.

2.2 AIM

Is the imaging and interpretation of fiducial position by the CK in-room imaging system accurate and appropriate in a Phantom model?

2.3 METHODS AND MATERIALS

Assessment was made of fiducial tracking in a phantom model, this was felt to be more comparable to a clinical situation than analysis of fiducial tracking by computer modelling (as reported by Murphy in the literature (6)).

It was thought to be important to analyse the interpretation of both static and migrating fiducials as this would more closely represent "real-life" clinical scenarios. An experimental system was therefore designed with 3 fixed (static) fiducials and 1 migrating fiducial.

Importantly, Accuray, the manufacturers of CyberKnife, believe that this is the first work analysing the interpretation of migrating fiducial position in a phantom model.

2.3.1 Phantom set-up

A solid water phantom (WT1) measuring 30cm x 30 cm, and 3cm thick was used. The phantom had 3 gold fiducials drilled into it at fixed positions. Each fiducial had dimensions 5 mm by 1 mm (Oncology Services Limited).

The solid water phantom had a 2cm diameter channel within it. A 2cm solid water tube fitted perfectly into this channel, and when the tube was fully inserted into the channel, the tube protruded from the phantom by 10.37mm. A gold fiducial of identical dimensions (5 mm by 1 mm) was drilled into the end of the tube and fixed in place with araldite epoxy resin glue.

A CT scan was taken of the phantom, with the phantom "sandwiched" between 2 solid water phantoms, each measuring 30cm x 30cm x 5cm thick. The purpose of these 2 additional phantoms was to anchor the fiducial-bearing phantom in place on the treatment couch, in order to eliminate the risk of the phantom being inadvertently moved during the experiment. The orientation of the fiducial-bearing phantom was such that the tube was protruding inferiorly. See Figure 5.

Figure 5*:*

A photograph of solid water phantom, with movable tube protruding from the inferior aspect of the phantom. Green laser lights (seen) were used to position the phantom. This photograph is taken with the phantom on the CyberKnife treatment couch, but orientation and set-up is identical to that at CT.

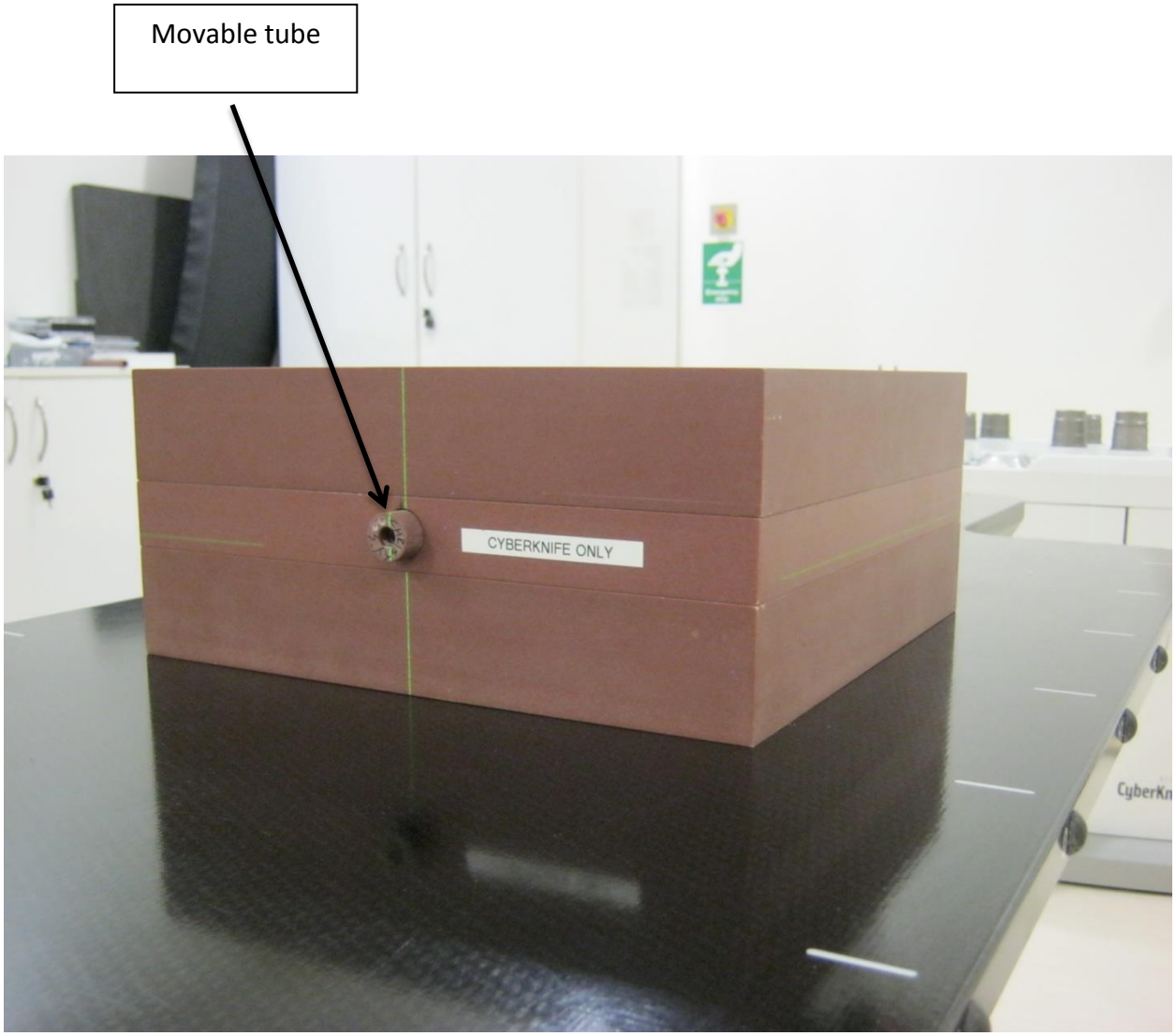

The 0^0 and 270^0 point was marked on both tube and phantom to ensure that there had been no rotation of the tube during the experiment. See Figure 6.

Figure 6:

Close-up photograph of the movable tube to illustrate marks on the tube and the main phantom that ensured consistency of set-up.

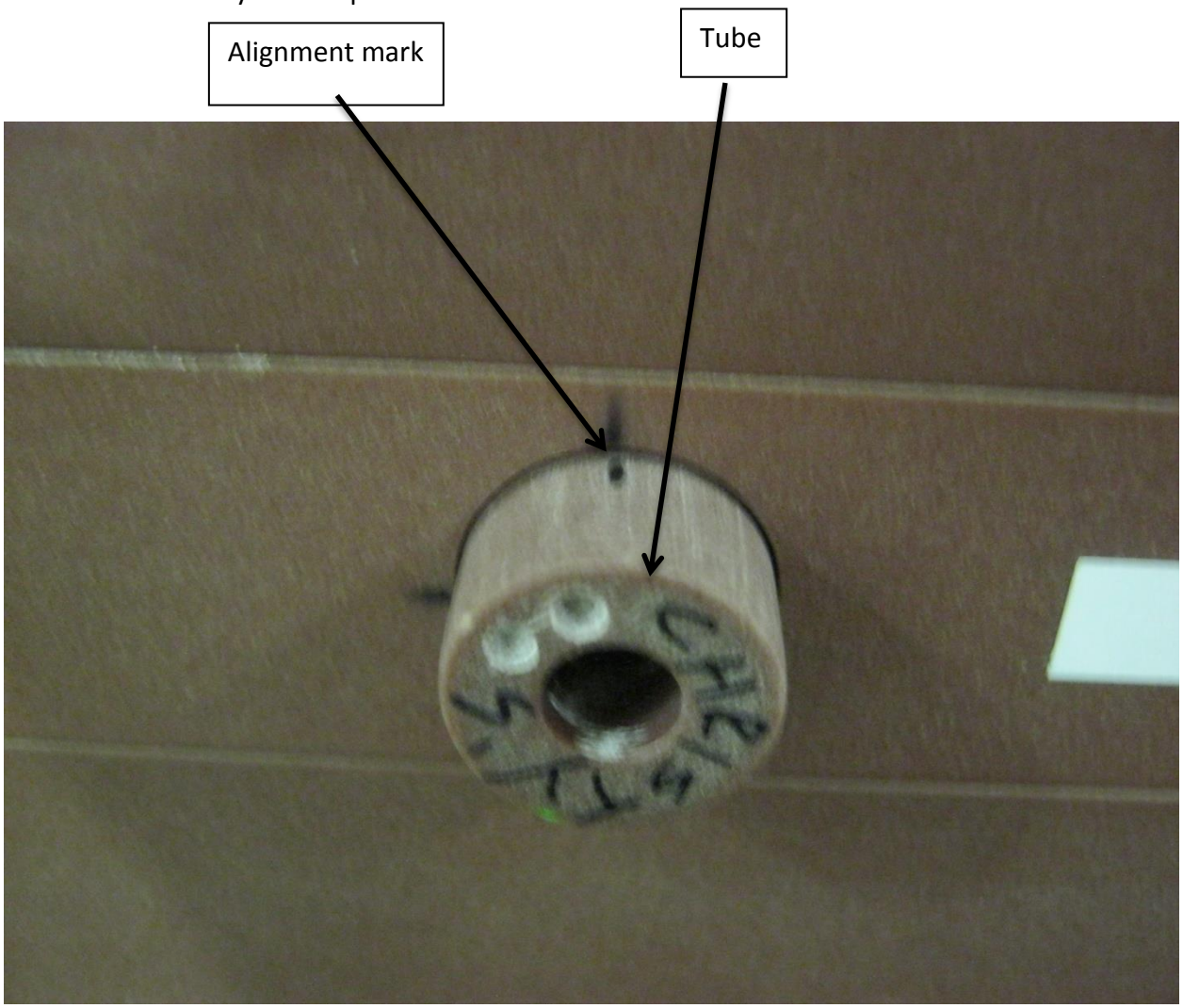

2.3.2 Treatment plan generation

A treatment plan for the phantom arrangement described above was generated on the CyberKnife planning system version 4.5 (Accuray Inc, California).

The planning system is able to automatically identify each of the 4 fiducials as “seed points”, but manual adjustments were made in order that the centre of each fiducial was accurately recorded. The fiducials were numbered 1-4, fiducials 1-3 were fixed fiducials within the main body of the phantom. The fiducial sited at the inserted end of the tube (which later represented the “migrating” fiducial), was labelled number 4. See Figure 7.

Figure 7: Image taken from MultiPlan system showing:

1. Top left pane: Rendered view of phantom taken from above
2. Top right pane: Axial view of phantom taken through a fiducial, artefact can be seen, the pink circle with crosshairs denotes the centre of this fiducial in the axial plane
3. Bottom right pane: Coronal view of phantom, the movable tube can be seen with an air-channel within it (shown as a black stripe), as before pink crosshairs denote the centre of the "migrating" fiducial in this plane, the 3 fixed fiducials can be seen in this view.
4. Bottom left pane: Sagittal view of phantom, the movable tube and migrating fiducial are again shown, as well as an additional fixed fiducial.

The image also shows a panel (far left) displaying the x/y/z co-ordinates of the centre of each fiducial.

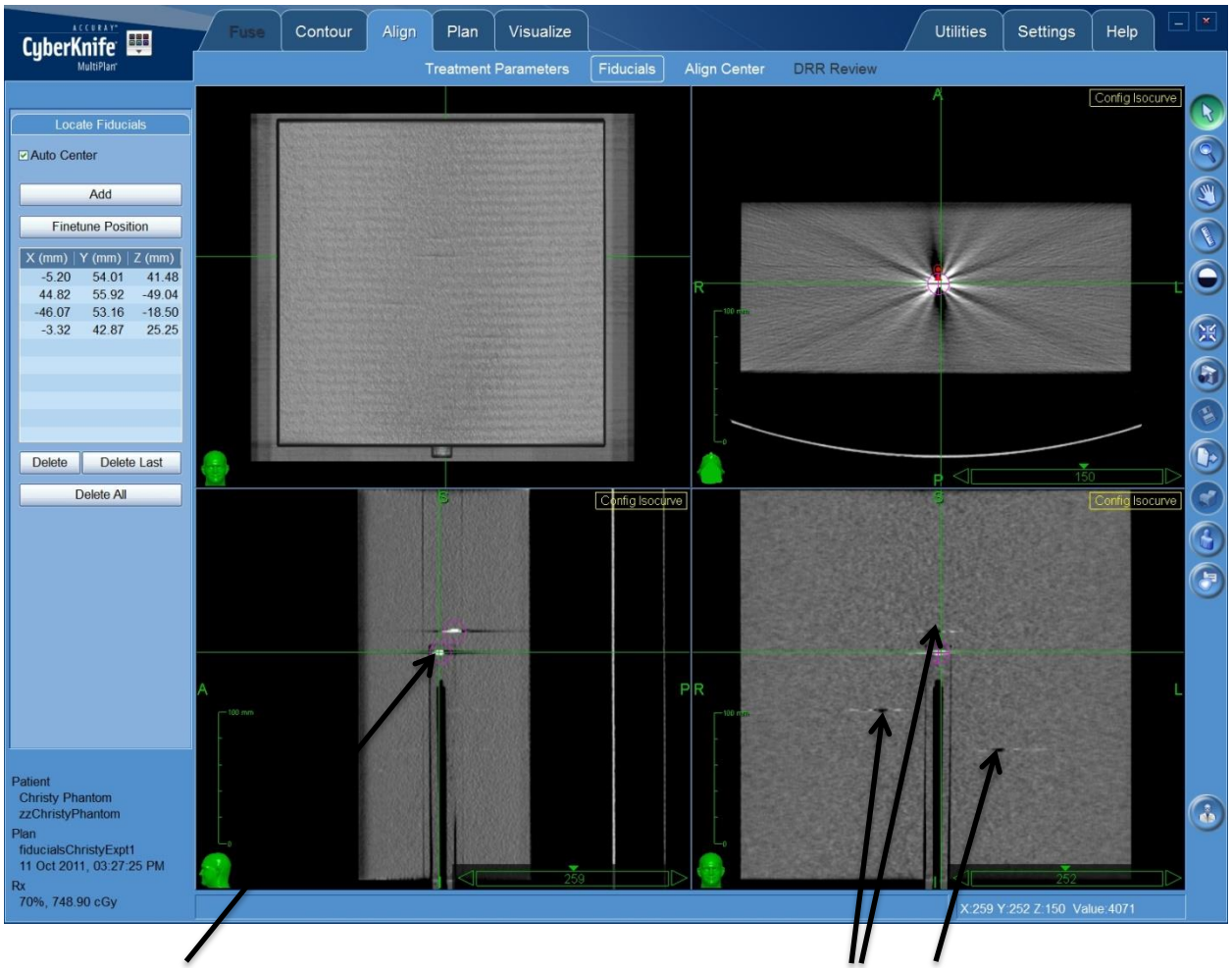

"Migrating" fiducial in tip of movable tube

3 x fixed fiducials

The inserted end of the tube was outlined as target, and an isocentric plan was generated to cover the target. The purpose of creating this plan was so that at treatment delivery the in-room Cyber Knife imaging system would generate paired live images to assess fiducial position.

2.3.3 Fixed Fiducial Tracking: 1 migrating fiducial, 1 fixed fiducial

The solid water phantom was arranged on the CyberKnife treatment couch exactly as it was at the time of the CT planning scan (see Figure 5). The treatment couch was moved such that the in-room lasers intersected over the phantom, at the imaging centre of the room. The starting position of the phantom was with the tube fully inserted. The orientation of the tube was checked by reviewing the position of the 0° and 270° marks on both the tube and phantom (see Figure 6). The starting position of the movable tube was with the tube protruding by 10.37mm, as measured with the depth gauge of digital callipers (see Figure 8). Callipers were supplied by Mitutoyo Corporation with a calibration certificate confirming their accuracy to within 0.01mm.

Figure 8:

Photograph showing the digital callipers. This was the starting position of the experiment, with tube protruding by 10.37mm. A depth gauge (seen resting on the index finger of left hand) was used to accurately measure tube protrusion.

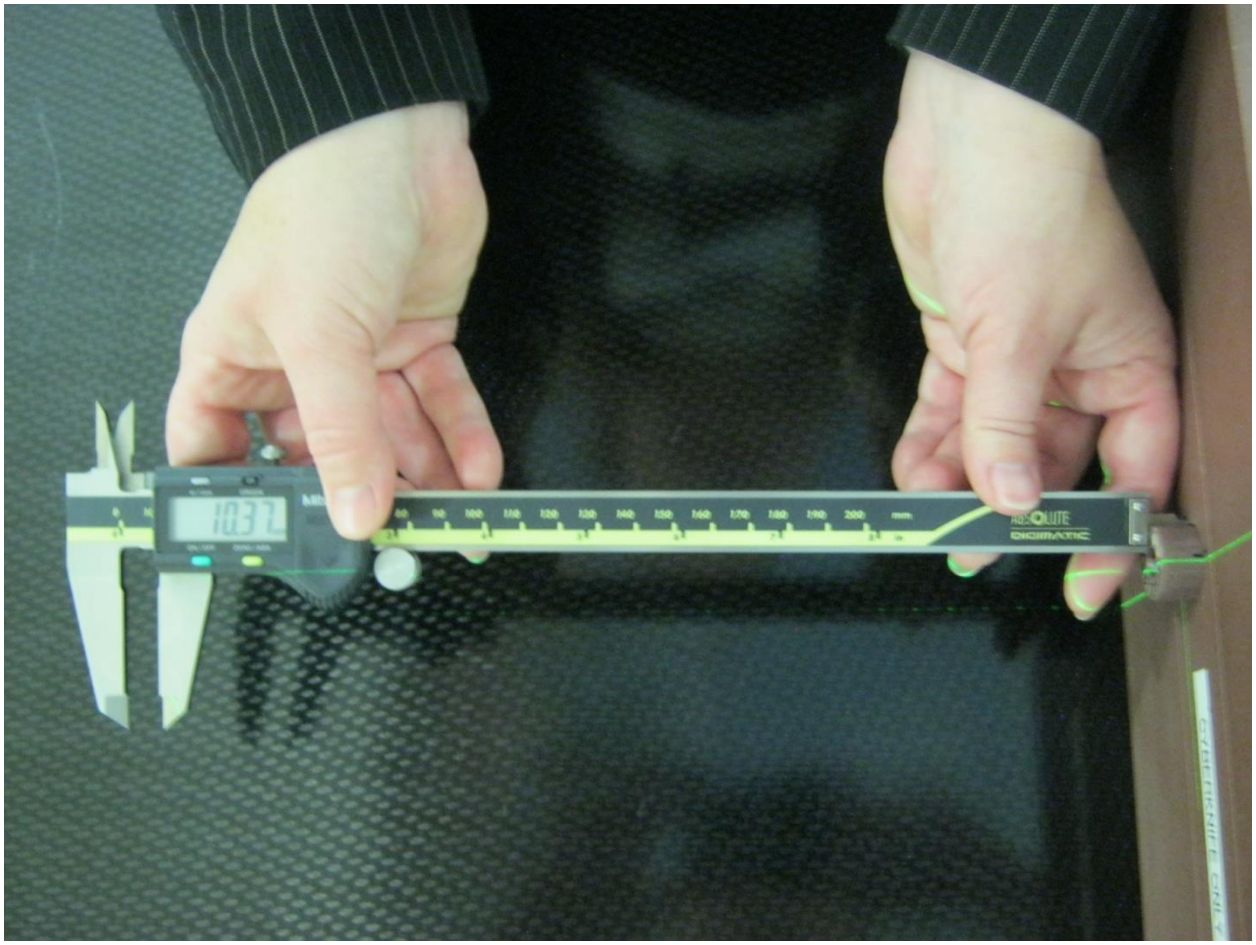

A pair of live X-Ray images were taken (120kV, 100mA) to assess the position of the phantom. The suggested couch corrections were applied, such that suggested couch corrections ultimately approximated 0, i.e. Suggested translational corrections ≤0.2mm, and rotational corrections ≤0.1°. As the migrating fiducial was to be moving in the superior-inferior direction, it was prioritised that the suggested translation correction in this direction was 0mm at Start.

A screen shot of the console data was taken at Start. See Figure 9.

Figure 9:

A photograph of the CyberKnife Treatment Console at the Start of the Experiment.
2 rows of X-Ray images can be seen. The top row labelled "A" refers to X-Ray images from Camera A. The bottom row shows images from Camera B. The 1st column of images are "DRRs" (Digitally Reconstructed Radiographs) generated from the Planning CT. The air in the movable tube (shown as black) is easily seen. Each fiducial 1-4 is highlighted by a green square. The 2nd column represents the "Live" X-Ray images that have been acquired. The fiducial tracking algorithm has correctly identified each fiducial (highlighted by green circles). The 3rd column shows an Overlay of DRR and Live images. The images overlay perfectly. To the right of the Overlay images is a column for "corrections". The Corrections approximate 0mm (0-0.1mm), the rotational corrections approximate 0^0 (0.2^0). Despite excellent alignment of the phantom, there is still a "Rigid Body Error" generated of 0.48mm. The significance of this is discussed later in this thesis.

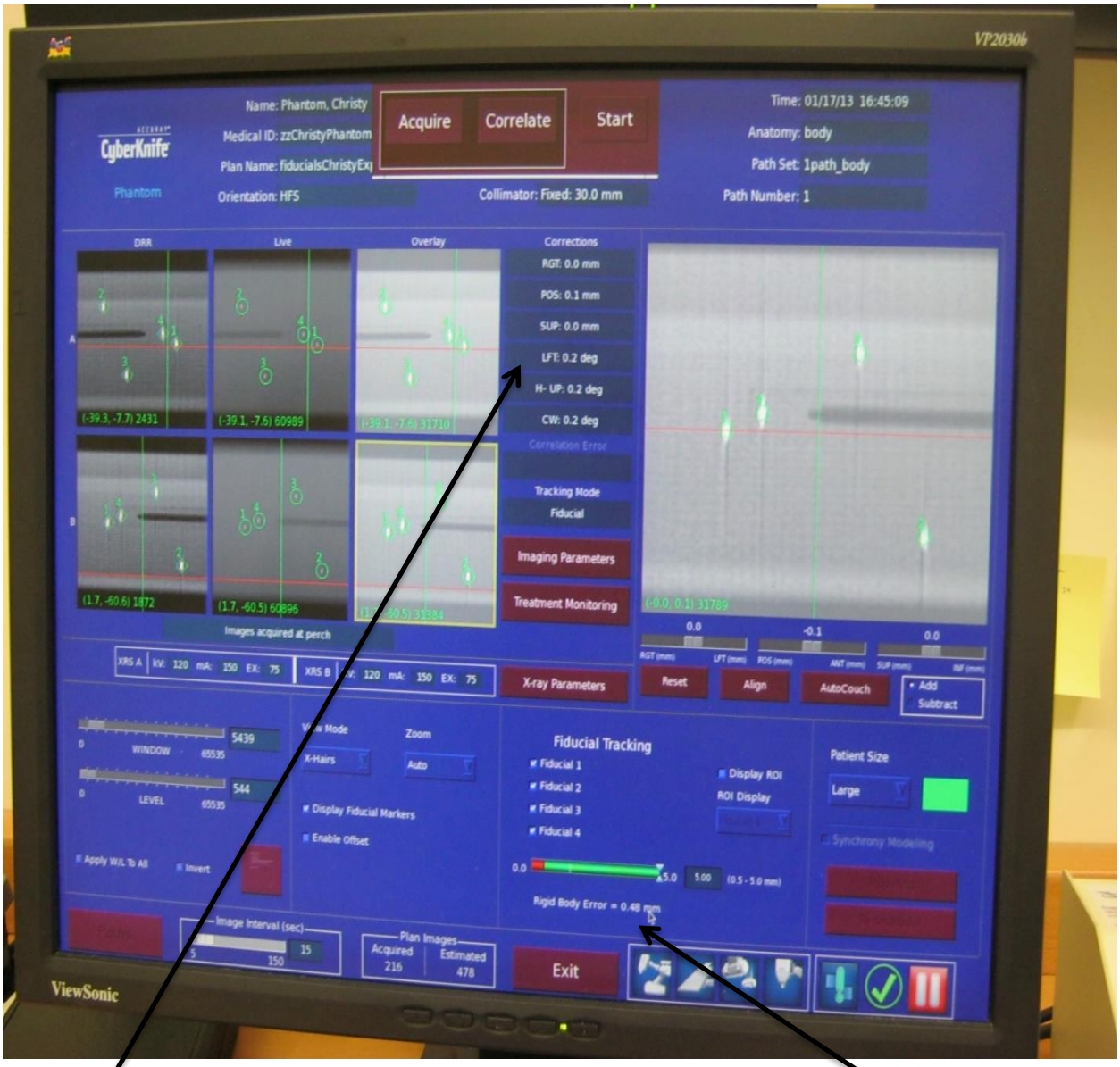

The tube was moved by hand to protrude by an additional 2mm, i.e. by 12.37mm. Therefore, fiducial 4 was positioned 2mm more inferiorly than the system was expecting. The accuracy of positioning was confirmed to be correct by using the depth gauge of the digital callipers.

A further pair of live images was acquired.

As verification that the tube had been moved accurately by the specified distance, the system was initially interrogated to generate offsets and Rigid Body Errors for Fiducial 4 only, then subsequently to also generate offsets and RBEs for Fiducials 4 and 1 together (Fiducial 1 was chosen as this was the closest fiducial to Fiducial 4).

Screen shots of the console data were taken after every shift of tube position, the tube was moved by 2mm increments.

The final position was 36.37mm protrusion of tube for the first experiment. At subsequent repeats of this first experiment, the final position of the tube was 26.37 mm, this provided data for at least 9 tube/fiducial positions for each experiment.

The experiment was repeated twice in order to generate standard deviations for the results achieved.

2.3.4 Fixed fiducial tracking, 1 migrating fiducial, 2-3 fixed fiducials

The solid water phantom was set up on the CyberKnife treatment couch exactly as described in Section 2.3.1. As before, in order to verify that the tube had been moved accurately by the specified distance, the system was initially interrogated to generate offsets and Rigid Body Errors for Fiducial 4 only.

In this Experiment, the system was then asked to "correlate", i.e. analyse fiducial position relative to each other for the following combinations of fiducials after each 2mm move:

Fid 4 only
Fids 1, 2, 4
Fids 1, 3, 4
Fids 2, 3, 4
All 4 Fiducials.

Screen shots of the console data were taken as before. The experiment was repeated twice in order to generate standard deviations for the results achieved.

2.4 RESULTS

2.4.1 Fixed Fiducial Tracking Accuracy: Interpretation of Fiducial position

In order to minimise the complexity of the analysis, although there were 3 fixed fiducials in the phantom, only the detection and correlation of fiducials 1 and 4 were analysed in this section.

The results of the 1st Run of the experiment are shown in Appendix 2.1. The experiment was repeated 3 times.

On the 1st Run of this experiment the tube was moved (in increments of 2mm) to a position 26mm away from the Start position. The Results for positions up to 16mm from Start position only are shown for ease of displaying the data.

The 1st column describes the move applied (in mm) to the tube (and therefore fiducial 4, the "migrating" fiducial). The tube was moved in an Inferior direction only, so in order to "adapt" to this, when the system is being asked to look at Fiducial 4 only (Fiducial 4 only ticked in the "Fiducial tracking" panel on the console, see Figure 9 page e), the system should generate a "superior" move as a correction. The 2nd column shows these corrections. Appendix 2.1 shows good agreement between move applied to the tube, and "superior correction". Between 0 and 16mm from starting position of fiducial 4, the mean difference between the callipers measurement and that of the CyberKnife system was 0.04mm (Range 0-0.1mm). This good agreement continued until the tube was 26mm from Start position. At this point, the superior correction was 0.2mm different to the move applied to the tube. The experiment was terminated at this point as a fiducial move of 26mm in a clinical situation would be certain to represent true migration (rather than deformation) and as such the fiducial would be unreliable for tracking purposes.

The figures in brackets in red type in the 2nd column are the Standard Deviations for the Superior move (mm) for fiducial 4 across the 3 runs of the experiment. For Run 2 the tube was moved to 20mm from Start position only, and for Run 3 to16mm. The experiments were consistent, Standard Deviations approximated 0 (Range 0-0.09).

Standard deviation = $\sqrt{\frac{\sum_{i=1}^{N}(x-\bar{x})^2}{N-1}}$

Appendix 2.1 shows Reference positions (in x, y and z axis) for Fiducials 1 and 4. These Reference positions are generated from the Planning CT and therefore are fixed. Indeed, the "Reference" positions for both Fiducials are consistent as expected, despite the moves being applied to the tube.

Fiducial 1

Fiducial 1 is a fixed fiducial therefore its "Live" (imaged) position should be consistent. The position of Fiducial 1 is accurately and consistently recorded between 0 and 14mm of the tube from its starting position. There are slight differences between the Reference and Live positions of Fiducial 1 (0.17mm in x axis, 0.29mm in y axis, and 0.06mm in z axis). These differences are consistent. The differences arise due to the process of the fiducial tracking algorithm. Each "kernel" represents a certain number of pixels, and the kernel can only be moved to its candidate location by a whole number of pixels.

At 16mm (Runs 1 and 3), and 18mm (Run 1) offset of the migrating fiducial from its expected position, the CyberKnife imaging system inappropriately identified Fiducial 1 and instead identified a point in space that was approximately the expected distance from Fiducial 4 (highlighted in yellow on the table). This was the case despite trying to "help" the system e.g. by decreasing the "tracking range" (the section of image in which the system will look for candidate fiducials). From the console data at "Start" the inter-fiducial marker distance between Fiducials 1 and 4 = 19.81mm. The inter-fiducial marker distance (where Fiducial 1 was mis-identified), and with tube at 16mm from the Start position = 22.53mm (on the 1st Run) and 22.45mm (on the 3rd Run). The system is therefore likely to be inappropriately identifying the same candidate fiducial or "feature". On the 2nd Run it was possible to help the system to correctly identify Fiducials 1 and 4 at 16mm offset of the tube from the Start position.

From 20mm to 26 mm inclusive, the system was then able to appropriately identify Fiducial 1.

Fiducial 4 (migrating fiducial)

Appendix 2.1 displays the Fid 4 (x) Live positions for the migrating fiducial. The tube was being moved in the x axis, therefore it was expected that the positions would change by 2mm each time (within the limitations of pixel size). The x locations displayed showed this happened consistently for the first Run (Mean shift= 2.04mm, range 1.9-2.2mm). On the second Run, the x axis displacement of migrating

fiducial 4 changed by a mean of 2.01 mm on each move (Range 1.9–2.1 mm). On the third Run, the x axis displacement of migrating fiducial 4 was accurately tracked for all positions 0-16mm with a mean shift of 2.01mm (Range 1.9-2.2 mm). Standard deviations for the observed shifts were 0.14mm, 0.1mm and 0.16mm on the 1st, 2nd and 3rd Runs respectively so the tracking is consistent.

Fiducial 4 (y) and (z) Live positions are shown in Table 1. The y location was accurately identified as -0.89 and the z location as 8.48 (within the limits of pixel size), up until the 14mm position. Thereafter the system had difficulty in capturing the fiducial accurately, and the reported position of Fid 4 was inaccurate, by 0.23mm.

On the second execution of the experiment, the system accurately tracked the x axis position of Fiducial 4 until 14mm. The 16mm position was inaccurately captured, but the system was able to accurately track the migrating fiducial in the 18 and 20mm positions. The Fid 4 (y) locations varied between -0.22 position and -0.67 across the tracking range (ref position = -0.88). The Fid 4 (z) locations varied between 8.26 and 8.48 (ref position= 8.62) other than at 16mm, where it was inaccurately identified at 6.48.

On the third execution of the experiment, the system accurately tracked the x axis position of Fiducial 4 up to and including the 16 mm position. The Fid 4 (y) locations varied between -0.45 and -0.67 (ref position = -0.88). The Fid 4 (z) location varied between 8.26 and 8.48 (ref position = 8.62).

Results overview: Fiducial 1 (Fixed fiducial)

Overall, the mean difference between Reference and Live positions of Fid 1 in x axis across all 3 executions was 0.17mm, as long as the fiducial was correctly identified. This was very stable i.e. as long as the fiducial was correctly identified, Reference position was always -41.69, and Live x position was always -41.86.

Overall, the mean difference between the Fiducial 1 Reference and Live positions in the y axis were small as long as the fiducial was correctly identified. Across all 3 executions the mean difference between Reference and Live positions was 0.24 mm.

The mean difference between the Fiducial 1 (z) Reference and Live positions was 0.06mm, (as long as the fiducial was correctly identified) averaged out over all 3 executions. This was therefore highly accurate.

In summary, the accuracy of fixed fiducial tracking for this experimental system is ≤ 0.24mm.

Results overview: Fiducial 4 (Migrating fiducial)

The mean difference between Fid 4 (x) Reference and Live positions at Start was 0.01mm, therefore excellent correlation. The tube was being moved in the direction of the x axis by 2mm increments, therefore the Fid 4 (x) Live position was expected to change by 2mm increments. In the 2nd and 3rd Runs, the position changed by on average 2.01mm. In the 1st Run, the position changed by on average 2.04mm. The migrating fiducial was therefore accurately tracked in the x axis, to within 0.1mm.

On the 1st Run the Fid 4 (y) axis Live position (which should not have changed as the tube was moved) was on average 0.01 mm different to the Reference position, so long as the fiducial was correctly identified. On the 2nd Run the difference was 0.39mm, and for the 3rd execution this was 0.31. Overall, the mean difference was 0.24mm.

The mean difference between Fid 4 (z) Reference and Live positions was 0.19mm for the 1st Run. For the 2nd and 3rd executions this difference was 0.19mm, and 0.26mm respectively. Overall, the mean difference was 0.23mm.

2.4.2 Fixed Fiducial Tracking Accuracy: Robot corrections

The experiment was conducted as described in section 2.3.1.

In this Experiment, the system was asked to "correlate", i.e. analyse fiducial position relative to each other, for the following combinations of fiducials after each 2mm move of the migrating fiducial:

Fid 4 only

Fids 1, 2, 4

Fids 1, 3, 4

Fids 2, 3, 4

All 4 Fiducials

When the Fiducials are imaged in a different arrangement to what was expected (i.e. with reference to the DRR generated by the Planning CT scan), the CyberKnife system will generate a Correction (see Figure 9 image of Console data) and a Centre Of Mass (COM) Translation (see Figure 10, "Translation (x,y,z)" is recorded in "Algorithm data" section). The COM refers to the COM of the fiducials. The "Correction" is reported as a Couch correction, i.e. the move that the Treatment couch would need to make in order that the target was correctly aligned for treatment (incorporating a rotation if necessary), but in practice it is the Robot that moves by the required amount to ensure that the treatment is delivered accurately. The COM Translation (by definition) does not incorporate any rotational corrections.

As can be seen from the Algorithm data section of Figure 11, the COM Translation is reported as an x, y, z shift. It is important to appreciate the x,y,z orientation of the CK room in order to understand the direction of shifts. The room is set up as follows:

X Sup (-) ⟷ Inf (+)

Y Right (-) ⟷ Left (+)

Z Post (-) ⟷ Ant (+)

This data was used, as well as the "Start" Translational corrections, in order to calculate the COM translational correction using the root of the sum of the squares formula. A shift was calculated (rather than simply using the x,y,z co-ordinates) in order that the relationship between migrating fiducial move and COM Translational correction (analogous to Robot corrections) could be explored.

An example calculation of COM Translation is shown on the next page.

At “Start” (i.e. 0mm move of Migrating fiducial):

Translation (x, y, z): 0.03, 0.22, 0.02 (See Figure 10). It can be seen that these Translations are analogous to the “Corrections” , the ant/post and the sup/inf translations approximate 0, whilst the left/right Correction approximates Left 0.2mm. A small rotation (0.1 deg to right) is noted which accounts for the very slight discrepancy between Translations and Corrections.

Figure 10:

A photograph of the CyberKnife Treatment Console at the Start of the Experiment. “Corrections” (in mm) are listed in the left of the image. The x,y,z Translations (in mm) are listed in the data panel

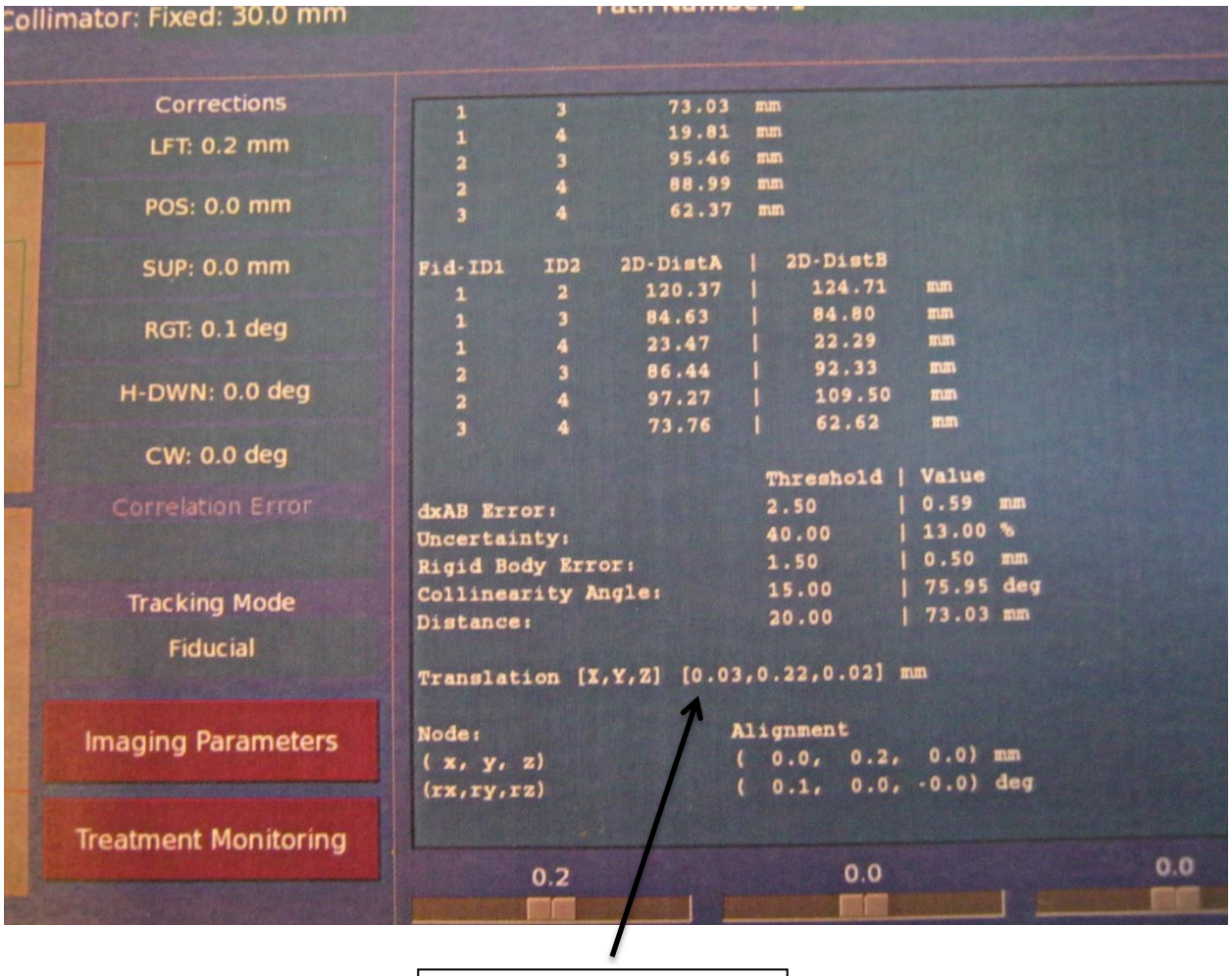

At 6mm move of Migrating fiducial (when considering Fids 1 and 4):

COM Translation shift = -2.91, 0.08, 0.04 (see Figure 11 below).

Figure 11:

Photograph of CK console data to illustrate robot corrections for a migrated fiducial

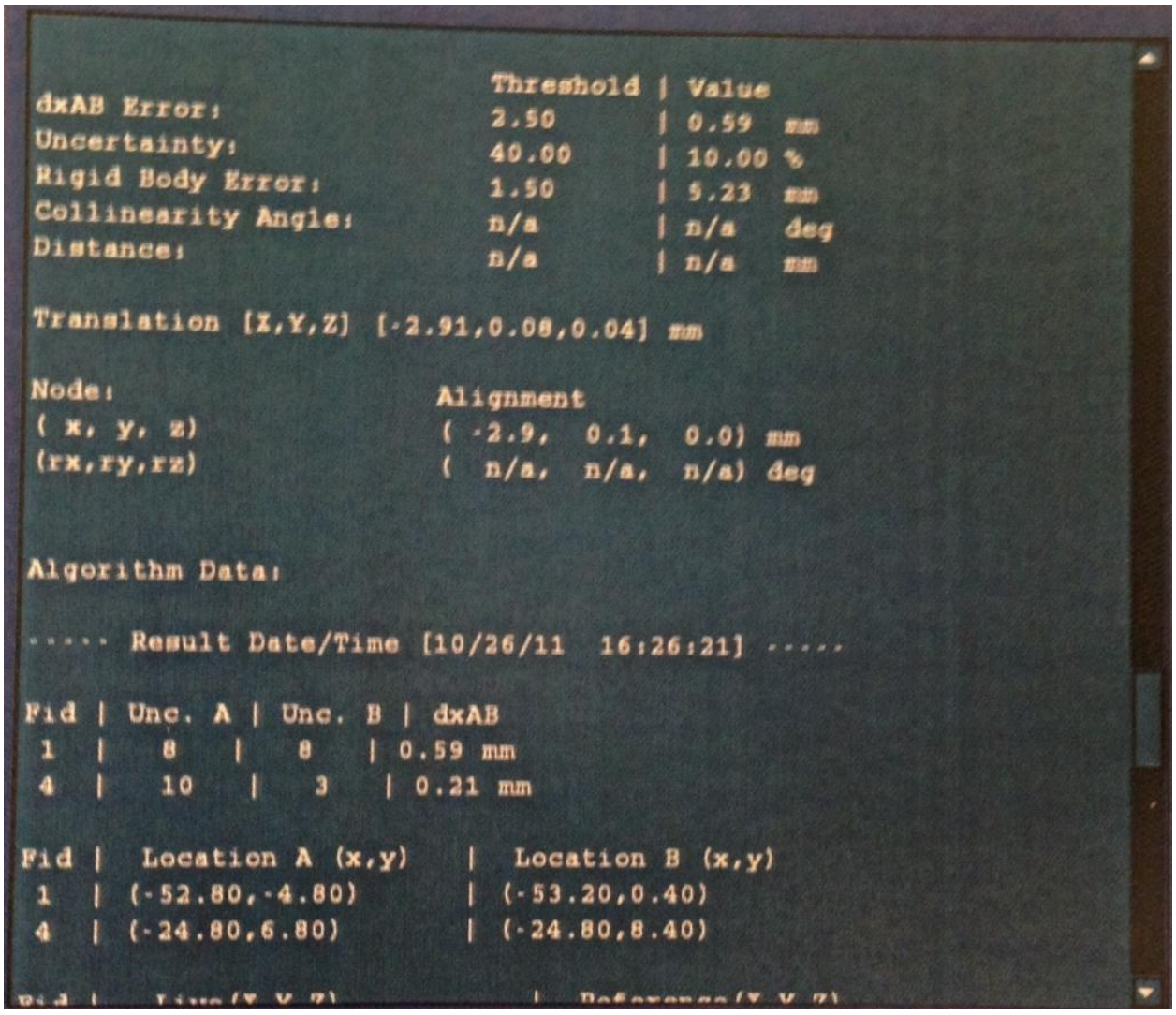

i.e. the suggested correction is in the superior direction by almost 3mm:

$$\sqrt{(0.03 + 2.91)^2 + (0.22 - 0.08)^2 + (0.02 - 0.04)^2}$$

= 2.94 (see Table 1, page 51).

This calculation was repeated for each 2mm move of the migrating fiducial, and according to the combination of fiducials being correlated.

Results are recorded in Table 1 (see next page) and are displayed in Graph 1 (page 53). Results are not displayed for "Fiducial 4 only", as for a treatment tracked by a single fiducial, the Centre of the Fiducial is the Centre of Mass. The "Corrections" for Fiducial 4 only are listed in the 2nd column of Appendix 2.1.

The COM Translational corrections show good reproducibility of results, as can be seen from the 3 Runs of the experiment correlating Fiducials 1 and 4, the curves on Graph 1 overlie each other. Standard deviation ranges between 0 mm and 0.15mm.

When correlating combinations of 3 fiducials, standard deviation ranged between 0mm and 0.07mm.

When correlating all 4 fiducials, standard deviation ranged between 0mm and 0.4mm.

Therefore for a given Move of the migrating fiducial, the suggested COM Translational corrections are consistent to within 0.4mm.

Table 1:

COM Translational correction (mm) vs. Migrating fiducial move (mm) according to combination of fiducials being assessed.

Figures in red font indicate where a Fiducial was misidentified.

Fiducial 4 distance moved (mm)	COM Translational Correction (mm)				
	Fids: 1 and 4	Fids: 1,2,4	Fids: 1,3,4	Fids: 2,3,4	Fids: All 4
0	0	0	0	0	0
2	0.89	0.56	0.76	0.73	0.52
4	2	1.25	1.44	1.41	1.02
6	2.94	1.93	2.13	2.09	0.79
8	3.88	2.61	2.81	2.78	
10	4.99	3.25	3.44	3.41	
12	5.93	2.25	2.07	2.08	
14	6.88				
16	13.7				

Graph 1 (page 53) and Table 1 above displays “move” applied to Fiducial 4 (in mm) compared to Centre of Mass translational correction (as reported by the CK system) according to the number and combination of fiducials being used (or “correlated”), for tracking purposes. It is important that the CK system suggests the appropriate translational correction, as the CK system will generate “Robot corrections” analogous to these corrections (as has been shown). The COM translational corrections have been plotted, rather than “Robot corrections”, because as a safety feature, once the Rigid Body Error>5, the system will not generate Robot corrections (and treatment is rendered “Undeliverable”), as it is considered that at this point (appropriately, given the tiny margins applied in SBRT) that the fiducials are no longer a good surrogate for tumour (see Figure 12). Plotting COM translations therefore (rather than Robot corrections) allows more data points to be plotted.

Graph 1 and Table 1 show that the COM translational correction is greatest when only 2 fiducials (fiducials 1 and 4) are being correlated, as the COM will be equally dependent on each fiducial. On reviewing the relationship between COM translational correction and move applied to Fiducial 4, the COM translational correction approximates Fid 4 move (mm) divided by 2 when measured to the nearest mm (when correlating 2 fiducials). At 16mm (from Start position), the CK in-room imaging system failed to accurately identify Fids 1 and 4, hence the erroneous reading of COM translational correction at 16mm (Table 1 red font).

Graph 1 and Table 1 show that COM translational correction, when correlating 3 fiducials (2 fixed fiducials and 1 migrating fiducial), approximates Fiducial 4 move (mm) divided by 3. At and beyond 12mm move of Fiducial 4, the CK system could not accurately identify both Fiducials 1 and 4.

Graph 1 and Table 1 show COM translational correction when correlating all 4 fiducials, approximates Fiducial 4 move (mm) divided by 4 for the first 2 data points (i.e. where Fiducial 4 is 2mm and 4mm away from Start position). Thereafter, the data points are erroneous because Fid 1 and 4 could not be accurately identified.

Where fiducials are accurately identified, in a Phantom experiment with fixed fiducials and only one "migrating" fiducial:

COM translational correction (mm)~ Move of migrating fiducial (mm) ÷ n

Where n = number of fiducials.

Graph 1: Migrating fiducial distance moved vs COM Translational Correction

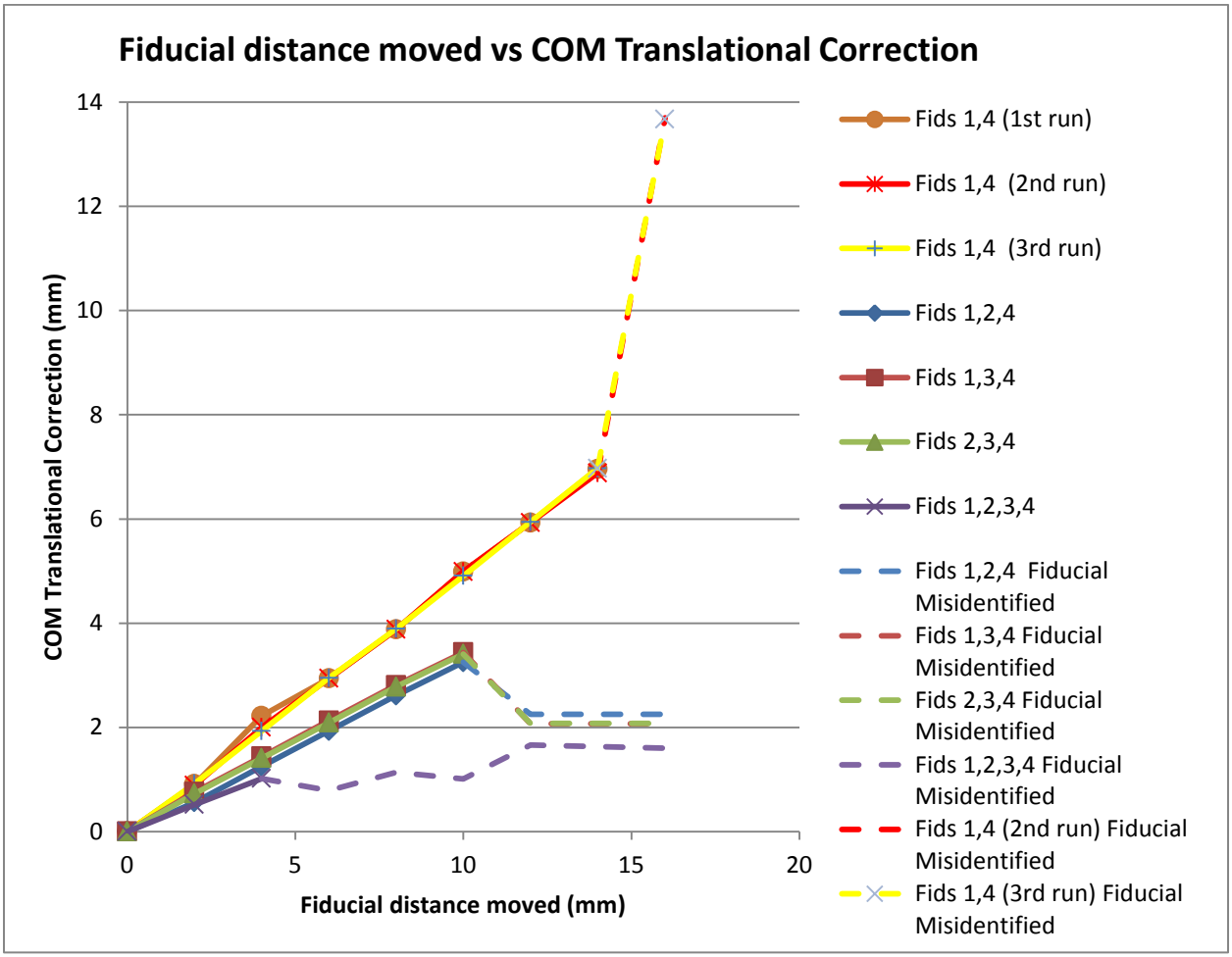

2.4.3 Rigid Body Error (RBE)

RBE refers to the discrepancy (in mm) in Fiducial positions (relative to each other) between the CT Planning scan and the time of treatment. The larger the RBE, the greater the change in Fiducial position from planning scan to treatment. Table 2 shows the Fiducial 1-4 inter-marker distance, and RBE for the 3 Runs of the experiment up to 14mm displacement of the tube. Figures in red represent RBE values greater than the "deliverable" threshold. The figures in blue font represent figures generated when at least 1 fiducial was misidentified. Full raw data is shown in Appendix 2.1 as before.

Table 2: Results from 1st Phantom experiment: focus on inter-fiducial distance and RBE

Move (mm) tube from Start	Fid 1-4 Distance (mm) Run 1	Fid 1-4 Distance (mm) Run 2	Fid 1-4 Distance (mm) Run 3	RBE: Run 1 (mm)	RBE: Run 2 (mm)	RBE: Run 3 (mm)
0	19.81	19.78	19.81	0.04	0	0
2	21.54	21.27	21.27	1.77	1.5	1.5
4	23.18	23.18	23.32	3.41	3.41	3.55
6	25	25	25	5.23	5.23	5.23
8	26.71	26.71	26.71	6.94	6.94	6.94
10	28.74	28.59	28.64	8.96	8.81	8.86
12	30.49	30.4	30.4	10.71	10.62	10.62
14	32.41	32.41	32.17	12.63	12.63	12.4
16	22.45	13.41	22.53	2.67	6.36	2.75

At the Start position, the Fiducial 1-4 distance was on average 19.8mm (range 19.78-19.81mm). At the Start position we know that there should be no Rigid Body Error (RBE), as the arrangement of fiducials should be identical to that at the time of the CT planning scan, i.e. there is "Rigid Body" geometry between planning CT scan and the time of the live paired imaging of the phantom by the CyberKnife system. The reported RBE at Start was on average 0.01mm (range 0-0.04mm).

The CyberKnife system was able to accurately identify both Fiducials 1 and 4 in this experiment up to and including the 14mm position. Considering only the 0-14mm positions the Fid 1-4 distances, and RBE's will be analysed.

The mean increase in Fid 1-4 distance across all 3 Runs was 1.8mm (Range 1.5-2.05, SD = 0.16) each time the tube was moved by 2mm. It was not expected that the Fid 1-4 distance would increase in 2mm increments as Fiducials 1 and 4 were not in the same x axis plane.

The mean increase in RBE Fid 1-4 was 1.8mm (Range 1.5-2.05, SD = 0.16).

On reviewing the RBE Fid 1-4, for each move, Fid 1-4 distance increase = RBE Fid 1-4 increase.

Therefore, as only one Fiducial is moving (Fid 4), and system is being asked to correlate only 2 Fiducials (Fids 1 and 4, Fids2&3 switched off), Fid 1-4 distance change = RBE Fid 1-4.

RBE is calculated by the CK system according to the following formula:

$\sqrt{(\Delta x^2 + \Delta y^2 + \Delta z^2)}$ to get the shift in fiducial positions between "Reference" locations and "Live" locations, where Δ = change in co-ordinates (Reference to Live)

To verify RBE reporting for RBE at 2mm shift of Fiducial 4 (see Appendix 2.1):

Calculate Reference (i.e. Planning scan) Fid 1-4 intermarker distance:

Δx = (-41.69+25.45) = -16.24
Δy = (-2.75+0.88) = -1.87
Δz = (-2.52-8.62) = -11.14

$$= \sqrt{(-16.24)^2 + (-1.87)^2 + (-11.14)^2}$$

= 19.78

Calculate Live Fid 1-4 inter-marker distance at 2mm shift:

Δx = (-41.86+23.6) = -18.26
Δy = (-2.46+0.67) = -1.79
Δz = (-2.46-8.26) = -10.72

$$= \sqrt{(18.26)^2 + (1.79)^2 + (10.72)^2}$$

= 21.25

21.25 (Live) – 19.78 (Ref) = 1.47 (i.e.1.5) (see Column 2, Appendix 2.1)

Therefore calculated and reported RBEs agree.

These calculations were repeated for the data in Table 1 and for all data, calculated and reported RBE's were in agreement.

Tables 3 and 4 show further RBE results, when correlating combinations of 2 and 3 fixed fiducials and the single migrating fiducial. Figures in red represent RBE values greater than the clinically "deliverable" threshold for a treatment plan. The figures in blue font represent figures generated when at least 1 fiducial was misidentified. Figures in purple font in brackets represent Standard deviation (SD).

Table 3:

Move of Migrating fiducial (mm) vs RBE (mm) when correlating combinations of 2 fixed fiducials and 1 migrating fiducial.

Fid 4 move (mm)	Fids 1,2,4 1-2 RBE	Fids 1,2,4 1-4 RBE	Fids 1,2,4 2-4 RBE	Fids 1,3,4 1-3 RBE	Fids 1,3,4 1-4 RBE	Fids 1,3,4 3-4 RBE	Fids 2,3,4 2-3 RBE	Fids 2,3,4 2-4 RBE	Fids 2,3,4 3-4 RBE
0									
2	0.22 (0.05)	1.5 (0.12)	1.94 (0.18)	0.7 (0.18)	1.5 (0.12)	0.85 (0.08)	0.19 (0.04)	1.94 (0.18)	0.85 (0.08)
4	0.22 (0.03)	3.51 (0.08)	3.59 (0.1)	0.7 (0.09)	3.51 (0.08)	2.48 (0)	0.19 (0.03)	3.59 (0.1)	2.48 (0)
6	0.22 (0.05)	5.19 (0.13)	5.13 (0.18)	0.7 (0.18)	5.19 (0.13)	3.73 (0.08)	0.19 (0.04)	5.13 (0.18)	3.73 (0.08)

Table 4:

Move of Migrating fiducial (mm) and RBE (mm) when correlating all 3 fixed fiducials and 1 migrating fiducial.

Fid 4 move (mm)	Fids 1,2,3,4 1-2 RBE	Fids 1,2,3,4 2-4 RBE	Fids 1,2,3,4 1-3 RBE	Fids 1,2,3,4 1-4 RBE	Fids 1,2,3,4 3-4 RBE	Fids 1,2,3,4 2-3 RBE	Fids 1,2,3,4 All 4 RBE
0	0.22 (0.03)	0.37 (0.01)	0.7 (0.09)	0.11 (0.02)	0.47 (0.08)	0.19 (0.04)	0.7 (0.09)
2	0.22 (0.03)	1.94 (0.18)	0.7 (0.09)	1.5 (0.19)	0.85 (0.08)	0.19 (0.04)	1.94 (0.18)
4	0.22 (0.03)	3.59 (0.1)	0.7 (0.09)	3.51 (0.08)	2.48 (0)	0.19 (0.04)	3.59 (0.1)
6	0.22 (0.03)	0.81 (0.03)	0.7 (0.09)	0.1 (0)	1.79 (0.13)	0.19 (0.04)	1.79 (0.13)

As can be seen from Tables 3 and 4, when the system is asked to correlate only fixed fiducials (e.g. 1-2RBE, 1-3 RBE and 2-3RBE) the RBE is small (Range 0.19-0.7mm), and the RBE is consistent and reproducible (SD = 0.03-0.18mm). These RBEs reported for fixed fiducial correlation are small enough to allow a treatment to be deliverable.

In contrast, when correlating a fixed fiducial (Fids 1-3) with a migrating fiducial (Fid 4), the RBE is larger. The reported RBEs remain consistent and reproducible (SD=0.01-0.19mm). As expected, the RBE increases as Fiducial 4 move increases.

When correlating 2 fixed fiducials and the migrating fiducial (Table 3) at a 2mm move of the migrating fiducial, the treatment would be considered “deliverable”. Even though the only migrating fiducial is fiducial 4, and all other fiducials (1-3) are fixed, the reported RBE varies from a minimum of 0.85mm (3-4RBE) to a maximum of 1.94mm (2-4RBE) when the migrating fiducial moves by 2mm.

Of note, when correlating 3 fixed fiducials with a migrating fiducial, at 6mm move of the migrating fiducial, the CK in-room imaging system starts to misidentify a fiducial (see Table 4). The RBE generated at a move of 6mm of the migrating fiducial is “deliverable” in all cases (RBE 0.1-1.79mm) despite this large fiducial migration (blue font for erroneous RBE due to misidentified fiducial but “deliverable” RBE. The implications of this will be discussed.

2.5 DISCUSSION

An important component of SBRT is that the margin between GTV (Gross Tumour Volume) and PTV (Planning Target Volume) is small, typically only 2-5mm.

This means that, as long as targetting by the SBRT system is accurate, there will be minimal normal tissue in the PTV, and High BED (Biologically Effective Dose) ablative doses of radiotherapy may be safely delivered (as long as appropriate dose constraints are respected)(7).

A caveat to the above is that it is vitally important that target outlining is accurate, and that SBRT treatment is delivered exactly as intended. If there are errors in either target outlining, or treatment delivery, there could be target miss (which would negatively impact on tumour control). There could also be overdose of nearby OARs (organs at risk), which could have a serious impact on acute and late toxicity.

2.5.1 Fixed fiducial tracking accuracy: Interpretation of fiducial position

Single fiducial:

When reviewing the results of the 1st experiment, the CyberKnife imaging system could accurately identify Fiducial 4 (the migrating Fiducial), when this was the only Fiducial the system was being asked to locate, out to at least 26mm (away from "Expected"position). The callipers used to measure the distance moved by Fiducial 4 were accurate to within 0.01mm, so this was considered the "gold standard" measure of distance moved. Against this standard, the system accurately calculated the "Superior correction" i.e. the move that the robot would need to make to line it up with Fiducial 4 to within 0.05mm (range 0-0.2mm). There was only a single discrepancy of 0.2 mm, this was at the most extreme position of Fiducial 4, 26mm away from where the system was expecting it to be. At this position, although the tube still fitted snugly into its channel, it is certainly plausible that it was more difficult to accurately move the fiducial-bearing tube. In routine clinical practice a fiducial detection accuracy of 0.05mm (as achieved out to 26mm) would be considered clinically acceptable, as given the GTV to PTV margins applied of a minimum of 2mm this should not lead to target miss or overdose of nearby OARs.

It should be borne in mind, however, that in this phantom experiment the system is being asked to locate a radio-opaque fiducial, in a homogenous solid-water phantom, and the y/z axis positions were exactly as expected from the CT-planning scan. This is likely to be an easier case to interpret than a clinical case where there is less contrast between fiducial and soft tissue, and y/z positions may have changed.

Multiple fiducials

The experiment next looked at whether the system could accurately detect both a migrating fiducial (Fiducial 4) and a fixed fiducial (Fiducial 1). The system could accurately detect both fiducials from 0mm to 14mm displacement of the migrating fiducial from its expected position, beyond this distance the migrating fiducial is misidentified. In clinical terms, a 14mm shift of a fiducial from its expected position is a relatively large distance. If this shift is due to a fiducial migration, a shift of this magnitude would lead a Radiographer/Clinician to question whether the fiducial was a good surrogate for tumour. When multiple fiducials are being tracked a RBE will be generated, and at a shift of 14mm the RBE will certainly be beyond the "deliverable" threshold (see Section 2.4.3) which is an important "safety mechanism", to limit the possibility of a treatment being delivered when the fiducials are no longer a good surrogate for tumour.

This phantom experiment has shown that when tracking 2 "fixed" fiducials, the CyberKnife system is able to accurately interpret fiducial position, even when one fiducial migrates to a clinically large distance of 14mm from its expected position (expected according to CT planning scan).

Graph 1 (page 53) shows that when the system is asked to track 3 fiducials, a migrating fiducial can be accurately detected to 10mm away from its expected position. Graph 1 also shows that when correlating all 3 fixed fiducials, a migrating fiducial can be accurately detected up to only 4mm away from its expected position.

Overall, this experiment has shown that the accurate interpretation of fiducial position is not only dependent on the distance that a migrating fiducial has moved relative to its reference position. It is also dependent on the number of other fixed fiducials available for correlation. The greater the number of fixed (accurately located) fiducials that the system has available to correlate, the shorter the distance over which the system can accurately locate a migrating fiducial. The reason for this is not entirely clear, but is likely to be related to the fiducial tracking algorithm.

As explained in the Introduction, the system assumes that the probability of a candidate fiducial being an actual fiducial is partly dependent on the discrepancy between its actual distance from other fiducials and the expected distance. The results from this experiment suggest that the probability calculations are dependent also on the number of accurately located fixed fiducials available for correlation. The calculated probability of a candidate fiducial being an actual fiducial is lower in the presence of a greater number of accurately located fiducials.

2.5.2: Fixed Fiducial Tracking: Robot Corrections

The results of the experiment correlating Migrating Fiducial distance moved vs COM Translational Correction show that as long as the migrating fiducial is correctly identified, the COM Translational Correction is appropriately reported. This was validated manually in the root of the sum of the squares calculations (See Section 2.4.2). This result gives confidence in the Corrections generated at the time of CyberKnife treatment.

The Corrections generated (based on COM Translational Corrections) show good reproducibility of results which further gives confidence that for a given fiducial arrangement in a patient, their treatment could be executed consistently and appropriately on consecutive treatment days. It is important to note though, that there would be a number of caveats to assuming that the clinical scenario would be analogous to this phantom scenario. Firstly, interpretation of fiducial position is more difficult in a clinical situation with multiple tissue densities in the "region of interest". Additionally, fiducials which are implanted into a tumour volume, or an adjacent structure, can rotate, and the tissue can deform, such that the orientation of the fiducial(s) compared to that at the time of Planning CT can change, making it harder for the in-room imaging system, and indeed the Treatment Radiographers to accurately identify the fiducial(s).

Robot corrections were analogous to COM Translational Corrections (see Figure 10) except where Rotational corrections were required.

Robot corrections were appropriately generated on all occasions that the RBE was "within threshold", but were not generated on any occasion that the RBE was out of threshold, see Figure 12.

Figure 12:

Screenshot showing RBE>5. The CK system has not generated Robot Corrections and the “Start” button is greyed out because delivering a treatment with such a high RBE would not be clinically appropriate.

It should be noted, however, that if a fiducial is misidentified, a RBE may be reported that allows a Correction to be generated (See Table 4, page 57, at Fiducial 4 move of 6mm), but in this scenario the Correction would be inappropriate because it would be based on an erroneous fiducial location and treatment could proceed inappropriately. The treatment radiographers are vigilant though and they would take appropriate measures, such as “switching off” a fiducial if they believed it had migrated. Other options are reducing the “tracking range” in order to prompt the system to look only in a limited window (where the radiographers can see the fiducial).

2.5.3. Rigid Body Error (RBE)

RBE: 1 fixed fiducial and 1 migrating fiducial

The RBE when assessing the above combination of fiducials is greater than a "deliverable" threshold (Threshold = 1.8-2) at and beyond a 4mm move of the migrating fiducial (see Table 3, page 56). These results were consistent and could be validated by calculating the RBE as explained in Section 2.4.3, which is reassuring when considering being able to deliver clinical treatments accurately and consistently on consecutive days. At a 2mm move of the migrating fiducial, the RBE is within threshold (RBE=1.5), and it could be argued that this might not be clinically appropriate. In a scenario where one fiducial is in the GTV (therefore the optimally placed fiducial), and the other fiducial is lying outside the PTV, a clinical event associated with a 2mm shift of the optimally placed fiducial relative to the other could be concerning with regards to the accuracy of fiducial tracking. If the optimal fiducial remains within GTV, and there is adequate expansion to PTV, a treatment is likely to proceed accurately. However, if the optimal fiducial has migrated out of the GTV by 2mm, this could compromise the accuracy of treatment delivery. Such a small shift is difficult to appreciate for the Radiographers. In delivering a treatment tracked with 2 fiducials, the RBE can be dependent on a shift of either fiducial, or both, and it is difficult to appreciate which fiducial may have moved (or both) by this distance with reference to bony anatomy.

A new feature of the CyberKnife Treatment Delivery System Version 9.6 is that a "red square" is placed next to the fiducial that is contributing the most do the RBE generated. The aim of this would be to guide the Radiographers, to either adjust patient positioning if possible, such that the arrangement of fiducials at planning is more closely recreated, or if it is believed that a fiducial has migrated such that it is no longer a surrogate for tumour, the migrated fiducial can be "switched off".

In this experiment fiducial 4 was always the migrating fiducial. However, when assessing the tracking of Fiducials 1 and 4 only, from 6mm displacement of the migrating fiducial (Fid 4), the system erroneously showed a "red square" adjacent to fiducial 1 (the fixed fiducial), see Figure 13 (page 64). In a clinical scenario where only 2 fiducials are being tracked, it would be difficult for the delivery system to assess which fiducial may have moved (or both may have moved by the same amount). None-the-less it was surprising that the error was attributed to fiducial 1 as the "Live" location of this fiducial was very close (<0.29mm) to its Expected ("Reference") position. In contrast, fiducial 4 "Live" location was different (by 6mm in the x axis) to the expected "Reference" position. It is important for Radiographers to be

sceptical of the “red square” guidance at the time of treatment, and to review the position of the fiducials on the Live images adjacent to bony anatomy in order to ensure that the decisions taken to optimise fiducial tracking are appropriate.

Of note, it would be possible for a treatment to be rendered “Undeliverable” due to a RBE>Threshold owing to a “potentially migrated” fiducial. The position of this fiducial relative to other implanted fiducials may appear different to that at the time of Planning CT, but the fiducial may not have migrated (and may still therefore be a good surrogate for tumour), it may be correctly located at the site of implantation, but there may be deformation of the target due to e.g. filling of an adjacent bowel/duodenum loop. This issue will be further discussed in Chapter 3.

Figure 13:

Screenshot showing that the CK system has interpreted (erroneously) that Fiducial 1 is contributing most to the Rigid Body Error (RBE), as shown by the red square next to Fiducial 1. The system is being asked to correlate only Fiducials 1 and 4 (see "live" images). Fiducial 4 is the "migrating" fiducial.

RBE: 1 migrating fiducial and 2/3 fixed fiducials

When correlating combinations of 2 fixed fiducials and the single migrating fiducial, RBE is within "deliverable" threshold for up to a 2mm move of the migrating fiducial (RBE<2mm), see Table 3. At 4mm move of the migrating fiducial and beyond the RBE is beyond "deliverable" threshold as before, which is clinically appropriate.

It is notable that whilst the RBE is small (0.19-0.7mm) when the system is asked to correlate only fixed fiducials (which we know cannot have moved), the RBE is not 0. The reported RBE represents the

inherent error in defining the centre of each fiducial at the time of planning, and in interpreting the centre of each fiducial (which is limited by pixel size) in the Live X-rays at the time of treatment.

As expected, the RBE is larger (0.85-1.94mm) when correlating one of the two fixed fiducials with the migrating fiducial (at a 2mm move). The range for RBE encountered is likely to be related to how accurately the centre of each fiducial was defined at the time of planning (again there are limitations to this according to pixel size), and also whether the centre of each fiducial falls into the centre of a pixel or not on the Live images.

Of note, when correlating 3 fixed fiducials with a migrating fiducial, at 6mm move of the migrating fiducial, the CK in-room imaging system starts to misidentify a fiducial (see Table 4 and Graph 1). The RBE generated at a move of 6mm of the migrating fiducial (with 3 fixed fiducials) is "deliverable" in all cases (RBE 0.1-1.79mm) despite this large fiducial migration. This is important to note as in these scenarios, when a fiducial is misidentified, it is erroneously located relatively close to its expected position, resulting in a RBE which is "deliverable" which will not be appropriate in a fiducial-tracked treatment with typical (small) radiosurgical margins.

When correlating other fiducial combinations (e.g.fiducial 1 and 4, see Appendix 2.1), once a fiducial is misidentified (at 16mm move of fiducial 4), the RBE>2.75mm which is greater than the deliverable threshold.

The treatment radiographers therefore need to be even more vigilant when multiple fiducials (e.g. 4) are sited than when 2 fiducials are sited.

2.6 CONCLUSIONS

In this novel experimental phantom model with 1-3 fixed fiducials and 1 migrating fiducial:

1. The imaging of fiducial position by the CK in-room imaging system is accurate (to within 0.24mm) and reproducible (SD=0-0.09mm) as long as fiducials are correctly identified.

2. Fiducials are correctly identified across a clinically appropriate tracking range for fixed fiducial tracking (within 4mm of expected position).

3. Accurate interpretation of fiducial position depends not only on the distance that a migrating fiducial has moved relative to its reference position; it is also dependent on the number of fixed fiducials available for correlation. The greater the number of accurately located fiducials, the less likely the CK in-room system is to accurately locate a migrating fiducial.

4. Robot corrections (to adapt to discrepancies in fiducial position between Planning CT and time of treatment) are consistent (SD=0-0.4mm) for a given move of a migrating fiducial.

5. Robot corrections are mathematically appropriate based on the observed shift in fiducial centre of mass (as shown by manual verifications based on the root of the sum of the squares formula).

6. Where all fiducials are accurately identified in this phantom experiment with fixed fiducials and one migrating fiducial,

   Robot correction ~ Move of migrating fiducial (mm) ÷ n
   Where n = number of fiducials.

7. Reported Rigid Body Error (RBE) results have been manually verified (based on the root of the sum of the squares formula).

8. RBE > "Deliverable" threshold (therefore Robot corrections not generated) occurred when migrating fiducial had moved ≥4mm from its position at Planning CT. This would be considered clinically appropriate for fixed fiducial tracking given the small treatment margins applied in stereotactic treatments. See Discussion for caveats to this statement.

9. RBE within “Deliverable” threshold (i.e. Robot corrections generated and treatment can proceed) was achieved when migrating fiducial was ≤ 2mm from its position at Planning CT. This would be considered clinically appropriate (as 2mm will be less than CTV-PTV margin for fixed fiducial-tracked treatment). See Discussion for caveat to this statement.

10. When correlating all 4 fiducials with a move of 6mm (from Planning CT position) of the migrating fiducial, a fiducial was consistently misidentified close to its Expected location such that the RBE was within “Deliverable” threshold. This scenario is potentially concerning and confirms the need for close vigilance by the treatment radiographers at time of CK treatment.

These pre-clinical experiments have provided a foundation for understanding the accuracy and interpretation of fiducial location by the CyberKnife fiducial tracking system. Chapter 3 explores fiducial tracking in a clinical model.

References

1. Dieterich S, Gibbs IC. The CyberKnife in clinical use: current roles, future expectations. Front Radiat Ther Oncol. 2011;43:181-94.
2. Kitamura K, Shirato H, Shimizu S, Shinohara N, Harabayashi T, Shimizu T, et al. Registration accuracy and possible migration of internal fiducial gold marker implanted in prostate and liver treated with real-time tumor-tracking radiation therapy (RTRT). Radiother Oncol. 2002;62(3):275-81.
3. Wunderink W, Mendez Romero A, Seppenwoolde Y, de Boer H, Levendag P, Heijmen B. Potentials and limitations of guiding liver stereotactic body radiation therapy set-up on liver-implanted fiducial markers. Int J Radiat Oncol Biol Phys. 2010;77(5):1573-83.
4. Penney GP, Weese J, Little JA, Desmedt P, Hill DL, Hawkes DJ. A comparison of similarity measures for use in 2-D-3-D medical image registration. IEEE Trans Med Imaging. 1998;17(4):586-95.
5. Hatipoglu S, Mu Z, Dongshan F. Evaluation of a robust fiducial tracking algorithm for Image-guided radiosurgery. Proceedings of SPIE 2007;6509.
6. Murphy MJ. Fiducial-based targeting accuracy for external-beam radiotherapy. Med Phys. 2002;29(3):334-44.
7. Benedict SH, Yenice KM, Followill D, Galvin JM, Hinson W, Kavanagh B, et al. Stereotactic body radiation therapy: the report of AAPM Task Group 101. Med Phys. 2010;37(8):4078-101.

Appendix:

Appendix 2.1: Results from first Phantom Experiment: 1 fixed fiducial and 1 migrating fiducial

Move of tube from Start (mm)	Sup move of Fid 4 (mm)	Fid 1 Ref (x)	Fid 1 Live (X)	Fid 1 Ref (y)	Fid 1 Live (y)	Fid 1 Ref (z)	Fid 1 Live (z)	Fid 4 Ref (x)	Fid 4 Live (x)	Fid 4 Ref (y)	Fid 4 Live (y)	Fid 4 Ref (z)	Fid 4 Live (z)	RBE Fid 1-4
0	0 (0)	-41.69	-41.86	-2.75	-2.46	-2.52	-2.46	-25.45	-25.5	-0.88	-0.45	8.62	8.48	0
2	2 (0.05)	-41.69	-41.86	-2.75	-2.46	-2.52	-2.46	-25.45	-23.6	-0.88	-0.67	8.62	8.26	1.5
4	3.9 (0.09)	-41.69	-41.86	-2.75	-2.46	-2.52	-2.46	-25.45	-21.4	-0.88	-0.45	8.62	8.48	3.55
6	6 (0)	-41.69	-41.86	-2.75	-2.46	-2.52	-2.46	-25.45	-19.5	-0.88	-0.45	8.62	8.48	5.23
8	7.9 (0)	-41.69	-41.86	-2.75	-2.46	-2.52	-2.46	-25.45	-17.6	-0.88	-0.45	8.62	8.48	6.94
10	10.1 (0.09)	-41.69	-41.86	-2.75	-2.46	-2.52	-2.46	-25.45	-15.4	-0.88	-0.67	8.62	8.26	8.86
12	12 (0)	-41.69	-41.86	-2.75	-2.46	-2.52	-2.46	-25.45	-13.5	-0.88	-0.67	8.62	8.26	10.62
14	14 (0.06)	-41.69	-41.86	-2.75	-2.46	-2.52	-2.46	-25.45	-11.6	-0.88	-0.67	8.62	8.26	12.4
16	16.1 (0)	-41.69	-31.8	-2.75	-1.34	-2.52	6.25	-25.45	-9.4	-0.88	-0.67	8.62	8.26	2.75

CHAPTER 3

Stability and reproducibility of fiducial placement and Organ at Risk position in CyberKnife patients

3.1 INTRODUCTION

Non-spine Body treatments are usually tracked by fiducials (gold markers implanted in or around tumour). They act as surrogates for tumour position and their position can be determined by an in-room KV imaging system. The accuracy of fiducial-based tracking depends on the assumption that the inter-relationship between fiducials/tumour and Organs At Risk (OAR) is the same at the time of planning CT as at the time of treatment (1). However, it is known that a number of factors could invalidate this assumption.

3.1.1 Fiducial migration: Principles

Fiducial migration describes the movement of the inserted fiducials from their original position (at the time of fiducial placement) to a remote position, where they are no longer an adequate surrogate for tumour position/movement. It is recommended that the Planning CT scan is performed at least a week after insertion of fiducials to allow time for fiducial migration to occur (2). In theory, fiducial position captured on a Planning CT scan a week after fiducial insertion should be stable. There have been instances at my Centre, however, where this has not been the case.

Clinical example one: One CyberKnife patient with renal cell carcinoma of the superior pole of the right kidney had 4 fiducials inserted around the tumour. Post-insertion CT imaging (one-week later) showed that 3 fiducials were not well sited, the most optimally placed fiducial lay at the superior edge of the kidney. The physicists advised that treatment should be tracked with reference to this single optimally-placed fiducial, the other 3 fiducials were too far from the target to be reasonable surrogates. At the time of treatment on Day 1 the radiographers noted the relative arrangement of the fiducials appeared different to the DRR arrangement. Given that a single fiducial was to be tracked (therefore RBE would not be generated), and fiducial arrangement suggested possible fiducial migration, a CT was performed to assess fiducial position in more detail. This CT scan showed fiducial migration of the “optimally-

placed" fiducial (which had been inserted into peri-nephric fat), and treatment was postponed until further (well-placed) fiducials had been sited.

A further 4 fiducials were sited, all within the PTV, and treatment proceeded without event. The patient has had a Complete Response to treatment and remains well.

Clinical example two: A further patient with recurrent colorectal cancer with a solitary mesenteric node had three fiducials sited into adjacent mesenteric fat. Post fiducial insertion images showed the fiducials were well sited, but on the Planning CT two of the three fiducials had significantly migrated. The patient underwent treatment planning as it was felt that the single well-placed fiducial would be appropriate for tracking. However, at Day 1 CT, the fiducial had moved by 3cm from its position at Planning CT, and the patient did not proceed to treatment. A further CT another week later showed the fiducial had moved again, this time by 2cm. Radiology input concluded that the fiducial was lying in mesenteric fat, which was moving with bowel motion, and moving differently to the tumour target.

Following these examples, the Centre changed its protocol and a Day 1 CT scan is now performed on all patients that are to be tracked with fiducial tracking where the tumour is subject to respiratory motion i.e. Synchrony™ cases. Equally, if the CyberKnife team feel that a Day 1 CT is warranted due to specific concerns, then this is arranged.

It is our firm recommendation that the Day 1 CT be incorporated into routine clinical practice in such clinical scenarios, and therefore the archive of Day 1 CT scans is an important data set for analysis.

Various factors may contribute to the likelihood of fiducial migration. Intuitively, the most likely factor contributing to fiducial migration is "stability" of the tissue the fiducial is inserted into. The stability of a tissue is hard to quantify. Stability may partially depend on the density of the tissue (which would be relatively easy to quantify from CT data by Hounsfield Units), but also crucially on the micro-structure of the tissue, including the arrangement and contribution of connective tissue such as cartilage and fibrin strands. The stability of the tissue that the fiducial is inserted into will be assessed, this will be a qualitative judgement. It is hoped that the results may allow feedback to Radiologists/Endoscopists that perform fiducial placement, in order to maximise the chances of a successful fiducial implantation.

3.1.2 Fiducial migration: Histopathology of tumour

Tumour targets for treatment by CyberKnife vary in size, shape, and tissue of origin. The strategy for fiducial placement varies according to size/shape of the tumour target, and the relationship of the target with adjacent critical structures. Factors linked directly to the histopathology of the tumour are also considered, such as the risk of "seeding". This is more common in Gastro-intestinal malignancy, it refers to a tumour "seeding" in a biopsy or fiducial insertion tract (3).

An important principle of fiducial guidance is that the inserted fiducials act as true surrogates for tumour position. Therefore, whether the tumour target is potentially static (e.g. inguinal lymph node), or mobile (e.g. early stage lung tumour), it is important that implanted fiducials move exactly as tumour moves (4).

Fiducials may be either inserted directly into the tumour target, or surrounding the tumour target.

As an example, if the tumour target is a small, early stage (Stage 1) lung tumour (Non-Small Cell Lung Cancer, NSCLC), a single fiducial can reasonably be inserted into the tumour. This is particularly true when the tumour target is uniformly round, as rotations cannot be tracked with a single fiducial in situ. Translations only (not rotations) can be tracked with the Synchrony respiratory tracking system for lung tumours with a single fiducial target (5). The risk of seeding with a NSCLC tumour is negligible (<0.06%) (3).

An alternative strategy for an early stage lung tumour is to site 3-4 fiducials around the lung tumour. A potential disadvantage is that the further a fiducial is sited from the edge of a tumour target, the greater the potential that the fiducial could move differently to the tumour target. The potential for pneumothorax also increases according to the number of passes of the fiducial-placement needles, and the needle gauge. Pneumothorax risk reported is highly variable (8-38%) (6, 7). A potential advantage of inserting multiple fiducials surrounding tumour target, is that the accuracy of outlining of the tumour target may be improved by avoidance of CT artefact from a fiducial sited in the centre of the target, although this is more relevant for smaller tumours (8). A further advantage is that treatment (with rotational data captured) can still proceed if 1 of the 4 sited fiducials migrates (9). The Synchrony system can track tumour target translations (to within 25mm movement) and rotations (to within 1^0 for pitch and roll, and 3^0 for yaw (10).

A different example of a tumour target is a liver metastasis. There is some evidence that gastro-intestinal malignancies can seed along needle track sites (3). Liver metastases are often irregular in

shape. The fiducial placement strategy for liver metastases is therefore to site 3-4 fiducials surrounding the tumour. Fiducials should be sited >2cm apart, and not in the same sagittal plane. They should be sited in normal tissue (to avoid the potential risk of seeding if this is a consideration bearing in mind the histopathology), but as close to the edge of tumour as possible to maximise the chances that the fiducials will move in the identical way to the tumour target (2, 9).

Due to the different fiducial placement strategies according to tumour type described above, the Histopathology of the tumour type will be recorded when evaluating the stability of fiducial position between insertion and Planning CT/1st Day CT.

3.1.3 Number of fiducials in/around target, and proximity of fiducials to tumour target

When a tumour target is relatively large and accessible (to radiologist-guided fiducial placement), with no risk of tumour seeding, at least 3 fiducials may be sited within the tumour target e.g. prostate. However, a combination of size, accessibility, and seeding issues means that it is often not feasible or appropriate to site 3 fiducials in tumour lung, liver and pancreas sites.

As explained, rotation of the target can be assessed using 3 or more fiducials. Murphy et al (9), showed that the number of fiducials sited is also relevant. He stated that "if the orientation of a target site is important in the dosimetry, then at least 4 fiducials should be used".

Where fiducials are sited outside the tumour target, the distance of the fiducials to the edge of the tumour may also be an important consideration, when evaluating the likelihood of a given fiducial being a good surrogate for tumour.

I will examine the impact of these factors on the stability of fiducial placement.

3.1.3 Tumour deformation

If multiple fiducials remain fixed in position at the site of their insertion, but if fiducial position changes *relative* to their neighbouring fiducials (due to deformation), this can pose difficulties with the feasibility of fiducial tracking. Tumour deformation can occur due to changes in adjacent OARs (such as organ filling) between Planning CT and Day 1 CT. Tumour deformation can also occur due to a direct tumour effect e.g. growth of NSCLC to occlude an airway with deformation of tumour target due to collapse of adjacent lung.

Prior to delivery of each treatment beam the CyberKnife treatment console will display the expected positions of each fiducial as a Digitally Reconstructed Radiograph (DRR) generated from the Planning CT. The in-room imaging system will capture X-Rays to check positioning of fiducials and these live images are correlated with the DRR. If the entire tumour target has moved e.g. due to movement of a neighbouring structure such as bowel, but the relative positions of fiducials are identical to that of Planning CT, the CyberKnife system can generate the required corrections, the robot position can adjust accordingly and treatment can be delivered according to the treatment plan. If, however, the positions of the fiducials change relative to each other due to tumour deformation, a "Rigid Body Error" (RBE) will be generated by the CyberKnife system. If the RBE generated due to fiducial shift is greater than a certain threshold, a beam will not be able to be delivered, as there could be target miss. This scenario presents difficulties for treatment radiographers at the time of treatment delivery.

It may be that certain tumour targets are more at risk of tumour deformation than others. The CT data sets provide 3D information and are a unique data set to assess for tumour deformation. In contrast, the 2D imaging that is available for review at the time of treatment (via the treatment console) is more difficult to analyse for deformation, because it is not possible to define the edge of target on the 2D plain XR imaging.

Tumour deformation between Planning CT and Day 1 CT will be analysed in this Chapter.

3.1.4 Tumour growth

After a patient's CT planning scan has been performed, other Planning scans e.g. PET and MRI may also be performed for fusing with the Primary (Planning CT) scan.

The tumour target will then be outlined by the Oncologist, sometimes in collaboration with other Specialists, such as Surgeons and Radiologists.

Once a tumour target has been defined, and dose prescription and dose constraints have been set, CyberKnife Physicists will undertake planning. Given the ablative doses prescribed to target, and the proximity of radiosensitive OARs, the process of planning can take a number of days. There is therefore the potential for tumour growth in the interval between a Planning scan and treatment. This depends partly on the "Volume Doubling Time" of the tumour (this varies widely according to Histopathology; it also depends on the time interval between CT Planning and Treatment.

I will outline the tumour volume on the Planning CT and 1st Day CT to quantify the possible impact of tumour growth on fiducial spacing/arrangement.

3.1.5 Dose-limiting Organ At Risk (OAR) shift towards PTV

On the planned Treatment start day (Day 1), if there is an apparent change in fiducial location/arrangement compared to the planning scan, it is clinically important to understand the reason(s) for this, in order that appropriate action can be taken to accurately deliver a treatment to the tumour target.

However, delivery of the intended dose to the tumour target is not the only consideration. An equally important consideration is: will the dose-limiting OAR receive a safe dose of radiotherapy?

The stability of dose-limiting OAR relative to tumour target was recorded. The direction and magnitude of any shift in position was noted, and the effect of the shift on dosimetry was quantified.

3.1.6 Planning margins

As described in Section 1.1.1, the ICRU 50 report defined standards for describing radiotherapy prescription volumes (11). The Gross Tumour Volume represents the gross palpable or visible extent of disease. The Clinical Target Volume (CTV) incorporates a margin of normal tissue for unknown microscopic spread or subclinical disease. The Planning Target Volume (PTV) includes all other errors and uncertainties e.g. tumour motion and set-up errors.

The margin applied to transform a CTV to a PTV is termed a planning margin. Planning margins reported in the literature for Synchrony-tracked treatments vary between 2 and 8mm, margins of 3-5mm are commonly employed (12)

Standard planning margins at my Centre for the tumour sites studied here are as follows:

Lung: CTV to PTV margin: 2mm

Liver: CTV to PTV margin: 2-3mm

Pancreas: GTV/CTV to PTV margin: 2-3mm

The appropriateness of the above planning margins will be evaluated in light of the outcomes of the assessments made.

3.2 MATERIALS AND METHODS

3.2.1 Notes review

The CyberKnife database was retrospectively interrogated to retrieve names and details for patients receiving fiducial-tracked treatment for the following tumour sites: Lung, Liver and Pancreas. For each tumour site, where possible, a sample of patients with multiple fiducials available for tracking was selected, as well as a sample of patients where only a single fiducial was available for tracking. The patients were otherwise unselected and were therefore considered a representative sample of CyberKnife patients treated at this centre.

Primary histopathology of tumour, and number of fiducials inserted was recorded for each patient. Date of Planning CT and Day 1 Treatment CT was also recorded.

3.2.2 Imaging Analysis: Tumour Volume

The GTV volume (in cc's) drawn by the patient's Clinician was recorded from the MultiPlan system. In order that the Planning CT volume and Day 1 Treatment CT volume could be most meaningfully compared, the Planning CT GTV was drawn by myself (with the Clinician's contour "switched off", so that it was not visible at contouring). Where additional scans were fused to the Planning CT to aid the contouring process (e.g. PET, Contrast CT), these were always reviewed.

This process was repeated for the Day 1 CT ("B scan"), although the Day 1 CT scans were always non-Contrast scans.

The Window and Level selected for contouring was noted. The percentage difference in volume between the Clinician GTV contour and my own GTV contour from the Planning scan was calculated. The Clinician GTV contour was taken as the "reference" volume for calculation purposes. Therefore a "negative" percentage difference represented a GTV which was larger from the Clinician contour, than the GTV volume contoured by myself.

The percentage change in GTV volume between Planning CT and Day 1 treatment CT (both contoured by myself) was also calculated and recorded. The Planning CT was taken as the "reference" volume for this calculation. Therefore a "negative" percentage difference represented a GTV volume which had been contoured smaller on the Day 1 CT scan as compared to the Planning CT.

Tumour deformation is difficult to quantify. A qualitative judgement on this was made.

3.2.3 Imaging analysis: Fiducial location

CT Planning and Day 1 Treatment CT scans for the above patients were uploaded onto the CyberKnife MultiPlan planning system version 4.5 (Accuray, California). Both scans were captured in exhale breath-hold, with identical imaging parameters. CT slice spacing was 1.25mm.

These scans had been previously fused on Day 1 of patient Treatment by the Physics team, in order to confirm that there had been no significant fiducial migration, or significant Organ At Risk shift, and to determine that the planned PTV appropriately covered the tumour as seen on the Day 1 scan.

When viewing the scans on Multiplan, the Planning CT scan was always designated the "A" scan, the Primary scan. The "Align" tab on the MultiPlan system was selected, and number of fractions, body site, and treatment path was selected in order that it was possible to proceed to the "Fiducial" tab.

A judgement was made as to the stability of fiducial insertion site. This qualitative judgement was recorded, and it was also noted whether or not the fiducial was implanted in the GTV.

The centre of each fiducial had already been set (at the time of treatment planning), but each position was verified in this work. This was done by viewing each fiducial on axial, coronal and sagittal viewing planes, and then selecting (by clicking the mouse) the centre of the fiducial. Any discrepancy in x/y/z co-ordinate of fiducial >1mm (between the recorded centre, and my own judgement), was recorded. If any fiducial had migrated, this was recorded. Where more than one fiducial was sited, fiducials were ranked according to their location: the most optimally placed fiducial was ranked 1.

The Centre of Mass (COM) of the fiducials is referred to as the "Treatment Centre", this was calculated and recorded. Treatment Centre x, y, z position can be calculated according to the following formula: $x= \sum x/n$, $y= \sum y/n$, $z= \sum z/n$, where n= number of fiducials. It was noted whether the Treatment Centre lay within the PTV.

The above process was repeated for the Day 1 CT scan (designated the "B" scan). Of note, when assessing the centre of each fiducial on the B scan, it was important to disable the "Auto-Centre" function on Multiplan. This is because "the system" is always looking primarily at the A scan, and if my judgement was that a fiducial on the B scan is lying in a slightly different position, I would not be able to designate the centre of the fiducial on the B scan (the Auto-Centre function would mean that the fiducial

centre would default to the centre of that fiducial on the A scan). The shifts between Planning CT and Day 1 CT were recorded for each fiducial, and for the fiducial COM.

Where a fiducial lay outside the PTV, the distance of the fiducial to the closest PTV edge was recorded. If the Physics team had decided to reject a fiducial for tracking prior to treatment the reasons for this were recorded. Equally, if a fiducial was rejected by Radiographers at the time of treatment delivery, the reasons for this were also recorded.

3.2.4 Imaging Analysis: Organ At Risk (OAR) position and Dosimetry

The dose-limiting OAR was selected for analysis. The OAR was contoured on the Day 1 CT, with the original OAR contour (as drawn by the Clinical team on the planning scan) "switched off" as before, so that it would not prejudice my contouring.

As an initial assessment, the proximity of the "Day 1 OAR" to PTV was measured and compared to the proximity of Plan CT OAR to PTV. If the Day 1 OAR contour had shifted closer to PTV than on the Plan CT, further analysis was undertaken as described below.

Unfortunately it is not possible in MultiPlan to simply copy the original treatment plan on to a new dataset containing new contours. It is possible however, to sum the dose from the original plan with a plan created on the new dataset. Therefore, a workaround was developed which involved creating a dummy plan containing negligible dose at the location of the OAR, which could then be summed with the original plan on the new dataset. To create the dummy plan a false target was created at the inferior/anterior extent of the CT dataset, far away from the original target/OAR structures. A plan was then created containing multiple beams directed at this false target, and all but one of the beams were set to 0MU, with the remaining beam set to 1MU (MultiPlan requires all plans to contain at least 1MU before they can be summed). A high resolution dose calculation was then performed over the whole CT, and the dose at the OAR from the dummy plan was confirmed to be negligible. Therefore, once the original plan and the dummy plan were summed on the new dataset, the dose displayed at the OAR location consisted only of dose contributions from the original plan.

3.3 RESULTS

3.3.1 Lung tumour site: Tumour volume

Histopathology and Tumour volume data for 10 patients with implanted fiducials are shown in Table 3.1.

Table 3.1: Lung tumour cases: Tumour volume

Patient	Histopathology	Interval Plan CT to Day 1 CT (Days)	Clinician GTV (cc)	Planning CT GTV CG (cc)	Day 1 GTV CG (cc)	Change Clinician GTV to CG Planning CT GTV (%)	Change CG GTV Planning to Day 1 CT (%)
1	NSCLC	7	1.7	1.8	1.3	+6	-28
2	NSCLC	7	2.9	N/A	N/A	N/A	N/A
3	Colorectal	4	16.6	18.5	18.2	+11	-2
4	NSCLC	7	35.6	41.3	44.4	+16	+7
5	NSCLC	12	63.6	53.8	58.6	-15	+8
6	Colorectal	8	2.1	2.5	2.6	+16	+4
7	Colorectal	5	10.4	7.7	6.6	-26	-14
8	Colorectal	8	21.2	21.1	19.4	-0.5	-8
9	NSCLC	6	74	62.5	64.6	-16	+3
10	NSCLC	4	1.7	0.9	0.9	-47	0
Mean		7	23	23.3	24.1	-6	-3

As can be seen from the above table, 6 of the patients were treated for Non-Small Cell Lung Cancer (primary disease), and 4 patients were treated for Colorectal Cancer metastasis.

The interval (days) between Planning CT and the Day 1 of Treatment CT for each patient is displayed in the 3rd column. The mean and median interval between scans for this group as a whole were 6.8 days and 7 days respectively. Standard deviation = 2.2 days.

Clinician GTV volume (cc) and Planning CT GTV volume (cc) drawn by myself ("CG" as my initials) are displayed. Both contours were drawn on the same Planning CT scan. It was not possible to outline the "GTV" of Patient 2. This patient underwent surgical resection of endobronchial disease, and fiducials were placed at the time, to define the area that would be at high risk for recurrence in the future. The Surgeon defined the target volume in this case. There was no visible disease at the time of Planning CT.

Despite the fact that the GTV was outlined on the same Planning CT scan by both the Clinician and myself, there is a wide variability in volumes. The Mean and Standard Deviation of the percentage difference between the volumes are -7.2%, and 21.1%, confirming the variability in contouring between Clinical Oncologists (inter-observer variability).

There was also a wide variability between the GTV volumes drawn by myself on the Planning CT compared to the Day 1 CT volume. The Mean and Standard Deviation of the percentage difference between the volumes are -4.1% and 11.2% respectively. For this analysis, there was no risk of inter-observer variability skewing the results, as the same observer contoured both volumes.

None of the patients were receiving anti-cancer therapy between Planning CT, and Day 1 CT, so it may have been expected that the Day 1 CT volumes would be larger than the Planning CT volumes, but this was not always the case. Of note, the Day 1 CT scans were always Non-Contrast, as described, which made it more difficult to define the target on several of the Day 1 CT volumes. Patient 7's GTV was particularly difficult to define, and this patient was notable for showing moderate variability between Planning CT and Day 1 CT volumes. Patient 1 also had a difficult GTV to define, especially on the non-contrast Day 1 CT due to surrounding vasculature.

The limitations described above mean that it would not be reasonable to draw any conclusions about tumour growth between Planning and Day 1 CT scans.

There was no tumour deformation noted in any of the above cases.

3.3.2 Lung tumour site: Fiducial Reproducibility

Fiducial reproducibility data for 9 patients with single-implanted fiducials is displayed in Table 3.2.

COM = Centre Of Mass of fiducials

Std Dev = Standard Deviation

Table 3.2 Lung tumour site: Single fiducial: Fiducial reproducibility

Patient	Plan CT fiducial			Day 1 CT fiducial			Fiducial shift (mm)			Plan CT COM			Day 1 CT COM			Shift in COM		
	x	y	z	x	y	z	x	y	z	x	y	z	x	y	z	x	y	z
1	52.56	8.12	76	52.94	8.33	77	-0.38	-0.21	-1	52.56	8.12	76	52.94	8.33	77	-0.38	-0.21	-1
2	-58.45	-27.74	119.38	-58.74	-29.76	120	0.29	2.02	-0.62	-58.45	-27.74	119.38	-58.74	-29.76	120	0.29	2.02	-0.62
3	34.97	-4.27	238.18	34.81	-4.82	237.5	0.16	0.55	0.68	34.97	-4.27	238.18	34.81	-4.82	237.5	0.16	0.55	0.68
4	-91.77	28.11	161.25	-92.07	26.7	162.5	0.3	1.41	-1.25	-91.77	28.11	161.25	-92.07	26.7	162.5	0.3	1.41	-1.25
5	-77.83	-27.68	10.38	-78.1	-27.41	10	0.27	-0.27	0.38	-77.83	-27.68	10.38	-78.1	-27.41	10	0.27	-0.27	0.38
6	68.74	-7.07	-5.71	69.93	-9.39	-5	-0.89	2.32	-0.71	68.74	-7.07	-5.71	69.63	-9.39	-5	-0.89	2.32	-0.71
7	-54.57	-37.8	79.74	-54.09	-37.91	80	-0.48	0.11	-0.26	-54.57	-37.8	79.74	-54.09	-37.91	80	-0.48	0.11	-0.26
8	81.36	-20.87	111.8	81.98	-21.37	111.25	-0.62	0.5	0.55	81.36	-20.87	111.8	81.98	-21.37	111.25	-0.62	0.5	0.55
9	-49.09	8.46	-40.42	-50.64	7.75	-41.25	1.55	0.71	0.83	-49.09	8.46	-40.42	-50.64	7.75	-41.25	1.55	0.71	0.83
Mean							0.55	0.9	0.7							0.55	0.9	0.7
Std Dev							0.41	0.77	0.29							0.41	0.77	0.29

There was agreement between fiducial location as registered by the Physics team, and as registered by myself to within 1mm, except for patient 2. For patient 2, there was agreement on x and z locations, but the y location that was registered varied by 3mm between the Physics team and myself. The fiducial for patient 2 had a large artefact on CT.

The "Means" displayed in Table 3.2 were calculated to be Mean shift of fiducials from the Plan CT position. The direction of shift from the original position was not significant, only the magnitude of shift, therefore any minus signs were ignored when calculating the Means.

For a single-fiducial tracked CyberKnife treatment, as there is only one fiducial, the fiducial location position (at Planning CT), and the Planning CT COM is the same. Table 3.2 shows that Plan CT fiducial = Plan COM for each patient (columns highlighted in yellow) and similarly Day 1 CT fiducial = Day 1 CT COM (columns highlighted in blue). Equally Fiducial shift = COM shift for each patient, as there is only a single fiducial located.

Mean apparent shift in fiducial/COM position between initial Planning CT and Day 1 CT for the patient group as a whole is 0.55, 0.9 and 0.7mm in x, y and z directions respectively. Standard deviations were 0.41, 0.77 and 0.29mm for x, y and z directions respectively. The possible limitations to the accuracy of the methodology to calculate these shifts will be discussed in the Discussion.

Fiducial location and reproducibility data for an example patient with multiple-implanted fiducials is displayed in Tables 3.3A. Full data on the first 6 patients with multiple fiducials implanted for treatment of lung tumours is displayed in Appendix 1.

Table 3.3A: Lung tumour site: Multiple fiducials: Fiducial reproducibility: Patient 1

		Fid 1	Fid 2	Fid 3
Plan CT fiducial	x	-16.76	-14.08	-16.29
	y	35.04	43.39	35.71
	z	33	9.89	1.38
Day 1 CT fiducial	x	-14.83	-10.71	-15.72
	y	37.56	48.94	36.56
	z	33.17	10	-1.25
Fiducial Shift (mm)	x	-1.93	-3.37	-0.57
	y	-2.52	-5.55	-0.85
	z	-0.17	-0.11	2.63
Plan CT COM	x	-15.71		
	y	38.05		
	z	14.75		
Day 1 CT COM	x	-13.75		
	y	41.02		
	z	13.97		
Shift in COM (mm)	x	-1.96		
	y	-2.97		
	z	0.78		

The Plan CT COM is reported in Multiplan, but it can also be calculated. The x location of the Plan CT COM is the average of the x locations of fiducials 1-3 (see Table 3.3A, page 83). The y and z locations of the Plan CT COM are calculated in a similar way.

The Day 1 CT COM for each patient was also calculated.

Fiducial reproducibility data for 9 patients with lung tumours and multiple implanted fiducials is displayed in Figure 3.3B.

Table 3.3B: Lung tumour site: Multiple fiducials: Fiducial reproducibility

Patient	Number of fiducials	COM Shift (mm)		
		x	y	z
1	3	-1.96	-2.97	0.78
2	2	0.1	0.08	0.98
3	3	-0.32	0.02	-0.08
4	3	0.42	0.21	-0.42
5	3	2.44	0.33	-1.11
6	4	0.23	-0.43	0.86
7	3	-0.05	-0.37	-0.14
8	3	-0.14	-0.15	0.83
9	3	-0.01	-1	0.04
Mean	3	0.63	0.62	0.58
Standard Deviation	0.47	0.86	0.87	0.39

The “Means” displayed in Table 3.3B were calculated to be Mean shift of fiducial COM from the Plan CT position to the Day 1 CT position. As before, the direction of shift from the original position was not significant, only the magnitude of shift, therefore any minus signs were ignored when calculating the Means.

The mean shift (in mm) for fiducial COM for the group of patients with lung tumours and multiple fiducials is 0.63, 0.62 and 0.58 in x, y, and z directions respectively. The Standard Deviations were 0.86, 0.87 and 0.39.

The magnitude of mean shifts in COM for the multiple-fiducial cases described, are similar to the single-fiducial cases (COM shift 0.55, 0.9 and 0.7mm in x, y and z directions).

For the lung tumour patients as a whole the shift in fiducial COM between planning CT and Day 1 CT is sub-millimetre, overall mean shift was 0.59, 0.76 and 0.64mm in x, y and z directions respectively.

3.3.3 Lung tumour site: Fiducial Location

Assessment of Planning CT and Day 1 CT fusion allows a check that there has been no fiducial migration, and that the arrangement of fiducials is similar on the Day 1 CT to the Planning CT. There are other benefits to this assessment but these will be discussed later.

Stability/reproducibility of fiducial position is not the only consideration, an optimally located fiducial is also important. A sub-optimum placement can lead to difficulties in tracking at the time of treatment delivery. As there are risks to fiducial placement (bleeding, pneumothorax), it is advisable that every fiducial placed contributes to tracking. These aspects are displayed in Table 3.4.

NSCLC = Non-Small Cell Lung Cancer, CRC = Colorectal Cancer

Table 3.4: Lung tumour site: Single implanted fiducial: Fiducial location

Patient	Pathology	Fiducial in GTV/PTV	Implant tissue	Distance fiducial to PTV (mm)	Fiducials rejected?
1	NSCLC	Yes	Tumour	N/A	No
2	NSCLC	Yes	Tumour	N/A	No
3	Melanoma	No	Lung	4.4	No
4	NSCLC	Yes	Tumour	N/A	Yes: a 2nd fiducial migrated
5	NSCLC	Yes	Tumour	N/A	No
6	NSCLC	Yes	Tumour	N/A	No
7	NSCLC	Yes	Tumour	N/A	No
8	CRC	Yes	Tumour	N/A	No
9	NSCLC	Yes	Tumour	N/A	No

For a single-fiducial tracked treatment it is ideal that the fiducial lies in the tumour, so that it can be a true surrogate for tumour. This was the case for 8 out of 9 cases (89%). Patient 3 had a fiducial placed 4.4mm from PTV. It was judged that the fiducial was close enough to the tumour to be a good surrogate, and the patient proceeded to treatment without event.

There were no instances of a fiducial migrating out of the lung tumour once placed. Patient 4 had 2 fiducials placed, 1 in tumour (which was used for tracking), and the other in lung. The fiducial placed in lung migrated however, it was deposited close to the pleural edge, and review of the Planning CT showed that it had slipped in between the pleural layers, and was lying in the pleural recess.

Fiducial location data for 9 patients with multiple fiducials available for tracking are shown in Table 3.5.
NSCLC = Non-Small Cell Lung Cancer, CRC = Colorectal Cancer, Path=Pathology

Table 3.5: Lung tumour site: Multiple implanted fiducials: Fiducial location

Patient	Path	Fiducial	Fiducial in GTV/PTV	Implant tissue	Plan CT Fid COM in PTV	Distance fiducial to GTV/PTV(mm)	Fiducials rejected?
1	NSCLC	1	No	Bronchus	No	29/22.9	Yes: Fids 1,2
		2				18.7/13.9	
		3				13.5/8.8	
2	NSCLC	1	No	Lung	No	16.7/13	Yes: Fid 1
		2	Yes	Tumour		N/A	
3	CRC	1	Yes	Tumour	Yes	N/A	No
		2	Yes	Tumour		N/A	
		3	No	Lung		9/1.6	
4	NSCLC	1	Yes	Tumour	Yes	N/A	No
		2					
		3					
5	NSCLC	1	Yes	Tumour	Yes	N/A	No
		2					
		3					
6	CRC	1	No	Lung	No	13.5/7.9	Yes: Fids 1,2,4
		2	No	Lung		22/17	
		3	Yes	Tumour		N/A	
		4	No	Lung		11.1/4.3	
7	CRC	1	Yes	Tumour	Yes	N/A	No
		2	No	Lung		6.7/4.1	
		3	Yes	Tumour		N/A	
8	CRC	1	No	Lung	No	21.4/16.5	Yes: Fid 1
		2	No/Yes	Lung		4.1/In PTV	
		3	No/Yes	Lung		11.2/In PTV	
9	NSCLC	1	Yes	Tumour	Yes	N/A	No
		2					
		3					

There was no apparent fiducial migration (between Planning CT and Day 1 CT) for the cases displayed above.

7 out of 9 patients (78%) had fiducials implanted into tumour. Patient 1 had no tumour visible, therefore fiducials could not be inserted into tumour. Patient 8 (CRC) had no fiducials implanted in tumour, but tumour seeding is thought to be a risk of directly implanting the tumour.

27 fiducials were sited in total. 15/27 (56%) fiducials were sited in tumour.

Of the 12 fiducials that were not sited in tumour, 8 may have been deliberately placed in lung (rather than tumour) to avoid the risk of seeding. 4/8 (50%) of the fiducials placed in lung (not tumour) in Colorectal cancer cases were rejected prior to treatment delivery. The cases with rejected fiducials are described in more detail below.

Fiducials 1 and 2 of case 1 (NSCLC) were both rejected, only the closest fiducial was used to track treatment. The rejected fiducials were located 29 and 18.7mm away from GTV respectively.

Fiducial 1 of case 2 was rejected, it was located 16.7mm from the GTV, the other fiducial available was located inside the tumour.

Fiducials 1, 2 and 4 of case 6 were rejected prior to treatment delivery. The fiducials were situated 13.5, 22 and 11.1mm respectively from the closest edge of the GTV. Treatment was tracked instead using Fiducial 3 alone, which was located inside the GTV.

Fiducial 1 in case 8 was rejected, it was sited 21.4mm from the tumour (GTV), in the lung apex. At attempted treatment delivery, if this fiducial was included in fiducial tracking, the Rigid Body Error (RBE) increased to 2.5, suggesting that the fiducial may be moving differently to tumour. It was felt safer to reject this fiducial and track from the remaining 2 fiducials, which were inside the PTV.

Mean distance between a rejected fiducial and GTV was 18.9mm. In contrast, the mean distance between an acceptable fiducial and GTV was 4.2mm.

Even if individual fiducials are not located inside a tumour target, it is optimum for the fiducial COM to lie within PTV, to increase the chance that the fiducials will be a good surrogate for tumour. 5/9 cases (56%) had the Plan CT fiducial COM lying in the PTV. The “rejection strategy” for fiducials in Cases 2, 6 and 8, meant that the fiducial COM at the time of treatment delivery was located inside the PTV in 8/9 cases (89%). It was not possible to employ a fiducial rejection strategy for Case 1 that would shift the fiducial COM to inside the PTV, because all fiducials were placed superiorly to the target.

For the lung tumour group as a whole, fiducial migration occurred in just 1/18 patients (6%), and in 1/37 fiducials placed (3%). Fiducial COM (at the time of treatment delivery) was located inside the PTV for 16/18 patients (89%). 8/37 fiducials placed (22%) were rejected. 1 fiducial was rejected at planning due to migration into the pleural space, and the further 7 fiducials were rejected prior to/at the time of treatment delivery as described.

3.3.4 Lung tumour site: Organ At Risk Reproducibility

Assessment of Planning CT and Day 1 CT fusion allows a check on fiducial stability and reproducibility. As described the assessment allows a final time for reflection on the optimum combination of fiducials to be tracked to maximise the chances of accurate tracking of tumour at the time of treatment delivery.

The PTV contour can be overlaid on the Day 1 CT to check that by eye there is adequate coverage of the tumour.

The further important check of the fusion assessment, is to check that the Organs At Risk (OAR) will be receiving a safe dose. If there is shift of OAR into the high-dose region on the Day 1 CT, a CyberKnife treatment plan that was “safe” (based on Planning CT positions of tumour/OARs), may become unsafe.

Table 3.6 displays data on OAR reproducibility for 10 patients for the lung tumour site (the same patients as in Table 3.1). In each case the OAR specified in the table was the dose-limiting OAR.

NSCLC = Non-Small Cell Lung Cancer, CRC = Colorectal Cancer

Table 3.6: Lung tumour site: Organ At Risk (OAR) Reproducibility

Patient	Pathology	OAR	Dose-limiting OAR shift to PTV	Min Distance OAR to PTV on Plan CT (mm)	Min Distance OAR to PTV on Day 1 CT (mm)
1	NSCLC	Aorta	No	19.1	19.1
2	NSCLC	N/A	N/A	-	-
3	CRC	Bronchus	N/A	-	-
4	NSCLC	Chest Wall	No	0	0
5	NSCLC	Chest Wall	Yes	1mm overlap with PTV	2.5mm overlap with PTV
6	CRC	Chest Wall	No	15	17.5
7	CRC	N/A	N/A	-	-
8	CRC	Bronchus	Yes	1.5	2.5
9	NSCLC	Chest Wall	No	1.9mm overlap with PTV	1.9mm overlap with PTV
		Bronchus	Yes	5.3	1.9
10	NSCLC	Spinal cord	No	8.1	8.1

Of the 10 patients reviewed in Table 3.6, 7/10 (70%) had OARs which were either unsuitable for assessment, or had an identical/more favourable set-up with respect to OAR position on Day 1 CT as compared to Planning CT.

Patients 2, 3 and 7 had OARs unsuitable for assessment. Patients 2 and 7 had a small, peripheral lung tumour, the tumours were located remote from OARs such as chest wall, bronchi, mediastinum and cord. Patient 3 had a central lung tumour encircling the bronchus (OAR), Day 1 CT appearances showed the tumour encircling the bronchus exactly as at the Planning CT.

Patients 1, 4 and 10 had a perfectly reproducible OAR position between Planning CT and Day 1 CT. The OARs were Aorta, Chest Wall, and Spinal cord respectively. Patient 6 had a more favourable OAR position at Day 1 CT as compared to Planning CT.

Patient 9 had a less favourable position of bronchus at Day 1 CT as compared to Planning CT, (although chest wall position was stable). However, bronchus was not drawn on the original Planning CT so the impact of the OAR shift on bronchus dosimetry cannot be explored further.

Patients 5 and 8 had a less favourable position of their dose-limiting OARs (chest wall and bronchus respectively) on Day 1 CT as compared to the Planning CT scan.

3.3.5 Lung tumour site: Organ At Risk (OAR) Dosimetry

The impact of the OAR shift on OAR dosimetry for Patients 5 and 8 is explored further in Table 3.7.

MPD = Maximum point dose (dose limit allowed to be delivered to 0.035cc of OAR)

Table 3.7: Lung tumour site: Organ At Risk (OAR) Dosimetry

Patient	Number of fractions	OAR		MPD (Gy)	1cc threshold (Gy)	4cc threshold (Gy)	30cc threshold (Gy)
5	5	Chest Wall	Protocol	43	35	N/A	37.3
			Plan CT	58.1	53.9	N/A	44.3
			Day 1 CT	57.7	53.9	N/A	43.9
8	4	Bronchus	Protocol	35	N/A	16	N/A
			Plan CT	34.3	N/A	13.4	N/A
			Day 1 CT	35.8	N/A	15.7	N/A

It can be seen that Patient 5's planned doses to Chest Wall exceeded protocol dose, when considering both MPD, and the threshold limits. This was due to a decision taken by the treating Consultant to prioritise dose delivery to PTV over OAR dose. The coverage of PTV was 98.97%, meaning 98.97% of the PTV target was being treated to the prescription dose or greater. "Good" coverage is >95% and "Excellent" coverage is >98%. In order to maintain coverage of the PTV in this case, given the proximity of Chest Wall and tumour, the Chest Wall was treated to doses beyond those stated in the protocol. It is

noted that the doses to Chest Wall based on the Day 1 CT position of Chest Wall are overall marginally safer than anticipated (0.7% reduction in MPD, 0.9% reduction in 10cc threshold dose, 30cc threshold dose stable), though still greater than protocol doses.

Patient 8 had doses to Bronchus that were within protocol limits according to the Plan CT/treatment plan. However, due to the shift of bronchus towards PTV on the Day 1 CT scan, the MPD to Bronchus now breaches the “safe” protocol limits. The 4cc threshold dose has also increased due to the shift, but the calculated dose remains within protocol limits.

Overall, 1/7 patients treated for lung tumours (14%) eligible for assessment had an OAR shift towards PTV on Day 1 CT which resulted in an increase in calculated dose to the dose-limiting OAR beyond “safe” protocol levels.

3.3.6 Liver tumour site: Tumour volume

Histopathology and Tumour volume data for 6 patients with implanted fiducials are shown in Table 3.8.

Table 3.8: Liver tumour cases: Tumour volume

Patient	Histopathology	Interval Plan CT to Day 1 CT (Days)	Clinician GTV (cc)	Planning CT GTV CG (cc)	Day 1 GTV CG (cc)	Change Clinician GTV to CG Planning CT GTV (%)	Change CG GTV Planning to Day 1 CT (%)
1	Colorectal	8	116.4	186.2	103.6	+60	-44
2	Melanoma	5	5.5	4.4	7.5	-20	+71
3	Colorectal	5	37.2	35.6	39	-4	+10
4	Carcinoid	13	132.3	142.6	N/A	+8	N/A
5	Breast	4	1.7	2.8	3.8	+65	+36
6	Breast	6	6.4	10.2	10.4	+59	+2
Mean		7	49.9	63.6	32.9	+28	+15

The patients studied were all treated for metastatic disease. The histopathology of their primary disease is listed.

The interval (days) between Planning CT and the Day 1 of Treatment CT for each patient is displayed in the 3rd column. The mean and median interval between scans for this group as a whole were 7 days and 6 days respectively. Standard deviation = 3 days.

Clinician GTV volume (cc) and Planning CT GTV volume (cc) drawn by myself ("CG" as my initials) are displayed. Both contours were drawn on the same Planning CT scan. Despite the fact that the GTV was outlined on the same scan by both the Clinician and myself, there is a wide variability in volumes. The Mean and Standard Deviation of the percentage difference between the volumes are +28%, and 34%, confirming the variability in contouring between Clinical Oncologists (inter-observer variability).

There was also a wide variability between the GTV volumes drawn by myself on the Planning CT compared to the Day 1 CT volume. The Mean and Standard Deviation of the percentage difference

between the volumes are +15% and 38% respectively. For this analysis, there was no risk of inter-observer variability skewing the results, as the same observer contoured both volumes.

Patient 4 had a target volume which I felt was impossible to contour without the aid of Contrast (which is never given for the Day 1 CT scans). Liver metastases tend to enhance well with venous-phase contrast, and outlining is particularly difficult on non-contrast scans. It is likely, therefore, that any observed difference in tumour volume between Planning CT scan and Day 1 CT scan is more likely to be due to contouring difficulties, than a true change in size.

Tumour deformation was noted in patients 2 and 3.

3.3.7 Liver tumour site: Fiducial Reproducibility

Liver metastases tend to be irregular in shape (so it is important for tumour rotations to be tracked), and they are often reasonably large by the time of treatment with stereotactic body radiotherapy. In addition colorectal cancer, which frequently metastasises to liver, is prone to seeding along the needle track. For all these reasons, liver metastases tend to be marked with multiple gold fiducials surrounding the tumour for tracking purposes.

There is, therefore, no single-fiducial group for comparison for liver tumour site.

Fiducial reproducibility data for 9 patients with multiple-implanted fiducials is displayed in Table 3.9.

COM = Centre Of Mass of fiducials

Table 3.9: Liver tumour site: Multiple fiducials: Fiducial reproducibility

Patient	Number of fiducials	COM Shift (mm)		
		x	y	z
1	4	-2.05	0.45	-3.33
2	3	0.22	0.19	0
3	4	-0.15	-0.81	-2.88
4	3	0.12	-1	-0.2
5	4	1.36	-0.35	-2.19
6	4	0.67	-0.04	0.47
7	4	-0.26	0.12	0.16
8	4	0.3	-0.46	-0.61
9	4	-0.21	-0.04	0.57
Mean	3.8	0.59	0.38	1.16
Standard Deviation	0.4	0.63	0.32	1.21

The “Means” displayed in Table 3.9 were calculated to be Mean shift of fiducial COM from the Plan CT position to the Day 1 CT position. As before, the direction of shift from the original position was not significant, only the magnitude of shift, therefore any minus signs were ignored when calculating the Means.

The mean shift (in mm) for fiducial COM for the group of patients with liver tumours and multiple fiducials is 0.59, 0.38 and 1.16 in x, y, and z directions respectively. The Standard Deviations were 0.63, 0.32 and 1.21. The mean shift in the z axis COM for liver tumours is >1mm, whereas for lung tumours COM shift was <1mm in all axes. The Standard Deviation for COM shift in the z axis for liver tumours is also >1. The possible reasons for this, and the implications, will be discussed in the Discussion.

3.3.8 Liver tumour site: Fiducial Location

As described, the general approach for siting fiducials to mark liver tumours is to site multiple fiducials surrounding the tumour. The fiducials should be located close enough to tumour to be a good surrogate for tumour motion as the liver moves with respiration/bowel filling.

Fiducial location data for 9 patients with liver tumours is shown in Table 3.10.

CRC = Colorectal cancer, HCC = Hepatocellular cancer

Table 3.10: Liver tumour site: Fiducial location

Patient	Pathology	Fiducial	Fiducial in GTV/PTV	Implant tissue	Plan CT Fid COM in PTV	Distance fiducial to GTV/PTV(mm)	Fiducials rejected?
1	Melanoma	1	No	Liver	No	32/24	Yes: Fids 1,2,4
		2	No	Liver		34/25	
		3	Yes	Tumour		N/A	
		4	No	Liver		22/14	
2	CRC	1	Yes	Tumour	Yes	N/A	Yes: Fid 1
		2	Yes	Tumour		N/A	
		3	No/Yes	Liver		1/0	
3	Carcinoid	1	Yes	Tumour	Yes	N/A	Yes: Fids 2,3
		2	No/Yes	Liver		1/0	
		3	No	Liver		16/8	
		4	No/Yes	Liver		1/0	
4	Breast	1	No	Liver	Yes	25/16	Yes: Fid 2
		2	No	Liver		12/6	
		3	Yes	Tumour		N/A	
5	Breast	1	No	Liver	No	10/1	Yes: Fid 2,3,4
		2		Liver		10/3	
		3		Liver		12/5	
		4		Liver		46/37	
6	CRC	1	No	Liver	No	11/8	Yes: Fid 3
		2	No/Yes	Liver		1/0	
		3	No	Liver		37/34	
		4	No	Liver		14/9	
7	HCC	1	No/Yes	Liver	Yes	1/0	Yes: Fid 2
		2	No/Yes	Liver		1/0	
		3	No/Yes	Liver		1/0	
		4	No	Liver		47/38	
8	CRC	1	Yes	Tumour	Yes	N/A	No
		2	No/Yes	Liver		1/0	
		3	Yes	Tumour		N/A	
		4	Yes	Tumour		N/A	
9	CRC	1	No	Liver	No	19/14	Yes: Fids 1,3,4
		2	Yes	Tumour		N/A	
		3	No	Liver		35/28	
		4	No	Liver		33/27	

There were no instances of a fiducial migrating from the site of implantation when fusing Plan CT and Day 1 CT.

As explained, the general approach for the above patients is to site multiple fiducials surrounding tumour. However, 6/9 patients (67%) and 8/9 patients (89%) had at least one fiducial sited in GTV and PTV respectively. Of the 3 patients with no fiducials sited in tumour the pathology of their primary disease was breast, colorectal and hepatocellular cancer.

34 fiducials were sited in total, 9/34 (26%) were sited in tumour. Of the 25 fiducials that were sited in liver (rather than tumour), 9/25 (36%) were sited to mark colorectal cancer metastases, 6/25 (24%) to mark breast cancer metastases, 4/25 (16%) to mark a hepatocellular metastasis and 3/25 (12%) to mark a carcinoid and a melanoma metastasis.

15/34 fiducials (44%) were rejected for tracking. Mean distance of a rejected fiducial to the closest GTV edge was 21mm (range 0-46mm). In contrast, the mean distance of an accepted fiducial to the GTV was 6mm (range 0-47mm).

The reasons for rejecting fiducials are explained in more detail below.

Patients 1 and 9 both had 4 fiducials sited. In each case, 3/4 of the fiducials were sited moderately far from the tumour target, but the remaining fiducial was located in tumour target. The 3 remote fiducials were rejected in each case, and treatment was performed tracking the solitary intra-tumour fiducial only.

Patient 2 had 3 well-placed fiducials, however, an intra-tumour fiducial was rejected at treatment delivery because its position was inconsistent (as viewed on the live X-rays and by reference to RBE readings). This metastasis appeared low-density and necrotic on CT. A potential contributing factor for patient 2 was tumour deformation. The metastasis was peripherally-located, and different duodenal filling between Plan CT and Day 1 CTs appeared to affect the position of fiducial 1.

Patient 3 had 2 fiducials rejected. One was 16mm from tumour, the other rejected fiducial was just 1mm from the edge of tumour. This patient may also have experienced tumour deformation. The metastasis was peripheral. Differential filling of bowel was noted between Plan CT and Day 1 CT. Of note, this patient had had prior hepatic resection therefore a number of loops of bowel were lying more superior than normal, adjacent to the tumour target.

Patient 4 had a single fiducial rejected. The fiducial was 12mm away from tumour. The fiducial was rejected for 2 out of the 3 treatment fractions (due to RBE increasing when it was included), but it was tracked without issues for the remaining fraction.

Patient 5 had 3 well-placed fiducials, and a further fiducial which was further from tumour. At treatment only the closest fiducial was tracked however. Inclusion of all other fiducials increased the RBE.

Patient 6 had 3 well-placed fiducials (within 15mm of tumour), and a fiducial lying 37mm from tumour which was rejected.

Finally, patient 7 had a necrotic tumour with 3 fiducials placed at the edge of the tumour, and a fiducial lying 47mm from tumour. At Plan CT/Day 1 CT fusion it was advised that tracking would be done by the 3 fiducials at the tumour edge, and reject the remote fiducial. In practice, however, one of the edge fiducials was rejected due to inconsistent position, and the fiducial that was 47mm away from tumour was tracked as it seemed to be a good surrogate for tumour, and to allow rotations to be tracked.

In summary, fiducials were rejected for reasons of:

1. Remote placement ≥ 10mm from tumour, 12/15 fiducials (80%)
2. Tumour deformation, 2/15 fiducials (13%)
3. Necrotic tumour, 1/15 fiducials (7%).

Assessing the fiducial COM, this was located in the tumour in 5/9 cases (56%). The rejection strategies employed which have been described, shifted the COM into the tumour in a further 2 cases (22%). The remaining 2 cases had the COM shifted the edge of PTV by the rejection strategy employed.

In summary, for liver tumour site, fiducial migration did not occur in the sample of patients studied. Fiducial COM was located in the tumour at the time of treatment delivery for 7/9 (78%) of patients. 15/34 fiducials (44%) were rejected for tracking. A majority of fiducials (80%) rejected were placed remote from tumour (≥10mm). Other fiducials were rejected due to issues related to tumour deformation and necrotic tumour.

3.3.9 Liver tumour site: Organ At Risk reproducibility

Table 3.11 displays data on OAR reproducibility for 6 patients for the liver tumour site. In each case the OAR specified in the table was the dose-limiting OAR.

CRC = Colorectal Cancer

Table 3.11: Liver tumour site: Organ At Risk (OAR) Reproducibility

Patient	Pathology	OAR	Dose-limiting OAR shift to PTV	Min Distance OAR to PTV on Plan CT (mm)	Min Distance OAR to PTV on Day 1 CT (mm)
1	CRC	Oesophagus	No	8	10
		Spinal cord	No	49	57
2	Melanoma	Chest Wall	No	1.5	2
3	CRC	Duodenum	No	1.6mm overlap with PTV	0.5mm overlap with PTV
		Bowel	No	13.5mm overlap with PTV	2mm overlap with PTV
4	Carcinoid	Bowel	Yes	4.3mm overlap with PTV	7mm overlap with PTV
		Liver	N/A	See text	See text
5	Breast	Duodenum	Yes	0.8	0.2
6	Breast	Chest Wall	No	0	0

Out of the 6 patients assessed, 2 patients (33%) had a shift in OAR position towards the PTV (on the Day 1 CT as compared to the Plan CT). Patient 6 appeared to have a stable OAR position on Day 1 CT compared to Plan CT. The remaining patients had a shift of OAR away from PTV (on Day 1 CT as compared to Plan CT).

Patient 4 had a large liver metastasis in a liver which had previously been resected. In this patient therefore, dose to liver was potentially limiting, and accurate outlining of liver volume was crucial. Liver volume as outlined on Plan CT for this case was 1343.6cc. Liver volume as outlined on Day 1 CT by the

author = 1344.6cc. These volumes are very similar, and the Day 1 CT liver volume was more generous, which is reassuring regarding liver doses received by this patient.

3.3.10 Liver tumour site: Organ At Risk dosimetry

The OAR dosimetry of the patients with a less favourable OAR position at Day 1 CT, in addition to the patient with a stable OAR position at Day 1 CT, is explored in Table 3.12.

Table 3.12: Liver tumour site: Organ At Risk (OAR) Dosimetry

MPD = Maximum point dose (dose limit allowed to be delivered to 0.035cc of OAR)

Patient	Number of fractions	OAR		MPD (Gy)	5cc threshold (Gy)	10cc threshold (Gy)	30cc threshold (Gy)
4	3	Bowel	Protocol	25.2	17.7	N/A	N/A
			Plan CT	26.2	18.4	N/A	N/A
			Day 1 CT	29.8	18.6	N/A	N/A
5	3	Duodenum	Protocol	24	16.5	11.4	N/A
			Plan CT	22.8	8.3	5.4	N/A
			Day 1 CT	27.7	8.9	6.1	N/A
6	3	Chest Wall	Protocol	36.9	N/A	30 (ideal)	30 (absolute)
			Plan CT	43.1	N/A	17.1	11.6
			Day 1 CT	42.2	N/A	16.5	11.4

It can be seen that Patient 4's planned doses to Bowel exceeded protocol dose, when considering both MPD, and the 5cc threshold limit. This was due to a decision taken by the treating Consultant to maximise dose delivery to PTV, whilst also bearing in mind OAR dose. The coverage of PTV in this case

was 93.9% (less than the ideal coverage of 95%). In order to maintain coverage of the PTV in this case, given the proximity of Bowel and tumour, the Bowel was treated to doses beyond those stated in the protocol. It is noted that the doses to Bowel based on the Day 1 CT position of Bowel were higher than anticipated (13.7% increase in MPD, 1.1% increase in 5cc threshold dose). This could increase the risk of morbidity for the patient.

Patient 4's Liver doses were also calculated. Protocol specifies that doses ≥21Gy should be received by ≤30% of liver volume, and doses ≥15Gy should be received by ≤50% of liver volume. Despite the large tumour/resected liver, planned doses were well within limits (14.3Gy to ≤30% liver, and 9.7Gy to ≤50% liver). Day 1 CT calculated doses to liver were identical to the planned doses.

Patient 5 had doses to Duodenum that were within protocol limits according to the Plan CT/treatment plan. However, due to the Duodenum shift towards PTV on the Day 1 CT scan, the MPD to Duodenum now breaches the "safe" protocol limits (21.5% increase in MPD compared to Plan CT doses). The 5cc and 10cc threshold doses also increased due to the shift, but the calculated doses remain within protocol limits.

Patient 6 had planned MPD to the Chest wall exceeding protocol limits, although 10cc and 30cc threshold doses were well within limits. Coverage of the PTV by the prescribed dose was 98.6% and the treating Consultant wished that the dose to PTV was not compromised in order to reduce chest wall doses. It is noted that doses to Chest wall are marginally reduced according to the Day 1 CT position of Chest wall (2.1% decrease) although the MPD still exceeds protocol limits.

Overall, 2/6 patients with liver tumours (33%) had an OAR shift towards PTV on Day 1 CT which resulted in an increase in calculated dose to the dose-limiting OAR beyond "safe" protocol levels. This could potentially increase the risk of toxicity.

3.3.11 Pancreas tumour site: Tumour volume

Histopathology and Tumour volume data for 4 patients with implanted fiducials is shown in Table 3.13. All pancreatic tumours studied were adenocarcinoma of pancreas.

Table 3.13: Pancreatic tumour cases: Tumour volume

Patient	Interval Plan CT to Day 1 CT (Days)	Clinician GTV (cc)	Planning CT GTV CG (cc)	Day 1 GTV CG (cc)	Change Clinician GTV to CG Planning CT GTV (%)	Change CG GTV Planning to Day 1 CT (%)
1	5	39	31.6	32.7	-19	+4
2	6	84.6	72.3	88	-15	+22
3	5	54.4	38.6	52.5	-29	+36
4	12	18.7	22.2	17.9	+19	-19
Mean	7	49.2	41.2	47.8	-11	+11

The mean and median interval (days) between Planning and Day 1 CT scans for patients with pancreatic tumours were 7 days and 5.5 days respectively. Standard deviation = 3 days.

Clinician GTV volume (cc) and Planning CT GTV volume (cc) drawn by myself ("CG" as my initials) are displayed. Both contours were drawn on the same Planning CT scan. Despite the fact that the GTV was outlined on the same scan by both the Clinician and myself, there is again a wide variability in volumes. The Mean and Standard Deviation of the percentage difference between the volumes are -11%, and 18%, confirming the variability in contouring between Clinical Oncologists (inter-observer variability). Of note, for the first 2 patients listed, the volume drawn by the Clinician was labelled as "Clinical Target Volume (CTV)". The visible disease may therefore have been outlined generously to incorporate microscopic spread of disease, and this may be an explanation for the Clinician volume being greater than the volume drawn by myself.

There was also a wide variability between the GTV volumes drawn by myself on the Planning CT compared to the Day 1 CT volume. The Mean and Standard Deviation of the percentage difference between the volumes are +11% and 18% respectively. For this analysis, there was no risk of inter-observer variability skewing the results, as the same observer contoured both volumes. However, as

before, the Day 1 CT scans were performed without intravenous contrast, and in all cases outlining on the non-contrast Day 1 CT scans was very difficult due to poor definition of structures.

There was no tumour deformation noted in any of the above cases.

3.3.12 Pancreas tumour site: Fiducial Reproducibility

Pancreatic tumours tend to be irregular in shape, so ideally multiple fiducials would be placed surrounding tumour target such that rotations can be tracked. However, optimum fiducial placement is often limited by the proximity of critical structures to the tumour (bowel, mesenteric blood vessels). Fiducials to mark pancreatic tumours can be placed percutaneously under CT guidance, endoscopically via stomach/duodenum, or laparoscopically.

Fiducial reproducibility data for 9 patients with single-implanted fiducials is displayed in Table 3.14.

COM = Centre Of Mass of fiducials

Table 3.14 Pancreas tumour site: Single fiducial: Fiducial reproducibility

Patient	Plan CT fiducial			Day 1 CT fiducial			Fiducial shift (mm)			Plan CT COM			Day 1 CT COM			Shift in COM		
	x	y	z	x	y	z	x	y	z	x	y	z	x	y	z	x	y	z
1	28.13	-18.75	0.74	29.01	21.55	0	-0.88	2.8	0.74	28.13	-18.75	0.74	29.01	21.55	0	-0.88	2.8	0.74
2	6.22	-54.21	-23.13	6.9	-54.89	-23.13	-0.68	0.68	0	6.22	-54.21	-23.13	6.9	-54.89	-23.13	-0.68	0.68	0
3	6.35	-65.28	-61.88	6.26	-66.79	-62.5	0.09	1.51	0.62	6.35	-65.28	-61.88	6.26	-66.79	-62.5	0.09	1.51	0.62
4	-21.65	-41.41	-110.39	-21.93	-41.76	-110	0.28	0.35	-0.39	-21.65	-41.41	-110.39	-21.93	-41.76	-110	0.28	0.35	-0.39
5	-41.81	-16.02	-27	-41.39	-17.02	-26.5	-0.42	1	-0.5	-41.81	-16.02	-27	-41.39	-17.02	-26.5	-0.42	1	-0.5
6	-29.2	-66.65	-5	-29.01	-66.79	-5	-0.19	0.14	0	-29.2	-66.65	-5	-29.01	-66.79	-5	-0.19	0.14	0
7	-4.79	-4.79	-32.05	-4.87	-5.02	-32.5	0.08	0.08	0.45	-4.79	-4.79	-32.05	-4.87	-5.02	-32.5	0.08	0.08	0.45
8	-13.96	-13.96	18.96	-13.96	-29.2	21.25	0	-1.3	-2.29	-13.96	-13.96	18.96	-13.96	-29.2	21.25	0	-1.3	-2.29
9	-5.08	-57.38	46.5	-5.11	-56.19	46.25	0.03	-1.19	0.25	-5.08	-57.38	46.5	-5.11	-56.19	46.25	0.03	-1.19	0.25
Mean							0.29	1.01	0.58							0.29	1.01	0.58
Std Dev							0.29	0.8	0.65							0.29	0.8	0.65

There was agreement between fiducial location as registered by the Physics team and as registered by myself to within 1mm.

The “Means” displayed in Table 3.14 were calculated to be Mean shift of fiducials from the Plan CT position. The direction of shift from the original position was not significant, only the magnitude of shift, therefore any minus signs were ignored when calculating the Means.

For a single-fiducial tracked CyberKnife treatment, as there is only one fiducial, the fiducial location position (at Planning CT), and the Planning CT COM is the same. Table 3.14 confirms that Plan CT fiducial = Plan COM for each patient (columns highlighted in yellow) and similarly Day 1 CT fiducial = Day 1 CT COM (columns highlighted in blue). Equally Fiducial shift = COM shift for each patient, as there is only a single fiducial located.

Mean apparent shift in fiducial/COM position between initial Planning CT and Day 1 CT for this patient group with pancreatic tumours and single-implanted fiducials was 0.29, 1.01 and 0.58mm in x, y and z directions respectively. Standard deviations were 0.29, 0.8 and 0.65mm for x, y and z directions respectively.

Summary data for 9 patients with pancreatic tumours and multiple implanted fiducials is shown in Table 3.15.

COM = Centre Of Mass of fiducials.

Table 3.15: Pancreas tumour site: Multiple fiducials: Fiducial reproducibility

Patient	Number of fiducials	COM Shift (mm)		
		x	y	z
1	3	0.68	1.87	0.2
2	4	0.24	0	-0.25
3	3	-0.25	0.49	0.09
4	3	1.51	-1.31	-0.1
5	3	0.2	-0.44	-0.06
6	2	0.17	0.51	0.05
7	2	2.93	-0.87	1.67
8	2	-0.33	0.44	-0.24
9	2	-2.72	-0.81	0.98
Mean	2.7	1	0.75	0.4
Standard Deviation	0.7	1.05	0.52	0.52

The “Means” displayed in Table 3.15 were calculated to be Mean shift of fiducial COM from the Plan CT position to the Day 1 CT position. As before, the direction of shift from the original position was not significant, only the magnitude of shift, therefore any minus signs were ignored when calculating the Means.

The mean shift (in mm) for fiducial COM for patients with pancreatic tumours and multiple fiducials was 1, 0.75 and 0.4mm in x, y, and z directions respectively. The Standard Deviations were 1.05, 0.52 and 0.52mm.

The magnitude of mean shifts in COM for the multiple-fiducial cases described, are similar to the single-fiducial cases (COM shift 0.29, 1.01 and 0.58mm in x, y and z directions).

For the pancreas tumour patients as a whole, the shift in fiducial COM between planning CT and Day 1 CT was sub-millimetre, overall mean shift was 0.65, 0.88 and 0.49mm in x, y and z directions respectively.

3.3.13 Pancreatic tumour site: Fiducial Location

As described, the general approach for siting fiducials to mark pancreatic tumours is to site multiple fiducials surrounding the tumour. This is most often performed percutaneously via CT guidance. The fiducials should be located close enough to tumour to be a good surrogate for tumour motion as the pancreas moves with respiration/bowel and duodenal filling.

The location of certain pancreatic tumours prevents a percutaneous approach due to access issues. If this is the case, either an endoscopic, or more rarely, a laparoscopic approach is undertaken.

Fiducial location data for 9 patients with pancreatic tumours and multiple implanted fiducials is shown in Table 3.16.

Lap = Laparoscopic approach to implant fiducials

CT = Percutaneous approach with CT guidance to place fiducials

EUS = Endoscopic UltraSound approach to site fiducials

Table 3.16: Pancreas tumour site: Fiducial location: Multiple-implanted fiducials

Patient	Approach	Fiducial	Fiducial in GTV/PTV	Implant tissue	Plan CT Fid COM in PTV	Distance fiducial to GTV/PTV(mm)	Fiducials rejected?
1	CT	1	No	Pancreas	Yes	44/42	Yes: Fid1
		2	Yes	Tumour		N/A	
		3	Yes	Tumour		N/A	
2	CT	1	No	Pancreas	Yes	11/5	Yes: Fids 1,2
		2	No/Yes	Pancreas		4/0	
		3	Yes	Tumour		N/A	
		4	Yes	Tumour		N/A	
3	CT	1	Yes	Tumour	Yes	N/A	Yes: Fid1
		2					
		3					
4	Lap	1	Yes	Tumour	Yes	N/A	No*
		2					
		3					
5	CT	1	No	Mesenteric fat	No	24/19	Yes: Fids 1,2
		2	No	Mesenteric fat		11/5	
		3	Yes	Tumour		N/A	
6	EUS	1	Yes	Tumour	Yes	N/A	No
		2					
7	CT	1	Yes	Tumour	Yes	N/A	Yes: Fid 1
		2					
8	EUS	1	Yes	Tumour	Yes	N/A	No
		2					
9	EUS	1	Yes	Tumour	Yes	N/A	Yes: Fid 2
		2	No	Mesenteric fat		3/1	

5/9 patients (56%) had fiducials placed percutaneously, 3/9 patients (33%) by endoscopic ultrasound, and a single patient (11%) had fiducials sited at laparoscopy.

Patient 4 had to have a second fiducial placement procedure due to migration of fiducials following the first implantation. There was no imaging taken immediately after the first laparoscopy, but at the first Planning CT all 3 fiducials had apparently migrated. The fiducials were located 3.2cm, 7.3cm and 8cm from the tumour. The fiducials may have migrated along fat planes as they came to rest in the perinephric fat. At repeat laparoscopy all 3 fiducials were placed in the tumour and this was a stable position.

There were no further instances of a fiducial migrating from the site of implantation when fusing Plan CT and Day 1 CT.

All patients had at least one fiducial placed in tumour.

24 fiducials were sited in total (excluding the 3 migrated fiducials from Patient 4).

18/24 (75%) were sited in tumour, 3/24 (12.5%) in pancreas, and 3/24 (12.5%) in mesenteric fat.

8/24 fiducials (33%) were rejected for tracking. Mean distance of a rejected fiducial to the closest GTV edge was 16mm (range 0-44mm). In contrast, all accepted fiducials were located inside the GTV (i.e. inside tumour). However, not all intra-tumour fiducials were accepted, 14/16 intra-tumour fiducials were accepted (88%).

6/9 patients (67%) had instances of fiducials being rejected.

Patient 1 had a pancreatic head tumour, and one rejected fiducial, this was located in the tail of pancreas 4.4cm from tumour. At treatment, it was noted to be moving differently to the 2 intra-tumour fiducials.

Patient 2 had two rejected fiducials lying only 11mm (fiducial 1) and 4mm (fiducial 2) from tumour. Fiducial 1 was rejected for each of the 3 treatment fractions as it moved differently to the 2 intra-tumour fiducials (fiducials 3 and 4). Fiducial 1 was located on the periphery of pancreas, adjacent to stomach. The stomach was noted to be fuller at Planning CT. Fiducial 2 was rejected for fraction 3 only, it was positioned at the interface between the tumour and the second part of the duodenum.

Patient 3 had an intra-tumour fiducial rejected because it was lying too close (13 mm separation) to the other intra-tumour fiducial. The orientation of fiducial 1 was also changed compared to the orientation

at Planning CT (long axis of fiducial orientated anterior/posterior at Planning CT compared to right/left at Day 1 CT), which contributed to tracking issues at the time of treatment delivery.

Patient 5 had 2 fiducials rejected, both were located in fat, anterior to the tumour. Fiducial 1 was located in peri-bowel fat. Both of these rejected fiducials moved differently to the remaining intra-tumour fiducial.

Patient 7 had an intra-tumour fiducial rejected (fiducial 1). This was located anteriorly in the tumour, and adjacent to the duodenum. It was noted that the stomach/duodenum was more dilated at planning CT than at Day 1 CT. Differential stomach/duodenum filling may have contributed to apparent fiducial shift between scans (shift for fiducial 1 was 1.31, 0.89 and 3.75mm in x, y, and z directions respectively).

Patient 9 had a fiducial rejected which was located in mesenteric fat anterior to the tumour, and adjacent to the pylorus of stomach. At Day 1 CT this fiducial appeared to have shifted position, although it was still lying in mesenteric fat. The fiducial had shifted by 4.81, 1.31, and 0.36mm in x, y and z axes respectively compared to the planning CT.

In summary, fiducials were rejected for reasons of:

1. Unstable fiducial placement in mesenteric fat, 3/8 fiducials (38%)
2. Fiducial placement in pancreatic periphery, adjacent to stomach/duodenum, different filling of stomach/duodenum on Planning CT vs Day 1 CT, 3/8 fiducials (38%)
3. Remote fiducial placement (>4cm from tumour) in pancreas, 1/8 fiducials (12.5%)
4. Fiducial placement too close to indwelling fiducial, 1/8 fiducials (12.5%)

Assessing the fiducial COM, this was located in the tumour in 8/9 cases (89%). The rejection strategies employed which have been described, shifted the COM into the tumour in the remaining case.

In summary, for pancreas tumour site and multiple-implanted fiducial cases, fiducial migration occurred solely following a laparoscopic approach to implant fiducials. Fiducial COM was located in the tumour at the time of treatment delivery for all patients. 8/24 fiducials (33%) were rejected for tracking. All fiducials sited in mesenteric fat were rejected as they were a poor surrogate for tumour motion. Fiducials placed at the periphery of pancreas, and adjacent to stomach/duodenum were rejected due to apparent shift from their position at Planning CT, which was likely to be explained by differential stomach/duodenal filling (at Day 1 CT compared to Planning CT). Further fiducials were rejected for

being too remote from tumour, (and therefore an inappropriate surrogate for tumour), and for being too close (<2cm) to other implanted fiducials.

A further 6 patients with pancreatic tumours and single-implanted fiducials were assessed. 4/6 patients (67%) had the fiducial placed by endoscopic ultrasound, and the remaining 2 patients (33%) had the fiducial placed laparoscopically. One of the laparoscopic cases had initially had 3 fiducials implanted, but 2 fiducials had migrated (to >10cm from the tumour) by the time of Planning CT leaving a solitary intra-tumour fiducial. The operation note described that the two migrated fiducials were both placed in fat adjacent to the tumour.

5/6 patients (83%) had the solitary fiducials placed in the tumour. The remaining patient had the fiducial sited via endoscopic ultrasound, the fiducial was lying in the duodenal wall, on the periphery of the PTV and just 3mm from tumour. The position at Planning CT and Day 1 CT was stable.

In summary, for the 15 patients with pancreatic tumours described above, the following has been observed:

1. All fiducials sited in fat (8 fiducials) were rejected for tracking (either due to fiducial migration, or due to being a poor surrogate for tumour motion).
2. 14/15 patients (93%) had at least one intra-tumour fiducial placed.
3. 14/15 patients (93%) had a fiducial COM located in tumour at the time of treatment delivery.
4. The remaining patient had the fiducial sited at the edge of the PTV and only 3mm from tumour.
5. Fiducial tracking issues were sometimes encountered when fiducials were located at the periphery of normal pancreas and adjacent to duodenum/stomach. The difficulties appeared to be related to differential stomach/duodenal filling at treatment compared to planning.

3.3.14 Pancreas tumour site: Organ At Risk reproducibility

Table 3.17 displays data on OAR reproducibility for 1 patient for the pancreas tumour site.

Table 3.17: Pancreas tumour site: Organ At Risk (OAR) Reproducibility

Patient	OAR	Dose-limiting OAR shift to PTV	Min Distance OAR to PTV on Plan CT (mm)	Min Distance OAR to PTV on Day 1 CT (mm)
1	Duodenum	Yes	6mm overlap	11mm overlap

3.3.15 Pancreas tumour site: Organ At Risk dosimetry

The OAR dosimetry of the above patient is displayed in Table 3.18.

Table 3.18: Pancreas tumour site: Organ At Risk (OAR) Dosimetry

MPD = Maximum point dose (dose limit allowed to be delivered to 0.035cc of OAR)

Patient	Number of fractions	OAR		MPD (Gy)	5cc threshold (Gy)	10cc threshold (Gy)
1	3	Duodenum	Protocol	24	16.5	11.4
			Plan CT	30.1	25.6	22.3
			Day 1 CT	31.2	28.6	23.6

It can be seen that Patient 1's planned doses to Duodenum exceeded protocol dose, when considering both MPD, and the 5cc/10cc threshold limits.

3.4 DISCUSSION

A key requirement for the accurate delivery of SBRT is that there is stability between Planning CT and the time of treatment. The tumour volume should be stable (in size and formation), and the positional inter-relationship of tumour, fiducials, and Organs at Risk (OAR) should also be stable.

"Planning margins" are added to the imaging-defined tumour volume (GTV) to account for potential differences in tumour position between planning and treatment, with the aim of avoiding geographical miss (11). However, selection of an "appropriate" planning margin is a challenge for clinicians. The margin should be sufficient to encompass tumour position across the full range of inter-fraction and intra-fraction motion. However, given the high BED doses of SBRT, the margin should be small enough to protect normal tissue. This is a difficult balance to strike. The consequence of a margin which is too tight is potential loss of tumour control, and the consequence of a margin which is too generous is potential toxicity (13).

The selection of an "appropriate" planning margin should be informed by, among other factors, the stability of tumour volume and the positional stability of tumour/fiducials/OAR.

3.4.1 Tumour growth

Cancer cells stimulate their own growth, resist anti-growth signals, and have an ability to multiply indefinitely (14). Tumours grow exponentially (15) and therefore there is the potential for there to be a noticeable increase in tumour volume between planning and treatment even if the time interval is relatively short.

The methodology described in section 3.2.2 aimed to assess this potential growth by comparing the measured tumour volume at planning versus treatment. However, it was not possible to accurately determine change in tumour volume, due to the limitations encountered in the accuracy of contouring which are described below.

A number of studies reported in the literature describe moderate to large inter-observer variability in tumour volume contouring (16, 17). This includes a wide variability for contouring of the tumour sites

studied here i.e. lung, liver, pancreas (18-21). Accurate contouring of tumour volumes is a challenge for oncologists, and the observed variations in contouring across several studies demonstrate this.

When considering the methodology for assessing tumour growth for the patients studied in section 3.2.2, an option would have been to contour tumour on both Planning and Day 1 CT scans, with no comparison to the clinician's contoured volume. However, it was felt that comparison to the clinician's contoured tumour volume was an important assessment to evaluate the validity of the tumour volumes observed. Consistency in contoured volumes would have given some confidence to the accuracy of contoured volumes, although the observed variation in the literature would indicate that the accuracy of volumes should be viewed cautiously. In practice, there was a wide variation in Planning CT tumour volume observed between the clinician and the author. This suggests that all tumour volumes should be viewed with caution. The variation could be explained in a minority of cases by the clinician labelling the tumour volume as GTV (Gross Tumour Volume, as defined on imaging), but in practice drawing a CTV (Clinical Target Volume, to incorporate GTV plus a margin to account for microscopic spread). In these instances, the clinician volume would be expected to be greater than the GTV drawn by myself. In the majority of cases, however, the likely scenario was that the differences in contoured volumes was due to inter-observer variability (consistent with the reported literature).

Intra-observer variability has been reported in the literature, although the variability is less than for inter-observer variability (17, 22). The studies report the variability for the same observer contouring the same scans. The variability would therefore be expected to be much less in these studies from the literature, compared to the assessment of tumour volume (between planning and Day 1 CT scans) in this current work. The assessment described in 3.3.1 compared volumes contoured on two different scans (captured approximately 1 week apart), so tumour growth is possible, indeed assessment of tumour growth was the aim of this section. A complicating issue for the assessment, however, was that the Day 1 CT scans were performed without the aid of intravenous contrast. It is known that intravenous contrast aids in the tumour definition of lung (23), liver (24) and pancreatic tumours (25). It was certainly my experience that it was more difficult to be certain of the edge of the tumour on the Day 1 CT scans due to the lack of contrast enhancement.

The growth rate of tumours shows considerable variability between tumours of different histology, as well as between primary and metastatic lesions. Growth rates are typically quantified as Volume Doubling Times (VDT). The VDT is defined as the time taken for a tumour to double in volume (26).

The observed changes in tumour volume are reviewed with reference to tumour VDTs and interval between scans for each of the tumour sites studied below.

3.4.1A: Lung tumour site

Ten patients with lung tumours were studied.

Six patients were treated for primary Non-Small Cell Lung Cancer (NSCLC). Mean VDTs for primary NSCLC have been reported as 158 days by Kanashaki et al (27) and 181 days by Winer-Muram et al (28). The mean interval between planning and treatment scans for the six NSCLC patients studied was 7 days as shown in Table 3.1. For the NSCLC group as a whole the mean percentage change in tumour volume between planning and treatment was -2%. An average shrinkage in tumour volume is unexpected (given the exponential growth patterns of tumours) and is likely to be due to the limitations in contouring described. The results are also skewed by patient 1, who had a recorded decrease in tumour volume by 28% between scans, this tumour volume was notably difficult to contour on the non-contrast Day 1 CT. The remaining NSCLC patients had stable, or modest increase in tumour volumes (+3 to +8%) as might be expected given the VDT and the 7 day interval between scans.

Four patients were treated for Colorectal cancer (CRC) metastasis. Mean VDTs for CRC metastasis has been reported as 71 days (29) and 56 days (30). The mean interval between planning and treatment scans for the four CRC patients studied was 6 days as shown in Table 3.1. For the CRC group as a whole the mean percentage change in tumour volume between planning and treatment was -5%. As before, an average tumour shrinkage would not be expected. 3/4 patients had a recorded shrinkage of tumour size. Only patient 6 had an increase in tumour volume between scans of +4%, this increase in tumour size may be feasible given the quoted VDTs of metastatic CRC and the scan interval (in this patient) of 8 days.

3.4.1B: Liver tumour site

Six patients with liver metastases were studied.

Two patients were treated for CRC metastasis. Mean VDTs for CRC metastasis to the liver has been reported as 155 days (Standard deviation = 34 days) (31). The mean interval between planning and treatment scans for the two CRC patients studied was 7 days as shown in Table 3.8. The average

percentage change for these patients was -17%, an observed shrinkage in tumour volume. According to the results Patient 1's tumour volume almost halved in size. This is again thought to be a result which reflects the challenges (and therefore inaccuracies) of contouring on a non-contrast CT for the Day 1 Treatment CT scan.

Two patients were treated for breast cancer metastasis. Mean VDTs for Breast cancer metastasis has been reported as 98 days (30). The mean interval between planning and treatment scans for the two breast cancer patients studied was 5 days as shown in Table 3.8. The average percentage increase in tumour volume between planning and treatment scans in these patients is 19%. However, the results are being skewed by patient 5 who had an apparent large increase (+36%) in tumour volume as compared to a small increase in volume (+2%) in patient 6.

A single patient with a melanoma metastasis was studied. Mean VDTs for melanoma metastasis have been reported as 64 days (range 8-212) (32). There was a 5 day interval between planning and treatment scans for this patient, with an apparent increase in tumour volume of +71%. Whilst metastatic melanoma is known to be a fast-growing tumour (note VDT can be as little as 8 days), it was notably challenging to outline this tumour on the Day 1 treatment CT scan, and I would be sceptical that this is a true and accurate result.

It was not possible to contour the metastasis the single patient with a carcinoid metastasis on the Day 1 CT scan.

3.4.1C: Pancreas tumour site

Four patients with pancreatic tumours were studied, all had primary disease. Mean VDTs for primary pancreatic cancer has been reported as 42 days (30) . Mean interval between planning and treatment scans for these patients was 7 days as shown in Table 3.13. For the group as a whole there was a mean increase in tumour volume at treatment of +11%. However, there was a wide variation in the change of tumour volume (range -19% to +36%). The apparent reduction in tumour volume of -19% for patient 4 should certainly be viewed with suspicion.

3.4.1D Summary: Tumour growth

Evaluating all patients studied (lung, liver, pancreas) for potential tumour growth between Planning and Day 1 treatment CT scans, the following observations are noted:

1. Mean interval between Planning and Day 1 Treatment CT scans is 7 days (for the group as a whole, and for each tumour site).

2. For all histopathologies studied, mean VDTs far exceeded the interval between scans, although it was noted that there was wide variation in VDTs reported in the literature.

3. In spite of careful contouring on Planning CT and Day 1 treatment CT scans, it was not possible to draw conclusions about tumour growth between scans due to:

a) the challenging nature of contouring (as experienced here and evidenced by inter- and intra-observer variablity reported in the literature), and

b) the limitation of having a non-contrast CT only available for contouring on the Day 1 Treatment CT.

4. The magnitude of inter- and intra-observer variability observed in these volume assessments suggests that contouring is likely to be a much larger source of potential error in SBRT delivery, as compared to the sub-millimetre accuracy of fiducial tracking demonstrated in Chapter 2. (Although it is noted that the studies in Chapter 2 were phantom studies, and fiducial tracking in clinical situations may be less accurate).

3.4.2 Tumour Deformation:

SBRT is a highly conformal radiotherapy technique. Treatment plans are produced where the prescription isodose line conforms tightly to the PTV contour (33). As a consequence of this conformality it is critical to consider, estimate, and account for all geometrical uncertainties, such as tumour deformation.

Assessment of tumour deformation has been performed in a variety of ways in the literature. The most sophisticated assessments of deformation incorporate statistical modelling and deformable registration tools. These assessments have demonstrated that tumour shape changes during radiotherapy treatment (compared to the formation at the time of planning images) for rectal and prostate tumours (34-36). The shape changes were shown to be significant, such that adaptive margins were suggested.

Harris et al assessed breast tumour cavity deformation with statistical modelling without deformable registration, using the cavity marker clips as fiducials (37). The authors proposed an adaptive strategy to compensate for the volumetric and shape changes observed.

Barker et al pursued a more subjective approach to assessment and confirmed visible changes in tumour formation during a radiotherapy course for Head and Neck cancer (38).

It was beyond the scope of this study to assess tumour deformation with statistical modelling and image registration tools. Further, it was not possible to pursue the approach of Harris et al as fiducials were not inserted into the edge of tumour volumes in the patients studied here.

Initially, it was explored whether a suitable surrogate measure for tumour deformation could be the maximum contour deviation of the Day 1 CT, measured as a perpendicular to the reference planning CT contour. A deviation of the Day 1 contour beyond the planning CT contour would be potentially significant because this would risk underdose of tumour. Equally, deviation of the Day 1 CT contour inside the reference planning CT contour may be significant as this would be likely to occur due to changes in normal tissues, and these could therefore be overdosed (e.g pancreatic head tumour could be deformed due to increased duodenal filling on Day 1 vs Planning CT, with possible overdose of duodenum).

In practice, however, it became clear that there were a number of issues with the approach proposed. Firstly, there was recognised intra-observer variability, as described in section 3.4.1, exacerbated by the

use of non-contrast CTs for the Day 1 CT scans, therefore I did not consider the contours valid for assessment. A further issue was that it became clear that the maximum contour deviation was not a representative measure for the overall change in contours between planning CT and Day 1 CT. This approach was ultimately abandoned for the above reasons.

It would have been possible to contour the areas where the Day 1 CT contour was larger (or smaller) than the reference planning CT contour and calculate the volume of these structures in MultiPlan. This assessment would have been more representative of potential tumour deformation than the perpendicular contour deviation approach initially proposed. However, it was recognised that this approach was labour-intensive, and I felt that the issues regarding the reliability of the contours drawn meant that pursuing this approach was unwarranted.

On subjective assessment of the tumour volumes for the cases studied (lung, liver, pancreas), within the limitations described regarding delineation uncertainties, tumour deformation between Planning and Day 1 CT scans was noted for two liver tumours only (patients 2 and 3). In each case, the likely cause of tumour deformation was differential duodenal/bowel filling.

3.4.3 Fiducial Migration:

Fiducial migration describes the movement of implanted fiducials from their original position, (at the time of initial fiducial placement) to a remote position where they are no longer an appropriate surrogate for tumour position/movement. Fiducial migration can occur early, where it is noted by the clinician at the time of fiducial deployment, or on the immediate post-placement imaging. "Delayed" fiducial migration can also occur, where the migration is noted on Planning CT scans which are typically captured 1 week after fiducial placement (2). Early migration is less problematic to the patient as an additional fiducial can be placed at the same session to replace the migrated fiducial. Delayed migration, only noted at Planning CT, could mean that the patient requires a second fiducial placement session, and ultimately suffers a treatment delay, and the attendant risks of a second procedure.

It is not possible to treat a patient using fiducials which are situated >5-6cm away from the tumour target. This is partly to ensure that all fiducials can be captured on the Field of View (FOV) of the CyberKnife treatment consoles, which measure 20x20cm (2). In addition, the greater the distance between a fiducial and tumour, the greater the risk of disparity between fiducial and tumour position.

This section will consider “fiducial migration” as those cases where fiducials migrate >5cm from the implanted position. A more moderate degree of fiducial migration sometimes occurs, however, these cases will be considered in the next section on fiducial reproducibility (section 3.4.4).

3.4.3A: Fiducial Migration: Lung tumour site

Kothary et al (2) commented that fiducial migration is most often seen in the lung. The group hypothesised that this could be due to the risk of pneumothorax, and fiducials dropping into the pleural space.

Fiducial migration rates reported in the literature vary widely (1-53%) according to the fiducials used, site of insertion, and insertion technique (39-41).

Schroeder et al (41) reported on migration rates following 234 fiducial placements sited at bronchoscopy. The first 4 patients had linear fiducials placed, but 53% of these fiducials migrated (delayed migration). This resulted in 2 patients requiring a second insertion procedure. The centre therefore switched to inserting coil fiducials, which may have design features to reduce the risk of migration. Subsequent to this switch in fiducial type, the migration rate was much improved at 1%.

Patel et al reported an 8% migration rate of fiducial markers (delayed migration). Fiducials were inserted percutaneously under CT guidance. 4 fiducial markers migrated into the pleural space, whilst a further marker migrated into the extra-pleural soft tissue.

Bhagat et al reported a 19% migration rate. Fiducials were inserted percutaneously under CT guidance. Out of 11 migrated fiducials, 10 had migrated into the pleural space, the remaining fiducial migrated into an airway, and was thought to have been subsequently coughed up. The group noted an increased risk of migration when a fiducial was placed a shorter distance from pleura, and when a fiducial was placed outside of tumour.

As described in Methods section 3.2.3, a qualitative judgement as to the stability of a fiducial implantation site was due to have been recorded for each fiducial placed. However, in practice, I felt unable to make an informed judgement as to the likely stability of each site. The making of this qualitative judgement at the time of first reviewing the cases was therefore abandoned. However, full analysis of migration results has led me to be more informed on the likely stability of implantation sites, as will be discussed in this section.

A total of 18 patients with lung tumours were assessed for fiducial migration. All fiducials were placed percutaneously under CT guidance. Fiducial migration occurred in just 1/18 patients (6%) and 1/36 fiducials placed (3%). The solitary migrated fiducial was deposited close to the pleural edge (3 mm from pleural edge) and on planning CT was noted to be lying in the pleural recess. The patient did not develop a pneumothorax post-insertion. Fortunately, the patient did not require a second fiducial insertion procedure, because a second fiducial was optimally placed within tumour.

The migration rates observed here compare favourably with those reported by Bhagat et al, and Patel et al, where fiducials were inserted with the same technique. In keeping with the observations of Bhagat et al, there were no instances of fiducial migration where the fiducial was placed inside tumour. In addition, the solitary case of fiducial migration occurred where a fiducial was placed close to the pleura.

3.4.3B: Fiducial Migration: Liver tumour site

Jarraya et al reported the results of a large study of 328 patients, and 1444 implanted fiducials (42). All fiducials were placed into the liver percutaneously under CT-guidance. The centre's policy was to avoid placing fiducials in tumour due to concerns over tumour seeding, and also a concern over the potential for tumour necrosis during treatment causing fiducials to shift (43). 834 fiducials placed were single fiducials, 610 fiducials were linked by a strand.

There were no instances of fiducial migration for linked fiducials. In contrast, there was a 2.7% immediate migration rate for single fiducials. Out of 9 immediately migrated fiducials, 4 migrated to the heart (requiring overnight observation but no intervention), 3 migrated to a subcapsular location, and 2 fiducials migrated to the Inferior Vena Cava. There were 3 patients (0.9%) who had delayed migration of fiducials noted at planning CT. The initial site of implantation for the migrated fiducials was not described further.

Kim et al (44) reported on fiducial migration rates for Ultrasound-guided fiducial placements for the treatment of malignancy in intra-abdominal lymph nodes, liver, pancreas and prostate. Overall, 77 patients and 270 fiducial placements were studied. Considering the 96 fiducials placed to mark hepatic tumours, there was one case of delayed fiducial migration (1%). The tumour was a hepatocellular malignancy, and the migrated fiducial was lying in the adjacent capsule.

Nine patients with liver tumours were studied here, with 34 implanted fiducials. Results are reported in section 3.3.8. All fiducials were placed percutaneously under CT guidance. There were no instances of fiducial migration observed (either immediate or delayed). Whilst this is a smaller sample of patients than those studied by Jarraya and Kim et al, the fiducial migration rate observed here compares favourably.

3.4.3C: Fiducial Migration: Pancreas tumour site

Fajardo et al (45) reported on 23 patients with 63 fiducials sited to mark pancreatic tumours. All fiducials were sited under Endoscopic Ultrasound (EUS) guidance. The group noted a fiducial migration rate of 9.5% (6/63 implanted fiducials). The intended site of implantation for all fiducials was described only as "the tumour area".

Sanders et al (46) reported on 51 patients who had undergone EUS-guided placement of fiducials to mark pancreatic tumours. A 7% delayed migration rate (occurring in 3/51 patients) was noted, and the patients had to undergo a second fiducial placement procedure. The intended site of implantation for fiducials at the outset was "into or adjacent to tumour". Out of the 3 patients described above that suffered a fiducial migration, 1 patient had a fiducial placed successfully in the tumour mass at the second EUS procedure. The remaining 2 patients had fiducials placed in the tumour mass, and also the left hepatic lobe at their 2nd EUS procedure. Following these instances of fiducial migration, the group aimed to site 2 fiducials in the tumour mass, and a further fiducial in the left hepatic lobe per patient. The authors noted that it was "unclear" why there were cases of delayed migration.

Kim et al (44) inserted fiducials via ultrasound guidance to mark pancreatic tumours in 39 patients. There were no instances of fiducial migration recorded in these patients.

Data for 9 patients with pancreatic tumours marked by fiducials are shown in Table 3.14. 5/9 patients (56%) had fiducials placed percutaneously under CT guidance, 3/9 patients (33%) by endoscopic ultrasound, and a single patient (11%) had fiducials sited at laparoscopy.

The patient who had 3 fiducials sited at laparoscopy (patient 4), had delayed migration of fiducials noted on Planning CT. There was no immediate post-implantation image taken, but at Planning CT fiducials were located 3.2cm, 7.3cm and 8cm from the tumour. Whilst the fiducial lying 3.2cm from tumour is

clearly <5cm from tumour, it is considered here because it had come to lie in a completely separate tissue, and was judged by the team to be likely to be a poor surrogate for tumour position. The fiducials may have migrated along fat planes as they came to rest in perinephric fat. At repeat laparoscopy a further 3 fiducials were successfully placed in tumour, with no subsequent migration.

There were no instances of fiducial migration for the remaining 8 patients with fiducials sited by EUS or CT guidance.

The site of fiducial implantation for the successful fiducials re-sited for patient 4, and the above 8 patients were: tumour (75%), pancreas (12.5%), and mesenteric fat (12.5%).

In summary, there were no cases of fiducial migration observed for fiducials placed under EUS guidance, or percutaneously under CT guidance. This was a small sample of patients, but the results compare favourably with the fiducial migration rates reported in the literature (7-9.5%).

Equally there were no cases of fiducial migration observed when fiducials were implanted into tumour or pancreas.

A fiducial migration rate of 50% was observed in a single patient with laparoscopically-placed fiducials. No fiducial migration was observed by this technique when fiducials were implanted into tumour.

The fiducial migration rate was noted to be 50% in fiducials implanted into mesenteric fat.

The case described was early in the learning curve for the Surgeon doing the fiducial placement. I feel that it is more likely that the significant predisposing factor for fiducial migration in this case, was the implantation in mesenteric fat, rather than the laparoscopic approach. Indeed, a laparoscopic approach was pursued in this case because the position of nearby critical structures prohibited safe placement under EUS or CT guidance.

Fiducial migration following implantation into fat or mesentery was also noted for the 2 clinical examples described in the Introduction (section 3.1.1). A further clinical example of fiducial migration following insertion into peri-cardiac fat has also been noted. 3 fiducials were placed percutaneously, with laparoscopic guidance. Immediately post-implantation, a Chest X-Ray suggested that all fiducials were well sited. But at Planning CT it was clear that the fiducials had migrated (delayed migration). The patient (who had a cardiac metastasis of carcinoid tumour to the left ventricular wall) had a repeat

fiducial placement procedure, percutaneously under CT-guidance, with 2 fiducials placed directly into tumour. The tumour-implanted fiducials did not migrate, and treatment was delivered without event.

Kim et al (44) noted 5 instances of fiducial migration when fiducials were inserted to mark intra-abdominal lymph nodes. The authors commented that migration may have occurred "possibly from movement of the mesentery".

3.4.3D: Fiducial migration: Summary

It is already known from the literature that fiducial migration is a recognised complication following fiducial implantation. Migration rates vary according to tumour site, fiducial type and implantation technique. Observed fiducial migration rates are 1-53%, 1-3.5%, and 0-9.5% for lung, liver and pancreas tumour sites respectively.

Fiducial migration rates noted in this study are 6%, 0%, and 11% for lung, liver and pancreas tumour sites respectively. These migration rates are broadly in line with those reported in the literature, confirming earlier findings.

The studies reported above have large focussed on immediate complications of fiducial placement e.g. pneumothorax/bleeding/pain (these complications are not considered in this study), as well as fiducial migration rates. One study (39) reported that fiducial migration was unlikely to occur where fiducials were inserted in tumour, and 2 studies reported increased risk of fiducial migration where fiducials were implanted close to pleura, or close to liver capsule (39, 44). The studies did not explore in any further detail, the risk of fiducial migration following implantation into different tissues.

The analysis described here demonstrates a new and important finding: fat (mesenteric, peri-nephric, peri-cardiac) is an unsuitable tissue for fiducial implantation, due to an extremely high fiducial migration rate. Fiducial migration following insertion into fat occurred for 4/4 fiducials in perinephric fat, 3/3 fiducials in peri-cardiac fat, and 5/9 fiducials inserted into mesenteric fat (2 migrated fiducials from the case described in the Introduction, and 3 fiducials from pancreas Patient 4). This represents an overall fiducial migration rate of 75% for fiducials implanted into fat, which is unacceptable given the risks of fiducial placement, and the treatment delay that occurs by requiring a second fiducial implantation procedure. It is likely that the density and tissue architecture of fat makes it an unsuitable tissue to anchor fiducials. In addition, mesenteric and peri-cardiac sites are subject to significant motion, which may contribute to dislodging implanted fiducials.

3.4.4 Fiducial Reproducibility:

As previously stated, it is important that the positional relationship of fiducials to each other, and to tumour and organs at risk (OAR), is stable at treatment with respect to their positions at planning CT.

Section 3.4.3 reviewed cases where fiducials had migrated >5cm from their site of implantation, and could therefore not be used to guide treatment delivery.

However, given the small planning margins applied in SBRT treatment, a fiducial shift/migration of only a few millimetres from the planning position to a different treatment position, could potentially cause a risk of geographical miss of tumour, and risk of overdose to OARs. The likelihood of this issue arising, and its potential impact on treatment delivery, is reviewed here.

3.4.4A Fiducial Reproducibility: Lung tumour site

Van der Voort van Zyp et al (47) explored fiducial stability in 42 patients with lung tumours treated by CyberKnife. Each patient had a planning CT scan followed by 2-3 repeat scans, taken at intervals during the treatment course. Slice spacing of the CT scans was 1.5-2mm. This group co-registered the CT scans by tumour-to-tumour soft tissue matching. The 3D marker co-ordinates where then determined on the planning CT scan and compared to the repeat CT scans. They found median marker displacement to be 1.3mm, median COM displacement was 1mm. As the CyberKnife real-time tumour-tracking system localises the tumour using the fiducial COM, the group explored whether a COM displacement of ≥2mm could be detected by changes in inter-marker distance. They found inter-marker distance change of >1.5mm predicted a COM displacement of ≥2mm in 96% of treatment fractions.

Hong et al (48) investigated fiducial stability in 32 patients with lung tumours who were to be treated with CyberKnife. The patients had 147 implanted fiducials. The patients had post-implantation CT scans co-registered with planning CT scans, this time co-registration was performed by fiducial-to-fiducial matching. Median fiducial migration was found to be 1.28mm, remarkably similar to the Van der Voort van Zyp group, despite the difference in methodology. They concluded that fiducial migration of this magnitude was unlikely to cause geographic miss.

Table 3.2 shows the mean fiducial displacement between planning CT and Day 1 treatment CT for 9 patients with lung tumours and single implanted fiducials. Co-registering CT scans by fiducial matching

(similar to Hong et al (48)) showed a mean fiducial shift of 0.72mm. Clearly, the most important step in assessing fiducial displacement is in deciding the centre of each fiducial. The process could be prone to inter-observer variability, but the variability between the Physicists and myself was found to be sub-millimetre apart from the y co-ordinate of a single fiducial. Appendix Table 1A shows fiducial displacements for 6 patients with multiple implanted fiducials. Mean fiducial shift observed in the group of 9 patients with multiple fiducials was 0.75mm. Mean fiducial shift for the lung group overall was 0.74mm.

Mean COM shift was 0.72mm in the single-fiducial group (as centre of single fiducial = COM). Mean COM shift for the multiple fiducial group was 0.61mm (Table 3.3B). Overall mean COM shift for the lung tumour group was 0.67mm.

The observed fiducial and COM shift observed here compares favourably with the results reported in the literature above. However, the studies cannot be directly compared due to a few key differences which will be discussed.

The larger CT slice spacing (1.5-2mm) of the Van der Voort van Zyp group (47) may increase the risk of potential error in recording the true centre of each fiducial, compared to the standard 1.25mm slice spacing at our centre. In addition, this group recorded fiducial and COM displacement at several time-points during treatment. It could therefore be expected that the effects of treatment could increase fiducial displacement, indeed the group found that an increased interval between planning CT and repeat CT was associated with a small but significant increase of 0.3mm/day in fiducial displacement. This group also co-registered CT scans by means of tumour-to-tumour matching, rather than fiducial matching, so it could be expected that fiducial displacements would be greater, although interestingly the fiducial displacements observed were very similar to the Hong et al group.

The Hong group used similar methodology to assess fiducial stability to the patients assessed here. The decision to measure fiducial displacement based on fiducial-to-fiducial matching was based on the fact that this is how the scans are co-registered on the first day of treatment at this centre. Equally, the CyberKnife radiographers will set the patient up according to the positioning instructions from the CT-simulator staff, but then will fine-tune patient position based on fiducial configuration.

The median interval between CT scans for the Hong group was 8 days, which compares well to the interval in the patients studied here (7 days). The Hong group assessed fiducial displacement between

immediate post-implantation CT scans, and planning CT scans, therefore the scans were both taken much sooner after fiducial placement. It is plausible that the initial inflammation immediately post-fiducial implantation could affect the spatial resolution of fiducials. Indeed, this is one of the reasons why it is recommended that Planning CT scans are performed approximately 1 week after fiducial insertion (2). This could have affected the results recorded by the group. In addition, there are histopathological responses to fiducial placement that evolve over time. Imura et al (49) investigated 7 patients who had had 16 marking fiducials sited at bronchoscopy. The patients underwent video-assisted thoracoscopic surgical (VATS) resection within 7 days of fiducial placement and the histological changes surrounding fiducials were reviewed. Fibrin exudation was noted at 1 or 2 days after insertion, and fibrotic changes (which might serve to anchor a fiducial in place) and hyperplasia of Type 2 pneumocytes were seen at 5 or 7 days after insertion.

In summary, the patients assessed here had a mean shift of fiducial position of 0.74mm which compares well with that reported in the literature (1.28-1.3mm). Similarly, mean shift in fiducial COM of 0.67mm compares well with the literature (1mm), although differences in methodology between the patients treated here and those in the literature are noted. As the CyberKnife real-time tumour-tracking system localises the tumour using the fiducial COM, COM shift analysis is more relevant to assessing the likelihood of a treatment being accurately delivered as intended. The results of COM shift being sub-millimetre (0.67mm) suggest that geographical miss would be unlikely.

3.4.4B Fiducial Reproducibility: Liver tumour site

Kitamura et al (50) investigated fiducial stability in a mixed group of patients with prostate cancer and liver tumours treated by conventionally-fractionated radiotherapy. Only the 4 patients with liver tumours will be considered here. The patients had a single fiducial inserted into tumour. Planning CT was performed in exhale, the slice gap was 1mm at the level of the fiducial marker, and 5mm elsewhere. This scan was considered the reference scan for comparison. CT scans were repeated weekly until the end of treatment. Several clinicians were asked to contour the single marker, as well as the liver contour on each CT scan. Inter-observer variability of the COM was within 0.4mm for the fiducial, and within 2mm for the liver. The mean fiducial shift noted was 0.2mm in Left/Right direction, 1.5mm in Cranio/Caudal direction, and 1.4mm in Anterior/Posterior direction. Shift was calculated by comparison of 3D co-ordinates from the treatment planning system. The group noted there was no influence of

time (since planning scan) on the magnitude of fiducial displacement (in contrast to the findings of Van der Voort van Zyp (47) for lung tumours).

Summary data for fiducial COM shift for 9 patients with multiple implanted fiducials is displayed in Table 3.9. The mean shift in fiducials, and fiducial COM is 0.59mm in x (Left/Right), 0.38mm in y (Ant/Post) and 1.16mm in z (Sup/Inf) directions respectively. Considering the shifts in individual fiducial positions from individual patient data it was noted that the mean displacements are skewed in some cases by one or two fiducials with a large shift (e.g. Patient 1, fiducials 1, 2 and 4). If these fiducials are subsequently rejected due to concerns that they are a poor surrogate for tumour movement (this issue will be discussed in the next section), the COM shift for the fiducials that are ultimately used at treatment delivery will be decreased, and the accuracy of treatment delivery will be likely to increase (as long as the fiducial rejection strategy employed is not flawed). There were no discrepancies in fiducial centre of >1mm between the Physics team and myself, confirming the sub-millimetre inter-observer variability in marking a fiducial accurately shown by Kitamura et al. Both the Kitamura group and ourselves observed sub-millimetre displacement in the Left/Right direction, but >1mm displacement in the cranio-caudal direction. The results for displacement in the Ant/Post direction are different however (1.4mm vs 0.38mm). The Kitamura group had a small sample size (4 patients), and it may be that the mean results were skewed by one or two patients whose fiducials had migrated. When assessing a single-fiducial scan it is harder to assess for true migration, as there is no possibility of calculating inter-marker distance as done by Van der Voort van Zyp (47).

3.4.4C Fiducial Reproducibility: Pancreas tumour site

Van der Horst et al (51) explored fiducial stability in 13 patients with pancreatic tumours and 2-3 implanted fiducials per patient. The patients were treated by Linac-based conventionally fractionated radiotherapy. Adjustments to patient position could be made following Cone beam CT analysis, but there was no intra-fractional tracking of tumour motion. The planning CT was the reference CT, it was performed a mean of 4.5 days post-implantation (range 2-12 days). The free-breathing on-treatment Cone beam CTs were compared with the Reference CT. CT scans were co-registered by fiducial-to-fiducial matching.

Comparison of fiducial position was made by review of fiducial marker pairs. Inter-observer variability was compatible with previous literature, mean = 0.4mm (SD 0.9mm). The largest mean displacements

were noted in the Sup/Inf directions. Fiducial COM varied by 1-25.6mm compared to the Reference CT, especially in the Sup/Inf direction. This is not surprising as the Cone Beam CTs were free-breathing (therefore could have been captured at an entirely different respiratory phase to the reference CT) and the pancreas is known to move considerably with respiration. Mean fiducials COM shift was 1.5mm. 1.5mm and 0.3mm in the Left/Right, Sup/Inf and Ant/Post directions respectively.

Fiducial stability data for 9 patients with pancreatic tumours and single-implanted fiducials is shown in Table 3.14. Mean observed shift for the fiducials between Planning and Day 1 Treatment CT were 0.29mm, 1.01mm and 0.58mm in Left/Right, Ant/Post and Sup/Inf directions respectively. Summary data for 9 patients with multiple implanted fiducials is shown in Table 3.15. The mean fiducial COM shift for these patients are 1mm, 0.75mm and 0.4mm in Left/Right, Ant/Post and Sup/Inf directions respectively. Inter-observer variability was again noted to be sub-millimetre. The different methodology does not offer direct comparison of the patient groups studied here with the Van der Horst group, most notably that the Cone beam CTs, and the Planning CT scans were captured in free breathing for the Van der Horst group, but in exhale breath-hold for the patients studied here. The planning CT scans must be taken in breath-hold for CK purposes, otherwise there is a risk that fiducial will be captured as smeared across several cranio-caudal scan levels, and the actual true centre of its position with respect to tumour will not be known.

3.4.4C Fiducial Reproducibility: Summary

The analysis of fiducial stability presented here has assessed fiducial position at Planning CT scan in comparison with fiducial position on the Day 1 treatment CT scan taken a mean of 7 days later. Scans were acquired with identical imaging parameters, in identical treatment position, and at the same respiratory phase (exhale breath-hold), so the scans were directly comparable.

Each scan represents a “snapshot” of tumour and fiducial position/configuration. The individual fiducial and fiducial COM displacements noted are examples of inter-fractional position variation. These inter-fractional position variations can introduce both random and systematic positioning errors, so it is important the variation is minimal to allow accurate tumour targeting.

Co-registering of CT scans by means of a single implanted fiducial showed fiducial shift of 0.55, 0.9 and 0.7mm in Left/Right, Ant/Post and Sup/Inf directions respectively for lung targets. Single-fiducial matching showed fiducial shift of 0.29mm, 1.01mm and 0.58mm for pancreas targets.

Co-registering of CT scans by a seed-point transformation on a single-implanted fiducial should be the least challenging of fusion tasks. The gold fiducials are dense, so they can be easily seen on CT scans, and fusing CT to CT (same modality) should be an easily-performed task. The only caveat to the above is that gold fiducials can be associated with a moderate amount of artefact, due to their high electron density. Despite the note on artefacts, I feel that the "fiducial shifts" for single-fiducial cases observed above (0.29-1.01mm) represent the margin of error in co-registering scans. It is known to be more challenging to fuse scans of different modalities (e.g. Prostate CT with Prostate MRI), therefore the potential fusion errors described above are likely to represent a best-case scenario. This observation is of particular interest when considering delineation uncertainty for prostate tumours in Chapter 5.

Considering cases of multiple-implanted fiducials, mean fiducial COM shift was 0.61mm, 1mm, and 0.72mm in lung, liver and pancreas sites respectively, which is broadly in keeping with the fiducial displacements described in the literature, within the limitations of different methodologies employed. Fiducials here were matched according to a "best-fit" scenario, respiratory phase was identical (assuming patient compliance). It is interesting that the liver fiducials show the greatest displacement overall. When attempting to fuse MRI liver and CT liver scans, it is notably challenging. The larger shift in fiducial COM for liver cases, together with the difficulties in fusing liver scans observed, suggest that the liver is especially prone to deformation.

Overall mean fiducial COM shift for all tumour sites studied is ≤1mm.

3.4.5 Fiducial Location:

The relationship between fiducial marker and tumour target volume constitutes the largest uncertainty of Synchrony-based SBRT, and optimal fiducial placement is essential (50). CyberKnife plans are chacterised by a sharp-dose gradient away from tumour, therefore any small geometric errors in fiducial tracking can lead to a large change in dose-delivery.

As previously stated, fiducials must be placed greater than 2cm from each other, less than 6cm from the tumour, have greater than 15^0 angle between fiducials, and they should not be super-imposed on the 45^0 oblique X-Ray views taken by the in-room imaging system (2, 52, 53).

It is also critical that fiducial markers are placed close enough to tumour to be an accurate surrogate for tumour position/motion. It is known that deformations, rotations or non-synchronous movements may induce changes in fiducial marker groups which do not necessarily correspond with displacements in distant parts of an organ containing tumour (4). In addition, if multiple fiducials are placed, they should ideally be placed with a configuration such that the COM of fiducials lies inside the tumour. This will maximise the likelihood that fiducial tracking will lead to accurate tumour tracking (54).

However, whilst the above guidance is well recognised, the literature does not report clear guidance on threshold distances for fiducial-to-tumour which are likely to ensure accurate treatment delivery.

3.4.5A Fiducial location: Lung tumour site

Van der Voort van Zyp et al (47) explored aspects of fiducial tracking in 42 patients with lung tumours as reported previously. A total of 111 fiducials were sited. The causes of fiducial displacement >5mm (from their position relative to tumour noted at Planning CT) were explored. Fiducial displacement >5mm occurred for 13/111 fiducials (12%). The most frequent cause of fiducial displacement was non-synchronous motion of fiducials and tumour (6/111 fiducials, 5%). After CT co-registration, tumour-to-tumour matching was noted to be good, but a different respiratory phase was noted as evidenced by rib/diaphragm position, therefore the authors considered non-synchronous motion (between tumour/fiducials) to be the issue. They noted all 6 fiducials were placed further from tumour than other markers. Mean distance of fiducial to tumour centre was 3.5cm (Range 2.7-8.4cm) for the fiducials displaying non-synchronous motion. Tumour diameter for the above patients was 2.5cm vs 6.9cm. The authors did not report further details of fiducials employed at treatment vs. fiducials that may have been rejected at treatment delivery.

Results of an evaluation of optimum fiducial placement for lung tumour patients was reported in Section 3.3.3. Table 3.4 displays results for 9 lung tumour patients with a single-implanted fiducial. 89% of cases had the fiducial placed in tumour. For the single patient with a fiducial placed outside the tumour, this fiducial was 4mm from PTV edge. The team judged that this fiducial was close enough to tumour to be a good surrogate for tumour.

Table 3.5 shows the results for 9 patients with lung tumours and multiple implanted fiducials (27 fiducials). 12/27 fiducials (44%) were sited outside of tumour, therefore they could potentially move

non-synchronously to tumour. 7/12 (58%) of these outside-of-tumour fiducials were rejected. The mean distance from rejected fiducial to closest tumour edge was 1.9cm (vs. 0.4cm for an accepted fiducial). Observations made by CyberKnife radiographers suggested that non-synchronous motion of fiducial/tumour was the reason for rejection in 1/7 rejections (14%), this fiducial was 2.1cm from the closest tumour edge, and was the only fiducial rejected during treatment delivery. The remaining 6/7 (86%) fiducial rejections, affecting 3 patients, were guided by physicists due to combined concerns over the distance of a fiducial to tumour edge (and possibility of non-synchronous fiducial/tumour motion), and also concerns about fiducial configuration (and fiducial COM lying in a sub-optimum location). Fiducial configuration/fiducial COM may have been the dominant concern for the physicists, because the rejection of fiducials advised shifted the fiducial COM from outside tumour, to inside tumour for 2 patients (4 rejected fiducials). The remaining 2 fiducial rejections advised for Patient 1, moved the fiducial COM closer to tumour. All fiducials for Patient 1 were sited superior to tumour target, and the closest fiducial was the only one used for tracking.

Taking the results from Section 3.3.3 overall, if a small, uniformly round, tumour target is to be tracked with a single fiducial, the fiducial should ideally be placed in the centre of tumour.

For larger, more irregularly-shaped lung tumours, multiple-fiducials are recommended for tracking. Four fiducials are ideal as the challenging nature of fiducial placement means that often a fiducial needs to be rejected (22% rejection rate overall), and 3 remaining fiducials allows rotations to be tracked. The fiducial configuration should be such that the fiducial COM lies inside the tumour. In practice, if an intra-tumour fiducial was placed (5 patients), any fiducial placed >1cm from tumour edge was rejected. All fiducials placed within 1cm of tumour edge were accepted in practice. Radiologists should aim to place fiducials within 1cm of tumour edge, as well as fulfilling the other fiducial placement guidelines which are well known (2, 52, 53).

3.4.5B Fiducial location: Liver tumour site

Jarraya et al explored fiducial tracking in 328 patients with liver tumours as described in Section 3.4.4B (42). Fiducials were placed in an “unintended” position in 27/328 patients (8%), where fiducial-to-tumour distance was ≥6cm. The radiologists commented that this was largely due to the irregular breathing pattern of the patients involved. 3/27 of these patients (11%) required a second fiducial placement procedure for fiducials that were not appropriate for tracking. The authors did not discuss

any issues relating to fiducial tracking with fiducials sited <6cm from tumour, but this was not the focus of the article.

The Synchrony system is designed to track the respiratory motion of tumour targets, to within an accuracy of 0.6-2.5mm (47, 55, 56). Lu et al (57) noted a larger deformation due to breathing of liver tissue compared to lung tissue.

However, the liver is known to be susceptible to deformation, and any non-respiratory motion will not be tracked by Synchrony.

Von Siebenthal et al discovered that deformation was particularly common and problematic in the anterior/inferior part of the liver (Couinaud segments IVb and V) (58, 59). The group used a gating technique to account for respiratory motion, but despite gating, systematic deviations from set-up position of >5mm due to deformation were noted for MR-defined liver sub-volumes in 58% of patients studied.

Seppenwoolde et al (54) explored fiducial tracking in 20 patients with implanted fiducial markers and liver tumours. All patients had abdominal compression immobilisation. The patients had a Planning CT scan which was contrast-enhanced in exhale breath-hold. The patients had repeat CT scans before each treatment fraction, which were co-registered with the Planning CT. The group evaluated the inter-fraction accuracy of liver tumour position prediction by fiducials as a function of fiducial-to-tumour distance. Sophisticated statistical analysis revealed that fiducials were more reliable than anatomical surrogates (ribs/diaphragm). The reliability of fiducials as a surrogate varied however, and was found to be related to fiducial-to-tumour distance. A fiducial to tumour COM distance of 20mm was associated with an error (1SD) of 1.25mm. If fiducial to tumour COM distance increased to 6cm, this error increased to 2mm. The authors did not go on to give any guidelines on a threshold recommended distance of fiducial-to-tumour.

Table 3.10 shows the results for 9 patients with liver tumours and multiple implanted fiducials (34 fiducials).

25/34 fiducials (74%) were sited outside of tumour, therefore they could potentially move non-synchronously to tumour. 14/25 (56%) of these outside-of-tumour fiducials were rejected, although 2 of these rejected fiducials were only 1mm from the tumour edge. The mean distance from rejected fiducial to closest tumour edge was 2.1cm (vs. 0.6cm for an accepted fiducial). The two rejected fiducials which

lay only 1mm from tumour edge were implanted for peripheral metastases. Both were recommended for tracking by the Physicists (given they were positioned at the tumour edge), but were rejected at treatment delivery due to non-synchronous motion with other fiducials. One fiducial (in patient 3) was sited close to the edge of liver, and adjacent to bowel, differential filling of this bowel between Planning CT and Day 1 CT was noted which shifted the Ant/Post fiducial position, and Sup/Inf fiducial position by 2.4 and 3.1mm respectively. The tumour was not located in the anterior/inferior portion of liver noted to be the most susceptible area to non-respiratory motion, however, previous hepatic resection had caused the bowel to shift superiorly to lie adjacent to tumour/liver, likely rendering the fiducial susceptible to instability, and rendering the tumour susceptible to deformation. The other rejected fiducial (patient 7) which lay only 1mm from tumour showed a stable position when co-registering Planning CT and Day 1 CT (within 0.5mm), however it was rejected at treatment delivery due to inconsistent positioning relative to the other implanted fiducials. Reviewing the CT placement of this rejected fiducial, this was a central metastasis, remote from bowel, and the reasons for the tracking difficulties cannot be easily explained, the necrotic nature of the tumour could possibly be implicated. The remaining 12/14 fiducials (80%) which were placed outside of tumour and were rejected were placed ≥1cm from tumour. 6/12 (50%) were rejected according to Physicist advice, to shift the fiducial COM to inside the PTV. 4/12 (33%) of the fiducials were rejected at treatment delivery due to non-synchronous motion compared to the other implanted fiducials. The reason for rejection for the remaining 2 fiducials was less clear from the records.

In summary, multiple fiducials are recommended for tracking. Four implanted fiducials are ideal as the challenging nature of fiducial placement means that often a fiducial needs to be rejected (44% rejection rate), and 3 remaining fiducials allows rotations to be tracked. The fiducial configuration should be such that the fiducial COM lies inside the tumour. In practice, any fiducial placed ≥1cm from tumour edge was rejected. 14/17 fiducials (82%) placed <1cm from tumour edge were accepted in practice. Radiologists should aim to place fiducials within 1cm of tumour edge. In addition, care should be taken with peripheral metastases to avoid placing fiducials at a liver edge adjacent to bowel/duodenum.

3.4.5C Fiducial location: Pancreas tumour site

Kim et al (44) inserted fiducials via ultrasound guidance to mark pancreatic tumours in 39 patients. They noted a failure to discriminate fiducials in 1 patient (3%). The fiducials were either too close, or superimposed on the 45^0 oblique X-Rays. The authors did not report any further issues with respect to fiducial tracking for pancreatic tumours.

Table 3.15 shows the results for 9 patients with pancreatic tumours and multiple implanted fiducials. 27 fiducials were sited in total, but 3 fiducials in one patient migrated, leaving 24 fiducials for analysis. 6/24 fiducials (25%) were sited outside of tumour (3 in pancreas, 3 in mesenteric fat) therefore they could potentially move non-synchronously to tumour. All fiducials sited outside tumour were rejected. Mean distance of a rejected fiducial to closest tumour edge was 16mm (range 0-44mm). In contrast, all accepted fiducials were placed in tumour.

The 3 fiducials sited in pancreas (in 2 patients) were rejected at the time of treatment delivery for non-synchronous motion compared to the other implanted fiducials. The 2 rejected fiducials that were sited for patient 2 were located at the periphery of the pancreas, adjacent to stomach or duodenum. While the rejected fiducials appeared stable on the co-registered CT scans, (sub-millimetre shift only), the stomach was noted to be fuller at Planning CT, and the non-synchronous motion of fiducials could be explained by deformation due to stomach/duodenum filling or motion.

The 3 fiducials (in 3 patients) that were sited in mesenteric fat were rejected at the time of treatment delivery, due to non-synchronous motion with the remaining intra-tumour fiducials. One of these fiducials had shifted by 4.8mm in the Left/Right, and 1.3mm in the Ant/Post direction compared to the Planning CT.

In summary, I feel that pancreatic tumours present the greatest challenge for fiducial placement out of the 3 tumour locations studied here. Four implanted fiducials are ideal as pancreatic tumours tend to be large and irregular, and the challenging nature of fiducial placement means that often a fiducial needs to be rejected (33% rejection rate), and 3 remaining fiducials allows rotations to be tracked. The fiducial configuration should be such that the fiducial COM lies inside the tumour. In practice, all fiducials placed

outside of tumour were rejected. Clinicians should therefore place at least one fiducial in tumour. Mesenteric fat should be avoided as a placement site due to the high risk (100%) of migration or non-synchronous movement with intra-tumour fiducials. It is recognised that fiducials are rejected when implanted at the edge of normal pancreas and adjacent duodenum/stomach. However, the great majority of pancreatic tumours arise at the head of the pancreas and are therefore nestled in the C-shape of the duodenum. It is therefore unrealistic to request Radiology/EUS colleagues to avoid siting fiducials at the periphery of the pancreas (given the competing constraints e.g. needing to be >2cm apart, not superimposing on 45^{o} views). Rather, the emphasis should be on the CyberKnife team to ensure identical patient preparation with respect to eating/drinking for planning and treatment days.

3.4.6 Organ At Risk Reproducibility and Dosimetry:

As previously described, CyberKnife plans are chacterised by a sharp-dose gradient away from tumour, therefore any small geometric errors in fiducial tracking can lead to a large change in dose-delivery. This is not only an important consideration with respect to tumour dose, it is equally important that doses delivered to Organs At Risk (OAR) are within safe limits.

3.4.6A Thoracic OARs

Thoracic OARs include Bronchus, Chest Wall, Great Vessels, Heart, Oesophagus, Spinal Cord, and Lung. The dose-limiting OARs in an individual patient plan will depend on the location and size of the tumour target.

Zou et al (60) explored dose to OARs that may have been delivered (compared to planned doses) in 15 patients that had undergone arc therapy to deliver SBRT. The initial planning involved contouring of the GTV on different respiratory phases of the 4D CT to construct an Internal Target Volume (ITV), this was then expanded to a PTV. The patients had restrospective analysis using computer simulation and deformable image registration modelling. Mean differences in dosimetric parameters (between planned doses and simulated doses) were <1 Gy for OARs. However, in patients where the target was adjacent to critical organs, doses to heart, great vessels and bronchus increased by 2Gy, 4.9Gy, and 6Gy respectively. It is important to note that the patients were treated in free breathing (with an ITV technique to account for respiratory motion of the tumour as described), therefore the results may not be comparable to patients treated with tracking (e.g. Synchrony).

Section 3.3.4 describes an analysis of the reproducibility of Thoracic OAR position (relative to tumour target) on the Day 1 CT compared to the Planning CT. This is therefore an assessment of the inter-fractional variability of Thoracic OAR position.

Table 3.6 displays data on the reproducibility of OAR position for 10 patients with lung tumours. 3/10 (30%) of the patients studied had an inter-fractional change in OAR position which had the potential to increase OAR dose. 2 of these patients were suitable for assessment of the dosimetric impact of the OAR positional change (see Table 3.7).

Chest wall was the OAR for patient 5. It can be seen from Table 3.7 that planned doses to chest wall exceeded protocol doses for maximum point dose (MPD) and the 1cc/30cc threshold doses by 35%, 54% and 19% respectively. As explained, this was accepted by the treating Consultant, because they did not wish for tumour dose to be compromised.

It is interesting to note that the doses to Chest wall, based on the position of this organ at Day 1 CT, are actually marginally lower than planned doses, despite my judgement that the Chest Wall had moved towards tumour target (therefore closer to the high-dose region). This can be explained by the fact that CyberKnife plans are heterogenous. The prescription isodose line for Patient 5 was the 64% isodose line, with a PTV coverage of 98.97%. This means that 98.97% of the PTV is being treated to 45Gy or more, the maximum dose inside the tumour is 70.3Gy, and large portions of the PTV are receiving doses much greater than 45Gy. As a consequence, if the observed shift of OAR towards tumour occurred away from the highest dose volume, the OAR shift may not have a negative impact on OAR MPD/threshold doses.

Patient 8 had planned doses to Bronchus within protocol limits, but a shift in Bronchus position observed on the Day 1 CT has caused a small increase in MPD to beyond protocol limits (breach of protocol limits by 2%).

Both of these patients may be at risk of toxicity due to breach of OAR dose constraints.

3.4.6B Abdominal OARs

Velec et al (61) explored dose delivered to abdominal OARs for patients with liver tumours treated with hypofractionated radiotherapy delivered by a linac-based technique. The patients were treated in free breathing, a majority were treated with abdominal compression. Treatment planning was performed on an exhale breath-hold scan. Simulations were performed based on the breathing motion observed by

4D CT, and a deformable image registration technique. Results of change in doses to abdominal OARs were expressed as a percentage change of prescribed doses. Mean changes are reported with range in brackets. Results were as follows: Bowel -4% (-15 to 0), Duodenum -4% (-25 to +1), Oesophagus +2% (-1 to +9), Stomach -2% (-13 to +4), Liver 0% (-3 to +4). The mean dose to OAR only increased for Oesophagus, but it was noted that 2 patients had an increased dose (from the simulation), to oesophagus or stomach that would have exceeded dose constraints. It is again important to note that the patient treatments/simulations did not incorporate tumour tracking.

It is interesting that mean doses to OARs decreased in the simulations for 4/5 of the abdominal OARs studied. The planning was performed in exhale breath-hold, and it is possible that the relative positions for OARs and tumour are more favourable on inspiration. Loo et al conducted a planning study which considered likely oesophageal dose in patients being planned for lung SBRT with central tumours, according to respiratory phase. The respiratory phase which gave the greatest separation of tumour and oesophagus was selected for planning. This work was presented at ASTRO 2014, a number of patients showed favourable separation of oesophagus and lung tumour target.

Sections 3.3.9 and 3.3.14 explore the reproducibility (inter-fractional variation) of abdominal OAR position for patients treated for liver and pancreatic tumours respectively.

Table 3.11 displays data on the reproducibility of OAR position for 6 patients with liver tumours. 2/6 (33%) of the patients studied (patients 4 and 5) had an inter-fractional change in OAR position which had the potential to increase OAR dose. The possible dosimetric impact of the OAR positional change was explored in Table 3.12.

Bowel was the OAR for patient 4. It can be seen from Table 3.12 that planned doses to bowel exceeded protocol doses for both maximum point dose (MPD) and the 5cc threshold dose by 4%. This was considered acceptable by the treating Consultant. The coverage of the PTV by the prescription dose in this case was 93.9%, and reducing dose to bowel would only have been achieved by compromising PTV coverage further. It is noted that doses to Bowel based on the Day 1 CT position of Bowel were higher than anticipated (18% increase in MPD over protocol doses, and 5% increase in 5cc threshold doses over protocol doses). This could increase the risk of toxicity for the patient.

Patient 5 had planned doses to Duodenum within protocol limits, but a shift in duodenal position observed on the Day 1 CT has caused an increase in MPD to beyond protocol limits (breach of protocol

limits by 15%). Although the 5cc and 10cc threshold doses remained within protocol limits, this patient could be at increased risk of duodenal toxicity.

Table 3.15 displays data on the reproducibility of OAR position for 1 patients with a pancreatic tumour. This patients studied had an inter-fractional change in OAR position which had the potential to increase OAR dose. The possible dosimetric impact of the OAR positional change was explored in Table 3.18.

Duodenum was the OAR for patient 1. It can be seen from Table 3.18 that planned doses to bowel exceeded protocol doses for both maximum point dose (MPD) and the 5cc/10cc threshold dose by 25%, 55% and 95% respectively. This was considered acceptable by the treating Consultant in order to maintain an optimum coverage. Unfortunately, the duodenal shift observed on the Day 1 CT increased the duodenal doses further such that doses to MPD and 5cc/10cc thresholds exceeded constraints by 30%, 73%, and 107% respectively. This patient may have therefore received double the recommended dose to 10cc of duodenum, they would therefore certainly be at risk of duodenal toxicity.

A further pancreatic case (not reviewed here) showed an alarming change in duodenal position between Planning CT and Day 1 CT, such that Treatment was deferred. The patient did not speak English and was diabetic. Even though eating/drinking guidance was explained to her with the aid of an interpreter, the team had concerns about her understanding of these instructions. Her diabetic control was also poor with labile sugar levels, and on the first day of treatment she had felt like she was having a hypoglycaemic episode and therefore ate. The team decided to replan treatment using information from the Planning CT and "Day 1" Treatment CT scans, and a therapeutic, and safe, treatment plan was produced. When the patient was scanned on the new Day 1 of treatment, interestingly the duodenal position was most analogous to the previous "Day 1" CT, justifying the re-plan.

3.4.6C OAR summary

There are some limitations to the methodology followed to explore OAR reproducibility and dosimetry.

Firstly, assessments require delineation of OARs on the Day 1 CT. Inter-observer variability has been discussed previously with respect to tumour volume assessment, and this is a potential source of error here. However, it is considered likely that OAR delineation is more consistent than tumour volume delineation. OARs are "standard structures", so clinicians become experienced at outlining them, in contrast every tumour is individual in terms of size and shape. The edges of OARs also tend to be better

defined on imaging than the edges of tumours. Despite these caveats, inter-observer variability is a potential source of error.

Secondly, the measurements made of the closest distance of OAR to tumour target were prone to error. An initial visual assessment of the CT was made to highlight the slice levels where OAR was closest to tumour target, and the shortest distance was measured on the candidate slices. Whilst every effort was made to be as accurate as possible, this was accepted to be a fairly crude form of assessment, and it would have been possible for this methodology to miss some cases where there was OAR shift towards tumour. Reassuringly however, Patient 6 from the liver group, who was judged to have a stable position of OAR on Day 1 CT and Planning CT, had a decrease in Day 1 CT doses to OAR.

Thirdly, each CT reviewed is just a snap-shot of OAR position. Even when an OAR appeared in a more concerning position on the Day 1 CT, the actual positions of the OAR on the remaining days of treatment could feasibly be more favourable to inter-fractional variation. Equally, a patient with an OAR position which appeared more favourable on Day 1 CT, could have a less favourable OAR position on treatment days.

It is noted that a number of the patient cases reviewed had planned doses to OAR which exceed “safe” dose constraints. Doses delivered to tumour targets are largely limited by the dose constraints of adjacent OARs, so choosing an appropriately high dose to tumour, while also selecting a safe dose to adjacent OARs, is a constant challenge for Clinical Oncologists. It is known that uncontrolled tumour growth and organ invasion can be hazardous to the functioning of OARs e.g. rib fracture/pain due to tumour involvement, tumour invasion of the gastro-intestinal tract causing obstruction or fistulae. These risks of uncontrolled tumour growth therefore have to be borne in mind when considering whether to reduce prescribed doses in order to stay within safe OAR dose limits.

It is worth noting here, that dose constraints in SBRT are guidelines only. SBRT is a relatively new technique in radiotherapy, and compared to conventional fractionation there is a relative lack of long-term data on OAR toxicity. Therefore, staying within OAR dose constraints is far from a guarantee of delivering a safe treatment, and equally OAR dose constraints may possibly be overly conservative.

When considering MPD, this means the hottest dose delivered to 0.035cc of OAR. This is likely to be situated where a high-dose volume of the tumour target is adjacent to OAR, but the MPD based on Day 1 CT data may be delivered to a different 0.035cc of OAR, which would be a protective factor for the

OAR being considered. This same principle could apply to the threshold doses, but without real-time intra-fractional imaging of OARs, with subsequent dosimetric analysis, the actual position of MPDs cannot be assessed.

A very recent area of development in radiotherapy technique is MR-guided radiotherapy delivery (62-64). Treatments can be gated according to tumour motion, or OAR motion. This may offer the potential to assess doses actually delivered, and crucially to adaptively replan if necessary.

3.5 CONCLUSIONS

The accuracy of fiducial-based tracking depends on the assumption that the inter-relationship between fiducials/tumour and Organs At Risk (OAR) is the same at the time of planning CT as at the time of treatment. However, a number of factors which could invalidate this assumption have been assessed here: tumour volumetric change, tumour deformation, fiducial factors (migration/instability/optimum location) and OAR stability. Discrepancies in fiducial/tumour/OAR position between planning and treatment due to the factors described above must be accounted for by planning margins. In addition, for lung, liver, and pancreas tumour targets, a Synchrony tracking error of 2mm must be incorporated into the planning margins applied due to a correlation error (47).

A summary of the assessment outcomes for the factors described, together with the solutions to overcome the issues encountered, appear below.

<u>Assessment Outcomes:</u>

1. Tumour volumetric change:

Delineation issues were the biggest source of uncertainty here. However, Volume Doubling Times are significantly longer than the short mean interval from planning to treatment, so this is not considered an important issue.

2. Tumour deformation:

This was noted to be a potential issue for 2 liver patients. This was not an issue for lung and pancreatic tumours in the patients studied here.

3. Fiducial issues:

a) Migration: this was noted to be a particular concern when fiducials were inserted into fat.

b) Instability: sub-millimetre instability was noted for lung/liver/pancreatic targets.

c) Optimum location: rejection rates for implanted fiducials due to sub-optimal location were high (lung rejection rate 22%, liver rejection rate 44%, and pancreas rejection rate 33%).

4. Organs At Risk: Inter-fractional OAR shift was noted to be a significant issue for the pancreatic tumour site.

Solutions proposed:

1. Tumour volumetric change:

Improve delineation by careful consideration of the optimum imaging modality to best define a tumour target. It is also important to optimise the fusion of secondary scans e.g. PET-CT, MRI to the primary Planning CT scan.

2. Tumour deformation:

Particular attention should be given to assessing this in liver tumours. This can only be assessed adequately by CT, not by the Live X-Rays taken at treatment delivery. This supports the strategy of performing a Day 1 CT scan. Due to the difficulty in appreciating the contour of some liver tumours, a Day 1 CT with IV Contrast enhancement should be considered in selected patients, especially if a small planning margin has been applied.

3. Fiducial issues:

a) Migration: fiducials should not be implanted in fat

b) Instability:

Day 1 CT should be performed for all fiducial cases (not just Synchrony cases) as analysis has shown that instability of fiducial position is not just influenced by respiration, it is also influenced by organ filling and inter-fractional motion.

c) Optimum location:

Lung (large, irregular tumours): site 4 fiducials (due to risk of fiducial migration/rejection), and place fiducials within 1cm of tumour edge.

Liver: site 4 fiducials (due to risk of fiducial migration/rejection), and place fiducials within 1cm of tumour edge. In addition, try to avoid siting fiducials at the periphery of liver, adjacent to bowel/stomach/duodenum.

Pancreas: site at least one fiducial in tumour. Implant 4 fiducials, as many as possible within tumour, while following standard fiducial guidelines.

4. Organs At Risk:

Consider daily treatment CT for pancreatic cases

Optimise patient preparation: eating/drinking instructions and ensure patient compliance.

For the future, consider adaptive SBRT techniques e.g. Viewray, where OAR can be imaged in real-time.

Key Developments:

1. Interaction with Radiologists to feedback on above fiducial insertion guidance

2. Confirmation of importance of Day 1 CT for Synchrony cases: expand to perform a Day 1 CT for all fiducial cases

3. Review of standard planning margins:

Lung/Liver/Pancreas:

Synchrony (2mm) + Delineation (1mm) + Fiducial instability (1mm)

Therefore new minimum planning margin recommendation = 4mm

Individualise margins:

Delineation error likely to increase to minimum 2mm if e.g. a liver metastasis only shows well on an MRI scan, due to the Fusion error of minimum 1mm observed here.

References

1. Molinelli S, de Pooter J, Mendez Romero A, Wunderink W, Cattaneo M, Calandrino R, et al. Simultaneous tumour dose escalation and liver sparing in Stereotactic Body Radiation Therapy (SBRT) for liver tumours due to CTV-to-PTV margin reduction. Radiother Oncol. 2008;87(3):432-8.
2. Kothary N, Dieterich S, Louie JD, Chang DT, Hofmann LV, Sze DY. Percutaneous implantation of fiducial markers for imaging-guided radiation therapy. AJR Am J Roentgenol. 2009;192(4):1090-6.
3. Robertson EG, Baxter G. Tumour seeding following percutaneous needle biopsy: the real story! Clin Radiol. 2011;66(11):1007-14.
4. Wunderink W, Mendez Romero A, Seppenwoolde Y, de Boer H, Levendag P, Heijmen B. Potentials and limitations of guiding liver stereotactic body radiation therapy set-up on liver-implanted fiducial markers. Int J Radiat Oncol Biol Phys. 2010;77(5):1573-83.
5. Ozhasoglu C, Saw CB, Chen H, Burton S, Komanduri K, Yue NJ, et al. Synchrony--cyberknife respiratory compensation technology. Med Dosim. 2008;33(2):117-23.
6. Geraghty PR, Kee ST, McFarlane G, Razavi MK, Sze DY, Dake MD. CT-guided transthoracic needle aspiration biopsy of pulmonary nodules: needle size and pneumothorax rate. Radiology. 2003;229(2):475-81.
7. Tanisaro K. Patient positioning after fine needle lung biopsy-effect on pneumothorax rate. Acta Radiol. 2003;44(1):52-5.
8. Habermehl D, Henkner K, Ecker S, Jäkel O, Debus J, Combs SE. Evaluation of different fiducial markers for image-guided radiotherapy and particle therapy. Journal of Radiation Research. 2013;54(suppl 1):i61-i8.
9. Murphy MJ. Fiducial-based targeting accuracy for external-beam radiotherapy. Med Phys. 2002;29(3):334-44.
10. La Rosa S, Mahadevan A, E H, L S, Wang F. The effect of respiration on fiducials implanted in the pancreas for CyberKnife treatment. CyberKnife Users Meeting. 2009.
11. ICRU. International Commission on Radiation Units and Measurements Report 50: Prescribing, Recording and Reporting Photon Beam Therapy. ICRU Reports. 1993;50.
12. Pepin EW, Wu H, Zhang Y, Lord B. Correlation and prediction uncertainties in the CyberKnife Synchrony respiratory tracking system. Medical Physics. 2011;38(7):4036-44.
13. Wang K, Heron DE, Clump DA, Flickinger JC, Kubicek GJ, Rwigema JC, et al. Target delineation in stereotactic body radiation therapy for recurrent head and neck cancer: a retrospective analysis of the impact of margins and automated PET-CT segmentation. Radiother Oncol. 2013;106(1):90-5.
14. Hanahan D, Weinberg RA. The hallmarks of cancer. Cell. 2000;100(1):57-70.
15. Shackney SE. Tumour growth, cell kinetics, and cancer treatment: McGraw Hill; 1993.
16. Jameson MG, Holloway LC, Vial PJ, Vinod SK, Metcalfe PE. A review of methods of analysis in contouring studies for radiation oncology. J Med Imaging Radiat Oncol. 2010;54(5):401-10.
17. Upasani M, Chopra S, Engineer R, Medhi S, Master Z, Mahantshetty U, et al. Inter and intraobserver variation in gross tumor delineation on megavoltage CT images in patients undergoing tomotherapy-based image-guided radiotherapy for postoperative vault recurrences. J Cancer Res Ther. 2011;7(3):292-7.
18. Caravatta L, Macchia G, Mattiucci GC, Sainato A, Cernusco NL, Mantello G, et al. Inter-observer variability of clinical target volume delineation in radiotherapy treatment of pancreatic cancer: a multi-institutional contouring experience. Radiat Oncol. 2014;9:198.
19. Jensen NK, Mulder D, Lock M, Fisher B, Zener R, Beech B, et al. Dynamic contrast enhanced CT aiding gross tumor volume delineation of liver tumors: an interobserver variability study. Radiother Oncol. 2014;111(1):153-7.
20. Persson GF, Nygaard DE, Hollensen C, Munck af Rosenschold P, Mouritsen LS, Due AK, et al. Interobserver delineation variation in lung tumour stereotactic body radiotherapy. Br J Radiol. 2012;85(1017):e654-60.
21. Spoelstra FO, Senan S, Le Pechoux C, Ishikura S, Casas F, Ball D, et al. Variations in target volume definition for postoperative radiotherapy in stage III non-small-cell lung cancer: analysis of an international contouring study. Int J Radiat Oncol Biol Phys. 2010;76(4):1106-13.
22. Roberge D, Skamene T, Turcotte RE, Powell T, Saran N, Freeman C. Inter- and intra-observer variation in soft-tissue sarcoma target definition. Cancer Radiother. 2011;15(5):421-5.

23. Roy AEF, Wells P. Volume definition in radiotherapy planning for lung cancer: how the radiologist can help. Cancer Imaging. 2006;6(1):116-23.
24. Sahani DV, Kalva SP. Imaging the Liver. The Oncologist. 2004;9(4):385-97.
25. Tummala P, Junaidi O, Agarwal B. Imaging of pancreatic cancer: An overview. Journal of Gastrointestinal Oncology. 2011;2(3):168-74.
26. Steel GG. Basic clinical radiobiology: Arnold; 1997.
27. Kanashiki M, Tomizawa T, Yamaguchi I, Kurishima K, Hizawa N, Ishikawa H, et al. Volume doubling time of lung cancers detected in a chest radiograph mass screening program: Comparison with CT screening. Oncology Letters. 2012;4(3):513-6.
28. Winer-Muram HT, Jennings SG, Tarver RD, Aisen AM, Tann M, Conces DJ, et al. Volumetric growth rate of stage I lung cancer prior to treatment: serial CT scanning. Radiology. 2002;223(3):798-805.
29. Sadahiro S, Suzuki T, Ishikawa K. Estimation of the time of pulmonary metastasis in colorectal cancer patients with isolated synchronous liver metastasis. Jpn J Clin Oncol. 2005;35(1):18-22.
30. Queens CC. CIHR_RFA_Report 3_Appendix2.
31. Finlay IG, Meek D, Bruntont F, McArdle CS. Growth rate of hepatic metastases in colorectal carcinoma. British Journal of Surgery. 1988;75(7):641-4.
32. Carlson JA. Tumor doubling time of cutaneous melanoma and its metastasis. Am J Dermatopathol. 2003;25(4):291-9.
33. Dieterich S, Gibbs IC. The CyberKnife in clinical use: current roles, future expectations. Front Radiat Ther Oncol. 2011;43:181-94.
34. Liu H, Wu Q. A "rolling average" multiple adaptive planning method to compensate for target volume changes in image-guided radiotherapy of prostate cancer. J Appl Clin Med Phys. 2012;13(1):3697.
35. Nijkamp J, de Jong R, Sonke JJ, Remeijer P, van Vliet C, Marijnen C. Target volume shape variation during hypo-fractionated preoperative irradiation of rectal cancer patients. Radiother Oncol. 2009;92(2):202-9.
36. Nijkamp J, de Jong R, Sonke JJ, van Vliet C, Marijnen C. Target volume shape variation during irradiation of rectal cancer patients in supine position: comparison with prone position. Radiother Oncol. 2009;93(2):285-92.
37. Harris EJ, Donovan EM, Yarnold JR, Coles CE, Evans PM. Characterization of target volume changes during breast radiotherapy using implanted fiducial markers and portal imaging. Int J Radiat Oncol Biol Phys. 2009;73(3):958-66.
38. Barker JL, Jr., Garden AS, Ang KK, O'Daniel JC, Wang H, Court LE, et al. Quantification of volumetric and geometric changes occurring during fractionated radiotherapy for head-and-neck cancer using an integrated CT/linear accelerator system. Int J Radiat Oncol Biol Phys. 2004;59(4):960-70.
39. Bhagat N, Fidelman N, Durack JC, Collins J, Gordon RL, LaBerge JM, et al. Complications associated with the percutaneous insertion of fiducial markers in the thorax. Cardiovasc Intervent Radiol. 2010;33(6):1186-91.
40. Patel A, Khalsa B, Lord B, Sandrasegaran K, Lall C. Planting the seeds of success: CT-guided gold seed fiducial marker placement to guide robotic radiosurgery. Journal of Medical Imaging and Radiation Oncology. 2013;57(2):207-11.
41. Schroeder C, Hejal R, Linden PA. Coil spring fiducial markers placed safely using navigation bronchoscopy in inoperable patients allows accurate delivery of CyberKnife stereotactic radiosurgery. J Thorac Cardiovasc Surg. 2010;140(5):1137-42.
42. Jarraya H, Chalayer C, Tresch E, Bonodeau F, Lacornerie T, Mirabel X, et al. Novel technique for hepatic fiducial marker placement for stereotactic body radiation therapy. Int J Radiat Oncol Biol Phys. 2014;90(1):119-25.
43. Olsen CC, Welsh J, Kavanagh BD, Franklin W, McCarter M, Cardenes HR, et al. Microscopic and macroscopic tumor and parenchymal effects of liver stereotactic body radiotherapy. Int J Radiat Oncol Biol Phys. 2009;73(5):1414-24.
44. Kim JH, Hong SS, Kim JH, Park HJ, Chang YW, Chang AR, et al. Safety and efficacy of ultrasound-guided fiducial marker implantation for CyberKnife radiation therapy. Korean J Radiol. 2012;13(3):307-13.
45. Davila Fajardo R, Lekkerkerker SJ, van der Horst A, Lens E, Bergman JJ, Fockens P, et al. EUS-guided fiducial markers placement with a 22-gauge needle for image-guided radiation therapy in pancreatic cancer. Gastrointest Endosc. 2014;79(5):851-5.

46. Sanders MK, Moser AJ, Khalid A, Fasanella KE, Zeh HJ, Burton S, et al. EUS-guided fiducial placement for stereotactic body radiotherapy in locally advanced and recurrent pancreatic cancer. Gastrointest Endosc. 2010;71(7):1178-84.
47. van der Voort van Zyp NC, Hoogeman MS, van de Water S, Levendag PC, van der Holt B, Heijmen BJ, et al. Stability of markers used for real-time tumor tracking after percutaneous intrapulmonary placement. Int J Radiat Oncol Biol Phys. 2011;81(3):e75-81.
48. Hong JC, Eclov NC, Yu Y, Rao AK, Dieterich S, Le QT, et al. Migration of implanted markers for image-guided lung tumor stereotactic ablative radiotherapy. J Appl Clin Med Phys. 2013;14(2):4046.
49. Imura M, Yamazaki K, Kubota KC, Itoh T, Onimaru R, Cho Y, et al. Histopathologic consideration of fiducial gold markers inserted for real-time tumor-tracking radiotherapy against lung cancer. Int J Radiat Oncol Biol Phys. 2008;70(2):382-4.
50. Kitamura K, Shirato H, Shimizu S, Shinohara N, Harabayashi T, Shimizu T, et al. Registration accuracy and possible migration of internal fiducial gold marker implanted in prostate and liver treated with real-time tumor-tracking radiation therapy (RTRT). Radiother Oncol. 2002;62(3):275-81.
51. van der Horst A, Wognum S, Davila Fajardo R, de Jong R, van Hooft JE, Fockens P, et al. Interfractional position variation of pancreatic tumors quantified using intratumoral fiducial markers and daily cone beam computed tomography. Int J Radiat Oncol Biol Phys. 2013;87(1):202-8.
52. Ryu SI, Chang SD, Kim DH, Murphy MJ, Le QT, Martin DP, et al. Image-guided hypo-fractionated stereotactic radiosurgery to spinal lesions. Neurosurgery. 2001;49(4):838-46.
53. Berbeco RI, Nishioka S, Shirato H, Chen GT, Jiang SB. Residual motion of lung tumours in gated radiotherapy with external respiratory surrogates. Phys Med Biol. 2005;50(16):3655-67.
54. Seppenwoolde Y, Wunderink W, Wunderink-van Veen SR, Storchi P, Mendez Romero A, Heijmen BJ. Treatment precision of image-guided liver SBRT using implanted fiducial markers depends on marker-tumour distance. Phys Med Biol. 2011;56(17):5445-68.
55. Kilby W, Dooley JR, Kuduvalli G, Sayeh S, Maurer CR, Jr. The CyberKnife Robotic Radiosurgery System in 2010. Technol Cancer Res Treat. 2010;9(5):433-52.
56. Chang SD, Main W, Martin DP, Gibbs IC, Heilbrun MP. An analysis of the accuracy of the CyberKnife: a robotic frameless stereotactic radiosurgical system. Neurosurgery. 2003;52(1):140-6; discussion 6-7.
57. Lu XQ, Shanmugham LN, Mahadevan A, Nedea E, Stevenson MA, Kaplan I, et al. Organ deformation and dose coverage in robotic respiratory-tracking radiotherapy. Int J Radiat Oncol Biol Phys. 2008;71(1):281-9.
58. von Siebenthal M, Szekely G, Lomax AJ, Cattin PC. Systematic errors in respiratory gating due to intrafraction deformations of the liver. Med Phys. 2007;34(9):3620-9.
59. von Siebenthal M, Szekely G, Gamper U, Boesiger P, Lomax A, Cattin P. 4D MR imaging of respiratory organ motion and its variability. Phys Med Biol. 2007;52(6):1547-64.
60. Zou W, Yin L, Shen J, Corradetti MN, Kirk M, Munbodh R, et al. Dynamic simulation of motion effects in IMAT lung SBRT. Radiat Oncol. 2014;9:225.
61. Velec M, Moseley JL, Eccles CL, Craig T, Sharpe MB, Dawson LA, et al. Effect of breathing motion on radiotherapy dose accumulation in the abdomen using deformable registration. Int J Radiat Oncol Biol Phys. 2011;80(1):265-72.
62. Glitzner M, Crijns S, de Senneville BD, Kontaxis C, Prins F, Lagendijk J, et al. SU-E-J-77: Dose Tracking On An MR-Linac for Online QA and Plan Adaptation in Abdominal Organs. Med Phys. 2015;42(6):3281.
63. Kupelian P, Sonke JJ. Magnetic resonance-guided adaptive radiotherapy: a solution to the future. Semin Radiat Oncol. 2014;24(3):227-32.
64. Mutic S, Dempsey JF. The ViewRay system: magnetic resonance-guided and controlled radiotherapy. Semin Radiat Oncol. 2014;24(3):196-9.

Appendix 1: Lung tumour site: Multiple fiducials: Fiducial reproducibility: Patients 1-6

Patient	No of fids	Plan CT fid			Day 1 CT fid			Shift (mm)			Plan CT COM			Day 1 CT COM			Shift In COM (mm)		
		x	y	z	x	y	z	x	y	z	x	y	z	x	y	z	x	y	z
1	3	-16.76	35.04	33	-14.83	37.56	33.17	-1.93	-2.52	-0.17	-15.71	38.05	14.75	13.75	41.02	13.97	-1.96	-2.97	0.78
		-14.08	43.39	9.89	10.71	48.94	10	-3.37	-5.55	-0.11									
		-16.29	35.71	1.38	-15.72	36.56	-1.25	-0.57	-0.85	2.63									
2	2	56.79	37.45	-1.25	56.36	37.81	-2.5	0.43	-0.36	1.25	54.62	27.88	-2.77	54.52	27.8	-3.75	0.1	0.08	0.98
		52.44	18.32	-4.29	52.68	17.79	-5	-0.06	0.35	0.89									
3	3	-55.22	-57.76	46.36	-55.52	-57.83	45.75	0.3	0.07	0.63	-61.9	-68.5	39.42	-61.58	-68.52	39.5	-0.32	0.02	-0.08
		-51.96	-70.26	36.38	-51.22	-70.73	37	-0.74	0.45	-0.62									
		-78.5	-77.46	35.5	-78	-77.01	35.75	-0.5	-0.45	-0.25									
4	3	-83.03	-29.45	78.75	-84.51	-29.84	78.75	1.48	0.39	0	-90.38	-45.19	70.38	-90.8	-45.4	70.8	0.42	0.21	-0.42
		-86.01	-54.06	71.67	-86.39	-53.95	72.5	0.38	-0.11	-0.83									
		-102.11	-52.05	60.71	-101.39	-52.34	61.25	-0.72	0.29	-0.54									
5	3	-65.06	47.92	50.31	-66.68	48.71	51.25	1.62	-0.79	-0.94	-62.95	41.11	43.47	-65.39	40.78	44.58	2.44	0.33	-1.11
		-55.56	33.75	44.41	-58.4	33.01	46.25	2.84	0.74	-1.84									
		-68.24	41.64	35.69	-71.09	40.62	36.25	2.85	1.02	-0.56									
6	4	-100.68	2.09	111.79	-101	2.5	111.3	0.27	-0.45	0.54	-104.21 (98.41)	-4.87 (1.27)	95.86 (93.75)	-104.44	-4.44	95	0.23	-0.43	0.86
		-105.95	-20.24	98.59	-107.3	-21.58	98.75	1.35	1.34	-0.16									
		-98.01	1.21	93.04	-97.14	1.27	92.5	-0.87	-0.06	0.54									
		-112.19	-2.54	80	-112.38	0	77.5	0.19	-2.54	2.5									

CHAPTER 4

Optimising the Accuracy of Radiotherapy Treatment Delivery for Prostate Cancer: A focus on Bladder Filling

4.1 AIMS

1. Develop Bladder Filling Guidelines for Radiotherapy and CyberKnife patients, based on optimal dosimetry/reproducibility.

2. Determine the relationship between the consistency of bladder filling (between planning and treatment), and the ability to track rotations of the tumour target for the CK treatment of Prostate cancer.

4.2 INTRODUCTION

In order for Radiotherapy to be delivered accurately, and for the tumour to be treated exactly as intended, it is critical that the set-up and conditions at the time of treatment delivery reproduce exactly the set-up/conditions of the Planning CT scan. An accurate assessment of how closely the set-up/conditions/relative locations of tumour target and internal Organs At Risk (OAR) on treatment matches the set-up at planning, can only be achieved with imaging. The ability to image at the time of treatment allows for Image-Guided Radiotherapy (IGRT) which is now considered a standard of care as set out in the National Radiotherapy Implementation Group (NRIG) report: "IGRT: Guidance for implementation and use" (1, 2).

Reproducible set-up, and treatment delivery accuracy is dependent on a number of factors including: patient set-up errors, patient movements, delineation (contouring) errors, and organ motion (3-5). Organ motion is particularly relevant for the Radiotherapy treatment of prostate cancer, due to the anatomical location of the prostate gland. It sits at the base of the bladder and lies directly anterior to the rectum (see Figure 4.1). This means that the prostate tumour target will move due to bladder filling (or emptying), and due to passage of gas (flatus) through the rectum (6).

Fig 4.1

Sagittal view of an MRI scan to illustrate the proximity of Organs At Risk (Bladder and Rectum) to the Prostate Gland

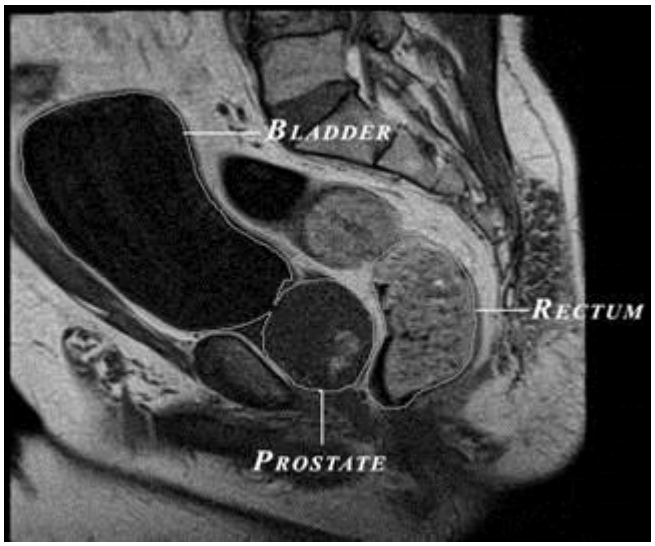

4.2.1 Prostate motion and sources of error in accurate targeting of tumour

The prostate gland is subject to Inter-fractional, as well as Intra-fractional, motion.

Inter-fraction motion is the motion seen between images taken on different treatment fractions. This motion can create errors in the geometric accuracy of treatment delivery, the error has systematic and random components.

Systematic inter-fraction error is the average variation in treatment position calculated from all treatment verification images/records across a course of radiation therapy for a given patient, compared with their CT planning scan (2).

Random inter-fraction error is the variability seen in patient positioning observed between daily treatment verification/images, this varies each day in direction and magnitude (2, 7).

Systematic errors can arise at the treatment preparation stage. Once "locked in" to the process, systematic errors will occur in each treatment fraction. Possible treatment preparation errors include:

Target delineation error

Target volumetric change (a change between Planning and Treatment due to tumour growth or regression)

Target positional change/target deformation (due to bladder filling and/or rectal distension)

Phantom transfer error (the error that accumulates when transferring image data from initial localisation at Planning CT, through the Treatment Planning System, and to the Linear Accelerator. This error is measured using a test phantom)

Patient set-up error (e.g. due to a change in patient's position, shape or size)

Random errors occur at the treatment delivery stage. Sources of error include:

Patient set-up error (varying changes in a patient's position between delivered fractions)

Target position and shape (between fractions due to target motion/deformation)

Intra-fraction motion is the variability seen in multiple images/assessments acquired in rapid succession during the delivery of a fraction of radiotherapy. Intra-fraction error is considered to be random, as the causes of error tend to be related to patient movement and organ filling.

4.2.2 Influence of Rectal gas/filling on prostate motion, target and OAR dose, and toxicity

As shown in Fig 4.1 the prostate gland lies anterior to the rectum. Therefore, any change in rectal filling (due to gas or faeces), either inter-fractionally, or intra-fractionally, can cause prostate motion. The consequence of such prostate motion is uncertainty in dose delivery to the tumour target, and OARs, during radiotherapy.

Ghilezan et al (4) used cine-MRI to quantify intra-fraction prostate motion, and concluded that the rectal filling status was the most important predictor of prostate motion. Padhani et al (8) also assessed the effect of rectal distension/movement on prostate gland position using cine-MRI, and confirmed that rectal filling status had an important impact on prostate motion.

A number of groups have attempted to reduce rectal distension, and optimise the reproducibility of rectal filling in order to minimise prostate motion. Strategies have included dietary modification, rectal preparation (including laxatives and enemas), and use of endorectal balloons (9, 10).

The possible consequence of rectal distension includes partial geometric miss of the prostate target, and therefore reduced tumour control, and this has been demonstrated in previous studies (11, 12). A limitation in these studies however, has been the lack of image-guidance during treatment (11). A study by Kupelian et al has demonstrated similar disease control between patients with distended vs non-distended rectum at the time of planning CT when ultra-sound based prostate position was verified daily (13), this supports the need for Image-guided Radiotherapy (IGRT).

A further refinement to radiotherapy dose delivery in recent years has been Volumetric Modulated Arc Therapy (VMAT). The technique can achieve highly conformal dose distributions, with improved target volume coverage and sparing of normal tissues, compared with conventional radiotherapy techniques (14). A group from Spain, Azcona et al (15), assessed the dosimetric impact of real-time prostate motion during VMAT on target dose. Real-time target (prostate) motion was determined using electronic portal imaging (EPI) data of the prostate fiducials. The team used an in-house simulation tool to calculate the dose received by the target (taking into account the observed prostate motion). They found that whilst the minimum dose to the PTV was only slightly degraded due to motion, the proportion of the GTV receiving the prescribed dose could be significantly affected by motion, dropping below 60% (compared to a desired coverage of >95%) in one trajectory in one patient. In contrast, the target dose delivered in those patients with minimal prostate motion, matched very well with the intended (planned) dose delivery. This supports the need for rigorous attention to rectal preparation, and use of IGRT, to maintain tumour control rates.

The main dose-limiting OAR for radiotherapy to the prostate gland is the rectum. It is important that planned dose-distributions to the rectum stay within "safe" dose limits. It is equally important that the delivered dose to the rectum remains within safe limits, in spite of any unplanned rectal/prostate motion. Thor et al applied motion models to two retrospective cohorts of prostate cancer patients that had had rigorous outcome data collection. There were strong associations for the planned and motion-simulated dose distributions, with rectal morbidity (especially rectal bleeding), at high doses (>55Gy) (16).

In summary, rectal preparation for the planning CT scan should result in a non-distended rectum. For accurate and optimum treatment delivery, the rectum should be non-distended, as per the planning CT, for each treatment day. IGRT should be employed in order that treatment can be delivered as intended, and prostate motion should be minimised. This should result in excellent tumour control rates, with minimal morbidity.

4.1.3 Influence of Bladder filling on prostate motion, target and OAR dose, and toxicity

In the past, patients receiving prostate radiotherapy were advised to empty their bladder before treatment. This was advocated in order to minimise inter-fraction variability (17).

However, dosimetric studies have shown that dose to OARs, including small bowel and bladder wall, are much higher when treating patients with an empty bladder (18-20). The clinical explanation for reduced high dose to the bladder wall with increased bladder filling, is that as bladder-filling increases, the bladder expands, partly within the high-dose region, but mainly outside this region. Simultaneously, the bladder wall stretches, with the overall result that the high-dose bladder wall volume decreases (18).

Fig 4.2

Lateral beam's eye view of rectum, bladder and conformal field of a patient. The view demonstrates the effect of bladder filling on the high-dose volume received by the bladder wall.

Taken from Lebesque et al, "Variation in volumes, dose-volume histograms, and estimated normal tissue complication probabilities of rectum and bladder during conformal radiotherapy of T3 prostate cancer" (12). The red outline represents the conformal field and therefore the high-dose region.

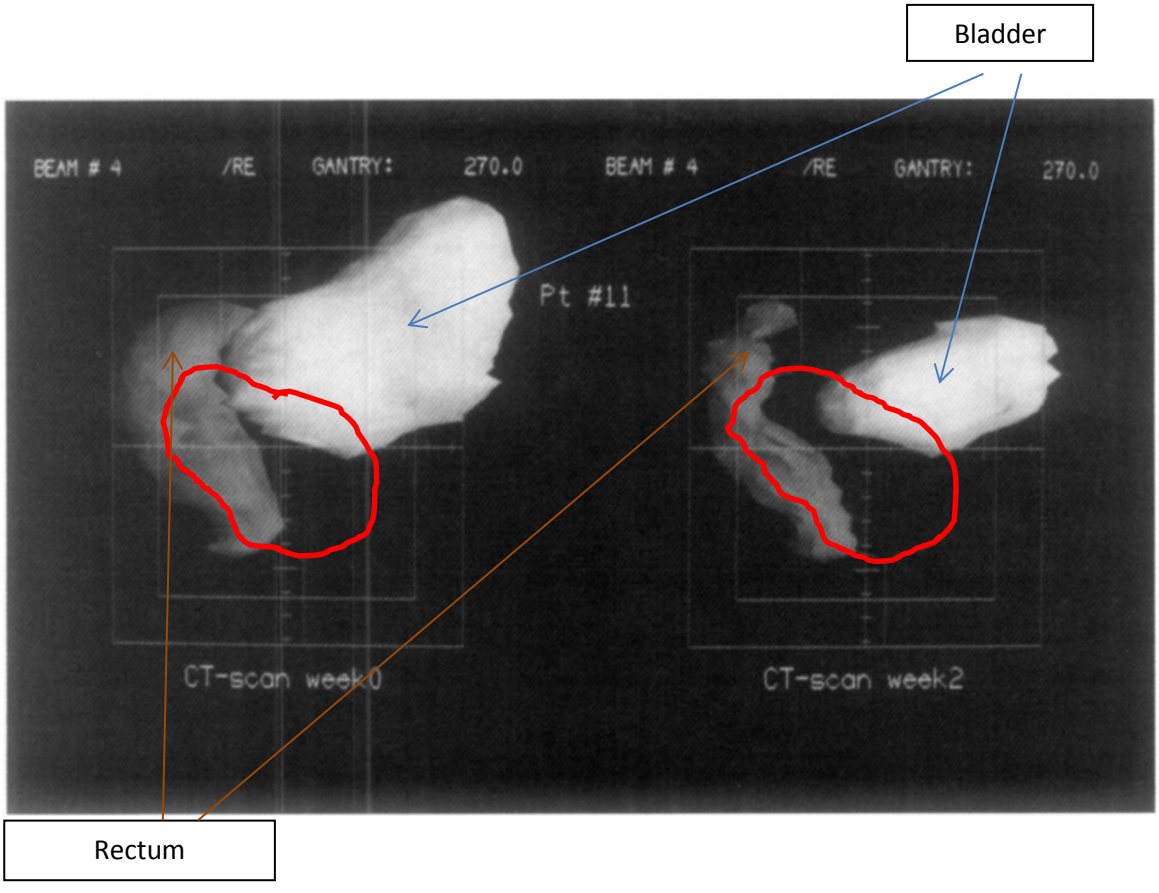

A study by Pinkawa et al showed that the dose to small bowel reached 90% of prescription dose in 37% of cases treated with an empty bladder, compared to only 3% of cases treated with a full bladder ($p<0.01$) (21). Importantly, a number of studies have shown that the increased dose received by OARs when irradiating the prostate with an empty bladder, translates into increased toxicity to the patient. Jain et al (22) performed a study on prostate cancer patients to evaluate whether using an IMRT technique to deliver elective pelvic nodal irradiation (vs. "4-field brick") reduced acute treatment toxicity. They found that bladder filling (full vs empty) had a greater influence on acute gastro-intestinal toxicity, particularly proctitis and flatulence ($p<0.0001$) ≥Grade 2 (G2) than the treatment technique employed ($p<0.0002$). In those patients treated with a 4-field brick technique, the rate of G2 toxicity was 14% for those treated with a full bladder, but as high as 40% for those treated with an empty bladder.

It is now widely accepted that patients receiving prostate radiotherapy should be treated with a "comfortably full" bladder. This is specified in national and international trials of prostate radiotherapy (PACE and CHHiP) (23, 24). However, achieving consistency of bladder filling on a daily basis for a course of conventionally fractionated External Beam Radiotherapy (which typically delivers 74Gy in 37 treatment fractions) is difficult to achieve. Even with the use of bio-feedback wide variations in bladder filling are observed (25, 26).

Ideal bladder preparation would have dosimetric advantages (bladder full enough to minimise dose to bowel and bladder wall), and would be consistent and reproducible on a daily basis (such that the treatment actually delivered to Prostate and OARs is exactly as intended).

The 1st aim of this Chapter is therefore:

To develop bladder filling guidelines for conventionally-fractionated Radiotherapy and CyberKnife patients, based on optimal dosimetry/reproducibility.

4.1.4 Prostate radiotherapy delivered by CyberKnife: hypofractionation

There is a good evidence base for the efficacy and tolerability of conventionally-fractionated external beam radiotherapy for the treatment of early stage, low to intermediate risk prostate cancer (prostate cancer which is confined to the prostate gland, with no capsular breach, Gleason≤4+3, PSA≤10-20) (27, 28). A typical dose/fractionation regime employed in conventionally-fractionated external beam radiotherapy is 74Gy/37 fractions/7.5 weeks (29). The BED for tumour control for this

regime (using alpha/beta for prostate cancer of 1.5Gy) = 173. The BED for late effects to bladder/bowel (using alpha/beta of 3) = 123.

The low α/β ratio (1.5Gy) of prostate cancer has stimulated interest in hypofractionated radiotherapy for prostate cancer. Delivery of hypofractionated regimes should optimise prostate tumour control rates, without negative consequences on late toxicity (30). Early results suggest that PSA relapse-free survival rates compare favourably with other definitive treatments for organ-confined disease, although longer-term outcome data is awaited (31).

The hypofractionated dose/fractionation regime for prostate cancer treated with CyberKnife at the author's centre is 35Gy/5#/1 week (BED tumour control= 198, BED normal tissues= 116), therefore hypofractionation delivers a higher BED to tumour (compared to conventional fractionation), while limiting BED to normal tissues.

4.1.5 Prostate radiotherapy delivered by CyberKnife: fiducial tracking

The importance of image guidance to guide prostate radiotherapy delivery has been described (1, 2). Standardly, three fiducials are inserted into the prostate (32, 33) to guide prostate radiotherapy for CK patients. In contrast to the patient groups described in Chapter 3 (lung, liver pancreatic tumours), prostate cancer patients do not undergo Day 1 Treatment CT at my Centre. This is considered reasonable practice, as the risk of fiducial migration outside of the prostate gland once implanted is negligible, and fiducial instability in the prostate is recognised to be sub-millimetre, and therefore within the accuracy of CT measurement (33-35).

At treatment, patients are positioned in immobilisation, exactly as at planning CT, and positional adjustments to the patient and couch are made according to information on fiducial position from the Live X-Rays. Treatment is able to proceed when the following criteria are fulfilled:

1. CyberKnife Radiographers are satisfied that the patient is well positioned

2. The Rigid Body Error (RBE) of fiducial arrangement is within acceptable limits

3. Suggested translations/rotations (to allow accurate treatment delivery) are sufficiently small that the CK robot can make the adaptations required

Once treatment has commenced, intra-fractional prostate motion is analysed by review of Live X-Rays, and evaluation of fiducial parameters (such as inter-marker distance and RBE).

Intra-rectal flatus can sometimes be appreciated on the Live X-Rays, but it is not possible to see bladder filling on the plain X-rays. Bladder filling during a CK prostate treatment (typically >40minutes) has the potential to change the fiducial configuration from that at CK planning. A change in fiducial configuration could potentially mean that rotational adjustments required are in excess of what the CK robot can adapt for. If this is the case, rotations may need to be "switched off" such that treatment delivery can proceed, tracking translations only. This is not ideal as tracking accuracy is improved by tracking both translations and rotations (36).

The author was called to the CK bunker for consultation on a problematic treatment delivery, and observed changes in pitch that were beyond what the robot could adapt for towards the end of treatment. The treatment had taken a long time to deliver and the patient commented post-CK that his bladder was very full. This prompted the author to consider the relationship between bladder filling and rotational tracking.

The rotational changes that the CK robot can adapt for are: Roll: 2^0, Yaw: 3^0, Pitch: 5^0.

The 2nd aim of this Chapter is therefore:

To determine the relationship between the consistency of bladder filling (between planning and treatment), and the ability to track rotations of the tumour target for the CK treatment of Prostate cancer.

4.3 MATERIALS AND METHODS

4.3.1 CyberKnife (CK) patients: Planning

A planning CT scan was performed 1 week after insertion of 3 gold fiducials into the prostate. A planning MRI scan was always performed immediately after the planning CT scan. This was a secondary scan to be fused with the planning CT to aid delineation of the target.

Patients were asked to keep a record of the fluids consumed on the day of the planning CT scan, and the time of the last fluids consumed before scanning.

Patients were catheterised prior to planning CT scan with an aseptic technique using a 12F rubber urinary catheter. Catheterisation was standard procedure for all CK patients undergoing treatment for primary prostate cancer. The aim of catheterisation was that the intra-prostatic urethra could be more easily visualised/delineated on CT. The dose to the intra-prostatic urethra could then be limited to safe dose constraints at the treatment planning stage.

All patients emptied their bladder before catheterisation (and recorded the time of voiding as requested), so in order to fill the bladder appropriately for the planning CT scan, sterile water was instilled into the bladder via the catheter. A bladder volume of approximately 180mls was considered optimum (full enough to improve bladder dosimetry, but empty enough for patient comfort during CK treatment). However, after each 60mls was instilled the patient was consulted as to their level of comfort. A minimum of 100mls was instilled. Once the bladder was filled as considered appropriate, the catheter was clamped, and the volume of fluid instilled into the bladder was recorded. This was standard pre-treatment planning procedure.

The department had recently purchased a BVI9400 bladder scanner (Verathon Medical UK, Sandford, UK). This is a portable 3D Ultrasound device that is designed to measure urinary bladder volumes. This Ultrasound device measures specifically the volume of urine (fluid), not “whole bladder” (i.e. the volume does not include bladder wall). The department was keen to use the bladder scanner to its full potential to help develop bladder filling guidelines.

Once the bladder had been filled as described, 3 ultrasound measurements of the urinary volume were taken in quick succession, and recorded. Patients were scanned by placing the ultra-sound transducer at the midline, 2cm above the pubic symphysis, and angled towards the bladder. The time of scanning was recorded.

The patient then proceeded to planning CT scan as standard (in immobilisation, 1.25mm slices).

Initially, the methodology was that the patients had 3 x bladder ultrasounds pre-CT, and then 3 x bladder ultrasounds immediately post-MRI. As an additional assessment as to the accuracy of the bladder ultrasound, the catheter was unclamped and the urine allowed to drain into the catheter bag. The volume of urine drained was recorded.

However, there were difficulties encountered with the above approach.

The patients often felt very full after MRI and wanted the catheter out immediately. It was not possible to perform ultrasound bladder scanning in the MRI room due to the incompatibility of the metal-containing ultrasound machine, and the magnet of the MRI scanner. It was often difficult to find a suitable room to perform ultrasound bladder scanning post-MRI in a timely way.

In addition, there were issues with measuring the volume of urine drained from the bladder post-MRI in the way described. One patient was so full that some urine bypassed the catheter. In others, urine did not completely drain via the catheter, some was retained.

For these reasons, the author felt it more constructive to abandon post-MRI measurements.

Following this change to the methodology, a further 3 bladder ultrasound measurements were recorded post-CT scan.

Urine volumes were subsequently estimated from the Planning CT scan as explained below.

“Bladder” was outlined on the planning CT in MultiPlan by the physics team. “Bladder wall” was created using the Boolean operator tool of MultiPlan, applying a 4mm internal margin on “Bladder” (37). Bladder volume minus Bladder Wall volume provided an estimate of urine volume at the time of planning CT.

4.3.2 CyberKnife (CK) patients: Dosimetry

Treatment planning was performed by the CK physicists as per standard protocol. Bladder wall dosimetry was recorded for analysis. Maximum Point Dose (MPD), dose to ≤ 5cc of bladder wall and ≤ 15cc of bladder wall (standard constraints) were recorded. PTV coverage and PTV volume were also recorded.

4.3.3 CyberKnife (CK) patients: Treatment

Patients were treated in 5 treatment sessions on consecutive days.

Patients were asked to record the quantity of fluids consumed prior to each CK treatment. They were advised to stop drinking 2 hours prior to each treatment.

For Day 1 of treatment, following standard protocol, patients were asked to void (just prior to treatment), and then drink 2 plastic cups of water (200mls). The cups were filled by a staff member. An Ultrasound bladder scan was performed prior to treatment (x 3 consecutive readings). The times of voiding, drinking and scanning were recorded.

The CK Radiographers then positioned the patient for treatment. The set-up time and start time was recorded.

Prior to treatment start, the inter-fiducial marker distances were recorded.

Each treatment session was observed and the following was recorded from the CK console data: translational and rotational robot corrections, Rigid Body Error (RBE). If rotational corrections needed to be disabled, or if couch corrections needed to be applied then this was also recorded.

Just before the end of treatment the CK Radiographers performed a "soft stop" of treatment delivery, and inter-fiducial marker distance was again recorded.

Immediately after each treatment session, the bladder was scanned (again, 3 x consecutive measurements). The time of scanning was recorded.

The average urine volume during treatment was calculated (end of treatment volume plus pre-treatment volume divided by 2). The average urine volume was compared to the planning CT urine volume in order to inform drinking instructions for the next day's treatment. The "baseline" pre-treatment water volume of 200mls was increased or decreased as considered appropriate.

4.3.4 Radiotherapy (RT) patients: Planning: Early patient group: pilot study

A planning CT scan was performed on each patient. The patients were not catheterised for scanning.

The initial protocol for these patients (in the pre-bladder scanner era) was to attend clinic 40 minutes prior to CT scan. The patients were asked to void, then drink 400-500mls within 5 minutes. The aim

was that when the patients were ready for CT scanning 40 minutes later, the bladder would be "appropriately full".

Once the bladder scanner was purchased, the CT simulator staff scanned the patients with the ultrasound bladder scanner (3 consecutive measurements) prior to proceeding to planning CT scan. Some patients were advised that more time/water was required to fill the bladder (times and volumes were recorded). A "threshold" bladder volume was not well defined in protocol at this point in time, however.

A bladder filling working party was established to analyse the early results from these pilot patients, and to refine the bladder filling guidelines in light of the results. The results will be reported in Section 4.4.

Urine volumes were subsequently estimated from the Planning CT scan as previously explained, with a few key differences. The RT patients were planned on Eclipse terminals. For these patients a 2mm thickness of bladder wall was assumed (38, 39).

The reasons for the different thickness of bladder wall assumed for the 2 groups of patients will be discussed and critiqued in Section 4.5.

4.3.5 Radiotherapy (RT) patients: Treatment

The pilot group of patients, were given identical drinking instructions for treatment fractions to their pre-CT instructions.

Three ultrasound bladder scan readings were taken prior to RT treatment. Given the much shorter treatment times in RT treatments (compared to CK), a post-treatment bladder scan was considered less informative and was therefore not undertaken.

4.3.6 Radiotherapy (RT) patients: Dosimetry analysis

As previously described, RT patients undergoing conventionally-fractionated for prostate cancer receive 33-37 treatment fractions. It is important for the accuracy of treatment delivery that there is image-guidance (1, 2). Standard protocol for these patients is to undergo Cone beam CT scan on the treatment couch just prior to radiotherapy delivery on Days 1-3 of treatment, then weekly Cone

beam CT scans thereafter. Any positioning errors noted on Cone beam CT are corrected before treatment delivery (40).

The Cone beam CT scans provide a helpful dataset for analysis of the impact of differential bladder filling on bladder and bowel dosimetry.

The bladder contour was outlined on the Cone beam CT scans for a sample of 3 patients. "Bladder wall" was created as before using an internal margin of 2mm on the bladder. The Cone beam CT scans were then blended with the original treatment plan for analysis of bladder/bowel doses received, which could be compared with planned doses.

4.3.7 Radiotherapy (RT) patients: Data collection

The author collected the bladder filling and dosimetry data for CK patients.

The bladder filling data for RT patients was collected by the treatment radiographers. The author analysed the results of the pilot group of RT patients and presented the outcomes in the RT department medical journal club, with suggestions for refinements to bladder filling guidelines. A "bladder filling working party" was subsequently established, which the author was an integral part of, and new guidelines were agreed.

The author designed the technique for assessing bladder dosimetry by use of the Cone beam CT scans in collaboration with the Physics department, and performed the dosimetric analysis on an example patient. The technique, and the DVH parameters of interest, were disseminated to a dosimetrist from the "bladder filling working party" for further analysis of a sample group of patients.

4.4 RESULTS

4.4.1 CK patients: Planning

The bladder filling results for 9 CK patients undergoing Planning CT scan are shown in Table 4.1 below.

Table 4.1: CK patients: Pre-treatment bladder filling

U/S = Ultrasound. ^{m} = Readings taken post-MRI rather than post-CT. * = see text below.

SD = Standard Deviation.

Patient	Fluid instilled into Bladder (mls)	U/S Bladder scan fluid volume pre-CT (mls)				Plan CT Urine Volume (cc)	% change Bladder scan pre-CT volume to Plan CT volume	U/S Bladder scan urine volume post-CT (mls)			
		1	2	3	Mean (SD)			1	2	3	Mean (SD)
1	180	207	249	247	234 (19)	**176**	-25	250^{m}	228^{m}	235^{m}	234^{m} (9)
2	180	218	221	235	225 (7)	**333**	+48	417^{m}	450^{m}	258^{m}	375^{m} (84)
3	180	332	318	342	331 (10)	**325**	-2	127*	122*	125*	125* (2)
4	180	308	314	296	306 (7)	**211**	-31	268^{m}	246^{m}	247^{m}	254^{m} (10)
5	180	250	266	262	259 (7)	**242**	-7	234	252	245	244 (7)
6	180	200	179	178	186 (10)	**173**	-7	182	183	195	187 (6)
7	150	106	127	127	120 (10)	**144**	+20	141	140	142	141 (1)
8	180	171	180	194	182 (9)	**204**	+12	274	290	267	277 (10)
9	180	249	250	248	249 (1)	**186**	-25	227	234	223	228 (5)
Mean	177				232	**222**	+4				230 (71)

8/9 patients (89%) could tolerate 180mls of water instilled into their bladder. The remaining patient (patient 7) felt reasonably full after 150mls of water was instilled.

On analysis of the Ultrasound bladder volume taken prior to CT, the mean volumes measured by bladder scanner were greater than the volume instilled for all patients except for patient 7. It would be expected that the volume of intra-bladder fluid recorded by bladder scanner would be >180mls because the bladder would have filled with urine to some extent in the interval between the patient voiding and the bladder scanner reading being taken. Mean interval between voiding and first bladder scanner reading was 23mins.

The likely explanation for the results for patient 7 is inaccuracies of the bladder scanner readings. There was no observation of fluid bypassing the catheter for this patient.

Mean pre-CT bladder scanner urine volume for the group as a whole was 232mls. For the 8 patients that had 180mls of water instilled into bladder, the mean bladder scanner urine volume pre-CT was 247mls. The range of mean urine volumes pre-CT for those with 180mls instilled into bladder was wide: 182-331mls. This is likely to reflect a significant individual variation in rate of bladder filling, which is dependent on multiple factors. These will be discussed further in the Discussion, section 4.5. Of note, the time interval between instilling water into the bladder and taking bladder scanner readings was minimal, and it was consistent across all patients studied, range was 2-3 minutes.

Examining the consistency of pre-CT bladder scan readings for each patient, these are largely consistent. The mean Standard Deviation for the group as a whole was 8mls (range 1-19). Interestingly, the largest Standard Deviation occurred in the first patient, so this may have represented a learning curve on taking the scan measurements.

The mean Planning CT urine volume was 222cc, which was remarkably consistent with the mean Ultrasound bladder scan volume pre-CT (232mls), a change of 4%. Note 1 ml= 1cc. However, there were wide individual variations in the consistency between bladder scan measurements, and the measurements calculated by CT. It would be expected that the urine volumes measured at CT would be larger, because the CT scans were taken at a later time point (5-10 minutes later) and therefore the bladder would have continued to fill. In fact, only 3 patients (patients 2, 7 and 8) showed an increase in urine volume at CT. The range of percentage variation between bladder scanner urine volumes, and planning CT urine volumes is -31% to +48%. Possible explanations for these observations will be discussed in Section 4.5.

Reviewing the results for post-CT bladder scanner readings, patients 1-4 had readings taken following MRI scan. The post-MRI readings were taken on average 1.5 hours after the pre-CT bladder scan readings, therefore, the readings might have been expected to be considerably more than the pre-CT readings. This was the case for patient 2, but not the other patients. The results for patient 3 cannot be interpreted sensibly because this patient had a significant amount of urine bypass the catheter post-MRI. For patients 1 and 4, the results may potentially be explained by a combination of inaccuracies in bladder scanner readings, and it was also possible that bladder filling rate may have slowed significantly due to the MRI scan taking place a long time after drinking. Patient 1 had last consumed fluids 4 hours 20 minutes prior to the post-MRI bladder scans. Patient 4 had not recorded their fluid intake.

Patients 5-9 had repeat bladder scanner readings taken immediately after planning CT scan. 4/5 patients (80%) showed an increase in bladder scan volumes, patient 7 had a slight decrease in volume recorded (-2%). Average change in volume between planning CT and post-CT bladder scan volume was +12% (-2 to +35%).

Post-CT bladder scanner readings were largely consistent, except for patient 2, who had a SD of 84mls. Of note, this patient had the largest urinary volumes recorded, so this could potentially suggest something about the accuracy of the bladder scanner at larger volumes.

Patients 1 and 3 had the catheter unclamped after the post-MRI bladder scanner readings, and the urine was allowed to empty into the catheter bag. This was subsequently measured in a measuring cylinder. The measured urine volume for patient 1 was 290mls, and for patient 3 was 120mls. The recorded volume for patient 3 was very similar to the bladder scanner readings (125mls). The volumes for patient 1 were less similar.

In summary, mean pre-CT bladder scanner urine volume measurements are consistent with mean planning CT urine volume measurements (only 4% difference), however, there are large individual patient variations. There are early suggestions that inaccuracies with bladder scanner measurements may be more significant at larger bladder volumes.

4.4.2 CyberKnife (CK) patients: Dosimetry

Table 4.2 shows bladder wall dosimetry for 9 patients undergoing CK treatment for primary prostate cancer.

MPD = Maximum Point Dose

Table 4.2: CK patients: Bladder wall dosimetry

Patient	MPD (Gy)	≤ 5cc threshold (Gy)	≤ 15cc threshold (Gy)	PTV coverage (%)	PTV volume (cc)
Protocol	**38**	**35**	**18.3**	**>95**	
1	37.3	32.6	14.9	98.8	49.7
2	37.9	33.6	17.1	99	70.8
3	37.8	34	18	96	42.6
4	37.4	34.1	17.5	97	99.8
5	37.4	33.6	14.9	98.6	40.9
6	37.3	30.1	14.4	99	54.5
7	37.8	34.9	16.5	98.1	80.3
8	37.2	33.3	18.4	89.4	121
9	37.5	34.3	17.8	95.7	47.7

Table 4.2 shows that for all 9 patients (the same patients as in Table 4.1) the bladder wall maximum point dose, and the 5cc threshold, were within protocol constraints. Patient 8 had up to 18.4 Gy delivered to ≤15cc of bladder wall, which is just outside of protocol. All other patients achieved protocol constraints.

Table 4.1 shows that patient 8 had a planning CT urine volume of 204 cc, which is just less than the mean volume for the group (222 cc). There were 4 patients (44%) with bladders which were less filled (≤186 mls), that would therefore potentially have had less favourable bladder filling to achieve bladder wall dosimetry within constraints. All of these achieved bladder wall constraints however, without compromising on PTV coverage.

Patient 8 had the largest PTV volume (121 cc) and PTV coverage was compromised (to 89.4%) in order to stay within bladder wall constraints as much as possible. It is likely that PTV volume (rather than bladder filling) was the dominant factor which caused a breach of bladder wall constraints, and also compromise of PTV coverage.

For all patients studied with a PTV volume of ≤100 cc, treatment plans were produced which were within safe constraints to bladder wall and other OARs, without dropping PTV coverage below the recommended lower limit of 95%. This supports planning CT urine volume of between 144mls and 333mls (and pre-CT bladder scanner volumes of 120-331mls) as an "optimum bladder volume" from a dosimetric perspective.

Reproducibility of bladder volumes on treatment is an important consideration and this is reported in the following section.

4.4.3 CyberKnife (CK) patients: Treatment bladder filling

Table 4.3 shows the results of bladder filling pre- and post-treatment for a patient undergoing CK treatment for primary prostate cancer.

BS = Bladder scan. BSV = Bladder scan volume.

Table 4.3: CK patient: Pre- and post-treatment bladder filling

Fraction	Fluids given (mls)	Time Void to Pre-CK BS (mins)	Time Void to Post-CK BS (mins)	Planning CT Bladder urine volume (cc)	Mean Pre-CK BSV (mls)	Mean Post-CK BSV (mls)	Average CK BSV (mls)	% change Plan CT Bladder urine volume to Mid-CK BSV
1	200	5	60	238	20	250	135	-43
2	250	3	54	238	0	306	152	-36
3	300	3	56	238	7	340	174	-27
4	350	5	55	238	0	327	163	-32
5	400	5	54	238	4	399	202	-15

The patient whose results are displayed in Table 4.3, was advised to drink an increased volume of fluids before CK treatment each day, as the average CK bladder scan volume was less than the volume recorded at planning CT for each fraction of treatment. The aim of the focus on bladder filling, and the individualised advice to patients, was to match the planning CT urine volume, and the average CK bladder scan volume (i.e. the likely bladder urine volume mid-way through a fraction of CK).

The advice given improved the consistency of bladder filling on treatment days. The application of "standard advice" on fraction 1 resulted in under-filling of the bladder on treatment by 43%. By fraction 5, refined bladder filling guidance which had been individualised to this patient, meant that the bladder was under-filled by 15% only. It is important to note that treatment times were remarkably consistent in this patient (as evidenced by the consistency of times between voiding and first post-CK bladder scan reading).

Table 4.4 shows the pooled results of bladder filling pre- and post-treatment for 6 patients undergoing CK treatment for primary prostate cancer.

BS = Bladder scan. BSV = Bladder scan volume.

Table 4.4: CK patients: Pre- and post-treatment bladder filling: summary results

Patient	Fraction	Fluids given (mls)	Time void to post-CK BS (mins)	Plan CT bladder urine volume (cc)	Mean Pre-CK BSV (mls)	Mean Post-CK BSV (mls)	Average CK BSV (mls)	% change Plan CT Bladder urine volume to Mid-CK Rx BSV
1	1	200	60	238	20	250	135	-43
	5	400	54		4	399	202	-15
	Mean (Range)	300 (200-400)	56 (54-60)		6 (0-20)	324 (250-399)	165 (135-202)	-31 (-43 to -15)
2	1	300	63	80	0	121	61	-24
	5	350	72		29	328	179	+123
	Mean (Range)	340 (300-350)	74 (63-81)		7 (0-29)	224 (121-462)	164 (61-231)	+105 (-24 to +189)
3	1	200	71	211	81	469	275	+30
	5	200	98		0	293	147	-30
	Mean (Range)	200 (200-200)	88 (63-107)		106 (0-174)	423 (256-704)	265 (147-433)	+26 (-30 to +105)
4	1	200	61	325	134	X	X	X
	4	200	61		9	336	173	-47
	Mean (Range)	200 (200-200)	58 (48-63)		77 (9-134)	304 (227-350)	181 (145-226)	-44 (-55 to -30)
5	1	200	100	144	27	337	181	+26
	5	250	72		5	158	82	-43
	Mean (Range)	230 (200-250)	84 (72-100)		17 (4-29)	234 (158-337)	125 (82-181)	-13 (-43 to +26)
6	1	200	68	204	0	230	115	-44
	5	250	85		63	411	237	+16
	Mean (Range)	250 (200-300)	86 (68-115)		32 (0-63)	308 (182-411)	138 (115-237)	-33

Patient 1 in Table 4.4 above is the same patient from Table 4.3 so the results will not be discussed further here.

Patients 3 and 4 were not advised to drink different amount of fluids than the standard 200mls. Both were patients that complied with voiding instructions with difficulty. This was the reason for the high pre-CK BSV's for these patients, even though the patients were asked to void immediately before arrival on the CK unit. Both patients were better at following this instruction towards the final fraction of CK. The author found it difficult to suggest a change to fluid consumption on the information gathered.

Patient 2 had a small bladder volume at CT. This was by design. The patient had attended for CK planning initially a number of months before. However, due to a combination of a large prostate gland, and the configuration of the bladder against the prostate, it was not possible to produce an acceptable treatment plan. The patient therefore underwent hormonal cytoreduction of the prostate gland. At repeat planning the aim was to scan the patient with a bladder volume of approximately 100mls rather than 180mls (as advised by the Physics team). This patient could not be catheterised therefore his bladder was filled by drinking at planning CT. Mean BSV prior to planning CT was 110mls. The patient was noted to have slow bladder filling at planning CT, which is the reason he was commenced on 300mls. This was not sufficient to adequately fill the bladder at fraction 1, but the adjustment strategy led to over-filling of the bladder on subsequent fractions, which was disappointing.

Patient 4 was so full at the end of his first fraction of CK, that he had to go immediately to the toilet without pausing for a post-CK BSV assessment. The fluids were not adjusted because he had such a high BSV before CK (134 mls), the author thought that the post CK BSVs may be acceptable for subsequent fractions if he voided just before CK.

As previously described, the aim of taking bladder filling measurements and individualising drinking instructions for patients, is to match average CK bladder volume to planning CT bladder volume. This aim was not achieved for patients 2 or 5, but was achieved for patients 1 and 6. Patient 3 had stable bladder volumes, and drinking instructions were not adjusted. Patient 4 could not be assessed fully due to the issues in measuring the post-CK readings for fraction 1.

It was previously highlighted that patient 1 had very consistent treatment times (and therefore consistent readings for Void to Post-CK BSV interval). The other 5 patients had wide variations in treatment times on a day-to-day basis, and this exacerbated the difficulty of deciding on an ideal volume of fluids for the patients to drink prior to CK.

An interesting and unexpected observation of daily assessment of post-voiding pre-CK bladder volumes, was an early indication of flow issues in some patients. Patients 1, 3, and 4, did not have any symptoms of poor urinary stream, or incomplete emptying, and the post-voiding volumes were reasonable. Patient 2 was asymptomatic until Day 5, and then complained of obstructive symptoms. An alpha-blocker was recommended given the post-voiding residual volume of 29mls and the symptoms. Patient 5 had a mean post-voiding volume of 8mls on Day 3, but on direct questioning he had obstructive symptoms therefore he was started on alpha blockade. The symptoms did not progress, and in fact the post-voiding volume improved marginally to 5mls on Day 5.

Patient 6 had a mean post-voiding volume of 63mls on Day 3, and was symptomatic. Alpha blockade was prescribed, but he did not wish to take medication and therefore was not compliant. Post-voiding residual volumes were stable for the remaining days of treatment.

In summary, individualising drinking instructions in order to optimise bladder filling is challenging. Individualised instructions led to optimised bladder filling in 2/6 patients (33%), but there was still room for improvement. A further patient had stable bladder volumes (comparing fractions 1 and 5), and drinking instructions were unchanged during treatment. One patient was difficult to assess, and 2 patients did not benefit from individualised instructions.

Half the group had obstructive symptoms accompanied by an increase in post-voiding residual volumes (arising on Days 3-5 of treatment), and were prescribed Tamsulosin.

4.4.4 CyberKnife (CK) patients: Treatment and Rotational tracking

Treatment delivery was observed for 7 patients undergoing CK treatment of primary prostate cancer. The frequency of rotational tracking, and couch adjustments made for rotations were recorded, results are displayed in Table 4.5.

The aim of the analysis was to determine the relationship between the consistency of bladder filling (between planning and treatment), and the ability to track rotations of the tumour target for the CK treatment of Prostate cancer.

Table 4.5: CK patients: Rotational tracking vs Consistency of bladder filling

RT = Rotational tracking. CA = Couch Adjustments. Rx = Treatment. # = Fraction

Patient	Percentage (%) of fractions with full RT	Percentage (%) of fractions requiring CA	Total CA made over Rx course	Problematic rotation	Most problematic fraction	Problematic quartile of Rx fraction
1	100	20	1	Roll	#4	First
2	100	100	29	Roll for 4#s Pitch for 2#s	Roll: #5 Pitch: #2	Roll: All Pitch: Final
3	100	60	5	Roll: for 2#s Pitch: for 1#	Roll: #2 & 4 Pitch: #1	Roll: Final Pitch: First
4	40	40	7	Pitch: all #s	#s 3-5	All quartiles
5	100	50	3	Pitch: for 2#s Yaw: for 1#	Pitch #1 &3 Yaw: #3	Pitch: First & Final Yaw: First
6	100	60	8	Roll: #1 & 5 Pitch: #2 & 5	Roll & Pitch: #5	#1 & 2:Final #5: First
7	100	60	8	Pitch: #2 & 4 Yaw: #2 & 3	Pitch: #2 Yaw: #2/3	Final

The relationship between consistent bladder filling, and the ability to track target rotations, was investigated due to an observation of significant pitch rotation (therefore rotations needed to be "switched off" for treatment to proceed) of a prostate target towards the end of a treatment fraction, in a patient who had a full bladder at the end of treatment.

Table 4.5 shows that only a single patient, Patient 4, (1/7, 14%) had to have rotational tracking disabled due to rotations being larger than what CK can adapt for. Pitch was the problematic rotation, which might be expected to be related to bladder filling (bladder filling would be less likely to cause a roll or yaw rotation). Of interest, the rotational tracking needed to be disabled with equal frequency in all quartiles of treatment fractions. Patient 4 had a planning CT urine volume of 211mls, and the patient exceeded a fill volume of 211mls in each fraction where rotational tracking was disabled (fractions 3-5). It might have been expected that rotational adjustments would be at a minimum where the bladder volume on treatment matched the planning CT, but this did not seem to be the case in this patient. As previously described, the rotational changes that the CK robot can adapt for are: Roll: 2^0, Yaw: 3^0, Pitch: 5^0 (for prostate treatments). However, there was an error made in the physics planning of this patient and the patient was set-up as a "Body" as opposed to a "Prostate" treatment. This meant that the rotations that could be adjusted for were: Roll 1.5^0, Pitch 1.5^0, and Yaw 3^0. Reviewing the pitch rotations observed for fractions 3-5, all were within 5^0, meaning that if the patient was set-up as a "prostate" patient, rotational tracking would have been employed in all treatment fractions (and therefore in all patients).

Patient 1 above is the patient that had consistent treatment delivery times, and no treatment delivery took >1 hour (see Table 4.2). As a guide, physicists aim to keep treatment delivery times to <1 hour for CK patients, for patient comfort, and in the knowledge that patients are more likely to move the longer a treatment takes to deliver. For this patient, only a single couch adjustment needed to be made in the entire course of treatment (for Roll in the first quartile of fraction 4), this adjustment brought the adjustment that the robot needed to make to within range, and treatment delivery proceeded without event.

Patient 2 above needed the largest amount of couch adjustments of all patients studied for delivery to proceed with rotational tracking enabled (29 for the entire treatment course). Roll was the most problematic rotation, and was responsible for 26/29 rotations (90%), the adjustments needed to be made equally in all quartiles of treatment delivery. Interestingly, this patient had a Left Total Hip Replacement. In order to maximise access for beam delivery (as beams would not be able to enter through the left metal hip), the patient was positioned in a roll in his immobilisation at planning CT, with his left hip down and the right hip up. This position was reproduced at treatment, but the position is likely to have been less stable than a patient lying supine on the couch (with no roll applied). The 3 couch adjustments made for pitch were made in the final quartile of treatment delivery in fractions 2 and 4. These were the treatment fractions associated with the largest post-CK

bladder volumes (373mls and 462mls respectively), therefore bladder filling could have been responsible for the need to make these couch adjustments.

Patient 3 only required 5 couch adjustments throughout the whole course of treatment. The only adjustments for Pitch were in the first 2 minutes of fraction 1 (when the patient had an empty bladder), and otherwise no adjustments were required. These pitch adjustments are likely to be related to set-up issues rather than bladder filling issues. The other adjustments were made for Roll in the final quartile of treatment delivery, at >60 minutes treatment delivery (for fractions 2 and 4). It may be that these minor couch adjustments needed to be made for patient movement.

Patient 5 only required 3 couch adjustments throughout the whole course of treatment, 2 for pitch (of note no data was recorded for fraction 5). The adjustment required for pitch on fraction 1 occurred at the end of treatment when the patient had a full bladder (so much so that he declined post-CK bladder scanning so that he could get promptly to the toilet). This adjustment may have been required therefore due to bladder filling (or patient discomfort). The other adjustments required were made early in fraction 3 and are likely to be related to set-up issues.

Patients 6 and 7 both required 8 couch adjustments total throughout the whole course of treatment, for 3 of the delivered fractions.

For patient 6, 3 of the adjustments were made in the final quartile of treatment delivery (for fractions 1 and 2), and the remainder were made early in fraction 5. This patient had long treatment delivery times (always > 60 minutes) due to interruption by passing flatus. Only 1 of the couch adjustments made in the final quartile was made for pitch. Fraction 4 was a particularly problematic treatment to deliver, lasting 115 minutes in total (including set-up time and interruptions). Set-up took a long time, and flatus was an issue during treatment delivery. The patient also needed to void twice during treatment, once 65 minutes following the pre-CK void, and then again 36 minutes later. Despite the issues with bladder filling for this fraction, no couch adjustments were required.

For patient 7, 6/8 of the couch adjustments required were for pitch, these adjustments needed to be made in the final quartile of treatment delivery (in fractions 2 and 4). These treatment fractions were not associated with the fullest bladders.

In summary, rotational tracking was employed for all fractions in 86% of the patients studied. The one patient where rotational tracking had to be disabled for 3 of the treatment fractions, would have had rotations compatible with rotational tracking if standard “prostate” adjustments were applied. Couch adjustments most frequently needed to be made in the final quartile (in 6/7, 86% patients),

but there was no clear relationship with bladder filling. In general, required couch adjustments did not impact on treatment delivery times, other issues were more problematic (flatus, patient positioning).

4.4.5 Radiotherapy (RT) patients: Planning: pilot study

The bladder filling results for 10 patients undergoing a planning CT scan for the conventionally-fractionated radiotherapy treatment of prostate cancer are displayed in Table 4.6. These patients were given bladder filling instructions as described in Section 4.3.4, and CT staff scanned patients according to their best judgement, before guidelines had been refined.

Analysis of this early group of patients was to help inform new guidelines.

Table 4.6: RT patients: Planning: Early patient group: pilot study:

BS = Bladder scan. BSV = Bladder Scan Volume

Patient	Fluids consumed (mls)	Interval void to BS (mins)	Mean BSV (mls) (SD)	Bladder urine volume (as % of fluids consumed)	Bladder volume judged suitable for CT scan
1	400	15	207 (21)	52	No
		40	334 (12)	84	Yes
2	400	25	312 (10)	78	No
		50	539 (11)	135	Yes
3	500	25	19 (1)	4	No
		50	159 (3)	32	No
		68	237 (27)	47	Yes
4	400	30	177 (6)	93	Yes
5	600	30	493 (48)	82	Yes
6	400	30	103 (5)	26	No
		43	294 (11)	74	Yes
7	400	30	228 (11)	57	Yes
8	500	35	307 (21)	77	No
		40	514 (49)	103	Yes
9	500	35	681 (29)	136	Yes
10	400	45	189 (21)	47	Yes

The fluids consumed by patients was largely within protocol (400-500mls), except for 1 patient that drank 600mls. Bladder urine volume at scanning as a percentage of fluids consumed in the department was noted to be highly variable. This is likely to be related to a number of factors such as: time interval to scanning, pre-hydration levels, cardiac output, renal function, and more.

The data completed in red font represents those patients and bladder scan volumes that were considered unsuitable for proceeding to immediate planning CT. The probability of having a BSV that was compatible with proceeding directly to planning CT was only 44% if the patients had a BS taken <40 minutes post-voiding (4 instances out of 9). In contrast, the probability of having a BSV compatible with proceeding directly to CT was 86% if a BS was performed at ≥ 40 minutes post-

voiding. The conclusion was therefore to wait a minimum of 40 minutes post-drinking before checking bladder volume with the bladder scanner.

The above data was evaluated to decide upon an appropriate bladder threshold at ultrasound scanning, to proceed to planning CT. The mean BSV of those that proceeded directly to CT was 369 mls. In contrast, the mean BSV of those that required extra time and/or water before proceeding to CT was 185mls, although a BSV of 177 was considered reasonable to proceed to CT in patient 4. A minimum of 160mls appeared to be required to proceed to CT.

In determining "bladder threshold" guidance, the pragmatic data observed above is not the only consideration. Reproducibility is also important, i.e. will the patient be able to maintain the optimum (planning CT) bladder volumes at treatment. Bladder dosimetry is also important.

4.4.6 Radiotherapy (RT) patients: Treatment: Pilot group

Considering the above group of 10 patients it seemed that 250mls was generally considered sufficient for proceeding to scanning, only twice was a bladder volume >250mls rejected for proceeding directly to planning CT.

The author wished to consider the reproducibility of volumes <250mls and >250mls.

Graph 4.1: Reproducibility of planning CT urine volumes of <250mls

BSV = Bladder Scan Volume

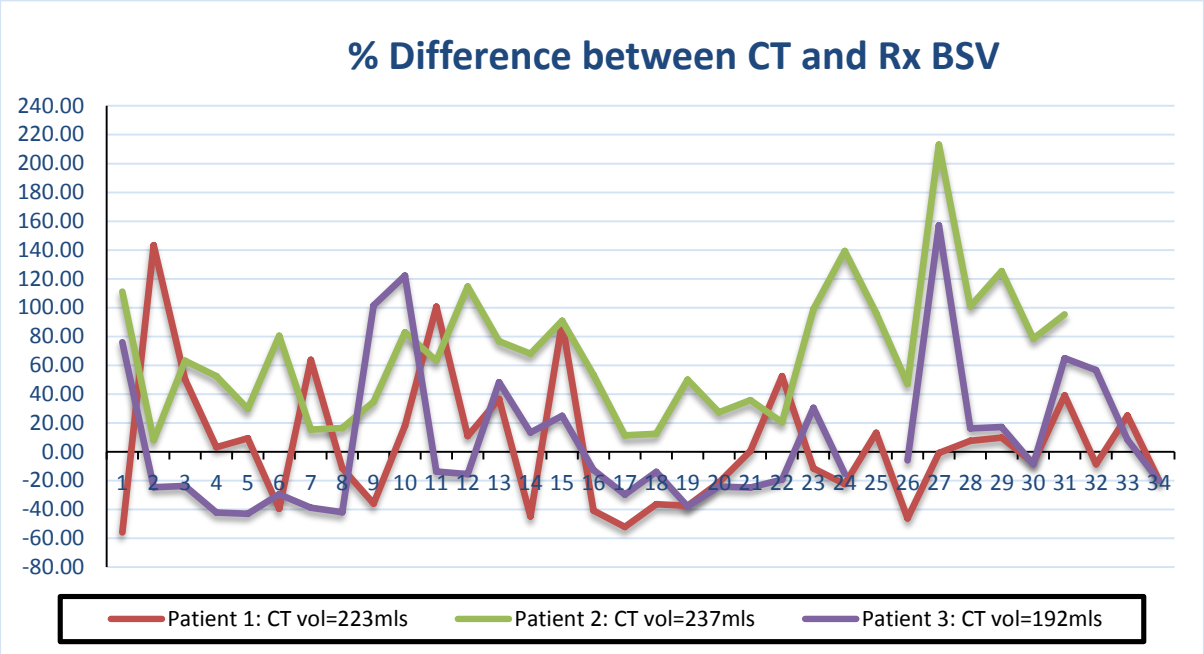

Graph 4.1 displays the on-treatment data for 3 prostate cancer patients with a planning CT volume <250mls which were treated before definitive bladder filling guidelines were refined. 0% difference between CT and Treatment BSV represents a perfect match between CT and on-treatment bladder filling. A recognised side-effect of radiotherapy to the prostate is urinary frequency, patients feel the need to empty their bladder more frequently, typically after 2 weeks of treatment. Therefore it might be expected that patients would find it harder to tolerate/achieve a fuller bladder towards the end of treatment.

Patient 2 however, achieved bladder volumes at treatment which were at least as full as at planning CT (237mls) throughout the whole course of treatment.

Patient 1, whose “baseline” planning CT urine volume was 223mls, achieved a bladder volume at least as full as at planning CT for 10 fractions in the first half of the treatment course, and for 7

fractions in the final half of their treatment course. So there may be a slight suggestion of bladder irritability in the final half of the treatment course. Overall the patient shows less variability from planning CT in the final half of treatment however, which may suggest that the patient has learned how to match his bladder volume to the planning CT volume.

Patient 3 had a "baseline" bladder volume at planning CT of 192mls. They were able to achieve at least this volume in 6 fractions of radiotherapy in the first half of treatment, and in 7 fractions in the second half of treatment. This suggests that bladder irritability as a side-effect of treatment is not having a significant impact on the consistency of bladder filling on-treatment in this patient.

Graph 4.2 shows the reproducibility of a comparator group of 5 patients with prostate cancer with a planning CT bladder volume of >250mls.

Graph 4.2: Reproducibility of planning CT urine volumes of >250mls

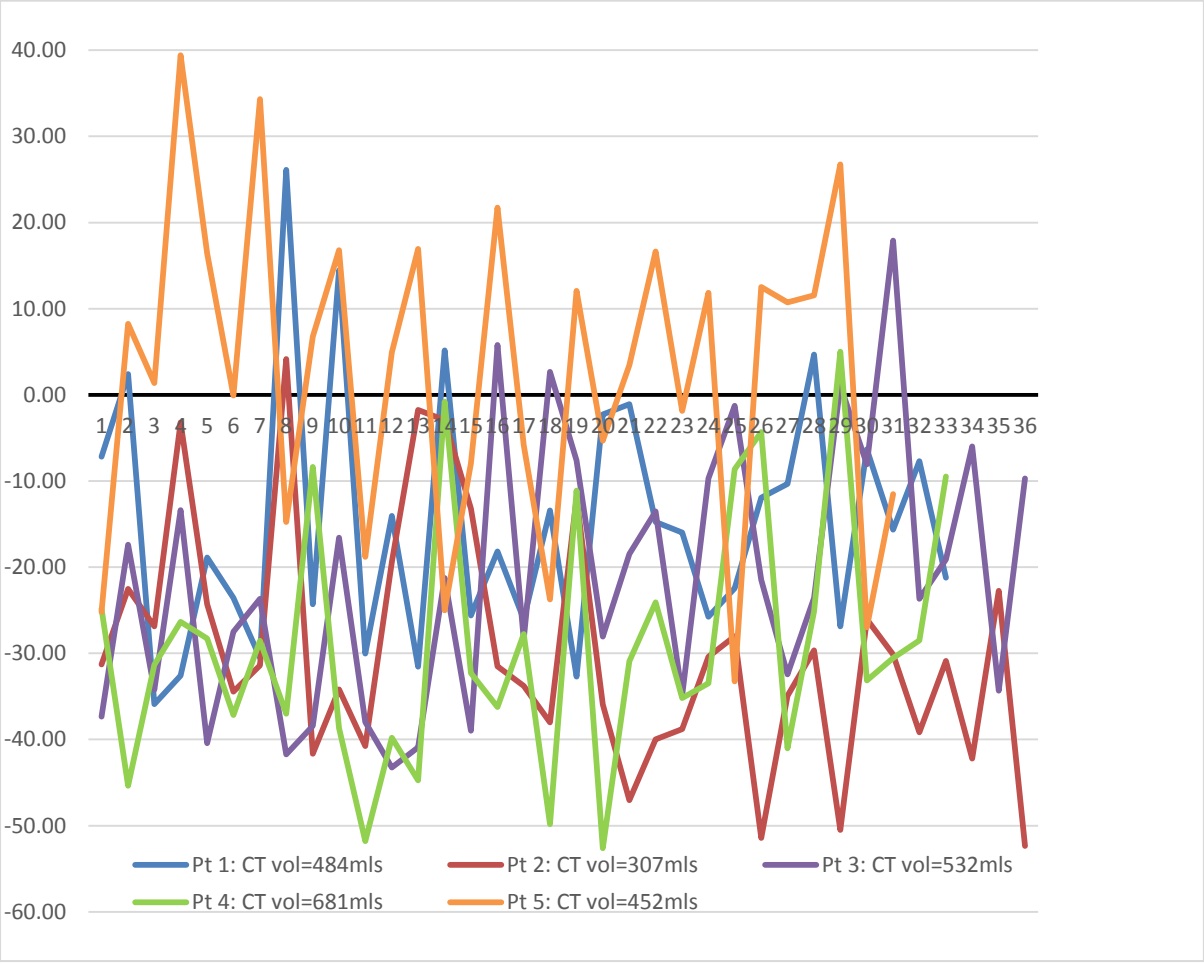

As can be seen from Graph 4.2, 4/5 patients studied (80%) achieved a bladder volume of baseline (i.e. planning CT volume) or greater in <20% of fractions. This group of patients therefore find it hard to achieve or tolerate bladder volumes of 250mls at treatment.

4.4.7 Radiotherapy (RT) patients: Treatment: Pilot group: Dosimetry analysis

A small sub-set of 3 patients was analysed to assess bladder dosimetry according to on-treatment Cone-Beam CT analysis (CBCT), as compared to planned dosimetry. This was related to degree of bladder filling.

Table 4.7 shows the planned dosimetry and CBCT-based dosimetry for the bladder in 3 patients receiving 74Gy/37 fractions to the prostate. Data for Patient 1 is shown in full, summary data is shown for patients 2 and 3.

CBCT = Cone-Beam CT, the number refers to the fraction of treatment, i.e. CBCT13 was performed prior to the 13^{th} treatment fraction.

HSC = Harley Street Clinic

QUANTEC = Quantitative Analyses of Normal Tissue Effects in the Clinic (41)

Rx = Treatment

V50 = % of Bladder receiving ≥ 50Gy

Table 4.7: Bladder dosimetry for patients receiving radical radiotherapy for prostate cancer

Scan	PTV Volume (cc)	Bladder CT Vol (cc)	V_{50} (%) HSC protocol	V_{60} (%) HSC protocol	V_{65} (%) QUANTEC	V_{70} (%) QUANTEC
Target		**150-250**	**<50%**	**<25%**	**<50%**	**<35%**
Pt 1 Plan	151	203	25.5	18.1	15.1	11.9
Pt 1 CBCT1		182	27.8	20.6	17.9	15.2
Pt 1 CBCT2		215	30.1	23.2	20.3	17.2
Pt 1 CBCT3		473	16.5	12.8	11.3	9.7
Pt 1 CBCT8		215	13.6	8.8	7.2	5.6
Pt 1 CBCT13		137	21.3	12.5	9.3	6.4
Pt 1 CBCT17		216	20.1	13.7	11.3	9
Pt 1 CBCT22		298	28.3	22.8	20.6	18.1
Pt 1 CBCT27		244	27.5	21.9	19.6	17.2
Pt 1 CBCT32		249	26.6	20.9	18.6	16.1
Pt 1 Mean On Rx		243.2	23.7	17.5	15.1	12.6
Pt 1 SD		86.5	5.3	4.9	4.7	4.5
Pt 2 Plan	94	172	16	11.9	9.8	7.5
Pt 2 Mean On Rx (Range)		239.7 (167-347)	11.7 (10.2-16.8)	7.7 (8-14)	5.9 (6.5-12.6)	4.1 (4.7-10.7)
Pt 2 SD		58.2	2.5	1.9	1.7	1.4
Pt 3 Plan	111	177	13.5	9	7	4.7
Pt 3 Mean On Rx (Range)		184 (130-279)	11.7 (5.6-13.9)	7.7 (3.6-10.4)	5.9 (2.7-8.7)	4.1 (1.7-6.9)
Pt 3 SD		48	2.5	1.9	1.7	1.4

The doses delivered to the bladder for the 3 patients displayed above are all within protocol limits. Exceeding the QUANTEC report limits would be associated with a risk of Grade 3+ urinary toxicity (CTCAE: Common Terminology Criteria Adverse Events v4.0). A grade 3 toxicity for urinary obstruction would mean that an elective operation is required (the need for catheterisation is a grade 2 toxicity).

Considering patient 1 that has full data displayed. This patient had the largest PTV of the patients in Table 4.7 (potentially making it harder for bladder dosimetry to be within standard dose constraints). The bladder volume at planning CT was 203cc, the range for bladder volume at CBCT on treatment was 137-473cc. In fact, the bladder was only under-filled at CBCT, as compared to planning CT, for fractions 1 and 13 (137cc and 182cc). An under-filled bladder on treatment could lead to the bladder doses being higher than planned, and indeed this was the case for the 1st fraction. However, this was not the case for fraction 13, all dose levels assessed were more favourable on treatment than on the planning CT for fraction 13.

The bladder was more generously filled at treatment than planning CT for 7/9 fractions (78%) for patient 1. This might have been expected to be associated with more favourable dosimetry. In fact, doses at treatment were higher than planning for 5/9 fractions (56%).

Patient 1 had an identical CBCT bladder volume on fractions 2 and 8 (215cc). Therefore, the dosimetry may have been expected to be very similar for these fractions. However, Table 4.7 shows that the dosimetry is markedly different.

The mean dosimetric parameters from the treatment CBCTs for patient 1 were more favourable than on the planning CT for all parameters except V70 (which was only marginally increased on treatment). This was a reassuring outcome.

Patient 2 had a smaller PTV (94cc), and a mean bladder volume on treatment (239.7cc) which was greater than at planning CT (172cc). In fact only one CBCT had a bladder volume less than the planning CT volume. In keeping with this, the mean treatment bladder dosimetry was more favourable than the planned dosimetry.

Patient 3 had a PTV of 111cc, and a mean bladder volume on treatment (184cc) which was greater than at planning CT (177cc). In keeping with this, the mean treatment bladder dosimetry was more favourable than the planned dosimetry.

Although the full data is not displayed in Table 4.7, both patients 2 and 3 had all dosimetric parameters lying well within protocol constraints for each CBCT assessed.

Comparing the 3 patients, patient 1 had the most generously filled bladder at planning, therefore potentially this would be associated with the lowest bladder doses. In fact, this patient had the highest doses delivered to bladder, which is likely to be due to the dominant factor that patient 1 had the largest PTV (151cc vs 94/111cc).

In summary, these 3 patients had bladder volumes at planning CT of <250cc. Each of the 3 patients studied had a mean bladder volume on treatment which was greater than the planning CT volume. The mean bladder dosimetry was improved on treatment compared to the planned bladder dosimetry for all patients and dosimetric parameters, except for V70 for patient 1. Although, this suggests the expected relationship between bladder filling and dosimetry (greater bladder filling leads to more favourable bladder dosimetry), this relationship is not clear cut. The wide variation in dosimetry noted for patient 1 on two CBCTs with identically filled bladders (fill volume 215cc), shows that other factors could be at play. This will be discussed further in Section 4.5.7.

In these patients with bladder volumes at planning of <250mls, all planned and treatment bladder dosimetry was well within treatment protocol. This supports an optimum bladder CT threshold of <250mls.

4.5 DISCUSSION

The prostate gland is susceptible to inter- and intra-fractional motion as described due to its anatomical location at the base of the bladder, and anterior to the rectum (6). Bladder filling is, therefore, a critical factor for radiotherapy teams to consider when treating all patients with prostate cancer, to ensure no target miss.

Equally, bladder filling can affect bladder dosimetry. The bladder is a hollow organ and can vary in both volume and position according to differences in filling, this presents a special problem with regards to relying on DVH data. However, the influence of irradiated bladder volume on acute and late urinary toxicity is well recognised (18).

Given the universal importance of optimum bladder filling on the delivery of safe and therapeutic external beam radiotherapy for prostate cancer, it is surprising that there is very little published literature on optimum bladder filling (25, 42). It is a topic that would value from further research.

4.5.1 CK Planning

Bladder filling instructions for prostate cancer patients undergoing CK treatment varies widely. Some centres advocate planning and treatment with an empty bladder for patient comfort and reproducibility (43). Other centres and trial protocols recommend voiding 30 minutes-1 hour prior to planning/treatment and drinking 200-250mls of fluid (23, 44). The optimum bladder volume in centres that advocate treating with a “partially full” bladder are not specified. Optimum bladder volume, together with strategies to achieve the optimum bladder volume consistently, were assessed here.

Table 4.1 shows that nearly all patients could tolerate a bladder volume of 180mls. The only patient that felt full at a lower bladder volume tolerated 150mls. It is worth noting that this was a subjective assessment, and it is also possible that filling a bladder per catheter, and with a bolus amount of 150-180mls, is more likely to make a patient feel uncomfortable than a gradual filling to the same level due to drinking.

As the simulation technique employed here introduced a known quantity of fluid into the bladder, it provides a useful guide as to the likely accuracy of the ultrasound bladder scanner. Comparing the volumes of fluid instilled, to the mean measured bladder scanner readings, the bladder scan volumes

were greater than the instilled volume (as would be expected due to bladder filling in the interval since patient voiding) for 89% of patients.

The reduced scanner reading in the remaining patient is likely to be due to the margin of error in bladder scanner readings. The manufacturer of the bladder scanner reports that the machine can measure bladder volume to within 15-20% accuracy (45). Patient 7 in Table 1 had 150mls instilled to the bladder, with a mean ultrasound reading of 120mls, which was 20% less than the volume instilled. This is therefore within the quoted range of error of the manufacturers.

Considering the 8 patients that had 180mls of water instilled into their bladder, the mean bladder scanner urine volume (prior to CT scanning) was 247mls. The range of urine volumes was wide (182-331mls), despite the fairly consistent time interval between void and first bladder scan reading of 23mins (range 21-31). Hynds et al (46) measured pre-treatment bladder inflow rate in patients undergoing simulation for prostate cancer radiotherapy. They calculated the rate to be 4.6mls/min (+/- 2.9mls/min). If the 8 patients studied here filled at the same rate for the average interval of 23mins between void and ultrasound scan, there would be an expected volume in the bladder of 286mls (180mls instilled + 106mls of filling), which is well within the range of measured urine volumes reported. Of note, the patients in the Hynds study were drinking a specified volume of fluids (500mls) prior to simulation, whereas the 8 patients studied by the author drank variable volumes of fluids on the day of CT (200-950mls) at varying intervals before bladder scanning.

Intra-patient bladder scanner readings taken prior to CT scanning were largely consistent (SD = 1-19mls) which gives some confidence to the accuracy of bladder scanner readings. Review of the methodology of other groups reporting on use of the bladder scanner suggests that single readings only were taken (46) . This may therefore be the first study to report on the reliability of the bladder scanner readings (although the other groups did compare bladder ultrasound volumes with CT volumes it is known that volumes assessed by differing imaging modalities can vary) (47).

The mean Planning CT urine volume for the 9 patients studied (222cc) was consistent with mean bladder scanner volume prior to CT scan (232mls), a variation of only 4%. However, there was wide variability noted in CT vs bladder scanner volumes for certain individual patients (-31 to +48%). Although 4 patients (44%) had measured bladder volumes which were more consistent and varied by <15% between the 2 modalities. The greatest disparity between volumes (48% difference) measured by different imaging modalities occurred in patient 2, who had the largest bladder volume assessed by CT. The bladder scanner may have underestimated urinary volume (equally CT may have over-estimated urinary volume). This greater variability observed at larger volumes confirms findings by

Hynds et al, who noted a statistically significant larger variability at larger bladder volumes (when assessing data by means of Spearman's correlation coefficient) (46). However, Hynds et al reported good correlation between CT scan bladder volumes, and bladder scanner readings for the 30 patients studied overall (Pearson correlation coefficient = 0.91, a value of 1 would indicate perfect correlation).

Reviewing the methodology of the Hynds et al paper for assessing CT-measured bladder volumes, it is not clear that any adjustment in volume was made for the likely thickness of bladder wall. In contrast, as described in Section 4.3.1, the CT-measured urinary volume was assessed in this study by assuming a bladder wall thickness (BWT) of 4mm, and subtracting "bladder wall" from "whole bladder" to derive urine volume. A mean BWT of 3.67mm was found in men with obstructive urinary symptoms and benign prostatic hypertrophy by Hakenberg et al (37). When it comes to assessing DVH data, it is more conservative (safer) to assume a thicker bladder wall hence selecting a BWT of 4mm for calculations in this study. However, this may over-estimate bladder thickness, as other studies report BWT of closer to 2mm, although this thickness was in healthy Korean adults (38). It is also important to note that bladder filling in itself can affect BWT, therefore BWT could be variable within the same patient. Morgan considers a BWT of <5mm normal if the bladder is empty, and states <3mm would be a "normal" bladder wall thickness if the bladder was distended (39). The patients studied here would be expected to have bladder outlet obstruction due to prostate cancer, often co-existing with Benign Prostatic Hypertrophy (BPH).

Calculating CT-assessed urine volume applying BWT of 4mm vs ~2mm has a significant effect on the volume calculations. Taking patient 4 as an example, the plan CT urine volume based on BWT of 4mm was 211cc vs urine volume of 242cc for BWT 2.6mm. Whole bladder for patient 4 was 293cc, which is similar to the mean bladder scanner reading of 306mls.

Considering post-CT bladder scanner volumes and the consistency with CT-assessed volumes, the average change in volume between planning CT and post-CT bladder scan volume was +12% (range -2 to +35%). This compared to the average change between pre-CT bladder scan volume and planning CT of -4% (range -31 to +48%). The moderate increase in mean difference between CT volume and the post-CT bladder scanner readings (as compared to pre-CT bladder scanner readings) may be due to the mean interval between CT and post-CT bladder scanner readings of 10 minutes (compared to an interval of 3 minutes between pre-CT bladder scanning and CT).

Intra-patient post-CT bladder scanner readings were largely consistent, except for patient 2 who had a SD of 84mls. This patient had the largest urinary volumes recorded, and may again be a suggestion that bladder scanner readings might be less reliable at larger volumes.

In summary, this appears to be the first study of the role of ultrasound volumetric imaging of the bladder in assessing bladder filling at simulation for hypofractionated SBRT of primary prostate cancer. It will be important to analyse dosimetric as well as on-treatment data for these patients, but the data reviewed above demonstrates that all patients could tolerate a minimum of 150mls at simulation. The bladder scanner was found to be reliable (intra-patient SD<19mls) at smaller bladder volumes (mean volumes <331mls), but may be less reliable at larger volumes (mean volume of 375mls, SD=84mls). This is the first radiotherapy study to assess the reliability of the bladder scanner by taking 3 consecutive bladder scanner readings, therefore these results are important. Despite the short interval between voiding and pre-CT bladder scanning (mean interval 23 mins), and the short interval between voiding and CT scan (27-35mins), there can be significant extra filling of the bladder, which supports not instilling more water than 180mls.

4.5.2 CK Dosimetry

Table 4.2 shows that in 8/9 of patients studied (89%) bladder wall dosimetry was within protocol constraints, and there was no compromise of PTV coverage. In the remaining patient the 15cc threshold dose was exceeded (marginally), and there was compromise of PTV coverage. Bladder wall was the dose-limiting OAR for this patient, rectal doses were well within constraint. As described in section 4.4.2, the breach of bladder wall dosimetry, and the compromise on PTV coverage, was most likely related to the large PTV size in this patient (121cc), rather than sub-optimal bladder filling.

There are no reports in the literature relating bladder wall dosimetry to bladder filling at planning CT for hypofractionated prostate treatments.

However, the literature does report on prostate volume limits for SBRT to the prostate. The PACE study is an International study of the efficacy of SBRT for prostate cancer, compared to surgery and conventionally-fractionated radiotherapy (23). The eligibility criteria requires a patient to have a prostate volume (not PTV) of ≤ 90 cc. Patient 8 had a prostate volume that would have been eligible (71cc) but the PTV coverage of 89.4% was not ideal and would have represented a protocol deviation.

Janowski et al reported on outcomes for patients treated with SBRT with prostate volumes ≥ 50 cc (48). Median prostate size was 62.9 cc (range 50 -138.7 cc). They reported a clinically acceptable Grade 3 + urinary toxicity rate of 3.5%, although nearly half of patients experienced Grade 2 urinary toxicity. The toxicity peaked at 1 month and 9 months post-treatment. The authors aimed for PTV coverage of 95%, but they did not comment on the frequency of exceeding bladder constraints, or compromising on PTV coverage.

It was noted in the patients studied here, that all with a PTV of ≤ 100 cc had target and bladder wall dosimetry within constraints. Patient 4 had a PTV of just under 100 cc, and had a prostate volume of 58 cc. Therefore a patient accepted for CK treatment with a prostate volume of ≤ 58 cc, and bladder filling on planning CT of minimum 144 mls (or pre-CT bladder scan volume of minimum 120mls) is likely to achieve a therapeutic (good PTV coverage) and safe (with respect to bladder wall dose) CK treatment plan.

4.5.3 CK Treatment: Bladder filling

There are no reports in the literature relating bladder wall dosimetry to bladder filling at planning CT for SBRT prostate treatments.

Section 4.4.3 describes the bladder filling achieved on-treatment in 6 patients undergoing CK for primary prostate cancer. The aim was to match the mid-CK urine volume with the planning CT urine volume. Standard bladder filling instructions were given to patients for their 1st day of treatment, thereafter the bladder filling instructions were individualised where possible to improve reproducibility of bladder volume (between planning and treatment).

In practice, whilst this was a small sample of patients, and therefore the author was still gaining in experience in individualising drinking instructions, it proved challenging to improve bladder filling reproducibility. Individualised instructions led to optimised bladder filling in patients 1 and 6 (33% of the group). However, others did not benefit from individualising instructions, or could not be fully assessed.

One factor that led to the difficulty in suggesting an ideal quantity of fluids for the patients to drink pre-CK was the widely variable time for treatment delivery. Treatment delivery times were the most consistent for patient 1, variation of only 10% of treatment time. In the remaining patients treatment delivery times varied by between 29% and 70% of the minimum treatment time. The reasons for prolongation in treatment delivery time were variable, and challenging to manage. Some

of the reasons were: varying lengths of time to achieve ideal patient set-up, flatus (causing the prostate to move out of position temporarily), and rotational changes in either prostate or patient position which required couch adjustments.

It is also possible that more consideration should have been given to a patient's general hydration level. It may have been sensible to suggest that a patient drinks a given (fixed) quantity of fluids for each treatment day.

Finally, patient compliance with voiding instructions could have been improved.

A consequence of bladder scanning pre- and post- each fraction of CK was that obstructive symptoms and signs were addressed at an early stage. Half the group had obstructive symptoms accompanied by an increase in post-voiding residual volumes (arising on Days 3-5 of treatment), and were prescribed alpha-blockade. Longer term follow-up of these patients is not yet available. In the publication by Janowski et al on prostate cancer patients receiving SBRT, 37% of patients were on alpha-blockade at the start of treatment, rising to 67% at 1 month post the start of treatment (48). The article does not report the time-point at which additional alpha-blockade was started.

In summary, optimising the reproducibility of bladder filling by individualising drinking instructions was challenging and unsuccessful in the majority of cases. The reasons for the difficulty include variable set-up/treatment delivery times, and patient compliance. Both of these factors are difficult to correct. A further factor could be a variation in general hydration levels each day of CK treatment, and this could potentially be addressed by additional drinking instructions.

Alpha-blockade was prescribed in 50% of patients, based on reported patient symptoms, and increases in post-voiding residual volumes.

4.5.4 CK Treatment: Rotational tracking

The author wished to consider the relationship between optimum bladder filling and the ability to track rotations of the tumour target for the CK treatment of prostate cancer following a chance observation. Attendance at the CK control room during a prostate treatment was required for a separate reason. It was noted that rotations needed to be switched off for the final part of the treatment fraction due to a pitch rotation greater than what could be adapted for. The same patient was extremely full at the end of treatment.

As explained, tracking accuracy is improved by tracking rotations (36), therefore if optimising bladder filling resulted in increased ability to track rotations, this could potentially improve the outcome of CK treatment for primary prostate cancer.

There are no reports in the literature relating bladder filling reproducibility to ability to track rotations for the CK treatment of prostate cancer.

Section 4.4.4 reports the results of 7 patients studied to assess the relationship between bladder filling and rotational tracking. 86% of patients (6/7) received CK treatment with rotational tracking employed for all treatment fractions. The remaining patient would have had rotational tracking employed for all treatment fractions if treatment had been planned with a prostate (rather than "body") treatment path/rotational adjustment capability.

Couch adjustments most frequently needed to be made to adjust for rotations in the final quartile of treatment fractions (for 86% of fractions), but there was no clear association with bladder filling as described. Patient movement could also be expected to be more likely (due to discomfort) in the final quartile of a treatment fraction. Couch adjustments were not the most important factor in prolonging treatment times. Patient set-up times, flatus, and other issues e.g. need to void, were more significant.

In conclusion, there was no relationship between the consistency of bladder filling (between planning and treatment), and the ability to track rotations of the tumour target for the CK treatment of primary prostate cancer.

4.5.5 Radiotherapy (RT) patients: Planning: pilot group

It is widely accepted that conventionally-fractionated radiotherapy for prostate cancer should be delivered with a "comfortably full" bladder. The aim of bladder filling is to minimise dose to bowel and bladder wall. Ideally bladder filling would be consistent between planning CT and each treatment fraction.

Bladder filling guidelines vary widely however. Centres/Trials advise patients to void 30-60 minutes prior to planning CT and then drink 300-500 mls of fluids (23, 46). These publications do not state an optimum bladder volume however. It is also unclear if the quantity of fluids/time interval between voiding and CT recommended, is evidence-based.

Haworth et al reported on the use of an ultrasound bladder scanner to aim to improve radiotherapy treatment delivery for patients receiving treatment to the prostate bed (49). The authors accepted a minimum pre-CT bladder scanner volume of 80 mls and a maximum volume of 350 mls.

Optimum bladder volume and drinking instructions were investigated further here. A pilot group of 10 patients undergoing conventionally-fractionated radiotherapy for prostate cancer were assessed. The results of the assessments were shown in Table 4.6.

Patients drank between 400 and 600 mls of fluids, a majority consumed 400 – 500 mls.

The patients had ultrasound bladder scanner volumes measured (to assess if bladder volume was appropriate for CT) between 15 and 68 minutes post-voiding. 5/10 patients (50%) needed to have their bladders scanned with the ultrasound device 2-3 times before proceeding to CT due to under-filling of the bladder. A clear threshold for bladder filling had not been set at this time point.

The probability of having a Bladder Scanner Volume (BSV) compatible with proceeding to immediate CT was only 44% if the BSV was taken <40 minutes post-voiding. In contrast, 86% of patients could proceed to immediate CT if the BSV was assessed at ≥ 40 minutes post-voiding.

This result conformed to the “bladder filling working party” that a BSV should be assessed 40 minutes post-voiding, and prior to Planning CT.

A minimum of 160 mls appeared to be required to proceed to CT. No patient was asked to void and recommence drinking instructions due to an over-filled bladder.

4.5.6 Radiotherapy (RT) patients: Treatment: pilot group

When considering optimum bladder filling instructions/bladder volume for prostate radiotherapy, the pragmatic data discussed in Section 4.5.5 is not the only consideration. Reproducibility, for each fraction of a patient's treatment, and dosimetry, are also important.

It has been described previously that for dosimetric reasons it is advantageous to fill the bladder (to move bowels and bladder away from the high-dose region), see Figure 4.2 in the Introduction. However, there is a risk that if a patient has a bladder which is "too full" at planning CT, the level of filling is difficult to reproduce consistently on treatment. This can be particularly challenging towards the end of a course of radiotherapy (due to bladder irritability) (18, 25).

There is little guidance on an "ideal" standard for bladder filling in the literature however. Haworth et al state that from previous unpublished work they found that >350mls is not reproducible on treatment (49). For practical reasons (to make bladder filling achievable) they recommended a tolerance range of 150mls in total, therefore, e.g. if planning CT for a patient had a bladder volume of 300mls, the tolerance range for them on treatment would be 200mls – 350mls.

Consistent bladder filling is challenging as previously described. Hynds et al, who assessed patients undergoing prostate radiotherapy with an ultrasound bladder scanner, concluded "in this cohort, bladder-filling instructions failed to provide a consistent and reproducible bladder filling from CT planning to treatment". The ideal bladder volume at planning CT was not stated, but the average volume at planning CT was 291mls (range 87-579mls). The average bladder volume fell during treatment, with a mean of all treatments of 189mls, and a mean bladder volume on the final day of treatment of 165mls. This suggests that the issue for poor reproducibility is under-filling of the bladder on treatment compared to planning CT volumes.

The author wished to consider reproducibility of bladder volumes comparing <250mls and >250mls. This was a somewhat arbitrary cut-point, although it was shaped by the experience of Haworth and Hynds et al (46, 49). 350mls or greater (from planning CT) was too large a volume to be reproduced according to the work by Haworth et al. Given the difficulties with reproducibility experienced by Hynds et al with a mean planning CT bladder volume of 291mls, a volume just less than this was selected.

The on-treatment bladder volumes for 3 patients with a planning CT volume of <250mls were displayed in Graph 4.1. The graph shows that under-filling of the bladder on-treatment was never an issue for patient 2. Patient 1 had greater reproducibility of CT bladder volume in the second half of

his treatment course, and patient 3 was able to achieve the planning CT volume or greater at least as often in the second half of his treatment course (compared to the first half of treatment). In this small sub-set of patients therefore, under-filling of the bladder on-treatment is not a significant issue.

The on-treatment bladder volumes for 5 patients with a planning CT volume of >250mls were displayed in Graph 4.2. 4/5 patients studied (80%) achieved a bladder volume of baseline (i.e. planning CT volume) or greater in <20% of fractions. This group of patients therefore find it hard to achieve or tolerate bladder volumes of 250mls at treatment, and under-filling of the bladder on treatment is a significant issue.

Concerns over reproducibility led the "bladder filling working party" to set 250mls as the upper threshold limit for optimum planning CT bladder volume. 150mls was set as a minimum theshold volume in order that bladder filling in the desired range was achievable. It was hoped that a bladder volume of 150mls would be sufficient to provide dosimetric sparing of the bladder and bowels.

4.5.6 Radiotherapy (RT) patients: Dosimetry

The results for planned and delivered dosimetry for 3 patients that completed a course of radical radiotherapy to the prostate were displayed in Table 4.7, Section 4.4.7.

Akin et al assessed bladder dosimetry in a group of 20 patients receiving radical radiotherapy in the post-prostatectomy setting (50). Bladder was re-outlined on Cone-Beam CT (CBCT) scans and the doses recalculated analogous to the Methodology described in Section 4.3.6. The group noted that most DVH parameters for bladder (V50, V60 and V65) were increased on treatment as compared to planning. This was statistically significant. The group applied tighter dose constraints than described in the QUANTEC report, but they were concerned to note that the V65 bladder limit was breached in 10%, and the V40 bladder limit was breached in 20% of the patients studied. The group concluded that the potential variability for bladder doses received on treatment supported an image guidance approach to treatment delivery.

Haworth et al used an ultrasound bladder scanner to try to improve radiotherapy treatment delivery in the post-prostatectomy setting. They assessed the relationship between change in bladder volume (between planning and treatment) and potential compromise of target coverage. Their analysis showed that there was no statistically significant relationship between bladder volume change and target coverage (49).

Image guidance is certainly important in ensuring accurate treatment delivery, but consistent patient preparation is also important, as bladder filling can affect the relative geometry of prostate/bladder/rectum, which can in turn affect dosimetry. Patient 1 in table 4.7 had variable bladder filling on treatment. If the planning CT bladder volume is taken as the reference volume (203cc), the bladder volume on treatment varied by -33% to +133%.

Despite this wide variation, bladder dosimetry was well within constraint limits on treatment which is reassuring. Bladder dosimetry was also consistently within constraint limits for patients 2 and 3, despite variable bladder filling on treatment.

As discussed in Section 4.4.7, patient 1 had an identical bladder volume at fraction 2 and 8. Intuitively, this might be expected to give near-identical dosimetry to the bladder, but in reality the dosimetry was very different. The possible causes for the disparity in bladder dosimetry observed include changes in rectal filling, and random inter-fractional changes in the relative positions of prostate/bladder/rectum. Haworth et al hypothesised that a possible reason for why they failed to demonstrate a relationship between change in bladder filling and target coverage, was the co-dependence on rectal filling.

Encouragingly, the 3 patients studied in Table 4.7 had more favourable bladder dosimetry on-treatment (except for a marginal increase in the V70 for patient 1), than at planning. However, there are some caveats to this observation.

The 3 patients studied all had mean bladder volumes which were greater on-treatment than at planning. This would be likely to make the bladder dosimetry more favourable. It would, therefore, be interesting and informative to perform dosimetric analysis on patients whose mean bladder volumes are reduced on treatment compared to planning.

It is also important, given the inter-relationship of prostate/bladder/rectum that bladder dosimetry is not considered in isolation. It is important to assess target coverage and rectal dosimetry for the above patients. It is important that the observed improvement in bladder dosimetry on-treatment is not at the expense of target coverage.

4.6 CONCLUSIONS

In order for Radiotherapy to be delivered accurately, and for the tumour to be treated exactly as intended, it is critical that the set-up and conditions at the time of treatment delivery reproduce exactly the set-up/conditions of the Planning CT scan.

Prostate is a difficult target for radiotherapy as it is susceptible to motion due to organ filling (bladder and bowel).

The research undertaken in this Chapter was designed to develop bladder filling guidelines for Radiotherapy and CyberKnife patients based on optimal dosimetry and reproducibility. In addition, the author wished to investigate the relationship between the consistency of bladder filling, and the ability to track rotations of the prostate for CyberKnife cases.

<u>Assessment Outcomes:</u>

1. Ultrasound bladder scanner reliability:

This is believed to be the first radiotherapy study to assess the intra-patient reliability of the scanner by taking 3 consecutive readings.

Bladder volumes <331mls: bladder scanner likely to be reliable (intra-patient SD = 1-19mls)

Bladder volumes ≥375mls: bladder scanner may be less reliable (intra-patient SD = 84mls)

2. CyberKnife:

a) Planning:

All patients could tolerate a minimum bladder volume of 150mls at planning CT.

Despite the short interval between patient voiding and CT scan, there can be significant extra filling of the bladder, which supports not instilling more water into the bladder than 180mls.

b) Dosimetry:

All patients with PTV of ≤100cc (equating to prostate volume of ≤58cc) had bladder wall dosimetry within constraints, with therapeutic coverage of the PTV. A “safe to bladder”, and therapeutic plan to a 100cc prostate PTV was produced for a patient with a bladder volume at CT of 144mls, therefore this would be a reasonable minimum volume at CT.

c) Treatment: Bladder filling:

Optimising the reproducibility of bladder filling by individualising drinking instructions was challenging and unsuccessful in the majority of cases studied.

Variable set-up/treatment delivery times contributed to the challenge.

Where treatment times were extended beyond what was expected, patients experienced full bladders, and voiding mid-treatment was sometimes required.

Pre-hydration could have been considered/addressed.

Alpha-blockade was prescribed in 50% of patients, based on symptoms and increases in post-voiding residual volumes, frequently for fraction 4.

d) Treatment: Rotational tracking:

86% of patients received CK treatment with rotational tracking employed for all treatment fractions. The remaining patient would have had rotational tracking employed for all fractions if a prostate path/rotational adaptation capability had been selected.

There was no relationship between the consistency of bladder filling, and the ability to track rotations of the prostate.

e) Protocol discussions:

A consequence of focussing on the bladder filling aspects of the CK Prostate protocol through this research, was that wider discussions were had within the CK team, and with Clinical Oncologists. The outcome of the discussions was that the team/Clinical Oncologists wished to move to a non-catheter planning technique for prostate targets.

3. Radiotherapy:

a) Planning:

The probability of having a bladder scan volume compatible with proceeding immediately to planning CT was 86% if there was an interval since voiding of at least 40 minutes, but only 44% if the interval was <40 minutes. 40 minutes was therefore set as the recommended interval between voiding and CT scanning.

The volume of fluids drunk by patients in the pilot study was 400-500mls. If a patient required extra time, due to under-filling of bladder, this had an impact on workflow in the radiotherapy department. To minimise the risk of under-filling, 500mls was selected as the recommended volume of fluids to drink pre-CT.

b) Treatment:

Reproducibility of bladder volumes was improved on treatment for a subset of patients with planning CT bladder volumes of <250mls vs a comparator group with planning CT bladder volumes of >250mls.

250mls was therefore set as the upper threshold limit for optimum planning CT bladder volume.

In order that obtaining a bladder volume in the desired range was achievable, a lower threshold limit of 150mls was proposed.

c) Dosimetry:

Bladder wall dosimetry was well within constraints for all patients studied.

These patients had bladder volumes at planning CT of 172-203mls, therefore well within the proposed ideal range for bladder volume at planning CT.

<u>Evidence-based bladder filling guidelines:</u>

A. CyberKnife:

1. Pre-hydrate by drinking minimum of 1.5litres of water per day in the 2 days leading up to planning scan/treatment. Continue to drink this volume whilst on treatment.

2. Attend clinic 1 hour prior to planning CT/treatment for bowel preparation.

3. Void, then drink 250mls of water, 40 minutes prior to CT scan.

4. Ultrasound bladder scan x 3 prior to CT planning scan. Aim is for bladder volume of 140-250mls. 140mls-200mls is likely to be ideal to avoid over-full bladder on treatment.

5. On Treatment:

Pre-hydration/bowel prep as described above.

Void immediately before CK treatment, then drink 250mls of water.

Ultrasound bladder scan x 3 pre- and post-treatment to individualise bladder filling instructions where appropriate.

B. Radiotherapy:

1. Pre-hydrate by drinking minimum of 1.5litres of water per day in the 2 days leading up to planning scan/treatment. Continue to drink this volume whilst on treatment.

2. Attend clinic 1 hour prior to planning CT/treatment for bowel preparation.

3. Void, then drink 500mls of water, 40 minutes prior to CT scan.

4. Ultrasound bladder scan x 3 prior to CT planning scan. Aim is for bladder volume of 150-250mls at planning CT.

5. On Treatment:

Pre-hydration/bowel prep as described above.

Void, then drink 500mls of water, 40 minutes prior to treatment.

Ultrasound bladder scan x 3 pre-treatment.

Individualise bladder filling instructions where appropriate.

<u>Further work:</u>

1. CyberKnife:

Audit the feasibility/implementation of the new bladder filling guidelines, and the planned dosimetry.

Adapt the drinking volume if necessary.

A non-catheter approach means that the prostatic urethra cannot be easily visualised, record likely maximum doses to prostatic urethra (by considering homogeneity index), and compare to catheter-based treatment plans.

2. Radiotherapy:

Audit the feasibility/implementation of the new bladder filling guidelines, and the planned dosimetry.

Analyse the dosimetry (through CBCT assessment) for a sub-set of patients whose mean bladder on-treatment was under-filled compared to planning CT.

Analyse the on-treatment dosimetry for prostate, rectum and bowel.

References:

1. NRIG. Image Guided Radiotherapy (IGRT): Guidance for implementation and use. 2012.
2. RCR I, SCoR. On Target: ensuring geometric accuracy in radiotherapy. 2008.
3. Njeh CF. Tumor delineation: The weakest link in the search for accuracy in radiotherapy. J Med Phys. 2008;33(4):136-40.
4. Ghilezan MJ, Jaffray DA, Siewerdsen JH, Van Herk M, Shetty A, Sharpe MB, et al. Prostate gland motion assessed with cine-magnetic resonance imaging (cine-MRI). Int J Radiat Oncol Biol Phys. 2005;62(2):406-17.
5. McLaughlin PW, Wygoda A, Sahijdak W, Sandler HM, Marsh L, Roberson P, et al. The effect of patient position and treatment technique in conformal treatment of prostate cancer. Int J Radiat Oncol Biol Phys. 1999;45(2):407-13.
6. Schild SE, Casale HE, Bellefontaine LP. Movements of the prostate due to rectal and bladder distension: implications for radiotherapy. Med Dosim. 1993;18(1):13-5.
7. Michalski A, Atyeo J, Cox J, Rinks M. Inter- and intra-fraction motion during radiation therapy to the whole breast in the supine position: a systematic review. J Med Imaging Radiat Oncol. 2012;56(5):499-509.
8. Padhani AR, Khoo VS, Suckling J, Husband JE, Leach MO, Dearnaley DP. Evaluating the effect of rectal distension and rectal movement on prostate gland position using cine MRI. Int J Radiat Oncol Biol Phys. 1999;44(3):525-33.
9. Nichol AM, Warde PR, Lockwood GA, Kirilova AK, Bayley A, Bristow R, et al. A cinematic magnetic resonance imaging study of milk of magnesia laxative and an antiflatulent diet to reduce intrafraction prostate motion. Int J Radiat Oncol Biol Phys. 2010;77(4):1072-8.
10. Wang KK, Vapiwala N, Bui V, Deville C, Plastaras JP, Bar-Ad V, et al. The impact of stool and gas volume on intrafraction prostate motion in patients undergoing radiotherapy with daily endorectal balloon. Radiother Oncol. 2014;112(1):89-94.
11. de Crevoisier R, Tucker SL, Dong L, Mohan R, Cheung R, Cox JD, et al. Increased risk of biochemical and local failure in patients with distended rectum on the planning CT for prostate cancer radiotherapy. Int J Radiat Oncol Biol Phys. 2005;62(4):965-73.
12. Heemsbergen WD, Hoogeman MS, Witte MG, Peeters ST, Incrocci L, Lebesque JV. Increased risk of biochemical and clinical failure for prostate patients with a large rectum at radiotherapy planning: results from the Dutch trial of 68 GY versus 78 Gy. Int J Radiat Oncol Biol Phys. 2007;67(5):1418-24.
13. Kupelian PA, Willoughby TR, Reddy CA, Klein EA, Mahadevan A. Impact of image guidance on outcomes after external beam radiotherapy for localized prostate cancer. Int J Radiat Oncol Biol Phys. 2008;70(4):1146-50.
14. Teoh M, Clark CH, Wood K, Whitaker S, Nisbet A. Volumetric modulated arc therapy: a review of current literature and clinical use in practice. Br J Radiol. 2011;84(1007):967-96.
15. Azcona JD, Xing L, Chen X, Bush K, Li R. Assessing the dosimetric impact of real-time prostate motion during volumetric modulated arc therapy. Int J Radiat Oncol Biol Phys. 2014;88(5):1167-74.
16. Thor M, Apte A, Deasy JO, Karlsdottir A, Moiseenko V, Liu M, et al. Dose/volume-response relations for rectal morbidity using planned and simulated motion-inclusive dose distributions. Radiother Oncol. 2013;109(3):388-93.
17. Zelefsky MJ, Crean D, Mageras GS, Lyass O, Happersett L, Ling CC, et al. Quantification and predictors of prostate position variability in 50 patients evaluated with multiple CT scans during conformal radiotherapy. Radiother Oncol. 1999;50(2):225-34.
18. Lebesque JV, Bruce AM, Kroes AP, Touw A, Shouman RT, van Herk M. Variation in volumes, dose-volume histograms, and estimated normal tissue complication probabilities of rectum and bladder during conformal radiotherapy of T3 prostate cancer. Int J Radiat Oncol Biol Phys. 1995;33(5):1109-19.
19. Fiorino C, Foppiano F, Franzone P, Broggi S, Castellone P, Marcenaro M, et al. Rectal and bladder motion during conformal radiotherapy after radical prostatectomy. Radiother Oncol. 2005;74(2):187-95.
20. Fokdal L, Honore H, Hoyer M, Meldgaard P, Fode K, von der Maase H. Impact of changes in bladder and rectal filling volume on organ motion and dose distribution of the bladder in radiotherapy for urinary bladder cancer. Int J Radiat Oncol Biol Phys. 2004;59(2):436-44.

21. Pinkawa M, Asadpour B, Gagel B, Piroth MD, Holy R, Eble MJ. Prostate position variability and dose-volume histograms in radiotherapy for prostate cancer with full and empty bladder. Int J Radiat Oncol Biol Phys. 2006;64(3):856-61.
22. Jain S, Loblaw DA, Morton GC, Danjoux C, Szumacher E, Chu W, et al. The effect of radiation technique and bladder filling on the acute toxicity of pelvic radiotherapy for localized high risk prostate cancer. Radiother Oncol. 2012;105(2):193-7.
23. Van As N TA. International randomised study of laparoscopic prostatectomy vs SBRT and conventionally fractionated radiotherapy vs SBRT for early-stage organ-confined prostate cancer. NCRN trials database. 2014.
24. Khoo VS, Dearnaley DP. Question of dose, fractionation and technique: ingredients for testing hypofractionation in prostate cancer--the CHHiP trial. Clin Oncol (R Coll Radiol). 2008;20(1):12-4.
25. Stam MR, van Lin EN, van der Vight LP, Kaanders JH, Visser AG. Bladder filling variation during radiation treatment of prostate cancer: can the use of a bladder ultrasound scanner and biofeedback optimize bladder filling? Int J Radiat Oncol Biol Phys. 2006;65(2):371-7.
26. Hynds S, McGarry CK, Mitchell DM, Early S, Shum L, Stewart DP, et al. Assessing the daily consistency of bladder filling using an ultrasonic Bladderscan device in men receiving radical conformal radiotherapy for prostate cancer. Br J Radiol. 2011;84(1005):813-8.
27. Nguyen PL, Zietman AL. High-dose external beam radiation for localized prostate cancer: current status and future challenges. Cancer J. 2007;13(5):295-301.
28. Grimm P, Billiet I, Bostwick D, Dicker AP, Frank S, Immerzeel J, et al. Comparative analysis of prostate-specific antigen free survival outcomes for patients with low, intermediate and high risk prostate cancer treatment by radical therapy. Results from the Prostate Cancer Results Study Group. BJU Int. 2012;109 Suppl 1:22-9.
29. Dearnaley DP, Sydes MR, Graham JD, Aird EG, Bottomley D, Cowan RA, et al. Escalated-dose versus standard-dose conformal radiotherapy in prostate cancer: first results from the MRC RT01 randomised controlled trial. Lancet Oncol. 2007;8(6):475-87.
30. Mangoni M, Desideri I, Detti B, Bonomo P, Greto D, Paiar F, et al. Hypofractionation in prostate cancer: radiobiological basis and clinical appliance. Biomed Res Int. 2014;2014:781340.
31. King CR, Freeman D, Kaplan I, Fuller D, Bolzicco G, Collins S, et al. Stereotactic body radiotherapy for localized prostate cancer: pooled analysis from a multi-institutional consortium of prospective phase II trials. Radiother Oncol. 2013;109(2):217-21.
32. Kothary N, Dieterich S, Louie JD, Chang DT, Hofmann LV, Sze DY. Percutaneous implantation of fiducial markers for imaging-guided radiation therapy. AJR Am J Roentgenol. 2009;192(4):1090-6.
33. Kumar KA, Wu T, Tonlaar N, Stepaniak C, Yenice KM, Liauw SL. Image-guided radiation therapy for prostate cancer: A computed tomography-based assessment of fiducial marker migration between placement and 7 days. Pract Radiat Oncol. 2014.
34. Delouya G, Carrier JF, Beliveau-Nadeau D, Donath D, Taussky D. Migration of intraprostatic fiducial markers and its influence on the matching quality in external beam radiation therapy for prostate cancer. Radiother Oncol. 2010;96(1):43-7.
35. Kitamura K, Shirato H, Shimizu S, Shinohara N, Harabayashi T, Shimizu T, et al. Registration accuracy and possible migration of internal fiducial gold marker implanted in prostate and liver treated with real-time tumor-tracking radiation therapy (RTRT). Radiother Oncol. 2002;62(3):275-81.
36. Murphy MJ. Fiducial-based targeting accuracy for external-beam radiotherapy. Med Phys. 2002;29(3):334-44.
37. Hakenberg OW, Linne C, Manseck A, Wirth MP. Bladder wall thickness in normal adults and men with mild lower urinary tract symptoms and benign prostatic enlargement. Neurourol Urodyn. 2000;19(5):585-93.
38. Jang HA, Lee JG, Bae JH. Measurement of Bladder Wall Thickness in the healthy Korean adults and its feasibility in diagnosing bladder outlet obstruction in the patients with lower urinary tract symptoms. Korean University Medical Centre, Seoul, Korea.84.
39. Morgan MA. Bladder wall thickening (differential). Radiopaediaorg/articles/bladder-wall-thickening-differential.
40. Das S, Liu T, Jani AB, Rossi P, Shelton J, Shi Z, et al. Comparison of image-guided radiotherapy technologies for prostate cancer. Am J Clin Oncol. 2014;37(6):616-23.
41. Marks LB, Ten Haken RK, Martel MK. Guest Editor's Introduction to QUANTEC: A Users Guide. International Journal of Radiation Oncology • Biology • Physics.76(3):S1-S2.

42. O'Doherty UM, McNair HA, Norman AR, Miles E, Hooper S, Davies M, et al. Variability of bladder filling in patients receiving radical radiotherapy to the prostate. Radiother Oncol. 2006;79(3):335-40.
43. Kole TP, Tong M, Wu B, Lei S, Obayomi-Davies O, Chen LN, et al. Late urinary toxicity modeling after stereotactic body radiotherapy (SBRT) in the definitive treatment of localized prostate cancer. Acta Oncologica.0(0):1-7.
44. Tang CI, Loblaw DA, Cheung P, Holden L, Morton G, Basran PS, et al. Phase I/II study of a five-fraction hypofractionated accelerated radiotherapy treatment for low-risk localised prostate cancer: early results of pHART3. Clin Oncol (R Coll Radiol). 2008;20(10):729-37.
45. http://verathon.com/products/bladderscan/.
46. Hynds S, McGarry CK, Mitchell DM, Early S, Shum L, Stewart DP, et al. Assessing the daily consistency of bladder filling using an ultrasonic Bladderscan device in men receiving radical conformal radiotherapy for prostate cancer. The British Journal of Radiology. 2011;84(1005):813-8.
47. Dubois DF, Prestidge BR, Hotchkiss LA, Prete JJ, Bice WS, Jr. Intraobserver and interobserver variability of MR imaging- and CT-derived prostate volumes after transperineal interstitial permanent prostate brachytherapy. Radiology. 1998;207(3):785-9.
48. Janowski E, Chen LN, Kim JS, Lei S, Suy S, Collins B, et al. Stereotactic body radiation therapy (SBRT) for prostate cancer in men with large prostates (>/=50 cm(3)). Radiat Oncol. 2014;9:241.
49. Haworth A, Paneghel A, Bressel M, Herschtal A, Pham D, Tai KH, et al. Prostate bed radiation therapy: the utility of ultrasound volumetric imaging of the bladder. Clin Oncol (R Coll Radiol). 2014;26(12):789-96.
50. Akin M, Oksuz DC, Iktueren B, Ambarcioglu P, Karacam S, Koca S, et al. Does rectum and bladder dose vary during the course of image-guided radiotherapy in the postprostatectomy setting? Tumori. 2014;100(5):529-35.

CHAPTER 5

Planning margins for Prostate Cancer patients: an analysis

5.1 INTRODUCTION

The importance of "planning margins" has been explained in previous Chapters. Planning margins need to take account of all uncertainties and errors during treatment planning and delivery (1). The Planning Target Volume (PTV) is treated to a high dose to ensure that the CTV receives a therapeutic dose despite small geometric errors in treatment planning/delivery (2).

"Systematic error" describes a deviation which occurs in the same direction and of a similar magnitude for each fraction through the treatment course. "Random errors" occur at the treatment delivery stage, and are varying (both intra- and inter-fraction) and unpredictable.

Sources of potential error between planned and executed radiotherapy delivery are discussed here.

5.1.1 Planning: Delineation error:

There are 3 components to delineation error.

The first is that all imaging modalities have limited spatial resolution. The magnitude of the resolution error is modality dependent, and varies according to the plane being considered (3, 4). Secondly, there can be intra-observer variation in outlining, as discussed in Chapter 3, where repeated delineations by the same observer yield different outlines (5, 6). Finally, inter-observer variability can be a factor which contributes to delineation uncertainty (5, 6).

Delineation error is a purely systematic error, it influences all treatment fractions in an identical way throughout the treatment planning process.

5.1.2 Planning & Treatment Delivery errors:

A) Organ motion:

At the planning CT scan, the target organ position is captured at a snap-shot position. All beams will subsequently be targeted at this arbitrary tumour position at planning CT. If the target position at planning CT is not representative of the position across all treatment fractions, this introduces a systematic error.

Organ motion also occurs within a treatment fraction (intra-fractional variation of target position). For the prostate, this occurs due to bladder filling and rectal motion due to flatus as discussed in Chapter 4 (7). In general, errors introduced once during treatment preparation (i.e. at planning CT, a systematic error), are more significant than day-to-day variation during treatment delivery (random error) (2).

B) Phantom transfer error:

This is the error that accumulates when transferring image data from initial localisation through the treatment planning system to the CyberKnife treatment delivery system (8). In order to regularly assess the magnitude of this error, an essential part of monthly quality assurance (QA) for CyberKnife is the film targeting test, or the "end-to-end" test. The test involves planning treatment delivery to a target in a phantom, and evaluating the doses delivered (by reference to film within the phantom). This test assesses treatment planning, robot motion, image processing, and Linac delivery (9).

Departmental QA shows the end-to-end error to be 0.42 mm (Range 0.26-0.66mm). The phantom testing described in Chapter 2 incorporated testing of errors in image processing and robot movements, but not dose delivery. The error from the testing described in Chapter 2 was 0.24mm.

The phantom transfer error is a systematic error because it occurs in the same direction, with similar magnitude, for each fraction of the treatment course (8).

C) Patient set-up error:

This describes all causes of treatment set-up error (meaning a discrepancy between intended and actual treatment position) not accounted for by phantom transfer error. The error comprises systematic and random components. Possible causes include changes in a patient's position, shape or size (8).

D) Fiducial tracking error:

When a patient is to undergo CyberKnife treatment that will be tracked via fiducials, they are set up according to fiducial position.

Initially, the patient lies down on the treatment couch, aided by the immobilisation specified by CT simulation. The CK Radiographers then align the patient approximately, with the help of in-room lasers, to bring the fiducials close to the imaging centre of the room. The first pair of live images is then taken, and adjustments to patient and couch position are applied until the fiducials are well visualised on the Live images, and the inter-fiducial distances are as established at planning CT (or very similar).
Errors in fiducial position, such as those described in Chapter 3, can therefore contribute to patient set-up errors.

Fiducials for prostate treatments are implanted directly into the prostate gland in all patients treated by CyberKnife. If there were a shift in the position of any fiducial compared to its corresponding position at planning CT this would be a source of error.

This error would be a systematic error if there were a change in position of a given fiducial between planning CT and the start of treatment, which was consistent for every treatment fraction. Equally, the error could be random if the positional change of the fiducial varied from day-to-day and during a treatment fraction.

5.2 AIMS

1. To quantify errors and uncertainties in CK treatment planning and delivery for prostate patients.

2. To calculate ideal planning margins for CK prostate patients.

5.3 MATERIALS AND METHODS

5.3.1 Treatment planning and delivery:

Comparison of inter-fiducial pair distances both inter-fractionally and intra-fractionally provided an assessment of fiducial instability as a potential source of error.

Inter-fiducial pair distances were calculated manually from the fiducial positions on the Planning CT scan (as described in Chapter 2) for 8 patients undergoing CK treatment for organ-confined prostate cancer.

CK Treatment delivery was observed in full for all 8 patients. Patients were treated in 5 treatment fractions on consecutive days.

Bladder preparation for the patients was described in Section 4.3.3.

The CK Radiographers positioned each patient for treatment according to standard procedures.

Immediately prior to delivery of the first treatment beam, the inter-fiducial marker distances (based on Live X-ray positions) were recorded.

Just before the end of each treatment fraction, the CK Radiographers performed a "soft stop" of treatment delivery, and inter-fiducial marker distance was again recorded.

During treatment delivery, translational and rotational corrections were recorded after each pair of live X-Rays were captured. Rigid Body Error was also recorded at intervals.

5.3.2 Statistical Analysis:

A) Inter-fiducial distance:

Planning CT, Pre-treatment and Post-treatment inter-fiducial distances were compared for each patient as a measure of the variability of fiducial position.

Inter-fiducial distances were also compared according to treatment fraction (e.g. fraction 1 vs fraction 5). The aim was to evaluate whether a change in target size/formation due to treatment effect has any impact on inter-fiducial distances.

Changes in inter-fiducial distances were compared to recorded Rigid Body Error (RBE).

B) Translational corrections:

For each patient, and each fraction, the mean translational corrections in Left/Right (lateral), Superior/Inferior (longitudinal), and Anterior/Posterior (vertical) directions were calculated.

Individual patient errors:

A Mean shift for lateral/longitudinal/vertical directions (considering all 5 treatment fractions) was recorded for each individual patient (m_{indiv}) along with the respective Standard Deviations (σ_{indiv}).

$\mathbf{m_{indiv}}$ = The individual mean set-up error for each lateral/vertical/longitudinal directions.

$$\boldsymbol{mindiv} = \frac{Mean\ Shift\#1 + Mean\ shift\#2 + \cdots .. + Mean\ shift\#n}{n}$$

Where # = treatment fraction, and n = number of treatment fractions.
For this sample of patients, n=5.

This is a **systematic** set-up error.

$\boldsymbol{\sigma_{indiv}}$ = The inter-fractional daily set-up error (in each direction) .

$$\boldsymbol{\sigma indiv} = \sqrt{\frac{(Mean\ Shift\#1 - \boldsymbol{m}\mathbf{indiv})^2 + \ldots\ldots (Mean\ shift\#n - \boldsymbol{m}\mathbf{indiv})^2}{\mathrm{n} - 1}}$$

This is a **random** error.

The denominator when calculating Standard Deviation above = number of fractions - 1.

Population errors:

This data was used to calculate Systematic and Random set-up errors for the **population** of prostate patients, which contribute to recommended planning margins. Calculations were performed according to guidance in the Royal College of Radiologists "On Target" document (8).

The overall population mean set-up error (M_{pop}) for the sample of 8 patients studied here, which should ideally be 0, is given by the following formula:

$$\boldsymbol{Mpop} = \frac{mindiv1 + mindiv2 + mindiv3 + mindiv4 + mindiv5 + mindiv6 + mindiv7 + mindiv8}{n}$$

Where n= number of patients. n = 8 for this sample of patients.

$\mathbf{M_{pop}}$ (population mean set-up error) is calculated for each lateral/ longitudinal/vertical directions.

The systematic error for the population, $\boldsymbol{\sum_{set\ up}}$, is defined as the Standard Deviation of the individual mean set-up errors around the overall population mean, $\mathbf{M_{pop.}}$ This is calculated according to the following formula:

$$\sum \boldsymbol{set\ up} = \sqrt{\frac{(m_{indiv1} - \mathbf{Mpop})^2 + (m_{indiv2} - \mathbf{Mpop})^2 + \cdots (m_{indiv8} - \mathbf{Mpop})^2}{\mathrm{n} - 1}}$$

Where n= number of patients. n = 8 for this sample of patients.

The population random error, $\boldsymbol{\sigma}_{\text{set up}}$, is the mean of all the individual random errors ($\boldsymbol{\sigma_1}$, $\boldsymbol{\sigma_2}$, ….$\boldsymbol{\sigma_8}$) .

$$\boldsymbol{\sigma set\ up} = \frac{\sigma 1 + \sigma 2 + \sigma 3 \ldots . + \sigma \mathrm{n}}{n}$$

C) Margin Calculations:

As described previously, the Planning Target Volume (PTV) is treated to a high dose to ensure that the CTV receives a therapeutic dose despite small geometric errors in treatment planning/delivery (2).

The population systematic error, $\boldsymbol{\sum_{set\ up}}$, was combined in quadrature with the other systematic errors previously described, to generate an overall systematic error, $\boldsymbol{\sum}$.

$$\sum = \sqrt{(\sum delineation^2 + \sum motion^2 + \sum phantom\ transfer^2 + \sum set\ up^2)}$$

Planning margins also need to take account of random error. $\boldsymbol{\sigma set\ up}$, calculated as described above, was incorporated into the margin recipe.

Several margin recipes have been published in the literature (10, 11), but the Van Herk formula was used here, as it is perhaps the most widely accepted (12) :

Planning Margin (mm) = $2.5\boldsymbol{\sum} + 0.7\boldsymbol{\sigma}$

D) Inter-fiducial marker analysis

Melanie Green, medical statistician performed statistical tests for trend.

5.4 RESULTS

5.4.1 Inter-fiducial pair distance: Planning vs Treatment

The results for inter-fiducial distances at planning (calculated from the fiducial positions on the planning CT scan), are displayed in Appendix 5.1.

The results for inter-fiducial distance measurements pre- and post- each CK treatment fraction are shown in Appendix 5.2.

Accuray recommend that fiducials are located >2cm apart, to ensure that the fiducial tracking system can appreciate fiducials as separate entities (13). Mean inter-fiducial distance for the 7 patients displayed in Appendix 5.1 is 23.6mm, which is within guidance. However, range = 16.3mm – 30mm.

Only 3/21 fiducial pairs sited (14%) were spaced by <2cm (Patient 3: fid 1/2; Patient 5: fid 1/2, and Patient 6: fid 1/3).

The exact arrangement and positions of the 3 intra-prostatic fiducials implanted for each patient can change due to inter-fractional motion. Comparing the inter-fiducial pair distances at planning CT (from Appendix 5.1), with the pre-CK inter-fiducial pair distances at fraction 1, (from Appendix 5.2) there is reasonable stability. All pre-CK fraction 1 inter-fiducial pair distances were within 3mm of the corresponding planning CT inter-fiducial pair distances. The majority (76%) of pair distances were within 1mm of the corresponding planning CT inter-fiducial pair distances.

5.4.2 Inter-fiducial pair distance: First fraction to Final fraction: Treatment analysis

Appendix 5.3 shows the change in inter-fiducial pair distance between the first and final recorded fraction for each patient. The table compares pre-CK inter-fiducial pair distances. This is a further assessment of inter-fractional fiducial motion.

The mean change in inter-fiducial pair distance (in mm) between the first and final fraction recorded was + 0.8mm (SD = 0.7). 5/7 patients studied (71%) and 17/21 inter-fiducial pair distance changes (81%) had increased spacing of fiducials in the final fraction, as compared to the first fraction.

Linear regression was used to explore any trend in inter-fiducial distance over the treatment period (fraction 1 to fraction 5) for the patient group. The dependent variable was fraction number, and the independent variable was the mean of pre- and post-treatment fiducial movement for D1, D2 or D2 (where D1 = Fid1-Fid2 distance, D2=Fid1-Fid3 distance, and D3=Fid 2-Fid 3 distance). There was no evidence of any trend (see Table 5.1 below).

Table 5.1: Test for trend: inter-fractional prostate fiducial motion: #1 vs #5

Fiducials	Coefficient (95% CI)	p-value
D1	0.019 (-0.126, 0.165)	0.788
D2	0.006 (-0.125, 0.136)	0.928
D3	0.034 (-0.148, 0.215)	0.708

Although a group trend in inter-fraction motion was not found, there was evidence of some substantial inter-fraction motion during treatment for some patients. Inter-fiducial distance (D1 [F1-F2], D2 [F1-F3] and D3 [F2 – F3]) was plotted for each patient (P1 = patient 1, P2= patient 2 etc) at planning (P) and for fractions #1 - #5 (Figure 5.1). Enlarged symbols signify a change in inter-fiducial distance from planning >1.5mm (patients 4, 5 and 7), indicating a clinically relevant inter-fraction displacement of fiducial COM of >2mm (14).

Figure 5.1: Inter-fractional change in marker pair distance: Planning vs #1 vs #5

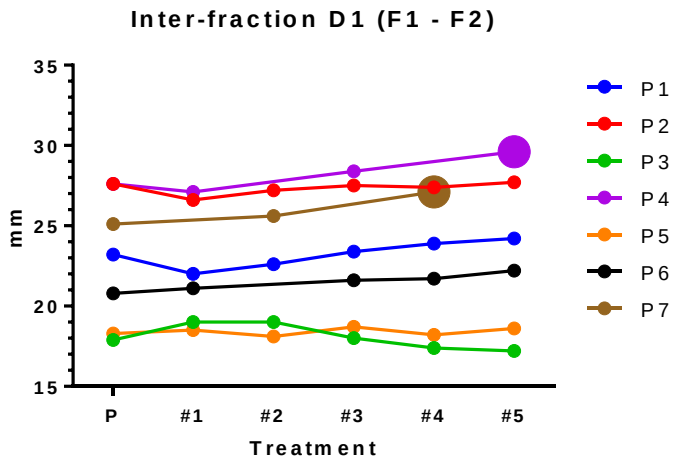

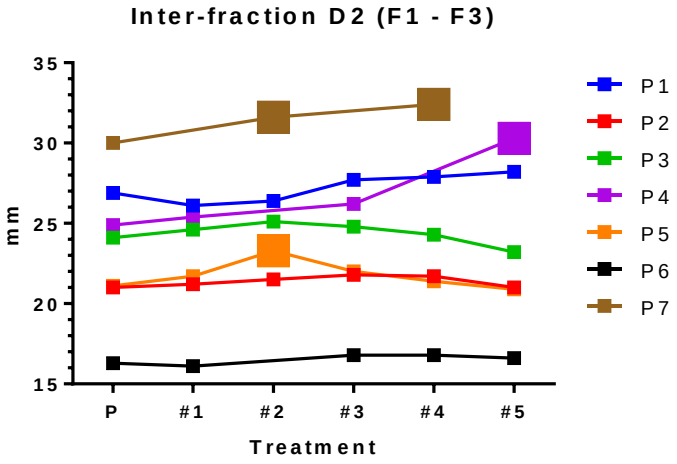

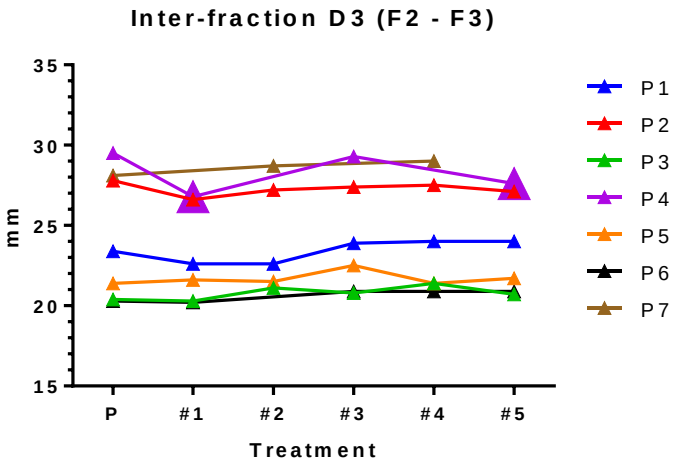

5.4.3 Inter-fiducial pair distance: Pre-CK vs Post-CK: Treatment analysis

A further assessment of any instability of fiducial arrangement for these prostate cases (and therefore a potential source of error) can be made by comparing inter-fiducial pair distances pre- and post- each CK treatment fraction using pair distances captured on the Live X-rays. This is a measure of intra-fractional motion, although based on only 2 "snap-shots" of fiducial position per fraction (just prior to commencing a treatment fraction, and immediately prior to completing a treatment fraction).

Appendix 5.3 shows the change in inter-fiducial pair distance (in mm) pre- and post- a CK fraction. A negative distance signifies that the fiducials have been imaged closer together on the post-CK images, compared to the pre-CK images. A positive distance change signifies that the fiducials have been imaged further apart. The mean change in pre- to post-CK inter-fiducial pair distance was +0.3mm, indicating that there is relative intra-fraction stability of pair distances. The range of measured changes in pair distances was -2.2mm to +3mm, however 81% of changes were sub-millimetre. Differences between the means of each inter-fiducial distance (D1 [F1-F2], D2 [F1-F3] and D3 [F2 – F3]) pre- and post-treatment were tested using the paired t-test; results are shown in table 5.2. No significant differences were observed in pre- and post-treatment D1 and D2, but there was borderline difference in D3 (p=0.059).

Table 5.2: Test for trend: intra-fractional prostate fiducial motion

Fiducials	Mean (pre-treatment)	Mean (post-treatment)	Difference	p-value
D1	22.74	22.87	-0.12	0.441
D2	23.69	23.78	-0.10	0.529
D3	23.80	24.13	-0.33	0.059

Where there was a large change in inter-fiducial distance observed (e.g. patient 3, #4/5 and patient 4, #5, highlighted in Appendix 5.3) it would be expected that this would be reflected in the Rigid Body Error (RBE). This is considered below.

5.4.4 Rigid Body Error (RBE): Treatment analysis

Appendix 5.5 displays the Rigid Body Error (RBE) readings for the patients studied.

As discussed in Chapter 2, the RBE refers to the discrepancy (in mm) in fiducial positions (relative to each other) between the CT planning scan and the time of treatment. The method of manually calculating RBE from inter-fiducial distance changes is demonstrated in Chapter 2 Section 2.4.3.

For tracking with multiple fiducials, the upper limit of RBE is often set at 2mm. It is possible to increase the acceptable RBE to allow treatment delivery if the RBE>2, but increasing the RBE threshold is considered carefully by CK radiographers, and Physics will be consulted. The greater the RBE, the greater the discrepancy between planning CT positions of fiducials and those at treatment, and in turn, the greater the risk of inaccuracies with treatment delivery.

Appendix 5.5 shows that only 2 fractions out of the 27 fractions reported (7%) were associated with a Mean RBE>2mm threshold (Patient 4: #5 and Patient 7: #4). However, Maximum RBE was >2mm threshold in 6/27 fractions (22%), always occurring in the 3rd to 5th fraction of treatment.

The highlighted data in Appendix 5.5, refers to those patients and fractions in Appendix 5.3 where there was a change of >2mm in on-treatment inter-fiducial pair distance. Each patient/fraction highlighted had a maximum RBE>2mm. For patient 4/#5, where 2 of the 3 inter-fiducial on-treatment pair distances changed by >2mm, the Mean RBE of 2.5mm was the largest for all patients and fractions studied. Patient 7/#4 in Appendix 5.5 had the 2nd largest Mean RBE (2.2mm), with only tiny changes in inter-fiducial pair distances shown in Appendix 5.3 (0-0.1mm). However, the inter-fiducial pair distance changes in Appendix 5.3 are based only on 2 snap-shots of fiducial positions (pre-CK and post-CK).

5.4.5 Translational corrections analysis:

Individual patient errors:

$\mathbf{m}_{indiv}$ = The individual mean set-up error for each lateral/ longitudinal/vertical directions, along with the respective Standard Deviations ($\boldsymbol{\sigma}_{indiv}$), were calculated as per description in Section 5.3.2B.

These values, for 8 CK prostate patients, are displayed in Table 5.1.

Table 5.1: Individual patient errors for CK prostate patients

Patient	Number of fractions (n)	Lateral (Left/Right) (mm)		Longitudinal (Sup/Inf) (mm)		Vertical (Ant/Post) (mm)	
		$\mathbf{m}_{indiv}$	$\boldsymbol{\sigma}_{indiv}$	$\mathbf{m}_{indiv}$	$\boldsymbol{\sigma}_{indiv}$	$\mathbf{m}_{indiv}$	$\boldsymbol{\sigma}_{indiv}$
1	5	-0.2	0.5	-1.9	1	1.8	0.7
2	5	-0.1	0.6	-0.1	0.6	1	0.8
3	5	0.6	0.6	0	0.3	1.2	0.4
4	4	0.2	0.9	-1.7	1.3	2.2	1.1
5	4	0.9	2.3	-1	2.2	1.7	1.2
6	5	0.4	1.1	-1	1.4	1.9	0.8
7	4	-1.3	3.8	-0.8	2	1.6	1.6
8	4	0.8	1	-0.7	1.4	1	1.6
Mean	5	0.2	1.4	-0.9	1.3	1.6	1

$\mathbf{m}_{indiv}$ = the systematic individual patient error, the range of $\mathbf{m}_{indiv}$ for the Lateral direction is -1.3mm to +0.9mm, for the Longitudinal direction: -1.9mm to 0mm, and for the Vertical direction: +1 to +2.2mm.

$\boldsymbol{\sigma}_{indiv}$ is the random individual patient error. The ranges of $\boldsymbol{\sigma}_{indiv}$ for Lateral direction is: +0.5-3.8mm, for Longitudinal direction: +0.3-2.2mm, and for the Vertical direction: +0.4-1.6mm.

Population patient errors:

The overall population mean set-up error ($\mathbf{M}_{pop}$) for the sample of 8 patients studied here, is the average of $\mathbf{m}_{indiv}$ values displayed in Table 5.1.

$\mathbf{M}_{pop}$ (population mean set-up error) for Lateral direction is +0.2mm, for Longitudinal direction -0.9mm, and for the Vertical direction +1.6mm.

The systematic error for the population, $\sum_{set\ up}$, is defined as the Standard Deviation of the individual mean set-up errors around the overall population mean, $\mathbf{M}_{pop.}$ This was calculated according to the formula described in Section 5.3.2B.

$\sum_{set\ up}$ for the population is 0.7mm, 0.7mm and 0.4mm in Lateral, Longitudinal, and Vertical directions respectively.

The population random error, $\boldsymbol{\sigma}_{set\ up}$, is the mean of all the individual random errors. Table 5.1 shows that $\boldsymbol{\sigma}_{set\ up}$ is 1.4mm, 1.3mm and 1mm in Lateral, Longitudinal, and Vertical directions respectively.

5.4.6 Margins calculations:

The population systematic error, $\sum_{set\ up}$, was combined in quadrature with the other systematic errors previously described, to generate an overall systematic error, $\sum$.

$$\sum = \sqrt{\sum set\ up^2 + \sum motion^2 + \sum delineation^2 + \sum end - to - end^2}$$

$\sum_{set\ up}$ for the population, as calculated above according to the "On Target" (8) document, was 0.7mm, 0.7mm and 0.4mm in Lateral, Longitudinal, and Vertical directions respectively. However, at the start of a CK treatment fraction the CK radiographers will set the patient up carefully as described in Section 5.3.1. They acquire a pair of Live images just before delivering the first beam, and the robot will adjust to correct for the translational and rotational changes (between DRR and Live images, based on fiducial position), before delivering the beam. This is an example of on-line correction. If the Live X-Rays acquired are an exact representation of fiducial position at the time of beam delivery, then the systematic set-up error is effectively 0mm (due to the on-line correction applied).

For this population $\sum_{set\ up}$ = 0mm, justification as above.

$\sum_{motion}$ describes the motion error for the population of prostate patients studied. The imaging frequency during a CK treatment fraction can be set by the CK radiographers, but for prostate patients the imaging frequency is often every 30 seconds at the start of treatment, moving to every 60 seconds once the radiographers are reassured that the translational and rotational adjustments are fairly stable. There is therefore the potential for residual motion of the prostate between a pair of acquired images and delivery of a treatment beam. This is a potential source of error. The calculations for "$\sum_{set\ up}$" described in Section 5.3.3 were based on translational adjustments applied by the CK robot in response to changes in fiducial position (on Live X-Rays compared to DRR) due to motion or deformation of the prostate. The values calculated are therefore appropriate for $\sum_{motion}$.

For this population $\sum_{motion}$ = 0.7mm (lateral), 0.7mm (longitudinal) and 0.4mm (vertical).

$\sum_{delineation}$ would ideally have been evaluated on the sample of 8 patients reviewed here by assessing intra-observer and inter-observer variation in outlining. However, a 2mm error is assumed as quoted in Nyholm et al (15). $\sum_{delineation}$ = 2mm.

$\sum_{end\text{-}to\text{-}end}$ = 0.42 mm as assessed by the Departmental QA ("end-to-end testing").

Therefore applying the above formula, $\sum$, the overall systematic error, is as follows:

$\sum_{lateral}$ = 2.2mm

$\sum_{longitudinal}$ = 2.2mm

$\sum_{vertical}$ = 2.1mm

Planning margins also need to take account of random error.

$\boldsymbol{\sigma}_{set\ up}$, calculated as described above, was incorporated into the margin recipe. $\boldsymbol{\sigma}_{set\ up}$ was 1.4mm, 1.3mm and 1mm in Lateral, Longitudinal, and Vertical directions respectively.

Van Herk Planning Margin (mm) = $2.5\sum + 0.7\boldsymbol{\sigma}$

Margins for each direction are as follows:

Lateral = 6.5mm

Longitudinal = 6.4mm

Vertical = 6mm

5.5 DISCUSSION

Planning margins need to take account of all uncertainties and errors during treatment planning and delivery, in order to ensure that a therapeutic dose is delivered to the tumour target. Potential sources of error have been described in Section 5.1. The author has undertaken work to quantify errors and uncertainties in treatment planning and delivery for CK prostate patients.

Once quantified, the errors and uncertainties have been incorporated into a margin recipe to generate "ideal" planning margins for CK prostate patients.

As described in Chapter 3, stability and reproducibility of implanted fiducials is critical for accurate treatment delivery in any CK treatment tracked using fiducials. Any discrepancy between fiducial location on the planning CT (an arbitrary snapshot of target/fiducial position) and treatment has the potential to lead to targeting error.

5.5.1 Inter-fiducial pair distance: Planning vs Treatment : Inter-fractional variation

Chapter 3 examined fiducial stability and reproducibility by comparing CT planning scan fiducial locations, to "first day of treatment" CT fiducial locations.

A "first day CT" is not performed for CK Prostate patients. This is considered acceptable as there have been no recorded cases of migration of fiducials outside of the prostate at this centre. However, as Chapter 3 illustrated, gross migration is not the only consideration. Fiducial migration within the prostate, where the fiducial has migrated a few millimetres from the site of implantation, can also have a deleterious effect on tumour targeting.

Inter-fiducial distance information is available from the CK console at the time of treatment. This has been recorded and analysed by the author to assess the reproducibility of fiducial location in prostate patients.

When comparing inter-fiducial distance at planning (from planning CT data) vs. inter-fiducial distance at treatment (from CK console data) as a measure of inter-fractional variation, the comparison was made with the first fraction of treatment, to eliminate treatment effect as a potential confounding factor. The only exception to this was patient 7, where inter-fiducial distances were not available on fraction 1, inter-fiducial distances were taken from fraction 2 instead.

Van der Horst et al (16) analysed marker pair distance changes between planning CT scan and first day of treatment CT in pancreatic tumours. The group found that 81% of marker pair distance changes were sub-millimetre.

Inter-fractional changes in marker pair distance for the prostate patients studied here were within 3mm for all patients, and 76% of inter-fractional marker pair distance changes were within 1mm. This is comparable to the results of the Van der Horst group.

The lung, liver and pancreas patients that were studied for fiducial reproducibility in Chapter 3 were assessed by co-registering planning and Day 1 treatment CT scans by means of the implanted fiducials. The CT scans were translated and rotated until an optimum match was achieved. This was the technique used by the Van der Horst group. This process might be expected to achieve a better match of fiducial position than the scenario faced by the CK radiographers at treatment, where a fiducial match can only be achieved by adjusting patient and couch position.

Despite the caveat about the different methodology, it is interesting to compare the fiducial reproducibility results from the lung, liver and pancreas patients with the prostate group.

Chapter 3 reported mean Centre of Mass (COM) of fiducials shift (between planning CT and Day 1 Treatment CT) as a measure of fiducial reproducibility. Taking COM as the measure of fiducial reproducibility (vs individual marker position) tends to minimise the magnitude of shift, due to the effect of individual marker shifts being averaged out (14, 16). Considering cases of multiple implanted fiducials, Mean COM shift for lung was sub-millimetre (0.6mm, 0.9mm and 0.7mm in x/y/z axes respectively), Mean COM shift for liver was 0.6mm, 0.4mm and 1.2mm in x/y/z axes respectively, and Mean COM shift for pancreas was 1mm, 0.8mm and 0.4mm in x/y/z axes respectively.

Therefore, despite the more challenging process required to achieve a fiducial match at treatment, it is encouraging that 76% of inter-fiducial marker pair distance changes (between planning and treatment) were within 1mm for prostate patients. The prostate inter-fiducial pair distance stability results compare favourably with the COM shifts observed (between planning and treatment) for lung, liver and pancreas patients previously studied by the author.

5.5.2 Inter-fiducial pair distance: First vs Final treatment fraction: Inter-fractional variation

Comparison of inter-fiducial pair distances between the first and final fraction recorded for each patient is a further measure of inter-fractional variation of fiducial position. However, this time there is the potential for the analysis to incorporate the effect of treatment.

Van der Horst et al (16) found that there was a mean change in pair distance of -0.03mm/day in pancreatic cancer patients tracked with implanted fiducials. This amounted to a mean change of 1.1mm over the course of treatment, with the markers moving closer together. The authors concluded that this was due to tumour shrinkage. This was however a different tumour type, and the patients were treated with conventional fractionation for 25 fractions.

Prostate brachytherapy is an example of extreme hypofractionation (single fraction treatment). A study of such patients by Cury et al (17) showed that 7 days after implantation, 68% of patients had an increase in volume of the prostate, associated with increased dimensions of the gland by 0.6mm, 0.5mm and 0.2mm in Ant/Post, Lateral and Sup/Inf dimensions respectively.

This is the first study to analyse change in inter-prostatic marker pair distance on treatment, treated with hypofractionated radiotherapy (35Gy/5#). The mean change in inter-fiducial pair distance between the first and final recorded fraction was +0.8mm (SD=0.7mm). 71% of patients studied had increased spacing of fiducials in the final fraction, as compared to the first fraction. The percentage of patients showing increased spacing of fiducials (which could be due to swelling of the prostate gland, or fiducial migration), is very similar to the results of Cury et al.

It may be intuitive that those patients whose fiducials became more spaced (due to possible prostate swelling), might also develop early obstructive symptoms (poor stream, residual urine volume). In fact, there was no correlation between increased fiducial spacing and obstructive symptoms. It may be that prostatic urethra dose is more closely correlated with early urinary symptoms.

5.5.3 Inter-fiducial pair distance: Pre- vs Post-CK Treatment: Intra-fractional variation

The Calypso system lends itself to measurement of intra-fractional assessment of fiducial marker stability in the prostate. Electro-magnetic transponders are implanted into the prostate to allow intra-fractional tracking of prostate motion. Transponder position is continuously monitored by a magnetic array which is positioned over the patient's pelvis. Tanyi et al (18) and Kupelian et al (19) assessed inter- and intra-fraction motion of the prostate assessed with Calypso. However, the

Calypso system reports COM of transponder position (or transponder "centroid"), rather than inter-fiducial pair distance.

Inter-fiducial distance information is available from the CK console at the time of treatment as previously described. This data was recorded immediately prior to delivery of the first treatment beam, and also just before completing treatment. This is a measure of intra-fractional motion, although based on only 2 images per treatment fraction which is a limitation.

The mean change in inter-fiducial pair distance was +0.3mm, and mean SD of pair distance was 0.5mm, signifying relative intra-fraction stability of pair distances.

In summary, analysis of inter- and intra- fractional variation of fiducial stability has shown that mean positional changes of fiducials are <1mm.

5.5.4 Rigid Body Error (RBE): Treatment analysis

The RBE refers to the discrepancy (in mm) in fiducial positions (relative to each other) between the CT planning scan and the time of treatment. The larger the RBE, the greater the risk of inaccuracy in treatment delivery.

As a Quality Assurance check, the CyberKnife tumour tracking system generates a warning if the distance between fiducial markers (reported as RBE) has deviated by >1.5mm from the reference configuration on the planning CT scan (9). This also gives the opportunity to the CK radiographers to "switch off" a fiducial which has clearly migrated and is no longer a good surrogate for tumour position.

Tumour localisation at treatment delivery of a CyberKnife plan is based on the COM of fiducials. Therefore, Van der Voort van Zyp et al (14) evaluated whether a clinically relevant displacement of > 2mm in the fiducial COM was accompanied by a change in the distance between markers of >1.5mm (reported as RBE). The group assessed 42 patients treated by CyberKnife for lung cancer. Planning CT scans and On-treatment CT scans were co-registered by means of soft tissue matching on the lung tumour. Fiducial stability (between planning and treatment) was analysed by displacement of fiducials, and displacement of fiducial COM.

The group found that median individual fiducial displacement was 1.3mm, and median displacement in fiducial COM = 1mm. Displacements in the fiducial COM of >2mm were detected by changes in inter-fiducial distance of >1.5mm (reported as RBE) in 96% of treatment fractions.

In comparison, considering the 7 prostate patients treated by CK, mean RBE was 1.1mm (see Appendix 5.5). Maximum RBE was >1.5mm in 13/27 observed treatment fractions (48%). Applying the findings of Van der Voort van Zyp, almost half of treatment fractions observed could have had a fiducial COM displacement of >2mm, for at least a portion of the delivered treatment fraction, this could be potentially significant.

As described, implantation of 3 intra-prostatic fiducials is the current standard at the author's centre. Implantation of a 4th fiducial per-patient would allow the possibility to "switch off" a fiducial at treatment delivery, if there had been apparent migration (compared to planning CT position), whilst still retaining the ability to track prostate rotations.

It is important to note that there were some limitations to the RBE results recorded by the author. As described, the CK radiographers can decide the frequency of imaging during delivery of a CK fraction (usually every 30 – 60 seconds). Therefore, the number of image pairs captured varied between fractions, and between patients. It was sometimes challenging for the author to record (by hand and in real-time) full translational, rotational and RBE data in between image pairs. Therefore, more RBE readings were available for some patients than others. The mean number of RBE records per treatment fraction was 18 (range 5-29).

Appendix 5.5 shows that 6/27 treatment fractions (22%) studied were associated with a Maximum RBE > 2mm. These large RBE values always occurred in the 3rd to 5th fraction of treatment. The above-threshold RBE values in these instances reflect a moderate change in fiducial position between planning CT scan positions, and the positions on treatment.

The observation that the larger RBE values tended to occur towards the end of a course of treatment fraction is interesting. If the reason for this was inflammation, it might be expected that the starting RBE would increase with each fraction, but this was not borne out in the results. It could be hypothesised that the effect of treatment on the prostate, makes the fiducials more prone to displacement (e.g. due to bladder/rectal filling) in the later, rather than the early, treatment fractions.

Whilst the RBE is a QA check that can flag up potential issues with targeting, the critical factor in accurate treatment delivery is stability of the fiducial COM. It would be possible for the 3 fiducials to migrate apart from each other (e.g. due to inflammation) whilst keeping an identical COM, this would increase RBE (flagging up a warning), but accuracy of treatment delivery would potentiallynot be affected (due to the identical COM), as long as the planning margins were sufficient.

5.5.5 Margins calculations:

Assessment of inter-fiducial distance and RBE as described above has provided critical information on fiducial reproducibility for CK prostate cases. However, other factors are of considerable importance when calculating optimum planning margins for the population of prostate patients treated by CK.

It is important that each source of potential error is minimised where possible. Equally, adequate planning margins must be applied which will allow for these errors, whilst ensuring that the target receives a therapeutic dose.

5.5.5A: Phantom transfer error:

Departmental QA has assessed this to be 0.42mm. The error is related to the technical accuracy of the CyberKnife system. The QA to monitor this source of error is undertaken monthly. Whilst it is likely for there to be minor random variation in this source of error (borne out in the monthly readings), the magnitude of any variation is likely to be small. It would be unlikely for there to be a significant improvement in this source of error, unless there is an upgrade to CK software/hardware at the author's centre.

5.5.5B: Set-up error:

As described in section 5.4.6, once a patient has been optimally set-up, a pair of live images is acquired just before delivering the 1st treatment beam. The robot will adjust for any translational or rotational changes (between planning CT and treatment) before delivering a beam. This error is therefore reduced to 0mm by online correction. However, this is an assumption. If there is a change in inter-fiducial positions, in between live imaging assessment and treatment delivery, there is a potential for error. This is considered to be a low risk given the time delay between imaging and delivery.

5.5.5C: Motion:

Fiducials implanted into the prostate act as surrogates for target motion. The prostate is subject to inter and intra-fractional motion, for example due to bladder and rectal filling.

Tanyi et al (18) assessed inter- and intrafraction of the prostate to inform PTV margin expansions in 14 patients undergoing 39 fractions of intensity-modulated radiotherapy (IMRT) for prostate cancer.

The group assessed motion by means of implanted transponders and the Calypso system. The observed intra-fraction movement was as much as 4.8mm, 8.6mm and 9.1mm in the lateral, longitudinal and vertical directions respectively.

In comparison, the maximum motion of prostate observed by fiducial tracking in the patients studied here was 7.2mm, 6.7mm and 7.5mm in lateral, longitudinal and vertical directions respectively.

Maximum motion in the vertical (Anterior/Posterior) direction was greatest in both studies.

In order to minimise errors in targeting due to prostate motion, strategies to reproduce bladder filling and rectal filling can be employed. Bladder filling is discussed in detail in Chapter 4. Bowel preparation for the patients studied here involve an enema 1 hour pre-planning CT and pre- each CK treatment fraction. In addition, Buscopan is administered 30 minutes before planning CT/treatment fractions.

However, other groups have gone further with bowel preparation, advocating a low-fibre diet from 5 days prior to planning scans until the end of treatment (20), and fasting from 4 hours prior to planning CT/treatment (21).

Section 5.4.5 displays the individual mean set-up errors in each direction. These were used to calculate population systematic errors for set-up/motion as described.

For this population $\sum_{motion}$ = 0.7mm (lateral), 0.7mm (longitudinal) and 0.4mm (vertical). These compare to errors determined with the Calypso system of 0.33mm (lateral), 0.7mm (longitudinal) and 0.52mm (vertical) in the Tanyi et al paper (18).

$\sigma_{set\ up}$, population random error for the 7 prostate patients studied here was 1.4mm, 1.3mm and 1mm in lateral, longitudinal and vertical directions. Population random error for the 14 prostate patients tracked with Calypso transponders in the Tanyi et al study (18) was 0.76mm, 1.29mm, and 1.38mm in lateral, longitudinal and vertical directions.

The longitudinal direction systematic and random errors were therefore remarkably consistent between the study groups. Whilst there was variation in lateral/vertical systematic and random errors this was sub-millimetre.

5.5.5D: Delineation:

There can be errors in delineation due to limited spatial resolution of the imaging modality used, as well as intra-and inter-observer variability (3-6). At the author's centre, the prostate is delineated

largely on MRI, which is co-registered to the planning CT scan. Chapter 3 discussed some of the issues around fusion uncertainties when outlining on a secondary scan (rather than the planning CT scan).

Nyholm et al (15) assessed inter-physician variability of prostate contouring on MRI and found that this was 0.7-1.7mm. The error for the patients studied here could be exaggerated if there was any error in CT-MRI fusion.

$\sum_{delineation}$ = 2mm was selected for calculation of PTV margins. Tanyi et al (18) did not incorporate a delineation error into their margin calculation.

5.5.5E: Marcel van Herk margin calculation:

The systematic error (∑) for the CK prostate population studied here having combined phantom transfer, set-up, motion and delineation errors in quadrature as described is 2.2mm in lateral and longitudinal directions, and 2.1mm in the vertical direction.

Applying the Marcel van Herk equation of Planning Margin (mm) = $2.5\sum + 0.7\sigma$ yields planning margins of 6.5mm in the lateral direction, 6.4mm in the longitudinal direction, and 6mm in the vertical direction. These would be the margins needed to deliver 95% of the prescription dose to 95% of the clinical target volume for 90% of the patients.

Tanyi et al calculated planning margins according to the same equation for their prostate patients tracked with Calypso guidance. Their margins were much smaller (1.4mm, 2.6mm and 2.3mm in lateral, longitudinal, and vertical directions respectively). But their margins did not incorporate delineation error, or phantom transfer error.

The systematic error, ∑, is given the largest weighting in the Marcel van Herk formula quoted above (2). In addition, given the way that ∑ is calculated in quadrature, the delineation error of 2mm, is the dominant factor in the planning margin calculation. To illustrate this, if the margins are recalculated, using a delineation error of 2mm, but setting all other systematic errors, and the random error as 0mm, the required margins are 5mm.

This underlines the importance of optimum imaging and fusion protocols.

5.5.5F: Limitations

Tanyi et al (18) demonstrated that margin requirements are less with Calypso set-up/tracking compared to other techniques (skin-mark alignment, bony anatomy alignment, image-guided marker alignment). However, the planning margins that the group calculated did not take into account delineation (as previously discussed), or rotational and deformation errors.

The CyberKnife can adapt for rotational changes in fiducial position, as long as these are within threshold. Rotational changes were tracked throughout for all patients studied here, except for patient 4, and as explained in Chapter 4, this was due to an exceptional circumstance in this patient.

Deformation of the prostate gland may be a more significant issue than rotation in CK prostate patients. Nichol et al (22) assessed prostate deformation in 25 patients with implanted fiducial markers that were treated to 78.9Gy in 42 fractions. The patients had 2 MRIs for assessment, one on the day of the Planning CT, and the second on a randomly allocated treatment day assigned by the study statistician. The scans were fused in a treatment-planning system by means of the fiducials, and the residual errors due to mismatch of the prostate surfaces due to prostate deformation were assessed. The maximum prostate deformations were as large as 6mm, 13mm and 7mm in the lateral, longitudinal, and vertical directions respectively, so deformation is not a trivial issue. An interesting observation was that the superior aspect of the prostate patients who had undergone a TURP procedure (Trans-Urethral Resection of Prostate) appeared to splay open on sagittal imaging when the bladder volume increased from smaller to larger.

Finally, the Marcel van Herk formula does not account for penumbral uncertainties at the collimator edge.

5.5.6 Current planning margins vs Calculated Marcel van Herk margins

The standard planning margins applied at the author's centre are: 5mm in all directions except posteriorly, where a 3mm margin is applied. The reason for the smaller margin in the posterior direction is not due to reduced motion in the posterior direction (indeed Tanyi et al (18) showed increased motion in this direction), but in order to protect the anterior rectal wall from toxicity.

The standard margins applied are clearly less than the calculated Marcel van Herk margins of 6.5mm, 6.4mm and 6mm. This is clearly concerning at first glance.

However, the standard planning margins of 5mm/3mm are widely employed internationally and there is outcomes evidence that the margins are sufficient. Chris King reported the pooled analysis

clinical outcomes of 1100 prostate cancer patients treated with CyberKnife to a median dose of 36.25Gy in 4-5 fractions with planning margins of 5mm/3mm (23). At 36 months follow up the 5 year biochemical Progression-Free Survival (bPFS) was 93%. A cohort of 135 patients with a minimum 5 years follow up have a 5-year bPFS of 99% and 93% for low and intermediate-risk prostate cancer respectively. These results compare favourably with the results of the RT01 study, (24) although comparison of outcomes is best assessed in a randomised trial, such as the PACE study (25). Another note of caution is that long-term data (i.e. 10 years plus data) for those treated with hypofractionation and small planning margins is still awaited.

So why might we get away with it?

Imaging:

It may be that the spatial resolution of MRI is such that observers are outlining the prostate generously, and in reality the actual outline of the prostate (the clinical target volume) lies within the MRI-visualised outline. If this were the case there may be no need to apply a "delineation" error when calculating PTV margins.

Anatomy:

Targeted transperineal biopsies of the prostate via multi-parametric MRI (mpMRI) and template guidance have become more common-place in recent years. The technique is being compared to trans-rectal ultrasound (TRUS) biopsy technique in the PROMIS study (26). For clinical oncologists, the additional spatial information provided by the mpMRI technique is of great importance in identifying where prostate cancer nodules lie. For peripherally located tumour nodules this is helpful in highlighting which margins may be at risk.

Equally, if a tumour nodule lies more centrally in the prostate, the CTV may already be generous.

Biology:

The dose-escalated arm of the RT01 study delivered 74Gy in 37 treatment fractions (24). There is now good evidence that the α/β ratio for prostate cancer is 1.5 (27), the calculated BED of the 74Gy/37# regime for tumour control is 173 (using α/β of 1.5 for tumour control). In comparison, the BED for 35Gy in 5 fractions, using the same α/β ratio is 198. Therefore, despite the sharp dose fall-off outside the prescription isodose line observed with CK treatments, it may be that the CTV is being treated to a biologically therapeutic dose.

Treatment planning and delivery:

There has been great progress in refinement of radiotherapy technique to treat prostate cancer in recent years. Image-guided radiotherapy is an especially important improvement to the technique (28). It is likely that despite the addition of smaller planning margins, we are more reliably delivering a therapeutic dose to the prostate target than ever before.

These are hypotheses only and the testing of these hypotheses is beyond the scope of this thesis.

5.6 CONCLUSIONS

The Aims of this Chapter were:

1. To quantify errors and uncertainties in treatment planning and delivery for CK prostate patients.

2. To calculate ideal planning margins for CK prostate patients.

Errors and Uncertainties taken from published data:

Systematic error:

Delineation $\sum_{delineation}$ = 2mm (15).

Errors and Uncertainties evaluated in this work:

Population Systematic errors:

Set-up error: $\sum_{set\ up}$ = 0mm

Motion error: $\sum_{motion}$ = 0.7mm (lateral), 0.7mm (longitudinal) and 0.4mm (vertical)

End-to-End error: $\sum_{end\text{-}to\text{-}end}$ = 0.42mm

Population Random errors:

$\boldsymbol{\sigma}_{set\ up}$ = 1.4mm (lateral), 1.3mm (longitudinal) and 1mm (vertical)

"Ideal" planning margins for CK prostate patients:

Applying the above sources of errors and uncertainties into the Marcel van Herk equation yields the following margins:

6.5mm, 6.4mm and 6mm in lateral, longitudinal and vertical directions respectively.

These would be the margins required to deliver 95% of the prescription dose to 95% of the CTV for 90% of the patients. The above margins do not incorporate rotational/deformation errors, or penumbral uncertainties.

The Van Herk margins calculated here are more generous than the "standard planning margins" applied (of 5mm in all directions except posteriorly = 3mm), which is potentially concerning. However, there is good clinical outcome data at 5yrs following the application of standard planning margins (23). Some potential reasons for this have been hypothesised.

Recommendations:

1. Do not reduce planning margins below "standard margins" of 5mm/3mm.

2. Patient selection: care with post-TURP patients, they may be more prone to prostate deformation.

3. Fiducial placement: Place 4 fiducials per patient. This will allow the CK Radographers the flexibility to "switch off" a fiducial, but still track rotations, if a fiducial has migrated, or the prostate has deformed (reflected in a high RBE).

4. Delineation:

Assess inter-observer and intra-observer error/uncertainty as this is potentially the biggest source of error.

Close liaison with radiology to optimise MRI sequences for target delineation and to aid CT-MRI fusion.

5. Motion:

Low-fibre diet to minimise rectal filling motion (20)

Follow bladder filling guidelines recommended in Chapter 4.

6. Outcome data:

Analyse clinical outcomes for disease control (measured by bPFS) as well as toxicity in-house.

Review published 10-year outcome data when it becomes available.

References:

1. ICRU. International Commission on Radiation Units and Measurements Report 50: Prescribing, Recording and Reporting Photon Beam Therapy. ICRU Reports. 1993;50.
2. van Herk M. Errors and margins in radiotherapy. Semin Radiat Oncol. 2004;14(1):52-64.
3. Goldman LW. Principles of CT: radiation dose and image quality. J Nucl Med Technol. 2007;35(4):213-25; quiz 26-8.
4. Senan S, De Ruysscher D. Critical review of PET-CT for radiotherapy planning in lung cancer. Crit Rev Oncol Hematol. 2005;56(3):345-51.
5. Upasani M, Chopra S, Engineer R, Medhi S, Master Z, Mahantshetty U, et al. Inter and intraobserver variation in gross tumor delineation on megavoltage CT images in patients undergoing tomotherapy-based image-guided radiotherapy for postoperative vault recurrences. J Cancer Res Ther. 2011;7(3):292-7.
6. Roberge D, Skamene T, Turcotte RE, Powell T, Saran N, Freeman C. Inter- and intra-observer variation in soft-tissue sarcoma target definition. Cancer Radiother. 2011;15(5):421-5.
7. Schild SE, Casale HE, Bellefontaine LP. Movements of the prostate due to rectal and bladder distension: implications for radiotherapy. Med Dosim. 1993;18(1):13-5.
8. RCR I, SCoR. On Target: ensuring geometric accuracy in radiotherapy. 2008.
9. CyberKnife CsH-TFf. Technical White Paper: An educational report on CyberKnife Quality Assurance testing. CRCPD publicationE-07-03. 2007;http://www.crcpd.org/Pubs/CyberknifeWhitePaper.pdf.
10. Stroom J, Gilhuijs K, Vieira S, Chen W, Salguero J, Moser E, et al. Combined recipe for clinical target volume and planning target volume margins. Int J Radiat Oncol Biol Phys. 2014;88(3):708-14.
11. Herschtal A, Te Marvelde L, Mengersen K, Hosseinifard Z, Foroudi F, Devereux T, et al. Calculating radiotherapy margins based on Bayesian modelling of patient specific random errors. Phys Med Biol. 2015;60(5):1793-805.
12. van Herk M, Remeijer P, Rasch C, Lebesque JV. The probability of correct target dosage: dose-population histograms for deriving treatment margins in radiotherapy. Int J Radiat Oncol Biol Phys. 2000;47(4):1121-35.
13. Kothary N, Dieterich S, Louie JD, Chang DT, Hofmann LV, Sze DY. Percutaneous implantation of fiducial markers for imaging-guided radiation therapy. AJR Am J Roentgenol. 2009;192(4):1090-6.
14. van der Voort van Zyp NC, Hoogeman MS, van de Water S, Levendag PC, van der Holt B, Heijmen BJ, et al. Stability of markers used for real-time tumor tracking after percutaneous intrapulmonary placement. Int J Radiat Oncol Biol Phys. 2011;81(3):e75-81.
15. Nyholm T, Jonsson J, Soderstrom K, Bergstrom P, Carlberg A, Frykholm G, et al. Variability in prostate and seminal vesicle delineations defined on magnetic resonance images, a multi-observer, -center and -sequence study. Radiat Oncol. 2013;8:126.
16. van der Horst A, Wognum S, Davila Fajardo R, de Jong R, van Hooft JE, Fockens P, et al. Interfractional position variation of pancreatic tumors quantified using intratumoral fiducial markers and daily cone beam computed tomography. Int J Radiat Oncol Biol Phys. 2013;87(1):202-8.
17. Cury FL, Duclos M, Aprikian A, Patrocinio H, Souhami L. Prostate gland edema after single-fraction high-dose rate brachytherapy before external beam radiation therapy. Brachytherapy. 2010;9(3):208-12.
18. Tanyi JA, He T, Summers PA, Mburu RG, Kato CM, Rhodes SM, et al. Assessment of planning target volume margins for intensity-modulated radiotherapy of the prostate gland: role of daily inter- and intrafraction motion. Int J Radiat Oncol Biol Phys. 2010;78(5):1579-85.
19. Kupelian P, Willoughby T, Mahadevan A, Djemil T, Weinstein G, Jani S, et al. Multi-institutional clinical experience with the Calypso System in localization and continuous, real-time monitoring of the prostate gland during external radiotherapy. International Journal of Radiation Oncology*Biology*Physics. 2007;67(4):1088-98.
20. Smitsmans MH, Pos FJ, de Bois J, Heemsbergen WD, Sonke JJ, Lebesque JV, et al. The influence of a dietary protocol on cone beam CT-guided radiotherapy for prostate cancer patients. Int J Radiat Oncol Biol Phys. 2008;71(4):1279-86.
21. Lei S, Piel N, Oermann EK, Chen V, Ju AW, Dahal KN, et al. Six-Dimensional Correction of Intra-Fractional Prostate Motion with CyberKnife Stereotactic Body Radiation Therapy. Front Oncol. 2011;1:48.

22. Nichol AM, Brock KK, Lockwood GA, Moseley DJ, Rosewall T, Warde PR, et al. A magnetic resonance imaging study of prostate deformation relative to implanted gold fiducial markers. Int J Radiat Oncol Biol Phys. 2007;67(1):48-56.
23. King CR, Freeman D, Kaplan I, Fuller D, Bolzicco G, Collins S, et al. Stereotactic body radiotherapy for localized prostate cancer: pooled analysis from a multi-institutional consortium of prospective phase II trials. Radiother Oncol. 2013;109(2):217-21.
24. Dearnaley DP, Sydes MR, Graham JD, Aird EG, Bottomley D, Cowan RA, et al. Escalated-dose versus standard-dose conformal radiotherapy in prostate cancer: first results from the MRC RT01 randomised controlled trial. Lancet Oncol. 2007;8(6):475-87.
25. Van As N TA. International randomised study of laparoscopic prostatectomy vs SBRT and conventionally fractionated radiotherapy vs SBRT for early-stage organ-confined prostate cancer. NCRN trials database. 2014.
26. El-Shater Bosaily A, Parker C, Brown LC, Gabe R, Hindley RG, Kaplan R, et al. PROMIS — Prostate MR imaging study: A paired validating cohort study evaluating the role of multi-parametric MRI in men with clinical suspicion of prostate cancer(). Contemporary Clinical Trials. 2015;42:26-40.
27. Brenner DJ, Hall EJ. Fractionation and protraction for radiotherapy of prostate carcinoma. International Journal of Radiation Oncology • Biology • Physics.43(5):1095-101.
28. Høyer M, Thor M, Thörnqvist S, Søndergaard J, Lassen-Ramshad Y, Muren LP. Advances in radiotherapy: from 2D to 4D. Cancer Imaging. 2011;11(1A):S147-S52.

Appendices:

Appendix 5.1: Inter-fiducial distances for CyberKnife prostate cancer patients (Planning)

Patient	Fid 1 to 2 distance(mm)	Fid 1 to 3 distance(mm)	Fid 2 to 3 distance(mm)
1	23.2	26.9	23.4
2	27.6	21	27.8
3	17.9	24.1	20.4
4	27.6	24.9	29.5
5	18.3	21.1	21.4
6	20.8	16.3	20.3
7	25.1	30	28.1

Appendix 5.2: Inter-fiducial distances for CyberKnife prostate cancer patients (Treatment)

= fraction. SD = Standard Deviation. Fid 1/2 = Distance between fiducial 1 and fiducial 2.

Patient	#	Pre-CK inter-fiducial distance (mm)			Post-CK inter-fiducial distance (mm)			Mean (mm)	SD (mm)
		Fid 1/2	Fid 1/3	Fid 2/3	Fid 1/2	Fid 1/3	Fid 2/3		
1	1	22	26.1	22.6	23.2	26.8	23.4	24	1.8
	2	22.6	26.4	22.6	24	27.6	24.2	24.6	1.9
	3	23.4	27.7	23.9	24.1	27.8	24.2	25.2	1.8
	4	23.9	27.9	24	24.6	28.4	24.4	25.5	1.9
	5	24.2	28.2	24	24.4	28.5	23.9	25.5	2
2	1	26.6	21.2	26.6	27.1	21.1	26.4	24.8	2.6
	2	27.2	21.5	27.2	27.7	21.5	26.2	25.2	2.7
	3	27.5	21.8	27.4	28.3	21.9	27.7	25.8	2.8
	4	27.4	21.7	27.5	28.1	21.6	27.5	25.6	2.8
	5	27.7	21	27.1	27.9	20.8	26.9	25.2	3.1
3	1	19	24.6	20.3	19.2	24.6	21	21.5	2.3
	2	19	25.1	21.1	19	25.7	21.7	21.9	2.7
	3	18	24.8	20.8	17.8	24.6	21	21.2	2.8
	4	17.4	24.3	21.4	19.8	26.3	22.5	22	2.9
	5	17.2	23.2	20.7	17.4	24.8	23.1	21.1	2.9
4	1	27.1	25.4	26.8	26.8	26.2	28.4	26.8	0.9
	3	28.4	26.2	29.3	27.8	24.7	29	27.6	1.6
	5	29.6	30.3	27.6	27.4	30.1	30.6	29.3	1.3
5	1	18.5	21.7	21.6	18.1	21.2	21.7	20.5	1.6
	2	18.1	23.3	21.5	18.3	21.6	20.9	20.6	1.9
	3	18.7	22	22.5	18.9	21.6	22	21	1.5
	4	18.2	21.4	21.4	18.1	20.2	20.7	20	1.4
	5	18.6	20.9	21.7	18.4	21.5	21.9	20.5	1.5
6	1	21.1	16.1	20.2	20.9	16.6	19.7	19.1	2
	3	21.6	16.8	20.9	21.8	16.6	20.8	19.8	2.2
	4	21.7	16.8	20.9	20.2	16.5	20.9	19.5	2.1
	5	22.2	16.6	20.9	22	16	20.7	19.7	2.5
7	2	25.6	31.6	28.7	25.7	32.5	29.4	28.9	2.6
	4	27.1	32.4	29	27.2	32.4	29	29.5	2.2
Mean		22.7	23.7	23.8	22.9	23.8	24.1	23.5	2.2
SD		3.9	4.2	3	3.8	4.5	3.2	3.1	0.6

Appendix 5.3: Change in inter-fiducial distance: 1st fraction to final fraction

Patient	Inter-fiducial pair distance change (mm)			Mean	SD
	Fiducial 1/2	Fiducial 1/3	Fiducial 2/3		
1	2.2	2.1	1.4	1.9	0.4
2	1.1	-0.2	0.5	0.5	0.5
3	-1.8	-1.4	0.4	-0.9	1
4	2.5	4.9	0.8	2.7	1.7
5	0.1	-0.8	0.1	-0.2	0.4
6	1.1	0.5	0.7	0.8	0.2
7	1.5	0.8	0.3	0.9	0.5
Mean				0.8	0.7

Appendix 5.4: Change in inter-fiducial pair distance at Treatment (pre- to post-CK)

Patient	#	Fid 1 to 2 Change Pre- to Post-CK (mm)	Fid 1 to 3 Change Pre- to Post-CK (mm)	Fid 2 to 3 Change Pre- to Post-CK (mm)	Mean (mm)	SD (mm)
1	1	1.2	0.7	0.8	0.9	0.2
	2	1.4	1.2	1.6	1.4	0.2
	3	0.7	0.1	0.3	0.4	0.3
	4	0.7	0.5	0.4	0.5	0.1
	5	0.2	0.3	-0.1	0.1	0.2
2	1	0.5	-0.1	-0.2	0.1	0.3
	2	0.5	0	-1	-0.2	0.6
	3	0.8	0.1	0.3	0.4	0.3
	4	0.7	-0.1	0	0.2	0.4
	5	0.2	-0.2	-0.2	-0.1	0.2
3	1	0.2	0	0.7	0.3	0.3
	2	0	0.6	0.6	0.4	0.3
	3	-0.2	-0.2	0.2	-0.1	0.2
	4	2.4	2	1.1	1.8	0.5
	5	0.2	1.6	2.4	1.4	0.9
4	1	-0.3	0.8	1.6	0.7	0.8
	3	-0.6	-1.5	-0.3	-0.8	0.5
	5	-2.2	-0.2	3	0.2	2.1
5	1	-0.4	-0.5	0.1	-0.3	0.3
	2	0.2	-1.7	-0.6	-0.7	0.8
	3	0.2	-0.4	-0.5	-0.2	0.3
	4	-0.1	-1.2	-0.7	-0.7	0.5
	5	-0.2	0.6	0.2	0.2	0.3
6	1	-0.2	0.5	-0.5	-0.1	0.4
	3	0.2	-0.2	-0.1	0	0.2
	4	-1.5	-0.3	0	-0.6	0.7
	5	-0.2	-0.6	-0.2	-0.3	0.2
7	2	0.1	0.9	0.7	0.6	0.3
	4	0.1	0	0	0	0.1
				Mean	0.3	0.5

Appendix 5.5: Rigid Body Error (RBE) for CK prostate patients

Patient	#	Mean RBE	Min RBE	Max RBE
1	1	0.5	0.2	1.3
	2	0.6	0.4	0.8
	3	0.8	0.2	1
	4	1.2	0.6	1.6
	5	1.5	0.5	2.3
2	1	1.3	1.2	1.5
	2	0.6	0.4	0.9
	3	1	0.7	1.9
	4	0.7	0.6	0.8
	5	0.7	0.5	0.8
3	1	0.9	0.3	1.6
	2	1.4	0.5	1.7
	4	1.6	0.8	2.2
	5	1.9	0.8	2.6
4	1	1.1	0.6	1.5
	3	1.3	0.4	2.3
	5	2.5	1.8	2.8
5	1	0.6	0.3	0.8
	2	0.5	0.1	0.7
	3	0.8	0.4	1.1
	4	0.4	0.2	0.7
	5	0.5	0.1	0.8
6	1	0.4	0.2	0.8
	4	1.1	0.9	1.4
	5	1.3	1	1.5
7	2	1.5	0.7	2
	4	2.2	1.4	2.5
Mean		1.1	0.6	1.5
SD		0.5	0.4	0.6

CHAPTER 6

Optimising dose-fractionation in Stereotactic Body RadioTherapy (SBRT)

6.1 INTRODUCTION

Patients referred for SBRT have either primary tumours for treatment, recurrence within a previously treated area, or oligometastatic disease. Prescription dose and number of fractions are selected according to the radiosensitivity of the primary tumour, as well as the radiation sensitivity of the surrounding normal tissues. Other factors such as previous radiotherapy are also considered.

Chapter 1, Section 1.3.5 describes an introduction to dose-fractionation issues in SBRT, but these are discussed further here.

6.1.1 The concept of Oligometastasis

Localised primary cancer is usually treated with curative intent with local treatments such as surgery and/or radiotherapy often in combination with a systemic therapy component for the elimination of micrometastatic disease. In contrast, patients with distant metastasis are usually treated with palliative intent with systemic therapy such as chemotherapy or hormone treatment.

More recently, however, the existence of a status intermedius between widespread metastatic disease and local, organ-confined disease has been hypothesised, this state has been coined as "oligometastatic disease" (1). Local therapies have been trialled in this group of patients in recent years, in the hope that the oligometastases seen on scans (usually defined as <5 in number) are the only sites of disease. This would make the local treatment potentially curative, although long-term local control is a more realistic aim.

Alternatively, the Norton-Simon hypothesis suggests that reducing tumour burden by local treatment may increase the efficacy of subsequent systemic therapy (2).

Approximately 20% of patients with oligometastic disease treated with SBRT are progression-free at 2-3 years after SBRT (3).

6.1.2 The importance of Biologically Effective Dose (BED)

The radiation schedules used in SBRT cannot be directly compared with those used in conventional radiotherapy, as explained in Chapter 1, because the dose per fraction is different.

To compare the regimes, therefore, Biologically Effective Dose (BED) must be calculated according to the following formula, where D = Total Dose (Gy), d = dose per fraction (Gy), and α/β is a useful measure of how a tumour/tissue will respond to different doses/fraction (4).

A majority of tumours are assumed to have an α/β ratio of 10 (5).

$$BED = D\ x\ \left(1 + \frac{d}{\alpha/\beta}\right)$$

There is a large evidence base on the importance of BED for Stage 1 Non-Small cell lung cancer (NSCLC). Zhang et al (6) performed a meta-analysis on 2587 patients across 34 studies to evaluate the optimal BED for SBRT for Stage I NSCLC. The delivered BED was divided into quartiles ($83.2Gy_{10}$=Low, $83.2\text{-}106Gy_{10}$=Medium, $106\text{-}146Gy_{10}$=Medium-to-High, and $>146Gy_{10}$=High). There was a statistically significant Overall Survival benefit at 2 years for those receiving Medium to Medium-to-High BED regimes.

There is also limited evidence on the importance of BED in controlling oligometastatic disease. Stinauer et al analysed the importance of BED in controlling 30 patients with 53 metastases. The primary pathology was renal cell cancer and melanoma, metastatic sites included lung, liver and bone. BED was a significant predictor of in-field control, with BED>$100Gy_{10}$ having a greater control rate. Modelling studies predicted that at least 48Gy in 3 fractions (BED $125Gy_{10}$) would be needed to achieve >90% 2-year control (7).

6.1.3 Dose-fractionation in SBRT for primary pancreatic cancer

Approximately 40% of patients present with locally advanced, inoperable disease without clinically detectable metastases. The treatment strategy for these patients often involves systemic chemotherapy at the outset, as pancreatic cancer tends to metastasise early in the course of its disease, and the patient may have occult metastases (8).

Conformal radiotherapy may also be delivered to the primary disease for symptom palliation, and to prevent local disease progression from causing morbidity or death. Radiotherapy is often given concurrently with 5-fu or Capecitabine systemic therapy. However, disease control rates can be low (50% disease progression at 6 months) (9). An additional drawback is the number of daily treatments, typically 28 fractions over 5.5 weeks , in a disease where the median prognosis is 8 months. A typical regime of 50.4Gy in 28# over 5.5 weeks (1.8Gy/fraction) is associated with a BED of 59.5Gy_{10}, assuming an α/β ratio of 10 for tumour control.

SBRT technique has a number of potential technical advantages over conformal radiotherapy which have been discussed in this thesis. The short duration of treatment (typically 3-5 fractions) is also an attractive feature for these patients who either ultimately have a limited prognosis, or who benefit from a shorter period of interruption of chemotherapy to control micro-metastatic disease.

Chang et al (10) delivered a single fraction of 25Gy for patients with unresectable pancreatic cancer. The BED of this regime = 87.5Gy_{10}. Freedom from local progression (FFLP) rate at 1 year was 84%, but Overall Survival at 1 year was only 21%, and a quarter of patients had Grade ≥ 2 toxicity at 1 year.

Mahadevan et al delivered induction Gemcitabine and selected out those patients with no metastases after 2 cycles to receive SBRT. Dose delivered was 24-36Gy in 3 fractions (BED = 43.2-79.2Gy_{10}). Local control rate was 85% at median follow-up of 21 months, Median Progression-Free Survival (PFS) was 15 months, and median Overall Survival (OS) was 20 months in those receiving SBRT. Late Grade 3 toxicity was observed in 9% (11). The authors concluded that the extreme hypofractionation of the above SBRT regime allowed minimal interruption to systemic therapy, which improved the overall survival of patients.

Overall, there is scope for refinement of dose-fractionation in order to improve local control rates, while limiting toxicity, and improving overall survival.

6.1.4 Dose-fractionation in SBRT for Lymph Node oligometastases

Patients treated with SBRT for lymph node oligometastases are a heterogenous group. They comprise a range of primary cancers, and a range of metastatic sites (e.g. cervical, abdominal, pelvic, supraclavicular). Disease-Free Interval, number of lymph node metastases, and metastasis size, (all factors which are known to affect local control rates and prognosis) often vary, which makes it hard to draw conclusions on optimum dose fractionation (3).

Literature reported on SBRT case series comprising various primary cancers (Prostate, Cervix, Gastric, Breast, Colorectal, Renal cell) treating various lymph node sites (abdominal, para-aortic, pelvic,

mediastinal) to a variety of BEDs ($60Gy_{10}$ – $125Gy_{10}$) show Local Control rates of 67.4%-100% at a follow-up of 2-4 years. Toxicity is also important: Grade 3+ toxicity rates were 0-20% (12-15).

As before, there is scope for refinement of dose-fractionation in order to improve local control rates, while limiting the toxicity of SBRT.

6.1.5 Dose-fractionation for Oligometastatic breast cancer

Milano et al analysed the results from a large series of patients (n=121) with oligometastases (16). Those patients with breast cancer histology (n=39) were evaluated separately, as this histology confers a better prognosis than other primary tumours. For breast cancer patients the 6-year local control rate was 87%. Freedom from Distant Metastasis rate was 36% at 6-years, indicating that some treated patients truly had oligometastatic disease (rather than radiologically-occult widespread metastases). BED was not specifically evaluated in this study, but 72% of non-brain metastases were treated with 50Gy in 10#, a BED of $75Gy_{10}$.

6.2 AIMS

To assess the effects of SBRT on tumour control and normal tissue toxicity, by comparing radiobiological calculations and RBE with clinical outcome. Three clinical models were chosen:

1. A radiobiological comparison between SBRT regimes delivered for the treatment of primary pancreatic cancer, and conventional radiotherapy schedules was performed.

2. The outcomes of SBRT treatment to lymph node oligometastases according to delivered BED were evaluated.

3. The outcomes of SBRT to oligometastatic breast cancer according to delivered BED were evaluated.

6.3 MATERIALS AND METHODS

6.3.1 SBRT vs Conventionally-fractionated radiotherapy for primary pancreatic cancer

42 patients with localised but inoperable pancreatic cancer were treated with 3-fraction SBRT on the CyberKnife platform at the author's centre. To give context to the radiobiological comparison (Aim 1) it is important to also evaluate outcome data (toxicity and disease control).

6.3.1A: Treatment planning and delivery: SBRT pancreatic cancer

The pancreas moves with respiration and bowel filling, as described in Chapter 3, therefore SBRT treatment to the pancreas is best tracked with implanted fiducials and the Synchrony system.

Approximately 1 week after fiducial placement, patients underwent a Planning CT scan. Patients were scanned supine in a patient-specific Vac-Bag immobilisation device for supporting the arms and upper torso, with knee and ankle supports as needed. Patients were advised to drink 300mls of cold water 30 minutes before the scan for duodenal filling. A non-contrast CT scan was performed, a Contrast CT scan was also performed to aid target definition in all patients. A PET scan was performed if it would aid localisation.

Gross disease (GTV) was outlined and expanded to PTV by adding a margin of 2-3 mm. Treatment was planned on the non-Contrast CT scan. Treatment was prescribed to 18-36Gy in 3#. Dose-fractionation was decided according to Clinician preference, and according to the proximity of dose-limiting Organs At Risk, and any prior Radiotherapy. The prescription isodose line was chosen to provide optimum coverage of the PTV. Treatment was delivered on consecutive days.

The patients drank 300mls of water prior to treatment to re-create the conditions on the Day of the Planning CT scans. Patients had a CT scan performed on Treatment Day 1 to check for fiducial stability prior to treatment, as described in Chapter 3. This scan was a non-contrast scan with the patient in the treatment position, taken in mid-breath hold.

Patients were given prophylactic anti-sickness medication (Ondansetron 4mg bd and Maxalon 10mg tds prn) unless contra-indicated.

Treatment planning and delivery parameters were recorded for all patients. This included prescription dose, number of fractions, prescription isodose, minimum and maximum dose to PTV, coverage and PTV size.

6.3.1B: Outcome data: SBRT pancreatic cancer

Toxicity and outcome data were prospectively collected. Patients were clinically reviewed 3 months after treatment, then at 3 or 6 monthly intervals thereafter, when post-treatment CT scans were acquired. Toxicity was assessed using CTCAEv4 criteria, and local failure was determined by the reporting radiologist and treating physician.

6.3.1C: Radiobiology: SBRT pancreatic cancer

Radiobiology calculations were performed for the 42 patients treated by SBRT. These were compared to calculations performed on a comparator external beam radiotherapy regime (50.4Gy/28#/5.5 weeks).

Radiobiology calculations were performed under the supervision and guidance of Roger Dale. The methodology for the calculations is explained here.

Pancreatic tumours are fast-growing. Volume Doubling Time (VDT) of pancreatic cancer has been shown to be 6 weeks. This is faster than the VDT of head and neck tumours (VDT = 8 weeks) (17).

Tumour cell repopulation is known to occur during a course of radiotherapy, and this is a factor that limits tumour control. It is therefore important to consider this factor when calculating the potency of a given radiotherapy regime.

The maximum repopulation correction factor (k value) was assumed to be 0.5Gy/day. This is the biological dose per day required to compensate for ongoing tumour cell repopulation. This was incorporated into BED calculations using the formula proposed by Dale et al (18) with the following justification by Roger Dale.

"It is assumed that the k value for pancreatic cancer is the same as that for Head and Neck tumours, i.e. k = 0.9Gy/day. In Squamous Cell Cancers of the Head and Neck the delay time before significant repopulation begins is ~28 days, but there is very little documentation about delay times for other tumour types. I have therefore assumed that the repopulation factor for the fastest-growing pancreatic cancers is an average of 0.5Gy/day over the entire duration of treatment."

Formula for BED, taking into account tumour repopulation:

$$BED = Total\ dose \times \left[1 + \frac{d}{\alpha/\beta}\right] - (k \times T)$$

Where T = overall treatment time in days.

This formula was used to calculate BED for the conventionally fractionated comparator, as well as the SBRT regimes delivered by CyberKnife at the author's centre. To allow fair comparison the formula above was also used to calculate the BED of alternative SBRT regimes described in the Discussion.

6.3.2 SBRT Dose-Fractionation for Lymph Node oligometastases

38 patients with unresectable lymph node metastases were studied. The patients were treated at the author's centre between 2009 and 2012.

6.3.2A: Treatment planning and delivery: Lymph Node oligometastases

Treatment technique varied according to the site of the lymph node target to be treated. Thoracic and upper abdominal lymph nodes move with respiration, and therefore these were tracked with implanted fiducials and the Synchrony system. Other nodes were tracked with X-Sight spine tracking, or fixed fiducial tracking.

For those patients with implanted fiducials, a planning CT scan was performed 1 week after fiducial placement. Patients were scanned supine in a patient-specific Vac-Bag immobilisation device. A non-contrast CT scan was performed. Contrast CT, PET and MRI scans was also performed if this would aid target definition, or definition of adjacent Organs At Risk. X-Sight Spine patients were planned on a non-contrast CT scan acquired in immobilisation with secondary scans performed as appropriate.

The target node(s) was outlined as Clinical Target Volume (CTV) and expanded to PTV by adding a margin of 0-5 mm. Treatment was planned on the non-Contrast CT scan. Treatment was prescribed to 18Gy in 1#, 24-36Gy in 3#, or 35-47Gy in 5#. Dose-fractionation was decided according to Clinician preference, and according to the proximity of dose-limiting Organs At Risk, and any prior Radiotherapy. The prescription isodose line was chosen to provide optimum coverage of the PTV. Treatment was delivered on consecutive days.

Patients that were to be tracked with fiducials/Synchrony had a CT scan performed on Treatment Day 1 to check for fiducial stability prior to treatment, as described in Chapter 3. This scan was a non-contrast scan with the patient in the treatment position, taken in mid-breath hold.

Supportive medication was prescribed to patients as appropriate.

Patient demographics, histopathology, prior treatment details and target details were recorded. Treatment planning and delivery parameters were also recorded. These included prescription dose, number of fractions, prescription isodose, PTV size, CTV-to-PTV margin, conformality and coverage.

BED was calculated according to the more commonly used equation (4):

$$BED = D\ x\ \left(1 + \frac{d}{\alpha/\beta}\right)$$

6.3.2B: Outcome data: Lymph Node oligometastases

Toxicity and disease control data were prospectively collected. Patients were clinically reviewed 3 months after treatment, then at 3 or 6 monthly intervals thereafter, when post-treatment CT scans were acquired. Toxicity was assessed using CTCAEv4 criteria, and local failure was determined by the reporting radiologist and treating physician.

6.3.2C: Statistical analysis: Lymph Node oligometastases

Local control was analysed according to BED as per Aim 2. A Weibull test with Gamma fragility was performed to analyse Progression Free Survival (PFS) by Histopathology, adjusted for BED. This test was performed with SPSS statistical software by Paul Seed, medical statistician, St. Thomas' hospital, London.

6.3.3 Dose-Fractionation for Oligometastatic breast cancer

57 patients with unresectable oligometastatic breast cancer were studied.

6.3.3A: Treatment planning and delivery: Oligometastatic breast cancer

Treatment technique varied according to the site of the oligometastasis to be treated. Targets that move with respiration were tracked with implanted fiducials and the Synchrony system. Other targets were tracked with X-Sight spine tracking, fixed fiducial tracking, or 6D Skull tracking as appropriate.

For those patients with implanted fiducials, a planning CT scan was performed 1 week after fiducial placement. Patients were scanned supine in a patient-specific Vac-Bag immobilisation device. A non-contrast CT scan was performed. Contrast CT, PET and MRI scans were also performed if they would aid target definition, or definition of adjacent Organs At Risk. X-Sight Spine and 6D Skull patients

were planned on a non-contrast CT scan acquired in immobilisation with secondary scans performed as appropriate.

The target(s) was outlined as GTV or CTV, and expanded to PTV by adding a margin of 0-5.1 mm. Treatment was planned on the non-Contrast CT scan. Treatment was prescribed to 12-48Gy in 1-5 fractions. Dose-fractionation was decided according to Clinician preference, and according to the proximity of dose-limiting Organs At Risk, and any prior Radiotherapy. The prescription isodose line was chosen to provide optimum coverage of the PTV. Treatment was delivered on consecutive days.

Patients that were to be tracked with fiducials/Synchrony had a CT scan performed on Treatment Day 1 to check for fiducial stability prior to treatment, as described in Chapter 3. This scan was a non-contrast scan with the patient in the treatment position, taken in mid-breath hold.

Supportive medication was prescribed to patients as appropriate.

Patient demographics, prior treatment details and target details were recorded. Treatment planning and delivery parameters were also recorded. These included prescription dose, number of fractions, prescription isodose, PTV volume, and GTV-to-PTV margin.

BED was calculated according to the formula below (4):

$$BED = D\ x\ \left(1 + \frac{d}{\alpha/\beta}\right)$$

6.3.3B: Outcome data: Oligometastatic breast cancer

Toxicity and disease control data were prospectively collected. Patients were clinically reviewed 3 months after treatment, then at 3 or 6 monthly intervals thereafter, when post-treatment CT scans were acquired. Toxicity was assessed using CTCAEv4 criteria, and local failure was determined by the reporting radiologist and treating physician.

6.3.3C: Statistical analysis: Oligometastatic breast cancer

Local control was analysed according to BED as per the Aim. Local Progression-free survival Kaplan-Meier curves were constructed in SPSS by Mel Green, medical statistician.

6.4 RESULTS

6.4.1 SBRT vs Conventionally-fractionated radiotherapy for primary pancreatic cancer

6.4.1A: Treatment planning and delivery: SBRT primary pancreatic cancer

The majority of pancreatic tumours in the 42 patients treated were locally advanced (90%) with T3/T4 staging. A majority of tumours (90%) were located at the pancreatic head. The patients were largely pre-treated, some patients had received multiple-modality treatment prior to CK. 77% had received prior chemotherapy, 23% prior radiotherapy and 21% prior surgery. All patients had an imaging-defined macroscopic target (i.e. none were treated adjuvantly).

Treatment planning and delivery variables are displayed in Table 6.1.

Table 6.1: Dosimetric variables for patients with primary pancreatic cancer treated by SBRT

Factor		
Number of fiducials	1	N = 8 (19%)
	2	N = 6 (14%)
	≥ 3	N = 28 (67%)
PTV (cc)	Median (range)	69.2cc (15.8-193.6)
	Mean (SD)	75.1cc (41.7)
Prescription dose (Gy)	Median (range)	27Gy (18-36)
	Mean (SD)	27Gy (29)
Number of fractions	3#	N=42 (100%)
BED	Median	$49.5Gy_{10}$ (27.3-77.7)
	Mean	$48.6Gy_{10}$
Prescription isodose (%)	Median (range)	67% (53-82)
	Mean (SD)	67% (7)
Coverage (%)	Median (range)	97.6% (80-99.5)
	Mean (SD)	96.6% (3.5)

The PTV volumes varied widely (15.8cc-193.6cc) which would be likely to have a bearing on both toxicity and local control. The patients studied were all treated with a 3-fraction regime, to a range of prescription doses, which will be discussed further in the section on Radiobiology (Section 6.4.1D).

6.4.1B: Outcome data: Toxicity: SBRT primary pancreatic cancer

Outcomes for Acute and Late toxicity are displayed in Table 6.2. Data is available for 40 and 32 patients respectively. Some data is missing due to incomplete follow-up information from treating/referring Physician. Mel Green (medical statistician) performed full statistical analysis to see if any Patient/Treatment/Delivery factors were related to Toxicity on Univariate or Multivariate analysis but there was no factor that reached statistical significance (p values 0.084-0.875 for acute toxicity and p values 0.212-0.991 for late toxicity) .

Table 6.2: Acute/Late toxicity data: primary pancreatic cancer treated by SBRT

Acute Toxicity (≤ 3months post-treatment)			
None	N=10 (25%)		
	Grade 1-2	Grade 3	Grade 4
Diarrhoea	N=6 (15%)	0	0
Nausea	N=8 (20%)	0	0
Vomiting	N=2 (5%)	0	0
Dyspepsia	N=2 (5%)	0	0
Anorexia	N=2 (5%)	0	0
Pain	N=7 (18%)	N=1 (2.5%)	0
Fatigue	N=10 (25%)	0	0
Jaundice	N=1 (2.5%)	N=1 (2.5%)	0
Late Toxicity (> 3months post-treatment)			
None	N=27 (84%)		
	Grade 1-2	Grade 3	Grade 4
Pain	N=1 (3%)	0	0
Nausea	N=1 (3%)	0	0
Bleeding	N=1 (3%)	0	0
Duodenal	0	0	N=2 (6%)

Note: sometimes a patient will experience more than one toxicity symptom so the percentages of acute/late toxicity do not add up to 100%.

In terms of acute toxicity, the most common all grade toxicities were fatigue (25%), nausea (20%) and abdominal pain (18%). The most severe toxicity experienced was G3 abdominal pain, experienced by one patient and managed with analgesia. A further patient developed G3 jaundice but went on to die of metastatic pancreatic cancer 4 months after development of this symptom, therefore the cause of jaundice may have been disease progression.

In terms of late toxicity, one patient had grade 2 nausea and pain 1-year post-CK. It was notable that the patient was of poor performance status pre-treatment (she was considered too frail for chemotherapy). A further patient who was taking Diclofenac had a duodenal haemorrhage 4 months after CK. The patient was transfused, the Diclofenac was stopped and he was started on a proton-pump inhibitor.

A further 2 patients had G4 duodenal strictures as late toxicity. The dosimetry vs late toxicity of the patients described will be discussed in the Discussion.

6.4.1C: Outcome data: Disease control: SBRT primary pancreatic cancer

Graph 6.1 shows Kaplan-Meier and log-rank survival analysis with respect to Freedom-from-local progression (FFLP) for 42 patients treated with SBRT for primary pancreatic cancer. The actuarial FFLP rate at 1-year was 44%.

Graph 6.1:

Freedom-from-local-progression for patients treated with SBRT for pancreatic cancer

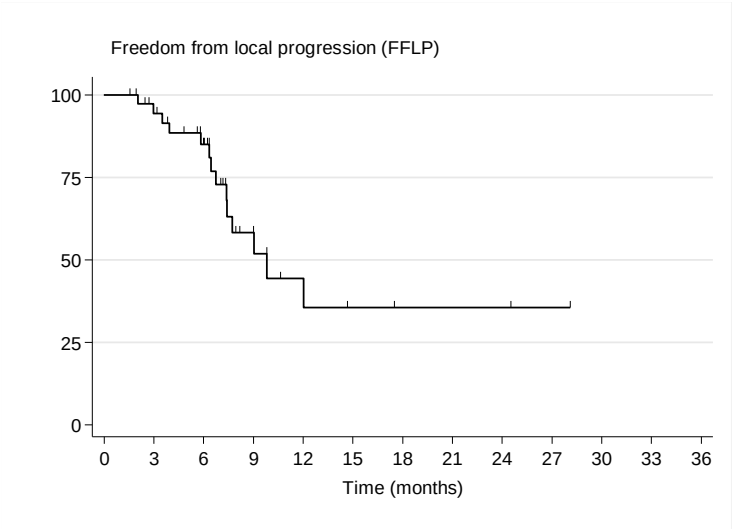

As discussed in the Introduction, pancreatic cancer is a disease which metastasises frequently, and early in the course of disease (8). It is therefore important to consider progression-free survival (PFS), which incorporates distant progression as well as local progression.

The Kaplan-Meier curve for progression-free survival (PFS) is shown in Graph 6.2.

The actuarial PFS at 1 year is 23%.

Comparing the FFLP curve (Graph 6.1) with the PFS curve (Graph 6.2) shows that more patients progressed with metastatic disease earlier than those that progressed with local disease.

Graph 6.2:

Progression-free survival (PFS) for patients treated with SBRT for pancreatic cancer

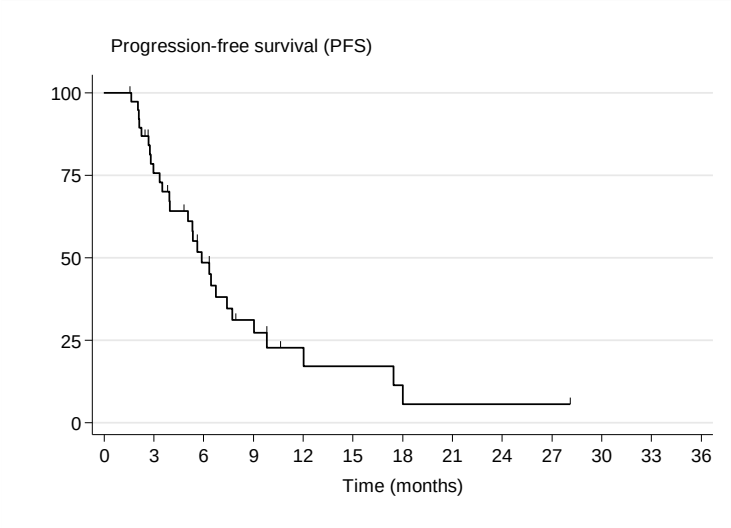

Finally it is important to consider Overall Survival.

Graph 6.3 shows the Overall Survival curve for the 42 patients treated with SBRT to primary pancreatic cancer. Overall survival at 1-year was 40%, with a Median Survival of 8.4 months.

Graph 6.3:

Overall Survival (OS) for patients treated with SBRT for pancreatic cancer

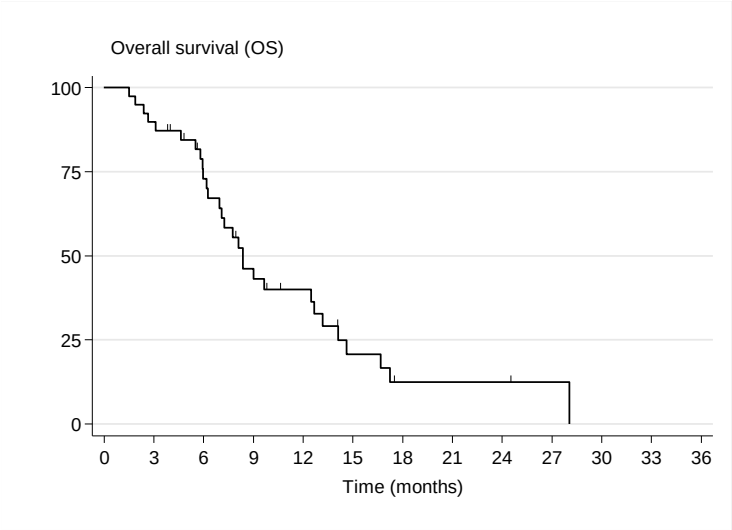

The above Outcome data will be fully discussed in the Discussion.

6.4.1D: Radiobiology: primary pancreatic cancer

Aim 1 was to perform a radiobiological comparison between SBRT regimes delivered for the treatment of primary pancreatic cancer, and conventional radiotherapy schedules. Radiobiological comparison needs to consider both tumour control and normal tissue toxicity.

Tumour control calculations:

Tumour α/β values tend to be related to growth rate, i.e. faster-growing tumours have high α/β ratios. As pancreatic cancer is fast-growing (17) a generic α/β value of 10Gy is assumed in these calculations.

Taking a Conventionally-fractionated external beam radiotherapy regime of 50.4Gy/28#/5.5weeks (9). For the purpose of this discussion this is considered the "Reference" radiotherapy schedule.

Formula for BED calculation, taking into account tumour repopulation:

$$BED = \left(Total\ dose \times \left[1 + \frac{d}{\alpha/\beta}\right]\right) - (k \times T)$$

Where k= maximum repopulation correction factor (units=Gy/day), d= dose per fraction (units = Gy) and T = overall treatment time (units = days).

k = 0.5Gy/day (justification as per Section 6.3.1C). T = 38 days.

BED = 40.5Gy_{10} (Reference: Tumour control)

Assuming that the Linear Quadratic model is valid for all potential fraction sizes, and back-converting from BED = 40.5$Gy_{10,}$ the 3-fraction CyberKnife tumour equivalents to the reference schedule is:

3 fractions of 7.85Gy = Total dose = 23.55Gy (CK: Tumour control)

(A fixed repopulation of 3 x 0.5Gy =1.5Gy was assumed in calculating the equivalent CK schedule).

Assuming that Conventionally-fractionated external beam radiotherapy treatments are planned according to ICRU guidelines (19), then all doses within the PTV should be in the range of 95-107% of prescribed dose. The minimum tumour dose is known to be the most significant determinant of local control, therefore re-calculating the Reference schedule taking into account the minimum dose to PTV: 47.88Gy/28#/5.5weeks:

Minimum BED = 37.1Gy_{10} (Reference)

Back-converting from BED as before, and assuming a 1.5Gy allowance for repopulation as before, the equivalent CK 3-fraction minimum dose equivalents is:

3 fractions of 7.4Gy = Total dose = 22.2Gy (CK minimum dose equivalent: Tumour control)

The CK planning system, MultiPlan, reports minimum total dose to the PTV. The range of minimum total dose to the PTV for the 42 CK patients studied here = 11.1Gy-34.5Gy. Among these 42 patients, 22 patients (52%) received minimum PTV total doses which were equal to, or greater than, 22.2Gy (i.e. the CK minimum dose equivalent to the Reference schedule). The other 20 patients (48%) received minimum PTV total doses which were, in radiobiological terms, less potent than those delivered by the Reference schedule (this suggests there would be scope to dose escalate if Normal tissue doses allow).

Normal tissue calculations:

When calculating BEDs to normal tissue in the upper gastro-intestinal tract, an α/β ratio of 3Gy is generally used. (Duodenum, Stomach and Small Bowel are the dose-limiting OARs when delivering radiotherapy to pancreatic tumours). In contrast to the considerations for tumour control, it is not the minimum dose that is relevant, but the higher delivered doses.

Calculations assume that some normal tissue volumes receive 100% of prescription dose. This is a reasonable assumption as tumours in the pancreatic head lie adjacent to the Duodenum, and once the tumour volume is expanded by a planning margin the PTV invariably overlaps Duodenum. Doses>100% of prescribed dose are not considered as treatment planning should not produce plans with a hot spot in normal tissue. BED is calculated according to the formula below, k value is not relevant in this situation, as the calculation is considering normal tissue (not tumour) response to radiotherapy. D =Total dose (Gy). D= Dose per fraction (Gy).

$$BED = D\ x\ \left(1 + \frac{d}{\alpha/\beta}\right)$$

Reference schedule (50.4Gy/28#/5.5w): = BED 80.6Gy_3 (Reference: Normal tissues)

Taking the minimum dose equivalent CK regime for tumour control calculated above (of 3 x 7.4Gy = Total dose 22.2Gy):

BED = 77Gy_3 (CyberKnife : Normal tissues)

Overall, this suggests that there is scope to dose escalate.

The calculations are summarised in Table 6.3.

The implications of the above calculations, and the recommendations for treatment planning for primary pancreatic cases treated by CyberKnife are discussed in the Discussion.

Table 6.3: BED summary for Reference Schedule vs SBRT (CK) for pancreatic cancer

Schedule	Total Dose (D) (Gy)	Fraction dose (d) (Gy)	Fraction number (n)	Treatment time (T) (days)	$BEDGy_{10}$ (Tumour Control)	$BEDGy_3$ (Normal tissues)
Reference (prescribed)	50.4	1.8	28	38	**40.5**	80.6
CK (equivalent to Ref for Tumour Control)	23.55	7.85	3	3	**40.5**	N/A
Reference (minimum PTV dose :Tumour control)	47.88	1.71	28	38	**37.1**	N/A
CK (equivalent to minimum of Ref :Tumour Control)	22.2	7.4	3	3	**37.1**	77

6.4.2 SBRT Dose-Fractionation for Lymph Node oligometastases

6.4.2A: Treatment planning and delivery: SBRT lymph node oligometastases

The 38 patients studied were largely pre-treated: 30 patients (78%) had previously received chemotherapy as treatment for their oligometastatic disease, and 14 patients (38%) had received prior radiotherapy to the target nodal sites. The patients had a median disease-free interval of 19 months (Range 5-106 months).

41 lymph node sites were treated (Range = 1-3 sites per patient). The anatomical distribution of the sites were as follows:

Neck 3 (7%), Thorax 14 (34.5%), Abdomen 14 (34.5%) and Pelvis 10 (24%).

The histopathology of the primary is shown in Table 6.4.

Table 6.4: Histopathology of primary tumour: Lymph node oligometastases

Histopathology	Number of patients (n)	Percentage (%)
Colorectal	12	31.5
Breast	8	21
Urological	6	16
Lung	4	10.5
Gynae	4	10.5
Other/Unknown 1^0	4	10.5
Total	38	100

Radiotherapy technique was described in Section 6.3.2. Treatment and delivery parameters are displayed in Table 6.5. BED was calculated according to the formula below:

$$BED = D\ x\ \left(1 + \frac{d}{\alpha/\beta}\right)$$

Table 6.5 Treatment and delivery parameters: Lymph node oligometastases

Parameter		
PTV volume (cc)	Median = 65cc	Range: 1.2 – 126.1cc
CTV-PTV margin (mm)	Median = 2mm	Range: 0 – 5mm
Dose-Fractionation	18Gy/1#	BED = 50.4Gy_{10}
	24-36Gy/3#	BED = 43 - 79Gy_{10}
	35-47Gy/5#	BED = 60 - 91Gy_{10}
BED	Median 59.5Gy_{10}	Range: 43Gy_{10} – 91Gy_{10}
	Mean 57Gy_{10}	
Prescription isodose line (%)	Median = 66%	Range: 48 – 78%
Conformality index (nCI)	Median = 1.2	Range: 1.06 – 1.65
Coverage (%)	Median 98.1%	Range: 96.7 - 99.9%

There was a wide range of PTV volumes treated, which would be expected to be reflected in toxicity and local control outcomes.

The BED of the SBRT regimes delivered ranged from 43 – 91Gy_{10}. The most commonly prescribed regimes were 24Gy/3# (BED = 43.2Gy_{10}) (13 patients, 34%) and 30Gy/3# (BED = 60Gy_{10}) (10 patients, 26%). The planned SBRT treatments had a high degree of conformality, and there was excellent coverage of the PTV with the prescribed dose.

6.4.2B: Outcome data: SBRT lymph node oligometastases

Outcome data was assessed at a Median follow-up of 15 months.

Acute Toxicity

The majority of patients (23 patients, 61%) had no acute side-effects following SBRT. 13 patients (34%) had Grade 1-2 acute reactions, largely grade 1 fatigue. A single patient had a Grade 3 acute toxicity reaction: this was pain escalation in a patient that was a disease progressor. The patient was managed with analgesia.

Late Toxicity

There were 2 cases of Grade 3 late toxicity (5%). Both patients had received prior radiotherapy to the target nodal site.

One patient experienced Grade 3 pneumonitis following SBRT to a large Internal Mammary Chain nodal mass (PTV = 126 cc). The pneumonitis resolved with steroid therapy.

A further patient experienced Grade 3 oedema (lower limb oedema) following SBRT to left inguinal lymph nodes. The patient had pre-existing oedema, and notably she was a disease progressor.

Local Control (LC):

The local control rate was 88%. There was in-field disease progression in 5 irradiated sites (5/41 nodal sites, 12%).

Progression-Free Survival (PFS):

Median PFS = 11 months, PFS at 1 year = 48%. Therefore, as for outcomes in primary pancreatic cancer, distant progression occurred earlier than local progression.

Overall Survival (OS):

Overall Survival at 1 year = 91%.

Aim 2 was to evaluate outcomes of SBRT to lymph node oligometastases according to delivered BED.

6.4.2C: Statistical analysis: SBRT lymph node oligometastases

BED vs Local Control:

The calculated BED (y axis) was compared to Local Control (x axis) in the dot-plot below. Each dot represents a patient. BED was calculated as described above assuming an α/β ratio of 10 for tumour control.

Dot Plot 1: BED vs Local progression status for SBRT to Lymph node oligometastasis

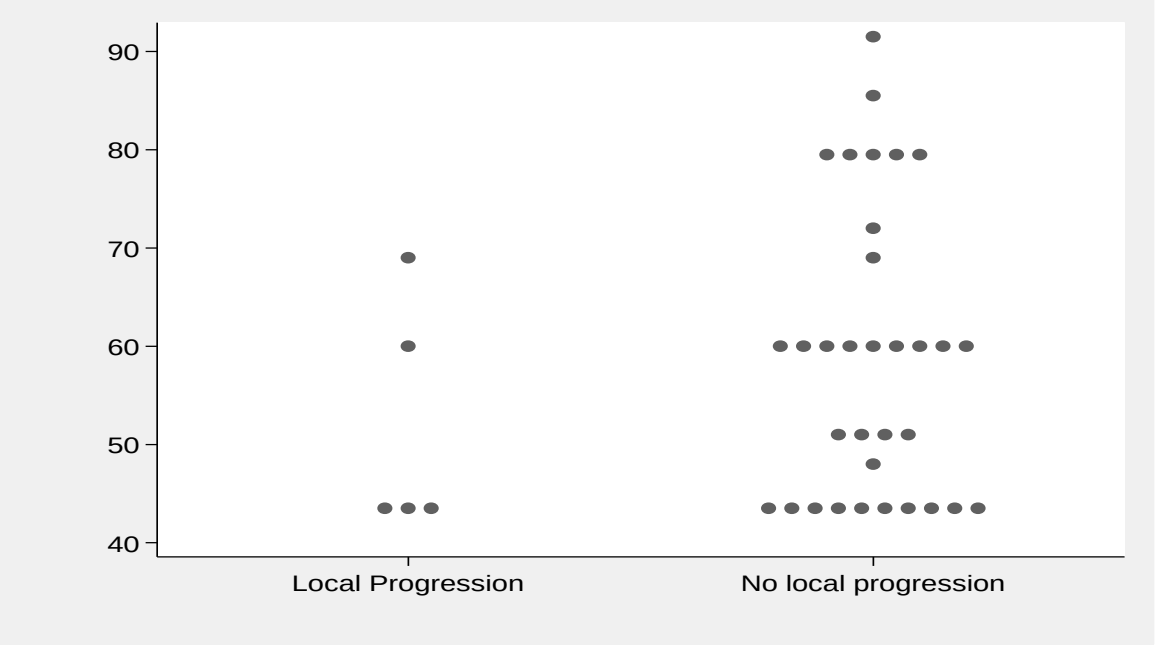

The dot-plot illustrates that the regime with the lowest BED (24Gy/3#, BED=43.2Gy_{10}) was associated with the highest risk of local progression.

Importantly, it can be seen that when patients were treated to a threshold BED of ≥ 72Gy_{10}, the local control rate was 100%. This equates to a prescribed dose of ≥ 36Gy/3# or ≥ 40Gy in 5#.

Histopathology vs PFS:

The radiation response of a tumour is known to vary according to its histopathology. Each primary tumour has an intrinsic Radiosensitivity (20). In addition, the biology of a tumour (e.g. the propensity to metastasis) varies according to the histopathology. Given the wide range of Histopathology in the sample of patients studied here, it was interesting to compare PFS by Histopathology. The importance of BED has been illustrated above, so the patients were stratified according to BED.

Graph 6.4 shows PFS for 5 histopathological categories of tumours, adjusted for BED.

Graph 6.4: PFS by Histopathology, adjusted for BED: lymph node oligometastases

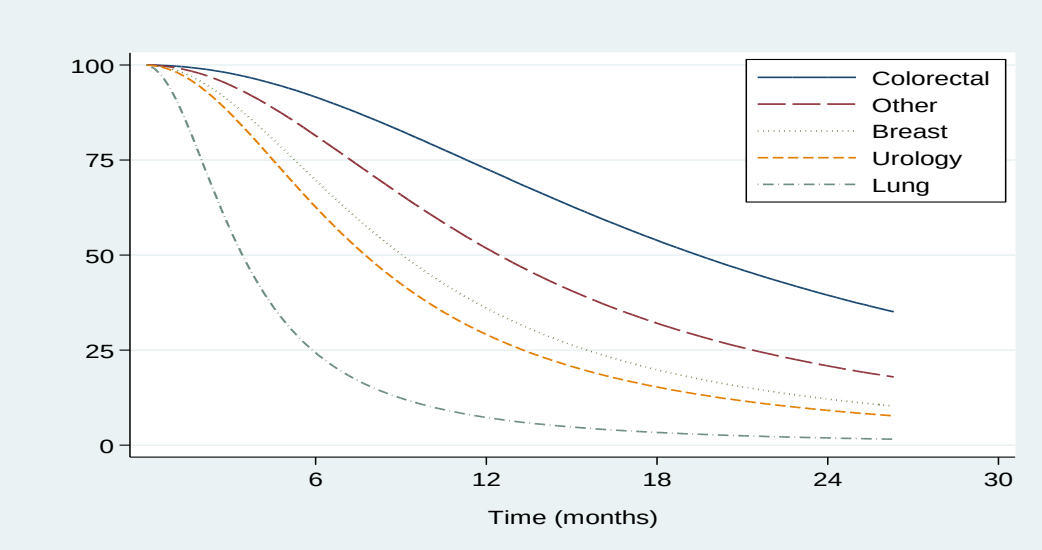

Graph 6.4 shows that in the sample of patients studied, the colorectal cancer patients had the most favourable PFS, the Median PFS for the Colorectal cancer histopathology group was 22 months.

The lung cancer group had the least favourable PFS, with a median PFS of just over 3 months.

6.4.3 Dose-Fractionation for Oligometastatic breast cancer

6.4.3A: Treatment planning and delivery: Oligometastatic breast cancer

57 patients received radiotherapy delivered with stereotactic technique to 84 unresectable oligometastases at the author's centre between May 2009 and March 2014. 42 patients (74%) had a solitary site of oligometastatic disease.

Chart 6.1 shows the distribution of oligometastases by anatomical site.

The most commonly treated anatomical site of metastasis was the brain, accounting for 41% of metastases. Spinal, lymph node, and non-spinal bone metastases made up a further 56% of the metastases.

Chart 6.1: Distribution of metastases by anatomical site: Oligometastatic breast cancer

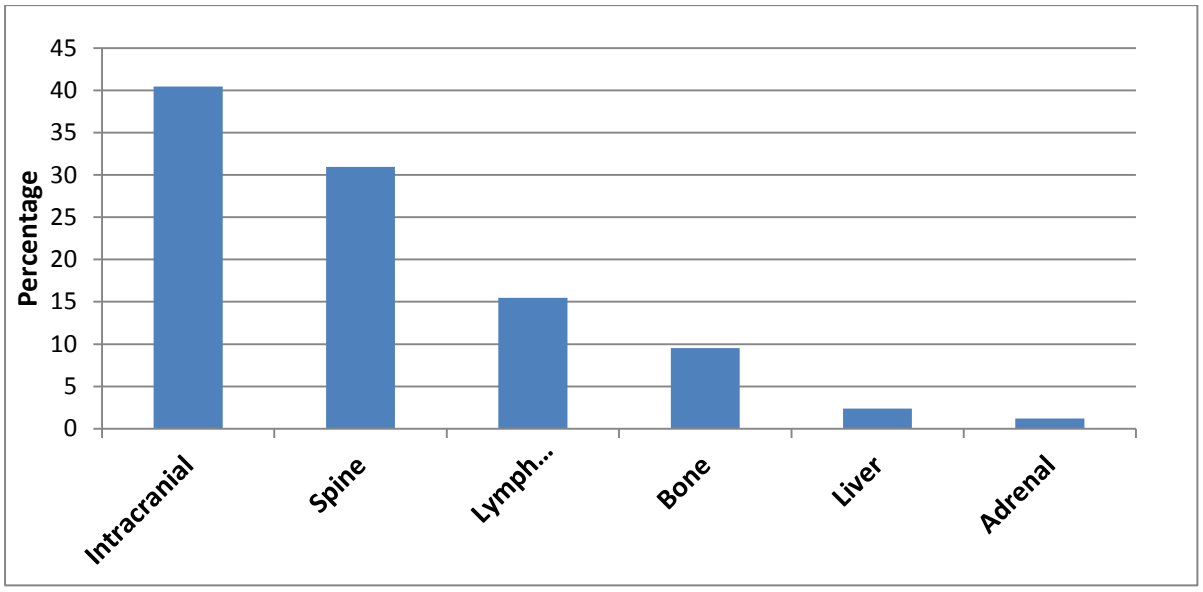

The treatment planning and delivery parameters are displayed in Table 6.6. BED was calculated as per the formula below. α/β = 10 for tumour control.

$$BED = D\ x\ \left(1 + \frac{d}{\alpha/\beta}\right)$$

Table 6.6: Treatment and delivery parameters: Oligometastatic breast cancer

Parameter		
PTV volume (cc)	Median (range)	11.4 (0.2-126.1)
GTV-PTV margin (mm)	Median (range)	2 (0-5.1)
Prescription dose (Gy)	Median (range)	26 (12-48)
Fraction number (n)	Median (range)	3 (1-5)
Dose per fraction (Gy)	Median (range)	9 (4-20)
Prescription isodose line (%)	Median (range)	61 (48-80)
BED (Gy_{10})	Median (range)	51.3 (16.8-124.8)

There was a wide range of PTV volumes treated, which would be expected to be reflected in toxicity and local control outcomes.

The BED of the regimes delivered ranged from 16.8 – 124.8Gy_{10}. The most commonly prescribed regimes were 30Gy/3# (BED = 60Gy_{10}) (16 metastases, 19%) and 24Gy/3# (BED = 43.2Gy_{10}) and 27Gy/3# (BED = 51.3Gy_{10}) both 14 metastases (17%).

6.4.3B: Outcome data: oligometastatic breast cancer

Outcome data was assessed at a Median follow-up of 13 months. Toxicity and local control was analysed per oligometastatic lesion. Overall survival was analysed per patient.

Acute Toxicity

Outcomes are shown in Table 6.7.

Table 6.7: Acute toxicity following stereotactic radiotherapy: Oligometastatic breast cancer

Toxicity grade (CTCAE v4.0)	None	Grade 1-2	Grade 3	No data
Toxicity incidence (%)	71.5	19	1.2	8.3

The vast majority of oligometastatic sites (71.5%) were treated without any acute toxicity. There were no cases of Grade 4 toxicity. The single case of Grade 3 toxicity was an incidence of skin ulceration following a high skin dose in a superficial bony target treated to BED112.5Gy_{10}.

Late Toxicity

Outcomes are shown in Table 6.8.

Table 6.8: Late toxicity following stereotactic radiotherapy: Oligometastatic breast cancer

Toxicity grade (CTCAE v4.0)	None	Grade 1-2	Grade 3	No data
Toxicity incidence (%)	83.3	2.4	4.8	9.5

The vast majority of oligometastatic sites (83.3%) were treated without any late toxicity.

There were no cases of Grade 4 toxicity. The Grade 3 acute skin reaction persisted after 3 months so was also counted as a late reaction. It subsequently healed. There were 2 cases of Grade 3 pain, and a single case of radionecrosis in an intra-cranial target.

Local Progression-Free Survival (Local PFS):

This is displayed in the Kaplan-Meier survival curve below.

It was noted on reviewing the outcomes that there was an increased incidence of local recurrence in the patients receiving stereotactic radiotherapy to intracranial metastases, therefore the Intracranial vs Body survival curves were compared.

Graph 6.5: Local PFS: Intracranial vs Body site: Oligometastatic breast cancer

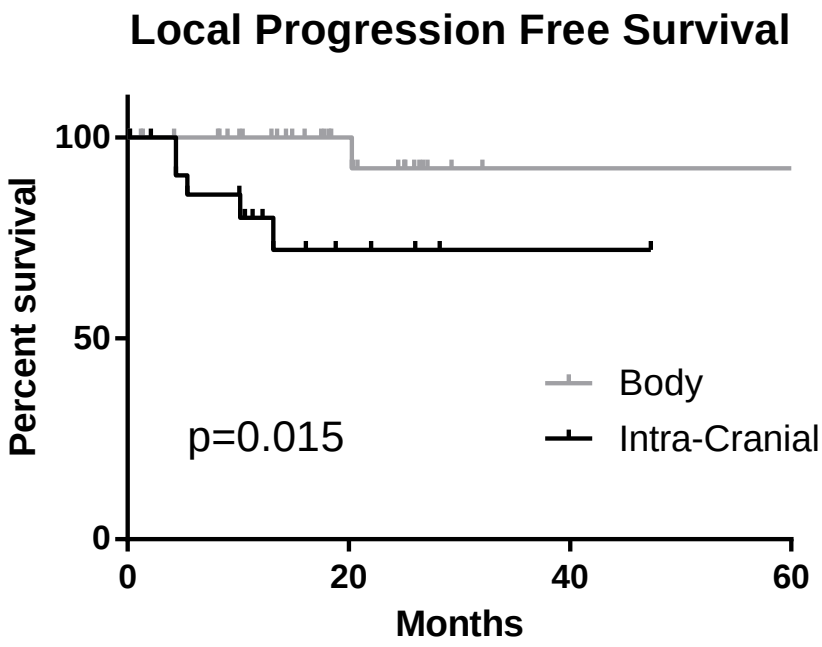

The local PFS for Body sites was promising at 92% at 2 years, the local PFS for intra-cranial sites was 74% at 2 years. This was a statistically significant difference. Intracranial oligometastases do significantly worse than body metastases (log-rank p=0.015).

Distant Progression:

Median freedom from distant disease progression, considering all 57 patients = 6 months.

Therefore, as for outcomes in primary pancreatic cancer, and lymph node oligometastases, distant progression occurred earlier than local progression.

Overall Survival (OS):

Overall Survival considering all 57 patients was 75% at 2 years.

6.4.3C: Statistical analysis: Oligometastatic breast cancer

Aim 3 was to evaluate outcomes of oligometastatic breast cancer according to delivered BED.

For the purposes of this analysis the author decided to focus on stereotactic radiotherapy delivered to body metastases.

BED vs Local Control:

The calculated BED (y axis) was compared to Local Control (x axis) in the dot-plot below. Each dot represents a "Body" oligometastasis. BED was calculated as described above assuming an α/β ratio of 10 for tumour control.

Dot plot 2: BED vs Local progression status:

Body metastases from oligometastatic breast cancer treated with SBRT

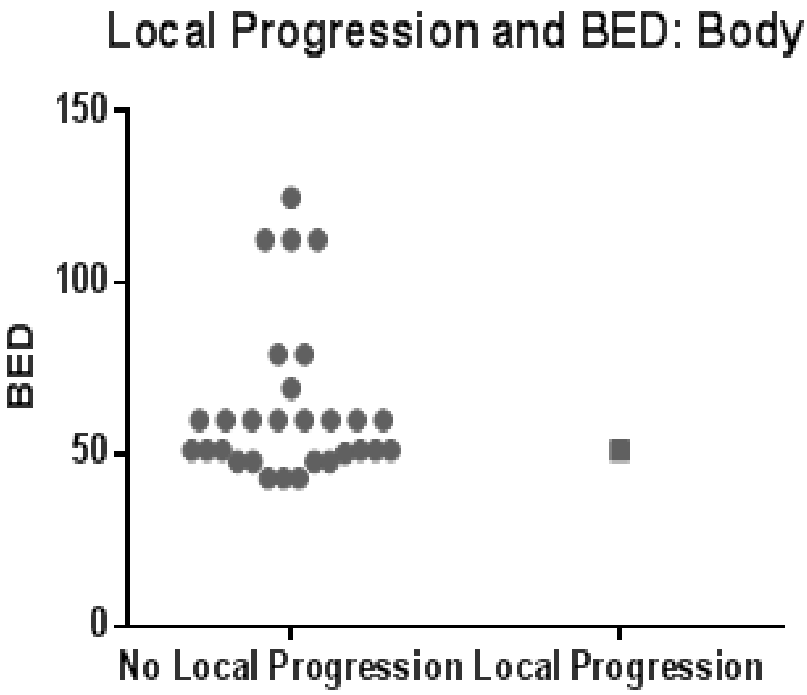

The dot-plot clearly shows that there was only a single case of local progression.

The solitary case of Body metastasis Local Progression was treated to BED 48Gy_{10} (30Gy/5#). Time to Local Progression was 20 months. Treating to ≥ 50Gy BEDGy_{10} (i.e. ≥27Gy/3# or ≥31Gy/5#) in this cohort gives 100% Local Control at Median follow-up 13 months.

6.5 DISCUSSION

Tumour control can be maximised, and normal tissue toxicity can be minimised, by optimising the accuracy of dose delivery. These aspects have been discussed in Chapters 3-5 (tumour delineation, optimum fiducial location, reproducible bladder filling, appropriate planning margin).

It is also important for the dose/fractionation regime selected to be optimum for tumour control, while being protective to Organs At Risk.

As explained in Chapter 1, the clinical evidence for the efficacy and safety of Conventionally-fractionated radiotherapy has been gathered over decades. In contrast, there is more limited long-term data for SBRT regimes, because the treatment approach is newer. Dose-fractionation regimes for Lung SBRT have been piloted in dose-escalation Phase 1 clinical trials (21). There is now good clinical data for optimum BED for Stage 1 lung cancer following a meta-analysis (BED>100Gy_{10} is associated with improved tumour control), but the evidence for other indications is less clear (22).

The BED formula can be used to compare the biological potency of a given SBRT regime with a conventionally-fractionated regime (which might be more familiar to an Oncologist). However, there are some caveats to this approach, the BED model tends to over-estimate the radiation effects of larger fraction sizes (23).

It is therefore extremely important that outcome data (toxicity and disease control data), is collected and critically analysed, in order to inform optimum dose/fractionation in SBRT.

6.5.1 SBRT vs Conventionally-fractionated radiotherapy for primary pancreatic cancer

The majority of pancreatic tumours lie in the head of the pancreas (24) where the tumour lies adjacent to duodenum, and in close proximity to small bowel and stomach. It is therefore critical to evaluate the toxicity of delivered SBRT regimes.

6.5.1A: Outcome data: Toxicity: SBRT primary pancreatic cancer

A number of studies have assessed the toxicity of SBRT regimes to treat localised pancreatic cancer.

Acute Toxicity

Certain studies report Grade 2+ Acute toxicity rates of 5-8% (10, 24). However, a further study (Hoyer et al, (25)) reported pronounced acute toxicity, with deteriorating performance status at 14

days, and progression to Grade 2+ toxicity in 79% of patients. Notably the Hoyer et al study did not employ real-time tumour-tracking (Synchrony), median PTV volume was large (136cc), and the prescribed dose was high (45Gy/3#, BED = 111Gy_{10}).

In contrast, the 42 patients whose treatment was described in Section 6.3.1 had Grade 3 acute toxicity rates of 5%, and there was no recorded Grade 4 acute toxicity. These rates are therefore comparable to the acute toxicity reported by Mahadevan et al, and Chang et al (10, 24).

The median PTV in the author's series (69.2cc) was notably smaller than the median PTV of the Hoyer et al series (136cc). In addition, the mean prescribed dose (27Gy/3#, BED = 48.6 Gy_{10}), was biologically much less potent than the regime delivered by Hoyer et al (BED = 111Gy_{10}). These differences may partially explain the differences in observed acute toxicity.

Outside of a randomised controlled trial, toxicity rates of different radiotherapy regimes should be compared with caution. That said, Grade 3 upper gastrointestinal acute toxicity was 7.3% in patients treated at 1.8-2Gy/fraction (conventionally-fractionated) to a median prescribed dose to the PTV of 54Gy in a study by Fuss et al (26).

In conclusion, the observed Grade 3 acute toxicity rate of 5% in the author's series is considered acceptable, and compares well with SBRT and conventionally-fractionated radiotherapy regimes reported in the literature.

Late Toxicity

Locally advanced pancreatic cancer has a poor prognosis, and this limited the reporting of late toxicity in studies. Hoyer et al had a 5% overall survival rate at 1 year (25). Chang et al (10) reported the late Grade 3+ toxicity rate "in the absence of progressive disease" as 9%. Mahadevan et al (24) selected chemo-responders to receive SBRT and had a Grade 3+ late toxicity rate of 6%.

In the current study, 2 patients (6%) experienced late Grade3+ duodenal toxicity (Grade 4 duodenal stricture). Both patients were treated in an early cohort at the author's centre and had a Maximum point dose (MPD) to the Duodenum which exceeded the current dose constraint of 24Gy to 0.035cc of Duodenum.

The first patient received a treatment dose of 25.5Gy/3# to the 58% isodose (BED= 45.7Gy_{10}) to an above average PTV of 79cc (compared to Median PTV of 69cc). MPD to Duodenum was 29.4Gy, (therefore exceeding the current MPD dose constraint of 24Gy).

A further patient experienced a duodenal stricture 14 months after SBRT and sadly died from perforation due to duodenal obstruction. The patient was treated to a median BED ($49.5Gy_{10,}$ 27Gy/3# to 70% isodose). Of note the PTV was large at 104cc (compared to Median PTV of 69cc). The patient also had a MPD to the Duodenum which exceeded the current dose constraint of 24Gy to 0.035cc. Duodenal MPD was 31.6Gy.

The reported Grade 4 toxicity rate of 6% is therefore comparable to the reported literature, and notably occurred only in those patients whose Duodenal MPD exceeded 24Gy (current constraint).

Statistical analysis:

Chi-squared test and ANOVA were used to test for association between treatment factors and toxicity. The treatment factors evaluated were: Number of fiducials, PTV (cc), PTV (min/mean/max dose), Prescribed dose, Prescription isodose, Coverage (%), and BED.

There was no statistically significant association (p values 0.084-0.991).

Summary:

The observed acute and late Grade 3+ toxicity rates (5% and 6% respectively) following SBRT to localised pancreatic cancer, compare favourably with toxicity rates reported in the literature.

There was no statistically significant association between treatment delivery factors and toxicity.

Late Grade 4 duodenal toxicity occurred only in those patients where Duodenal MPD constraint was exceeded.

Disease outcome data and radiobiological calculations will be discussed in the subsequent sections, but these results suggest there may be scope for cautious dose escalation, although Duodenal MPD constraint should be respected.

6.5.1B: Outcome data: Disease control: SBRT primary pancreatic cancer

The poor prognosis of pancreatic cancer patients is largely related to the propensity for early metastatic progression. Median time to disease progression is often 6 months, predominantly due to distant progression (27). However, achieving local control is important to prevent symptoms of local disease (such as abdominal pain, and jaundice). It is also important to secure local control because a certain percentage of patients progress locally only (10).

Wong et al reported disease control outcomes for patients receiving 50.4Gy/28 fractions over 5.5 weeks (at 1.8Gy/fraction). The patients received concurrent 5fu chemotherapy by protracted venous infusion. Median Local progression-free survival, and Median Distant progression-free survival was 6 months. Median overall survival was 9 months (27).

There would be a number of potential advantages of an SBRT strategy for the treatment of localised pancreatic cancer. There is a potential to deliver an increased BED to the tumour, the shorter fractionation allows for greater patient convenience, and the shorter fractionation allows minimal interference with chemotherapy delivery.

Outcomes for SBRT for the treatment of primary pancreatic cancer have been reported by Chang, Hoyer, and Mahadevan et al (10, 24, 25).

Chang et al delivered 25Gy/1# to pancreatic tumours using the CyberKnife treatment platform (10). Their radiobiological calculations determined that this dose was equivalent to 74Gy to tumour if delivering 1.8Gy/fraction. A majority of the patients had localised disease. The authors concluded that while the local control rates were promising, they would move to fractionated SBRT schedules to aim to reduce morbidity.

Hoyer et al delivered 45Gy/3# with a Linac-based SBRT technique (25). The regime was toxic as described in Section 6.5.1A.

Mahadevan et al selected chemo-responders with locally advanced pancreatic cancer to receive SBRT delivered by CyberKnife (24-36Gy/3#, based on duodenal tolerance) (24). The patients were then offered Gemcitabine for 6 months, or until tolerance or disease progression. The outcomes from this study are more encouraging. The authors felt that the promising outcomes were largely due to minimal interruption of systemic chemotherapy.

The disease control outcomes of these studies will be compared with those at the author's centre, and hypotheses for the different outcomes will be put forward.

Patients studied at the author's centre were a heterogenous group. 23% had not received chemotherapy prior to SBRT, because they were judged too frail. 23% had received prior radiotherapy, thereby limiting the SBRT dose that could be safely delivered. Treatment doses were 18-36Gy/3#, dose was largely adapted according to duodenal tolerance as per Mahadevan et al.

Local control analysis:

Actuarial Freedom From Local progression (FFLP) was 85% at 6 months, and 44% at 1 year at the author's centre. This compared favourably to the patients in the Hoyer (25) et al study (FFLP at 6 months = 57%), which is encouraging given that the toxicity outcomes of the author's SBRT regime were also more favourable.

The FFLP rate also compared favourably to the outcome of 50.4Gy/28#/5.5 weeks (BED 40.5Gy_{10}) with 5fu delivered by Wong et al (50% FFLP at 6 months)(9). The improvement may have been related to the higher BED delivered by the SBRT regime (Mean BED 48.6Gy_{10}), but may also be related to refinements in treatment delivery with SBRT e.g. tracking of respiratory movement.

However, FFLP at 1 year (44%) was poorer at the author's centre than the SBRT studies of Mahadevan et al and Chang et al (78-84%) (10, 24). Chang et al delivered a regime much more potent (BED = 87Gy_{10}) than the author's regime (Mean BED = 48.6Gy_{10}) which may partially explain the difference in control. Mean BED of Mahadevan et al (56.4Gy_{10}) was also more potent than the author's regime, but the potency of the regimes is more similar. On review of the treatment planning and delivery technique, the approach is very similar between the authors, the most notable difference was in the number of fiducials implanted. Chang and Mahadevan et al both followed a strategy of implanting 3-5 fiducials for all patients, whereas only 67% of the author's patients were tracked with 3+ fiducials. If there were inaccuracies in treatment delivery due to sub-optimal number of fiducials implanted it would be expected that FFLP rates may decrease, and Toxicity rates may increase. Statistical analysis was performed to evaluate if the number of fiducials implanted (≤2 vs ≥3) was associated with toxicity, but this was not found to be the case (p value 0.084 for acute toxicity and p value 0.718 for late toxicity). A formal statistical test for association between number of fiducials implanted and FFLP has not yet been undertaken, but it would be interesting to do this.

Progression-free survival (PFS) analysis:

PFS at the author's centre was 49% at 6months, and 23% at 1 year.

This compares favourably with the PFS of Hoyer et al SBRT regime (PFS at 1 year = 9%)(25), and was similar to the PFS of Wong et al (50.4Gy/28#, 50% PFS at 6 months)(9).

The PFS of the SBRT regime at the author's centre compared favourably to Chang et al (PFS 26% at 6 months, and 9% at 1 year) (10), although it is noted that 19% of the Chang et al cohort had established metastatic disease at the time of SBRT, whereas all patients treated at the author's centre had localised disease only.

However, Mahadevan et al (24) had superior PFS results, Median PFS = 9.6 months. All patients treated by Mahadevan et al were chemo-responders, which would naturally select a better prognosis cohort of patients. In contrast, 23% of the author's cohort had not received prior chemotherapy because the patients were considered too frail. In addition, the patients in Mahadevan et al's study were treated with adjuvant Gemcitabine chemotherapy, which was re-commenced soon after SBRT. Data on subsequent treatments has not been formally analysed at the author's centre, but this would be interesting. It may also be informative to statistically compare the PFS outcomes of chemotherapy-naïve patients with those pre-treated with chemotherapy.

Overall Survival (OS) analysis:

Median Overall Survival at the author's centre was 8.4 months. Overall survival was 40% at 1 year.

This was similar to the Median Overall Survival of the 50.4Gy/28# chemoradiotherapy regime delivered by Wong et al (Median Overall Survival 9 months) (26).

However, the SBRT regime delivered by Hoyer et al was associated with poorer survival (Median survival 5.4 months, survival 5% at 1 year). This may have been related to the toxicity of the regime (25).

Overall survival of the Chang et al SBRT regime was 21% at 1 year, therefore poorer than the outcomes at the author's centre, though again it is noted that 19% of the Chang et al cohort had established metastatic disease at the time of SBRT (10).

The most encouraging Overall Survival was observed by Mahadevan et al, median overall survival was 14.3 months (24).

Summary:

The SBRT regime delivered at the author's centre (Mean BED 48.6Gy_{10}) was associated with the following outcomes at 1 year: FFLP 44%, PFS 23%, and OS 40%.

FFLP was improved compared to the biologically less potent regime delivering 50.4Gy/28# (BED 40.5Gy_{10}) (27), perhaps due to refinements in treatment delivery with SBRT technique (e.g. tracking

of respiratory motion), as well as the increased biological potency of the SBRT regime. FFLP was also improved compared to the potent SBRT regime delivering 45Gy/3# (BED 111Gy_{10})(25), underlining the importance of accurate treatment delivery.

FFLP at the author's centre compared less favourably, however, with SBRT regimes tracked with Synchrony, which were biologically more potent (Mean BED 56.4-87Gy_{10}) (10, 24).

The poor outcomes for PFS and OS across all studies indicates that improvements in systemic therapy will be crucial in improving the prognosis of pancreatic cancer. However, the improved local control that can be achieved with SBRT (vs. 50.4Gy/28#/5.5 weeks), as well as the shorter fractionation (beneficial for patient convenience and minimal interruption of systemic treatment) supports the SBRT technique for the treatment of localised pancreatic cancer in well-selected patients. However, the FFLP rates show that there is clearly scope for improvement of SBRT technique/Dose-fractionation selection.

6.5.1C: Radiobiology: primary pancreatic cancer

Aim 1 was to perform a radiobiological comparison between SBRT regimes delivered for the treatment of primary pancreatic cancer, and conventional radiotherapy schedules. The results of the calculations are reported in Section 6.4.1D.

The analysis above has shown that SBRT regimes delivered at the author's centre had improved FFLP rates compared to conventional ("reference") radiotherapy schedules (50.4Gy/28#, BED 40.5Gy_{10}).

There is scope for improvement in FFLP rates, however, to improve the FFLP rates to those of the more potent SBRT regimes delivered by Chang and Mahadevan et al (10, 24). Improved FFLP should not be at the expense of worsened toxicity.

When considering FFLP rates with the reference schedule of 50.4Gy/28#, it is worth noting that this is associated with a low tumour BED (40.5Gy_{10}). This figure will be even lower in patients exhibiting the fastest repopulation. The reference BED of 40.5Gy_{10} , even when applied to a reasonably radiosensitive tumour ($\alpha = 0.35Gy^{-1}$) is unlikely to control tumours containing more than about 1 million clonogenic cells (20).

In the worst cases, the reference schedule dose losses to tumour repopulation may be 30% or more, and any form of radiotherapy which involves an accelerated schedule, e.g. SBRT, will reduce such losses.

The analysis performed in Section 6.4.1D shows that SBRT regimes can emulate the potency of the reference schedule, and half of the treatments at the author's centre delivered dose schedules which would be expected to produce disease control outcomes comparable with those from the reference schedule (based on minimum doses delivered to the PTV). Given the low overall toxicity (discussed in Section 6.5.1A), there could be scope for dose escalation based on gradual increase in minimum PTV dose, while respecting the Duodenal MPD dose constraint. This suggestion would be supported by the fact that when considering the CK regime that will deliver the minimum dose equivalent of the reference schedule (22.2Gy/3#), the $BEDGy_3$ for Normal tissues ($77Gy_3$) of this regime is less than the $BEDGy_3$ of the reference schedule ($80.6Gy_3$), see Table 6.3. Minimum dose to PTV is currently not the most considered parameter in CK treatment planning. A "good" CK treatment plan will have 95% of the PTV treated by the prescription isodose, but due to the sharp dose fall-off of CK plans, plans with >95% coverage could still have low minimum doses to the PTV. This analysis has highlighted that Minimum dose to the PTV in CK plans should be >22.2Gy (in a 3 fraction plan).

The 3-fraction regimes delivered at the author's centre are less likely (than single fraction regimes) to involve fraction sizes beyond the normally accepted reliability of the LQ model (10Gy fractions), and therefore the regimes would be a reasonable candidate for carefully-monitored dose escalation (23) as described above.

6.5.2 SBRT Dose-Fractionation for Lymph node oligometastases

Aim 2 was to evaluate the outcomes of SBRT to lymph node oligometastases according to delivered BED.

In contrast to the treatment of localised primary pancreatic cancer, conventionally-fractionated radiotherapy would not usually be employed to treat a solitary lymph node metastasis. Systemic therapy would be the standard of care, but this approach is rarely ablative. Systemic therapy is therefore the Control arm in the CORE study, a randomised trial which will shortly be opened in the UK, comparing systemic therapy vs systemic therapy + SBRT to oligometastases (≤ 3 metastases) (28).

This discussion will therefore focus on the outcomes of SBRT to treat lymph node oligometastases. Review of the literature reveals that studies reporting SBRT outcomes for lymph node oligometastases are a heterogenous group. They comprise a range of metastatic sites, prognostic factors (disease-free interval, number of sites, tumour volume) as well as varying tumour pathology, making it difficult to draw conclusions on optimum dose-fractionation (3).

Local control analysis:

The primary pathology of lymph node oligometastases treated by SBRT studies in the literature include: Prostate, Cervix, Gastric, Breast, Colorectal and Renal cell. The BED of the regimes delivered varied widely ($60Gy_{10}$ – $125Gy_{10}$), as did the outcomes: Local Control 67.4-100% at a follow-up of 2-4 years (12-15).

Considering the 2 studies that showed the most encouraging Local control rate, the first study was a small study (n=7) by Kim et al delivering SBRT to para-aortic lymph nodes from recurrent gastric cancer. Local control rate was 100% at a median follow-up of 26 months. Interestingly, the highest BED of the above studies ($125Gy_{10}$, 48Gy/3# to 80% isodose) was delivered, and importantly toxicity was acceptable (no Grade 3+ toxicity recorded). Patients were treated with a CyberKnife technique with 6 implanted fiducials per patient (15).

The next most promising study of SBRT for lymph node oligometastases (for local control) was performed by Casamassima et al (13). This was a study of 25 patients with lymph node oligometastases from prostate cancer. The lowest BED of the above studies was delivered (BED $60Gy_{10}$, 30Gy/3#), but an encouraging local control rate of 90% at 3 years was achieved with no Grade 2+ toxicity. SBRT was delivered using a Linac-based technique.

The observation that the 2 most encouraging SBRT lymph node oligometastasis studies (in terms of local control) employed the lowest and highest BED regimes, suggests that histopathology of the primary may be an important consideration in dose selection.

Local control rate at the author's centre was 88% at a median follow-up of 15 months (n=38, Median BED 59.5$Gy_{10,}$ majority 24Gy/3#), with Local-PFS at 1 year 80%. Toxicity was acceptable (Acute toxicity Grade 3+: 3%, Late Toxicity Grade 3+: 5%). The cohort at the author's centre had mixed histology of the primary site, similar to the study by Bignardi et al (n=19, Median BED = 79Gy_{10}, majority 45Gy/6#) which had comparable outcomes (Local control = 77.8% at 2 years, Grade 3+ Toxicity: 5%). Interestingly, the Bignardi et al study treated to a higher median BED, but of note no patients studied had received prior radiotherapy to the target site (compared to 38% of those studied at the author's centre had received prior radiotherapy, which limited the re-treatment dose).

Progression-Free survival (PFS) and Overall Survival (OS) analysis:

The SBRT studies reported in the literature have a wide range of PFS and OS outcomes, as would be expected given the wide range of histopathologies included, together with variable prognostic factors such as disease-free interval and tumour volume. PFS at 1 year was 29.5-80%, OS rates at 1 year were 76-100% (12-15).

At the author's centre, PFS at 1 year was 48%, and OS at 1 year was 91%, therefore the outcomes were in keeping with those in the literature. The heterogeneity of the patients included in the studies prevent further comparison. The outcome of randomised trials, such as the CORE trial, will allow comparison of outcomes stratified by prognostic and treatment factors.

BED vs Local Control:

The studies reported in the literature discussed above did not formally study local control with respect to delivered BED. This analysis was not possible in some studies due to small numbers of patients, and in other studies due to more standardised dose-prescription.

A range of BEDs were delivered at the author's centre (Range: 43Gy_{10} – 79$Gy_{10,}$ 9 x BED levels delivered). This is well illustrated in the dot-plot in Section 6.4.2C, where BED is plotted against Local Control. The dot-plot clearly shows that the regime with the lowest BED (24Gy/3#, BED = 43.2Gy_{10}) is associated with the highest risk of local progression. The dose-prescription was limited in these cases by a combination of prior radiotherapy and normal tissue dose constraints. It is therefore possible that radio-resistance of these tumour targets was partially responsible for the poorer local control rates. This outcome for the 24Gy/3# dose level fits with a dose-escalation trial by Salama et

al (29), a study evaluating SBRT to a variety of metastases (lung/liver/bone/lymph node/brain). Those who received 24Gy/3# (the lowest BED regime tested) had poor local control (45.7%).

Importantly, the dot-plot also shows that when patients were treated to a threshold BED of ≥ $72Gy_{10,}$ the local control rate was 100% at a median follow-up of 15 months (equating to a prescribed dose of ≥ 36Gy/3# or ≥ 40Gy in 5#). There was no Grade 3+ toxicity in patients treated to this dose level. The Kim et al study that achieved 100% local control at 26 months follow-up treated to a BED above the $72Gy_{10}$ threshold so these results are in keeping. In addition, the Salama et al dose-escalation trial showed that for the 4 patients prescribed 48Gy/3# (BED $125Gy_{10}$) a local control rate of 100% was achieved (29). However, the Bignardi et al cohort were treated to BED $79Gy_{10,}$ and there were local recurrences noted in 2 patients, both recurred within 1 year, the paper did not comment further on characteristics of the 2 patients that recurred locally (e.g. PTV volume, tumour pathology, coverage)(12).

<u>Histopathology vs PFS:</u>

The biology of a tumour (e.g. the propensity to metastasis) varies according to the histopathology. As well as the wide range of delivered BEDs, there was a wide range of histopathologies treated in the author's cohort which warranted analysis. Given the importance of BED, the analysis by Histopathology was stratified according to BED.

Graph 6.4 shows PFS by Histopathology, adjusted for BED. The Colorectal cancer patients had the most favourable PFS: Median PFS for the Colorectal cancer histopathology group was 22 months, which is encouraging in a cohort of patients that was heavily pre-treated (78% prior chemotherapy). It is interesting that the Colorectal group had the superior PFS, as Takeda et al reported that lung metastases from Colorectal cancer had substantially worse local control rates than metastases from other primaries (including lung cancer primaries)(30). However, a study by Milano et al showed no significant differences in outcomes between colorectal cancer and other (non-breast) primaries (16).

In contrast, the lung cancer group had the least favourable PFS, with a median PFS of just over 3 months (the time point that the first post-SBRT imaging would be performed). All cases of progression in the lung group were distant progression, therefore, patient selection factors (such as disease-free interval, number of metastases) are likely to be implicated.

Summary

The SBRT regime delivered at the author's centre (Median BED 59.5Gy_{10}) was associated with the following outcomes at 1 year: Local-PFS 80%, PFS 48%, and OS 91%. Toxicity was acceptable (Grade 3+ toxicity: ≤ 5%).

PFS and OS rates are comparable with other series quoted in the literature.

Analysis of outcomes according to BED has shown that tumour targets treated to a threshold BED of 72Gy_{10} (equating to 36Gy/3# or 40Gy/5#) have a local control rate of 100% at a median follow-up of 15months. There was no G3+ toxicity in patients treated to this dose level. It will be important to confirm whether the observed local control rate is maintained with longer follow-up.

The PFS of patients was analysed by histopathology of the primary, adjusted by BED. Colorectal cancer histology was associated with the most favourable PFS (Median PFS =22 months). There were relatively small numbers in each histopathology group, larger numbers will allow analysis of the reasons for the differences observed, specifically looking at prognostic factors such as disease-free interval, tumour volume, and number of metastases.

6.5.3 SBRT Dose-Fractionation for Oligometastatic breast cancer

Aim 3 was to evaluate the outcomes of SBRT for oligometastatic breast cancer according to delivered BED.

As for the treatment of lymph node oligometastases, systemic therapy would be the standard of care for oligometastatic breast cancer. Breast cancer is one of 3 histopathologies being evaluated in the CORE trial (the other histopathologies are prostate and lung)(28).

The literature regarding SBRT for oligometastatic breast cancer comprises a range of metastatic sites, therefore a variety of organs are the Organs At Risk, which in turn affects the doses which can safely be delivered to the oligometastases. The largest study on SBRT for oligometastatic breast cancer was conducted by Milano et al (16).

Local control analysis:

At the author's centre Local Progression-Free Survival (Local PFS) was 92% at 2 years for Body sites (extra-cranial).

Local PFS for intra-cranial sites (i.e. Brain metastases) was 74% at 2 years (see Graph 6.5).

There was a statistically significant difference between the outcomes of intracranial vs extracranial metastases, intracranial oligometastases do significantly worse (log-rank p=0.015).

Grade 3+ toxicity rate was 5%.

Milano et al analysed a subgroup of 39 patients with oligometastatic breast cancer treated with a Linac-based SBRT technique (16). The most commonly treated metastases were located in Liver, Bone and Lung. A single patient was treated for a brain metastasis. Local control rate at 2 years was 87%. The local control rate at 4 and 6 years was also 87% suggesting that local recurrences will occur within 2 years. Performing univariate and multivariate analysis, the authors found that local control was favourable for bone metastases (0/17 bony metastases recurred locally) vs. non-bone metastases (10/68 non-bone metastases progressed locally).

The Local PFS rates at the author's centre for extracranial breast cancer metastases (92% at 2 years) compared favourably with the Local control rate of Milano et al (87% at 2 years). A single patient (3%) of the Milano et al cohort had intracranial metastasis, shown in Section 6.4.3B to have poorer local control, which would slightly negatively bias the Milano et al cohort. Taking this into

consideration, the Local PFS (92%) at the author's centre still compares favourably to the Milano et al cohort.

Freedom from Distant Metastasis (FFDM) and Overall Survival (OS) analysis:

Median FFDM at the author's centre, considering all 57 patients, was 6 months. Therefore, as for outcomes in primary pancreatic cancer, and lymph node oligometastases, distant progression occurred earlier than local progression. In contrast, Milano et al reported a FFDM of 52% at 2 years, which would be a far more encouraging outcome. However, the author's centre would count any new distant metastasis. In contrast, the definition of FFDM applied by Milano et al was "widespread distant progression, not amenable to resection or locally ablative therapy". This difference in endpoints would therefore negatively bias against the author's centre.

Overall survival at the author's centre was 75% at 2 years (considering all 57 patients). The 2 year overall survival for the Milano et al cohort was 74% at 2 years, which is remarkably similar. It is encouraging that overall survival is similar across the 2 cohorts of patients given the proportion of patients with intracranial disease in the author's cohort (41%) vs Milano et al cohort (3%). Intracranial metastases are associated with a worse prognosis than extracranial metastases.

BED vs Local Control (Body sites):

This Thesis/Chapter is exploring aspects of SBRT, so the author has decided to focus on extra-cranial (body) metastases for this analysis.

Section 6.4.3C displayed a dot-plot for Local progression (x axis) vs delivered BED (Gy_{10}). Each dot represents a treated "Body" oligometastasis. It can be clearly seen that there was only a single case of local progression. This solitary case was treated to a BED of $48Gy_{10}$ (30Gy/5#). Treating to BED ≥ $50Gy_{10}$ (equating to ≥ 27Gy/3# or ≥31Gy/5#) in this cohort gives 100% local control at a Median follow-up of 13 months.

Interestingly, the solitary case of local progression was a patient with sternal metastasis (PTV=20cc), whilst the Milano et al paper showed that bony metastases had the best local control rates. There could be a few potential reasons for the disease progression (which was an edge-of-target progression). The patient had been treated with 2 lines of chemotherapy previously. The patient had had a good response to treatment but there was a PET-positive focus of residual disease post-chemotherapy. This was accepted for SBRT treatment. The GTV was grown by a small planning margin (1.25mm) to create the PTV. The patient may have recurred due to a) micrometastatic deposits being present in the sternum adjacent to the GTV post-chemotherapy, this could have been

incorporated into a CTV expansion, or b) planning margin inadequate (given Synchrony case, target best seen on a PET which needed fusing to primary CT), or c) aggressive tumour biology, the patient recurred simultaneously at other distant sites (mediastinal lymph nodes), or a combination of these possibilities.

It will be interesting to see if the encouraging Local control outcomes for extra-cranial sites will persist at longer follow-up (beyond 2 years).

Summary:

At the author's centre, Local PFS for SBRT to extra-cranial oligometastatic breast cancer was 92% at 2 years. Toxicity was acceptable (Grade 3+ toxicity = 5%).

Considering the entire cohort of 57 patients (41% brain metastases, 59% extra-cranial metastases), those with extracranial disease had significantly improved Local PFS (vs. intracranial metastases), p = 0.015.

Overall survival (considering all 57 patients) was 75% at 2 years, which compares well with Overall Survival outcomes reported in the literature.

At an early median follow-up of 13 months, SBRT delivery to a threshold BED of ≥ $50Gy_{10}$ (equivalent to ≥ 27Gy/3# or ≥ 31Gy/5#) to extra-cranial metastases gives 100% local control.

This is the first work evaluating local control according to BED for breast oligometastasis treated by SBRT. It will be important to see if the Local control outcomes are borne out on longer follow-up beyond 2 years.

6.6 CONCLUSIONS

It is important that the dose/fractionation regime that is selected in SBRT should be optimum for tumour control, while also being protective to Organs At Risk. Selection of dose/fractionation regimes based on extrapolation from conventionally-fractionated data may not be sound due to the limitations of the Linear Quadratic formula at the high doses per fraction delivered in SBRT. It is therefore important that outcome data is critically analysed, in order to inform optimum dose/fractionation in SBRT.

The Aims of this Chapter were:

1. To perform a radiobiological comparison between SBRT regimes delivered for the treatment of primary pancreatic cancer, and conventional radiotherapy schedules.
2. To evaluate the outcomes of SBRT to lymph node oligometastases according to delivered BED.
3. To evaluate the outcomes of SBRT to oligometastatic breast cancer according to delivered BED.

Primary pancreatic cancer:

The SBRT regimes delivered at the author's centre (Mean BED 48.6Gy_{10}) were associated with the following outcomes at 1 year: FFLP 44%, PFS 23%, and OS 40%.

This FFLP rate (following SBRT) is improved compared to a standard reference conventional radiotherapy schedule of 50.4Gy/28#/5.5 weeks (BED 40.5Gy_{10}).

There is, however, scope for improvement in the FFLP rates to those achieved by other more potent SBRT regimes reported in the literature (FFLP at 1 year 78-84% following BED 56.4Gy_{10} -87Gy_{10}), although it would be important that improved FFLP should not be at the expense of worsened toxicity.

The radiobiological comparison performed between the reference schedule (50.4Gy/28#/5.5weeks, BED 40.5Gy_{10}) and the SBRT regimes delivered at the author's centre, as per Aim 1, has shown that half the SBRT treatments delivered would be expected to produce FFLP outcomes comparable with those of the reference schedule (based on minimum doses delivered to the PTV). Given the low overall toxicity experienced by patients treated with SBRT at the author's centre, there would be scope for dose escalation based on increase in minimum PTV dose, while respecting the Duodenal MPD constraint. The radiobiological comparison which has been performed supports that this should be possible, potentially without an increase in toxicity.

Minimum dose to the PTV is currently not the most considered parameter in CyberKnife treatment planning. This novel radiobiological analysis has highlighted that Minimum dose to the PTV in 3-fraction CyberKnife treatment plans should be >22.2Gy. This sets out new planning guidance in SBRT for localised pancreatic cancer.

Lymph node Oligometastases:

The SBRT regimes delivered at the author's centre (Median BED 59.5Gy_{10}) achieved the following outcomes at 1 year: Local PFS 80%, PFS 48%, and OS 91%. Toxicity was acceptable (Grade 3+ toxicity ≤ 5%). PFS and OS rates are comparable with other series quoted in the literature.

Analysis of outcomes according to BED, as per Aim 2, has shown that tumour targets treated to a threshold BED of 72Gy_{10} (equivalent to 36Gy/3#, or 40Gy/5#) have a local control rate of 100% at a median follow-up of 15 months. There was no Grade 3+ toxicity in patients treated to this dose level. If these results are confirmed on longer follow-up, this is important data. Previous studies have shown 100% local control rate with BED125Gy_{10}, and equally, poor local control at BED 43.2Gy_{10} (confirmed also in this work), but if BED 72Gy_{10} is shown to secure 100% local control long-term, then it will be a more favourable regime than BED 125Gy_{10} as it would be associated with a safer toxicity profile. The recommendation is that 36Gy/3#, or 40Gy/5# should be the preferred dose prescription for lymph node oligometastasis.

Comparing the histopathology of primary tumours, adjusted by BED, Colorectal cancer histology was associated with the most favourable PFS (Median PFS = 22 months).

Oligometastatic breast cancer:

The SBRT regimes delivered at the author's centre (Median BED 51.3 Gy_{10}) achieved Local PFS of 92% at 2 years for extra-cranial metastases. Toxicity was acceptable (Grade 3+ toxicity = 5%). The patients with extra-cranial metastases (59% of the cohort) had statistically significantly improved Local PFS compared to patients with intracranial metastases receiving hypofractionated radiotherapy with a stereotactic technique ($p = 0.015$).

Analysis of Local control according to BED, as per Aim 3, for SBRT to extra-cranial metastases showed that delivery of a threshold BED of ≥ 50Gy_{10} (equivalent to ≥ 27Gy/3# or to ≥ 31Gy/5#) gives 100% local control at a median follow-up of 13 months.

This is the first work evaluating local control according to BED for breast oligometastasis treated by SBRT. It will be important to see if the Local control outcomes are borne out on longer follow-up beyond 2 years.

References

1. Hellman S, Weichselbaum RR. Oligometastases. Journal of Clinical Oncology. 1995;13(1):8-10.
2. Norton L, Simon R. The Norton-Simon hypothesis revisited. Cancer Treat Rep. 1986;70(1):163-9.
3. Tree AC, Khoo VS, Eeles RA, Ahmed M, Dearnaley DP, Hawkins MA, et al. Stereotactic body radiotherapy for oligometastases. Lancet Oncol. 2013;14(1):e28-37.
4. Jones B, Dale RG, Deehan C, Hopkins KI, Morgan DAL. The Role of Biologically Effective Dose (BED) in Clinical Oncology. Clinical Oncology. 2001;13(2):71-81.
5. Williams MV, Denekamp J, Fowler JF. A review of αβ ratios for experimental tumors: Implications for clinical studies of altered fractionation. International Journal of Radiation Oncology • Biology • Physics.11(1):87-96.
6. Zhang J, Yang F, Li B, Li H, Liu J, Huang W, et al. Which Is the Optimal Biologically Effective Dose of Stereotactic Body Radiotherapy for Stage I Non–Small-Cell Lung Cancer? A Meta-Analysis. International Journal of Radiation Oncology • Biology • Physics.81(4):e305-e16.
7. Stinauer M, Kavanagh B, Schefter T, Gonzalez R, Flaig T, Lewis K, et al. Stereotactic body radiation therapy for melanoma and renal cell carcinoma: impact of single fraction equivalent dose on local control. Radiation Oncology. 2011;6(1):34.
8. Rossi ML, Rehman AA, Gondi CS. Therapeutic options for the management of pancreatic cancer. World Journal of Gastroenterology : WJG. 2014;20(32):11142-59.
9. Wong AA, Delclos ME, Wolff RA, Evans DB, Abbruzzese JL, Tamm EP, et al. Radiation dose considerations in the palliative treatment of locally advanced adenocarcinoma of the pancreas. Am J Clin Oncol. 2005;28(3):227-33.
10. Chang DT, Schellenberg D, Shen J, Kim J, Goodman KA, Fisher GA, et al. Stereotactic radiotherapy for unresectable adenocarcinoma of the pancreas. Cancer. 2009;115(3):665-72.
11. Mahadevan A, Miksad R, Goldstein M, Sullivan R, Bullock A, Buchbinder E, et al. Induction Gemcitabine and Stereotactic Body Radiotherapy for Locally Advanced Nonmetastatic Pancreas Cancer. International Journal of Radiation Oncology • Biology • Physics.81(4):e615-e22.
12. Bignardi M, Navarria P, Mancosu P, Cozzi L, Fogliata A, Tozzi A, et al. Clinical Outcome of Hypofractionated Stereotactic Radiotherapy for Abdominal Lymph Node Metastases. International Journal of Radiation Oncology • Biology • Physics.81(3):831-8.
13. F C, L M, C M. Efficacy of eradicative radiotherapy for limited nodal metastases detected with choline PET scan in prostate cancer patients. Tumori. 2011;97:49-55.
14. Choi CW, Cho CK, Yoo SY, Kim MS, Yang KM, Yoo HJ, et al. Image-Guided Stereotactic Body Radiation Therapy in Patients With Isolated Para-Aortic Lymph Node Metastases From Uterine Cervical and Corpus Cancer. International Journal of Radiation Oncology • Biology • Physics.74(1):147-53.
15. Kim M-S, Yoo SY, Cho CK, Yoo HJ, Yang KM, Kang JK, et al. Stereotactic Body Radiotherapy for Isolated Para-aortic Lymph Node Recurrence after Curative Resection in Gastric Cancer. Journal of Korean Medical Science. 2009;24(3):488-92.
16. Milano MT, Katz AW, Zhang H, Okunieff P. Oligometastases Treated With Stereotactic Body Radiotherapy: Long-Term Follow-Up of Prospective Study. International Journal of Radiation Oncology*Biology*Physics. 2012;83(3):878-86.
17. Queens CC. CIHR_RFA_Report 3_Appendix2.
18. Dale RG, Hendry JH, Jones B, Robertson AG, Deehan C, Sinclair JA. Practical Methods for Compensating for Missed Treatment Days in Radiotherapy, with Particular Reference to Head and Neck Schedules. Clinical Oncology.14(5):382-93.
19. ICRU. International Commission on Radiation Units and Measurements Report 50: Prescribing, Recording and Reporting Photon Beam Therapy. ICRU Reports. 1993;50.
20. Steel GG. Basic clinical radiobiology: Arnold; 1997.
21. Rusthoven KE, Kavanagh BD, Burri SH, Chen C, Cardenes H, Chidel MA, et al. Multi-Institutional Phase I/II Trial of Stereotactic Body Radiation Therapy for Lung Metastases. Journal of Clinical Oncology. 2009;27(10):1579-84.
22. Zhang J, Yang F, Li B, Li H, Liu J, Huang W, et al. Which Is the Optimal Biologically Effective Dose of Stereotactic Body Radiotherapy for Stage I Non–Small-Cell Lung Cancer? A Meta-Analysis. International Journal of Radiation Oncology*Biology*Physics. 2011;81(4):e305-e16.

23. Murphy JD, Christman-Skieller C, Kim J, Dieterich S, Chang DT, Koong AC. A Dosimetric Model of Duodenal Toxicity After Stereotactic Body Radiotherapy for Pancreatic Cancer. International Journal of Radiation Oncology • Biology • Physics.78(5):1420-6.
24. Mahadevan A, Jain S, Goldstein M, Miksad R, Pleskow D, Sawhney M, et al. Stereotactic Body Radiotherapy and Gemcitabine for Locally Advanced Pancreatic Cancer. International Journal of Radiation Oncology*Biology*Physics. 2010;78(3):735-42.
25. Hoyer M, Roed H, Sengelov L, Traberg A, Ohlhuis L, Pedersen J, et al. Phase-II study on stereotactic radiotherapy of locally advanced pancreatic carcinoma. Radiotherapy and Oncology.76(1):48-53.
26. Fuss M, Wong A, Fuller CD, Salter BJ, Fuss C, Thomas CR. Image-Guided Intensity-Modulated Radiotherapy for Pancreatic Carcinoma. Gastrointestinal Cancer Research : GCR. 2007;1(1):2-11.
27. Wong AA, Delclos ME, Wolff RA, Evans DB, Abbruzzese JL, Tamm EP, et al. Radiation Dose Considerations in the Palliative Treatment of Locally Advanced Adenocarcinoma of the Pancreas. American Journal of Clinical Oncology. 2005;28(3):227-33.
28. Aitken K, Tree A, Thomas K, Nutting C, Hawkins M, Tait D, et al. Initial UK Experience of Stereotactic Body Radiotherapy for Extracranial Oligometastases: Can We Change the Therapeutic Paradigm? Clinical Oncology.27(7):411-9.
29. Salama JK, Hasselle MD, Chmura SJ, Malik R, Mehta N, Yenice KM, et al. Stereotactic body radiotherapy for multisite extracranial oligometastases. Cancer. 2012;118(11):2962-70.
30. Takeda A, Kunieda E, Ohashi T, Aoki Y, Koike N, Takeda T. Stereotactic body radiotherapy (SBRT) for oligometastatic lung tumors from colorectal cancer and other primary cancers in comparison with primary lung cancer. Radiotherapy and Oncology.101(2):255-9.

Acknowledgements

This research was undertaken at The Harley Street Clinic, London. I am grateful that THSC was financial sponsor for my course fees. I would like to thank Professor Pat Price, and Dr Nicholas Plowman for their invaluable help and support as MD (Res) supervisors.

The MD(Res) is registered with the Bart's Cancer Institute of Queen Mary University of London. I particularly acknowledge the encouragement and guidance of Dr John Marshall and Gunnel Hallden.

The work has been done in close collaboration with other CK Radiographers (Alexandra Aitken, Bronwyn Middleton, and Ankuree Patel) and Physicists within the hospital. I have also benefitted from collaboration with Medical statisticians and Radiobiologists. I acknowledge the contribution of:

Kelvin Hiscoke: Radiotherapy phantom discussions: Chapter 2.

Dr Ian Cowley: CK planning/delivery assistance, RBE discussions: Chapters 2 and 5.

Angelina Piccini: Data collection RT patients, Chapter 4.

Andrew Robinson: Prostate planning margins discussions, Chapter 5.

Roger Dale: Radiobiology calculations (pancreas), Chapter 6.

Melanie Green: Statistical support: Chapters 5 and 6.

Alexandra Aitken: Granting of Private Study Leave to complete writing-up.

I would also like to recognise the support and encouragement of my Research Office colleagues and friends, Andrew Edwards and Lynsey Rice.

Abstracts and Publications

International Presentations:

2012:

RadioSurgery Society (RSS), USA: SBRT to Lymph Node oligometastases

ARO Forum, USA: SBRT for IMC/Sternal metastases from Breast cancer

2013:

ESTRO (GVA): SBRT for IMC/Sternal metastases from Breast Cancer

RSS, USA: SABR to Lymph Node Oligometastases (update): Oral/ poster: Prize-winning

SABR for Pancreas cancer: Lessons to learn from toxicity: Oral/poster: Prize-winning

2014:

ASTRO, USA: Stereotactic Radiotherapy to Oligometastases in Breast cancer: Poster

RSS, USA: SABR for the treatment of recurrent breast cancer presenting with IMC nodal/sternal disease: Oral

2015:

ECCO, Vienna: DVH analysis of SBRT treatment of primary pancreatic cancer: Setting new dose-volume constraints: Poster

BIR/SABR, NI: SBRT for Oligometastatic breast cancer: Oral

Publications:

"Stereotactic ablative body radiotherapy (SABR) for primary and secondary lung tumours"

Christy Goldsmith and Andrew Gaya, Cancer Imaging (2012)12 (2), 351-360.

"Single-fraction and Fractionated Radiosurgery for Base-of-Skull tumours: Four year experience in a UK centre"

Christy Goldsmith, Hannah Wilson, Pat Price, Keyoumars Ashkan, Melanie Green, Timothy Cross, Ronald Beaney, Rhiannon Davies, Nick Plowman

British Journal of Neurosurgery: Accepted pending revisions: Sept 2015